

# The Development and Investigation of Catalytic Photochemical Radical Reactions Mediated by Visible Light

by

John Duy Nguyen

A dissertation submitted in partial fulfillment  
of the requirements for the degree of  
Doctor of Philosophy  
(Chemistry)  
in The University of Michigan  
2014

Doctoral Committee:

Associate Professor Corey R. J. Stephenson, Chair  
Professor Bart M. Bartlett  
Assistant Professor Amanda L. Garner  
Professor John Montgomery

To my family and friends

## ACKNOWLEDGEMENTS

The work in this thesis was accomplished through the support, help, and encouragement from many people. First and foremost I offer my sincerest gratitude to my advisor, Corey R. J. Stephenson for providing me with the opportunity to conduct research in his group as well as guidance and advice throughout my development as a scientist and a professional.

I have benefited, throughout my time at Boston University and the University of Michigan, from the guidance and input of numerous faculty members and staff members. Thank you to John Porco, John Snyder, and Ramesh Jasti for their intellectual support, technical assistance and motivational encouragement during my time at Boston University. I would like to express my gratitude to my dissertation committee members at the University of Michigan for their valuable time and helpful suggestions. I sincerely wish to thank Professor John Montgomery for his help and suggestions during my original research proposal exam. In addition, I am indebted to Professor Bart Bartlett and Professor Amanda L. Garner for their advice toward obtaining a postdoctoral position. Many thanks to Dr. Eugenio Alvarado and Dr. Chris Kojiro for assistance with NMR spectroscopy as well as Mr. Jim Windak and Mr. Paul Lennon for helping with mass spectroscopy.

I also wish to give thanks to the past and present members in the Stephenson group for their friendship, encouragement, and assistance. Dr. Jagan M. R. Narayanam and Dr. Joseph W. Tucker both served as my mentors as I began my graduate studies. I respectfully acknowledge the following project collaborators: Joseph Tucker, Jagan Narayanam, Marlena Konieczynska, Carl-Johan Wallentin, Erica D'Amato, Chunhui Dai, Bryan Matsuura, Jim Devery, and James

Douglas. Special thanks must also be given to Dr. David Freeman, Dr. Joseph Tucker, Dr. Laura Furst, Dr. Milena Czyz, Dr. Jim Devery, Dr. James Douglas, Dr. Elizabeth Swift, Bryan Matsuura, Joel Beatty, Mitch Keylor, Tim Monos, Katarina Makaravage, Lara Cala, Fabio Hernandez, and Rory MacAtee for their support and friendship. I have also had the opportunity to work with several outstanding undergraduates, visiting students, and graduate students as their mentor including Katarina Makaravage, Gabe Magallanes, Lara Cala, Jerome Gaborit, Peter Finkbeiner, Ellen Piel, Barbara Reiss, and Erica D'Amato.

I would like to thank my friends and family outside of the graduate chemistry community. My parents, Nathan and Victoria, taught me through their words and actions the importance of persistence, patience, self-respect, and sympathy, which have enabled my accomplishments thus far. Although my mother passed away several years ago, I think about her every day and her memory motivates me to new heights. My sister, Nikki, niece, Thuong, nephew, Them, and my high school and college friends: Anthony Hoang, Chris Lee, Brian Khy, Joseph Valdez, Alfredo Nava, Michael Chun, Conor McKiernan, Ben Hadden and Kenny Mayoral have constantly served as a grounding force, reminding me of the world outside of the laboratory. From the depths of heart, I would like to sincerely thank Erica D'Amato for her love, support, and encouragement. She never doubted that I could achieve my goals even when I did. When I was at my lowest points, she was there to hold me up. I may very well be the luckiest guy in the world. Erica, I love you.

Finally, I would like to thank the Chemistry Department, the American Chemical Society, Amgen, and AstraZeneca for financial support.



## TABLE OF CONTENTS

Dedications .....	ii
Acknowledgments.....	iii
List of Tables .....	viii
List of Figures.....	ix
List of Abbreviations .....	xiii
Abstract.....	xvi
<b>Chapter 1. Enabling Novel Photoredox Reactivity via Photocatalyst Selection</b>	
A. Introduction .....	1
B. Reductive Quenching .....	8
a) Reductive Dehalogenation	
b) Intramolecular Radical Additions	
c) Intermolecular Radical Additions	
d) Nucleophilic Addition to Iminium Ions Derived from Tetrahydroisoquinolines	
e) Radical Cation Diels-Alder Reactions	
f) Photocatalytic Activation of Carbon-Oxygen Bonds	
g) Formal [3+2] Cycloadditions of Aminocyclopropanes	
h) Use of Reductive Quenching in Total Synthesis	
C. Oxidative Quenching.....	19
a) Atom Transfer Radical Addition (ATRA)	

b) Oxytrifluoromethylation of Alkenes	
c) Trifluoromethylation of Arene and Heteroarenes	
d) Deprotection of PMB Ethers	
e) Dehalogenation of Unactivated Alkyl, Alkenyl and Aryl Iodides	
f) Batch to Flow Deoxygenation	
g) Control of Living Polymerization	
D. Conclusions and Future Prospects.....	27
<b>Chapter 2. Radical Reductive Dehalogenation and Reductive Cyclization</b>	
A. Introduction.....	30
B. Background.....	32
C. Reductive Hydrodeiodination.....	34
D. Deoxygenation Protocol.....	40
E. Reductive Hydrodebromination.....	46
F. Mechanism and Mechanistic Investigations.....	48
a) Reductive Hydrodeiodination	
b) Reductive Hydrodebromination	
G. Conclusions.....	50
Experimental Section.....	51
<b>Chapter 3. Radical Atom Transfer Radical Addition Reactions</b>	
A. Introduction.....	105
B. Background.....	106
C. Atom Transfer Radical Addition via Oxidative Quenching.....	109
D. Atom Transfer Radical Addition via Reductive Quenching.....	115

E. One-Pot Reductive Coupling .....	123
F. Mechanism and Mechanistic Studies.....	124
G. Conclusions.....	129
Experimental Section .....	130
<b>Chapter 4. Photochemical Strategy for Lignin Degradation at Room Temperature</b>	
A. Introduction.....	168
B. Strategy .....	176
C. Chemoselective Benzylic Oxidation.....	178
D. Photoredox-Mediated Reductive Cleavage of C <sub>α</sub> -O Bonds.....	181
E. Two-Step Protocol for Lignin Degradation .....	185
F. Mechanism and Mechanistic Studies.....	186
G. Conclusions.....	187
Experimental Section .....	188
<b>Chapter 5. Conclusion and Future Prospects .....</b>	<b>208</b>
<b>Bibliography .....</b>	<b>210</b>

## LIST OF TABLES

<b>Table 2.1</b> Optimization of hydrodeiodination of alkyl iodides .....	35
<b>Table 2.2</b> Reduction of alkenyl iodides and intramolecular reductive cyclizations.....	38
<b>Table 2.3</b> One-pot deoxygenation of alkyl alcohols .....	45
<b>Table 3.1</b> Optimization and control experiments for intermolecular ATRA .....	108
<b>Table 3.2</b> ATRA using oxidative quenching photocatalysis.....	109
<b>Table 3.3</b> Catalyst screenings.....	111
<b>Table 3.4</b> Solvent screening .....	112
<b>Table 3.5</b> Newly optimized conditions for ATRA via oxidative quenching .....	113
<b>Table 3.6</b> Optimization of ATRA of C <sub>8</sub> F <sub>17</sub> I onto 5-hexen-1-ol .....	118
<b>Table 3.7</b> ATRA of various perfluoroalkyl iodides .....	119
<b>Table 3.8</b> Substrate scope for iodoperfluoroalkylation of alkenes and alkynes.....	120
<b>Table 4.1</b> Investigation of visible light-mediated oxidation of benzylic alcohols .....	179
<b>Table 4.2</b> Selective benzylic oxidation with [4-AcNH-TEMPO]BF <sub>4</sub> .....	180
<b>Table 4.3</b> Optimization of reductive C <sub>α</sub> -O bond cleavage & control reactions .....	182
<b>Table 4.4</b> Substrate scope of visible light-mediated C <sub>α</sub> -O bond cleavage .....	184

## LIST OF FIGURES

<b>Figure 1.1</b> Generalized Jablonski diagram for $\text{Ru}(\text{bpy})_3^{2+}$ .....	2
<b>Figure 1.2</b> Photocatalytic cycle of $\text{Ru}(\text{bpy})_3^{2+}$ .....	3
<b>Figure 1.3</b> Tuning redox potentials via ligand substitution .....	4
<b>Figure 1.4</b> Seminal 2008 photoredox publications .....	8
<b>Figure 1.5</b> Reductive dehalogenation of activated carbon-halogen bonds .....	9
<b>Figure 1.6</b> Proposed catalytic cycle for reductive dehalogenation .....	10
<b>Figure 1.7</b> Intramolecular radical cyclization of electron rich heterocycles .....	11
<b>Figure 1.8</b> Expansion of intramolecular radical cyclization .....	12
<b>Figure 1.9</b> Intermolecular radical coupling .....	13
<b>Figure 1.10</b> Aza-Henry and subsequent expansion to other nucleophiles .....	14
<b>Figure 1.11</b> Proposed catalytic cycle for the aza-Henry reaction .....	14
<b>Figure 1.12</b> Radical cation Diels-Alder .....	16
<b>Figure 1.13</b> Proposed catalytic cycle for radical cation Diels-Alder radical .....	16
<b>Figure 1.14</b> Formal [3+2] cycloaddition of amino cyclopropanes .....	17
<b>Figure 1.15</b> Proposed mechanism of formal [3+2] cycloaddition of amino cyclopropanes .....	17
<b>Figure 1.16</b> Key radical coupling en route to gliocladin C .....	18
<b>Figure 1.17</b> Key radical coupling en route to aplyviolene .....	19
<b>Figure 1.18</b> Initial discovery of ATRA .....	20
<b>Figure 1.19</b> Optimized ATRA protocol .....	20

<b>Figure 1.20</b> Possible mechanisms for ATRA.....	21
<b>Figure 1.21</b> ATRA fluorous tagging.....	21
<b>Figure 1.22</b> Oxytrifluoromethylation of styrenyl alkenes.....	22
<b>Figure 1.23</b> Trifluoromethylation of electron rich heteroarenes using Ru(phen) <sub>3</sub> Cl <sub>2</sub> .....	23
<b>Figure 1.24</b> Trifluoromethylation of electron poor heteroarenes using Ir(Fppy) <sub>3</sub> .....	24
<b>Figure 1.25</b> Oxidative PMB deprotection.....	24
<b>Figure 1.26</b> Proposed catalytic cycle for the PMB deprotection.....	24
<b>Figure 1.27</b> Reduction of unactivated C–I bonds.....	26
<b>Figure 1.28</b> Comparison of batch vs batch to flow deoxygenation.....	27
<b>Figure 1.29</b> Application of visible light-mediated ATRA to living polymerization.....	28
<b>Figure 2.1</b> Improved methods for radical reductive deiodination.....	31
<b>Figure 2.2</b> Radical reductive hydrodeiodination of alkyl iodides.....	36
<b>Figure 2.3</b> Radical reductive hydrodeiodination of aryl iodides.....	37
<b>Figure 2.4</b> <i>fac</i> -Ir(ppy) <sub>3</sub> -mediated isomerization of cinnamyl alcohol substrates.....	37
<b>Figure 2.5</b> Reductive hydrodeiodination utilizing flow chemistry.....	40
<b>Figure 2.6</b> Conceptual goal toward catalytic visible light-mediated deoxygenation.....	42
<b>Figure 2.7</b> Schematic for visible light-mediated one-pot deoxygenation protocol.....	43
<b>Figure 2.8</b> Increased efficiency of deoxygenation in a flow reactor.....	44
<b>Figure 2.9</b> Light-mediated methods for reductive radical debromination.....	47
<b>Figure 2.10</b> Effect of heating upon reductive radical debromination.....	47
<b>Figure 2.11</b> Visible light-mediated debromination of alkyl and aryl bromides.....	47
<b>Figure 2.12</b> Deuterium labeling study.....	48
<b>Figure 2.13</b> Evidence for an operative oxidative quenching mechanism.....	49

<b>Figure 2.14</b> Proposed mechanism for the radical reductive hydrodeiodination reaction.....	49
<b>Figure 2.15</b> Proposed mechanism for the radical reductive hydrodebromination reaction .....	50
<b>Figure 3.1</b> Photoredox catalyzed ATRA.....	105
<b>Figure 3.2</b> Initial observation of ATRA product under photoredox conditions.....	106
<b>Figure 3.3</b> Initial results for intramolecular ATRA .....	107
<b>Figure 3.4</b> Synthetic utility of ATRA products.....	110
<b>Figure 3.5</b> Expansion of photocatalytic ATRA via oxidative quenching .....	115
<b>Figure 3.6</b> Post-transformational fluorous quenching.....	122
<b>Figure 3.7</b> Discovery that ethanol is an efficient H-atom source.....	123
<b>Figure 3.8</b> One-pot reductive coupling protocol .....	123
<b>Figure 3.9</b> Proposed mechanisms for photoredox-catalyzed ATRA .....	125
<b>Figure 3.10</b> Evidence for radical polar crossover mechanism.....	126
<b>Figure 3.11</b> Light/dark experiment .....	127
<b>Figure 3.12</b> Evidence for propagation mechanism .....	128
<b>Figure 4.1</b> Representation of lignin biopolymer and common linkages .....	170
<b>Figure 4.2</b> Summary of biorefinery.....	171
<b>Figure 4.3</b> Products formed from oxidative degradation of $\beta$ -O-4 lignin model systems .....	173
<b>Figure 4.4</b> Stahl's chemoselective oxidation of $\beta$ -O-4 lignin model systems .....	174
<b>Figure 4.5</b> Hartwig's reductive cleavage of $\beta$ -O-4 lignin model systems .....	174
<b>Figure 4.6</b> Redox-neutral degradation of $\beta$ -O-4 lignin model systems.....	175
<b>Figure 4.7</b> Strategic photoredox approach to degradation of lignin model systems.....	177
<b>Figure 4.8</b> Hasegawa's reductive opening of epoxides (top). Reductive cleavage of C $_{\alpha}$ -O bond (bottom) .....	177

<b>Figure 4.9</b> Utilizing continuous flow and lower catalyst loading .....	186
<b>Figure 4.10</b> Proposed mechanism of C-O bond cleavage .....	187



## LIST OF ABBREVIATIONS

abs	absorbance
Ac	acetyl
aq	aqueous
Ar	aryl
ATRA	atom transfer radical addition
AIBN	azobisisobutyronitrile
BArF	[B[3,5-(CF <sub>3</sub> ) <sub>2</sub> C <sub>6</sub> H <sub>3</sub> ] <sub>4</sub> ] <sup>-</sup> anion
BF <sub>4</sub>	tetrafluoroborate anion
Bn	benzyl
Boc	<i>tert</i> -butoxycarbonyl
Bu	<i>n</i> -butyl
bpy	2,2'-bipyridine
bpz	2,2'-bipyrazine
CAN	cerium(IV) ammonium nitrate
Cbz	carboxybenzyl
CFL	compact fluorescent lightbulb
cm	centimeter
°C	degree Celsius
COD	1,5-cyclooctadiene
Cu	copper
CV	cyclic voltammetry
d	doublet
DABCO	1,4-diazabicyclo[2.2.2]octane
DBU	1,8-diazabicyclo[5.4.0]undec-7-ene
DCM	dichloromethane
DDQ	2,3-dichloro-5,6-dicyano-1,4-benzoquinone
dF(CF <sub>3</sub> )ppy	2-(2,4-difluorophenyl)-5-(trifluoromethyl)pyridine
DIPEA	<i>N,N</i> -diisopropylethylamine
DMF	dimethylformamide
DMSO	dimethylsulfoxide
dr	diastereomeric ratio
dtbbpy	4,4'-di- <i>tert</i> -butyl-2,2'-bipyridine
δ	chemical shift in parts per million
E <sub>0,0</sub>	zero-zero excitation energy
E <sub>red</sub>	reduction potential
EDG	electron-donating group
ee	enantiomeric excess
eq	equation

equiv	equivalents
ESI	electrospray ionization
Et	ethyl
<i>fac</i>	facial
Fmoc	9-fluorenylmethoxycarbonyl
g	grams
h	hours
HMDS	hexamethyldisilazide
HRMS	high resolution mass spectroscopy
Hz	hertz
HMPA	hexamethylphosphoramide
Ir	iridium
IR	infrared
isc	intersystem crossing
<i>J</i>	coupling constant
K	Kelvin
L	liters
LAH	lithium aluminium hydride
LED	light emitting diode
Li	lithium
$\lambda_{\text{ex}}$	excitation wavelength
$\lambda_{\text{max}}$	maximum wavelength
m	multiplet
<i>m</i>	meta
M	molar concentration
Me	methyl
mg	milligrams
MHz	megahertz
$\mu\text{L}$	microliters
min	minutes
mL	milliliters
MLCT	metal to ligand charge transfer
mm	millimeters
mmol	millimoles
mol	moles
MW	molecular weight
NBS	<i>N</i> -bromosuccinimide
nm	nanometers
ns	nanosecond
NMR	nuclear magnetic resonance
<i>o</i>	ortho
[O]	oxidant
<i>p</i>	para
PC	photocatalyst
PF <sub>6</sub>	hexafluorophosphate anion
Ph	phenyl

phen	phenanthroline
PMB	<i>para</i> -methoxybenzyl
PMP	<i>para</i> -methoxyphenyl
ppm	parts per million
ppy	2-phenylpyridine
Pr	propyl
q	quartet
rt or RT	room temperature
Ru	ruthenium
s	singlet
SCE	saturated calomel electrode
t	triplet
TBS	<i>tert</i> -butyldimethylsilyl
TBDPS	<i>tert</i> -butyldimethylsilyl
TEMPO	2,2,6,6-tetramethylpiperidyl-1-oxyl
Tf	triflyl
THF	tetrahydrofuran
THP	tetrahydropyran
TLC	thin layer chromatography
TMS	trimethylsilyl
$t_R$	residence time
Ts	<i>para</i> -toluene sulfonate
TTMSS	tris(trimethylsilyl)silane
UV	ultraviolet light
V	volts
W	watt

## ABSTRACT

Metal-based polypyridyl photocatalysts such as  $[\text{Ru}(\text{bpy})_3]\text{Cl}_2$ ,<sup>1</sup>  $[\text{Ir}(\text{ppy})_2(\text{dtbbpy})]\text{PF}_6$ ,<sup>2</sup>  $[\text{Ir}\{\text{dF}(\text{CF}_3)\text{ppy}\}_2(\text{dtbbpy})]\text{PF}_6$ ,<sup>3</sup> and *fac*- $\text{Ir}(\text{ppy})_3$ <sup>4</sup> have been shown to be effective for the cleavage of C–Y bonds (Y = Cl, Br, I, O, N, P, H, and B) mediated by single electron transfers.<sup>5</sup> All of the photocatalysts mentioned above share similar modes of action and are all excited by visible light via absorption of a photon by the ground state photocatalyst to generate a spin-allowed high energy singlet excited state. In terms of electron transfer processes, the excited state species is “bipolar” in nature and can either undergo a single electron oxidation (oxidative quenching) or a single electron reduction (reductive quenching). The oxidative quenching pathway involves a direct single electron transfer (SET) from the excited state of the catalyst ( $^*\text{PC}^n \rightarrow \text{PC}^{(n+1)}$ ) to the substrate to reduce the C–Y bond, while the reductive quenching pathway involves two SET processes whereby the excited state is reduced by an electron donor to generate a strong reductant ( $\text{PC}^{(n-1)}$ ) which can then transfer an electron to the substrate to effect reduction of the C–Y bond. I have successfully utilized these photocatalysts to reduce C–Cl, C–Br, C–I, and C–O bonds to generate carbon-centered radicals capable of undergoing H-atom abstraction (Chapter 2), intramolecular cyclization (Chapter 2) and intermolecular coupling (Chapter 3). In addition, these methods have been applied to biomass conversion (Chapter 4).

## Chapter 1: Enabling Novel Photoredox Reactivity via Photocatalyst Selection

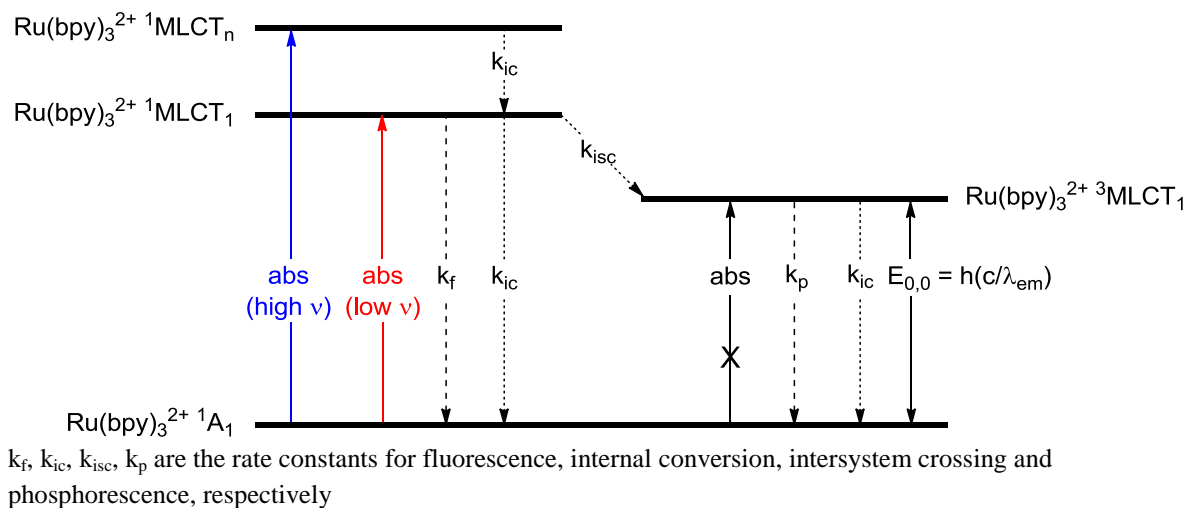
\*Portions of this chapter have been published in Douglas, J. J.; Nguyen, J. D.; Cole, K. P.; Stephenson, C. R. J. *Aldrichimica Acta* **2014**, *47*, 15.

### Introduction

Visible light active metal complexes have been extensively studied in numerous contexts since the first reported synthesis of tris(bipyridine)ruthenium(II) chloride ( $[\text{Ru}(\text{bpy})_3]\text{Cl}_2$ ) in 1936.<sup>6</sup> The optical and redox properties<sup>7</sup> of  $\text{Ru}(\text{bpy})_3\text{Cl}_2$  and related complexes has allowed for their use in the development of fields including photochemistry, electrochemistry and photocatalysis.<sup>8</sup> For decades, with few exceptions, studies into the visible light-induced redox properties of these catalysts were conducted by inorganic and physical chemists for applications including water splitting,<sup>9</sup> photovoltaic cells<sup>10</sup> and energy storage.<sup>11</sup> Complexes of this type have attracted chemists due in large part to the extended excited state lifetime of  $\text{Ru}(\text{bpy})_3\text{Cl}_2$  and related complexes. This confers the ability to undergo electron or energy transfer processes, allowing reactivity from the visible light induced excited state.

The following discussion regarding the physical properties of photoredox catalysts focuses on  $\text{Ru}(\text{bpy})_3\text{Cl}_2$ . However, the processes discussed are applicable to a wide variety of ruthenium- and iridium-based polypyridyl complexes. All light promoted transformations must first begin with absorption of a photon by the ground state photocatalyst,  $\text{Ru}(\text{bpy})_3^{2+} \text{}^1\text{A}_1$ , to generate a spin-allowed high energy singlet excited state. Despite the exact mode of excitation, these complexes typically relax initially to the lowest spin-allowed excited state  $^*\text{Ru}(\text{bpy})_3^{2+}$

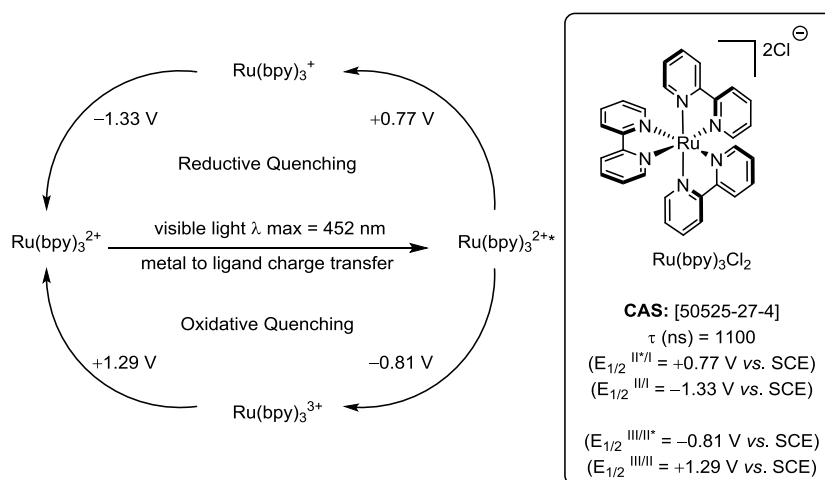
$^1\text{MLCT}_1$  from numerous singlet excited states  $^*\text{Ru}(\text{bpy})_3^{2+} \ ^1\text{MLCT}_n$ . This is advantageous as it alleviates the requirement of irradiation at a particular wavelength to initiate productive excitation of the catalyst. Broad spectrum irradiation from a less specialized apparatus can be employed, although  $\text{Ru}(\text{bpy})_3\text{Cl}_2$  has a maximum absorbance peak at 452 nm with a high molar extinction coefficient ( $14,600 \text{ M}^{-1}\text{cm}^{-1}$ ).<sup>1</sup> The  $^*\text{Ru}(\text{bpy})_3^{2+} \ ^1\text{MLCT}_1$  state rapidly undergoes intersystem crossing ( $k_{\text{isc}}$ ) to the triplet manifold followed by internal conversion to generate a long-lived first triplet excited state,  $^*\text{Ru}(\text{bpy})_3^{2+} \ ^3\text{MLCT}_1$  (Figure 1.1).<sup>12</sup> This intersystem crossing is so efficient that the quantum yield for the  $^*\text{Ru}(\text{bpy})_3^{2+} \ ^3\text{MLCT}_1$  state is essentially unity.<sup>13</sup> As a result, fluorescence,  $k_f$ , and internal conversion from  $^*\text{Ru}(\text{bpy})_3^{2+} \ ^1\text{MLCT}_1$  are minor deactivation pathways. Furthermore,  $^*\text{PC} \ ^3\text{MLCT}_1$  is sufficiently long lived to undergo bimolecular quenching reactions via either energy or electron transfer processes.<sup>14</sup> Unimolecular deactivation of  $^*\text{Ru}(\text{bpy})_3^{2+} \ ^3\text{MLCT}_1$  can occur through a variety of pathways, including luminescence or radiationless decay (Figure 1.1).



**Figure 1.1** Generalized Jablonski diagram for  $\text{Ru}(\text{bpy})_3^{2+}$ .

The detailed photochemical processes regarding the excited state species have been thoroughly investigated, with a synopsis designed for the organic chemist available.<sup>15</sup> In basic

terms, upon absorption of visible light, MLCT generates an excited state species that is “bipolar” in nature, it can either undergo a single electron reduction (reductive quenching)  $\text{Ru}(\text{bpy})_3^{2+*} \rightarrow \text{Ru}(\text{bpy})_3^+$  or a single electron oxidation (oxidative quenching)  $\text{Ru}(\text{bpy})_3^{2+*} \rightarrow \text{Ru}(\text{bpy})_3^{3+}$  (Figure 1.2). It is also important to note that the species resulting from either oxidative or reductive quenching ( $\text{Ru}(\text{bpy})_3^{3+}$  or  $\text{Ru}(\text{bpy})_3^+$ ) are themselves strong oxidants and reductants, respectively, thus the possibility for SET must be considered from multiple species. *Herein, “reduction potential” is exclusively used to describe the potential associated with the electrochemical half-reaction written in the direction where the more oxidized species is reduced, i.e.,  $\text{Li}^+ + e^- \rightarrow \text{Li}$ , ( $E_{\text{red}} [\text{Li}^+/\text{Li}] = -3.39 \text{ V}$ ).*

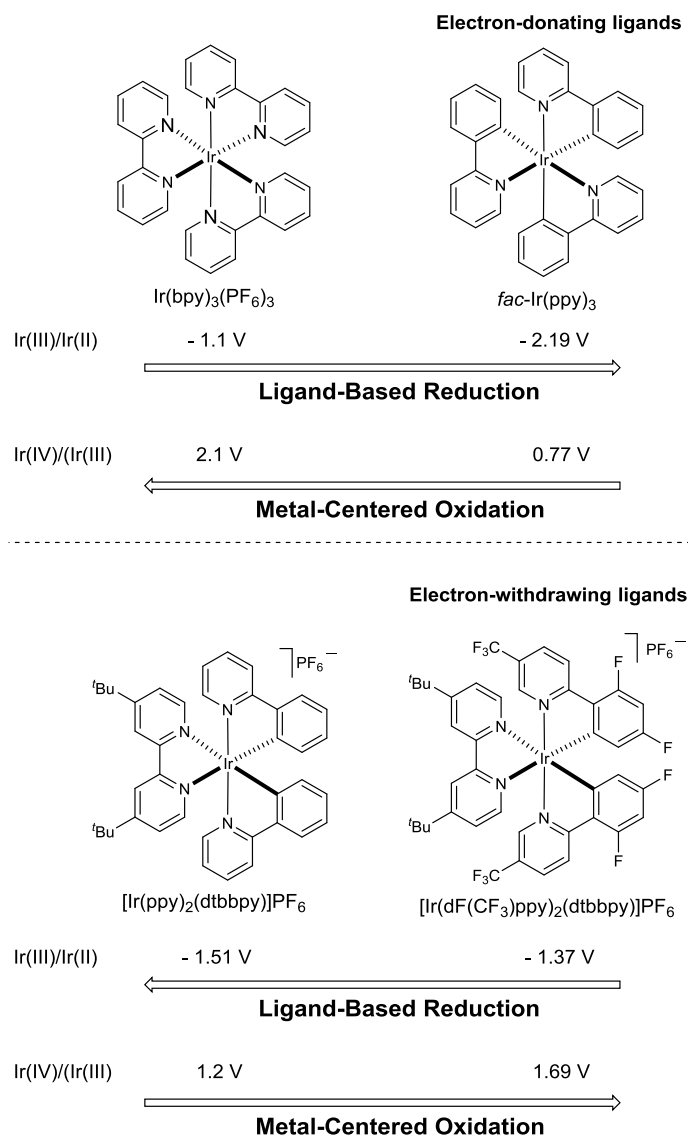


**Figure 1.2** Photocatalytic cycle of  $\text{Ru}(\text{bpy})_3^{2+}$ .

Light active metal-centered polypyridyl complexes have been studied extensively and applied diversely due to their chemical stability, redox properties, excited-state reactivity, luminescence emission, and excited-state lifetime.<sup>8</sup> Ru(II) and Ir(III) polypyridyl complexes are by far the most commonly utilized in organic chemistry for a range of radical based bond dissociations and bond formations mediated by single electron transfers. The success of these

complexes for photoredox catalysis stems largely from the ability to tune the redox properties of the catalyst by modification of the ligands as well as ligand combinations.

In general, the ground state oxidations of these complexes occur at the metal center, while the ground state reductions occur at the ligands. Therefore, electron-donating ligands tend to increase the ease of metal-centered oxidation and increase the difficulty of ligand-based reduction. For example,  $\text{Ir}(\text{bpy})_3(\text{PF}_6)_3$  has a ground state oxidation of  $[\text{Ir}(\text{IV})/\text{Ir}(\text{III}) = 2.1 \text{ V}]$



**Figure 1.3** Tuning redox potentials via ligand substitution.



and a ground state reduction of [Ir(III)/Ir(II) = - 1.1 V],<sup>16</sup> but replacing the neutral bipyridine ligands with negatively-charged and strong  $\sigma$ -donating phenylpyridine ligands to form *fac*-Ir(ppy)<sub>3</sub> causes the oxidation to occur more easily [Ir(IV)/Ir(III) = 0.77 V] and the reduction to become more difficult [Ir(III)/Ir(II) = - 2.19 V] (Figure 1.3, top).<sup>17</sup> On the other hand, electron-withdrawing ligands tend to increase the difficulty of metal-centered oxidation and decrease the difficulty of ligand-based reduction. For example, [Ir(ppy)<sub>2</sub>(dtbbpy)]PF<sub>6</sub> has a ground state oxidation [Ir(IV)/Ir(III) = 1.2 V] and a ground state reduction of [Ir(III)/Ir(II) = - 1.51 V],<sup>2</sup> but modifying the unsubstituted bipyridine ligands with electron-withdrawing fluoro and trifluoromethyl substituents to form [Ir(dF(CF<sub>3</sub>)ppy)<sub>2</sub>(dtbbpy)]PF<sub>6</sub> causes the oxidation to become more difficult [Ir(IV)/Ir(III) = 1.69 V] and the reduction to become easier [Ir(III)/Ir(II) = - 1.37 V] (Figure 1.3, bottom).<sup>3</sup>

Although the discussion above has focused on the oxidation of the metal center and the reduction of the ligand from the unexcited complex, organic chemists are more concerned with the reverse process in which reduction of Ru(III) or Ir(IV) generates Ru(II) or Ir(III), respectively, or the oxidation of Ru(I) or Ir(II) generates Ru(II) or Ir(III), respectively, because the catalysts are typically undergoing oxidative or reductive quenching from the excited state when they are used for organic transformations. For example, in the typical usage of the reductive quenching cycle of Ru(bpy)<sub>3</sub>Cl<sub>2</sub>,<sup>1</sup> light irradiation of the complex initiates a metal to ligand charge transfer event to produce an excited state that can be envisioned as a Ru(III) metal center and a radical anion bipyridine ligand. An electron donor reduces the metal center from Ru(III) to Ru(II), but the complex is typically described as Ru(I) due to the presence of the radical anion bipyridine ligand. Electron transfer from the ligand to a substrate molecule regenerates the unexcited Ru(II) complex. Therefore, a Ru(II) complex or Ir(III) complex with a

more difficult ligand-based reduction generally means that the Ru(I) or Ir(II) ground state is a strong reductant. Accordingly, a Ru(II) complex or Ir(III) complex with a more difficult metal-centered oxidation generally means that the Ru(III) or Ir(IV) ground state is a strong oxidant.

The redox potentials associated with the ground states are typically measured using cyclic voltammetry and spectroscopic data, but the redox potentials associated with the excited states are approximated using the ground state potentials and the zero-zero excitation energy, which is derived from the maximum emission of the catalyst.<sup>18</sup> As a result of the dependency of the ground state redox potentials on excited state redox potentials, larger values for the ground state redox potentials typically result in small values for the excited state redox potentials. The low values of the excited state redox potentials can prove detrimental for organic reaction development because ground states can only be accessed if the excited states can be oxidatively or reductively quenched when the catalyst is excited by visible light. For example, *fac*-Ir(ppy)<sub>3</sub><sup>17</sup> is a very strong single electron reductant through the reductive quenching cycle [Ir(III)/Ir(II) = -2.19 V], but the zero-zero excitation energy is 2.50 eV which dictates that the excited state oxidation potential is only 0.31 V [Ir(III)<sup>\*</sup>/Ir(II)]. This weak oxidation potential makes it difficult to access the Ir(II) ground state, and without the appropriate quencher the strong reductive power of the *fac*-Ir(ppy)<sub>3</sub> via reductive quenching cannot be utilized. However, *fac*-Ir(ppy)<sub>3</sub> is also a very strong single electron reductant through the oxidative quenching cycle [Ir(IV)/Ir(III)<sup>\*</sup> = -1.73 V], which dictates that the ground state oxidation potential is 0.77 V [Ir(IV)/Ir(III)]. This moderate oxidation potential is able to oxidize tertiary amines readily, and as a result, the oxidative quenching of *fac*-Ir(ppy)<sub>3</sub> has been utilized numerous times for organic transformations.<sup>19</sup> Consequently, the development of a successful photoredox catalyzed reaction depends strongly on the choice of catalyst, substrate, and additives (i.e. quencher).

The choice of metal center and ligands goes beyond simply shifting the redox potentials of the complex and can affect deactivation pathways, zero-zero excitation energy, and oxygen sensitivity.<sup>8</sup> These factors have traditionally been less of a concern to organic chemists, but could prove to be essential factors for designing new libraries of photocatalysts for organic transformations.

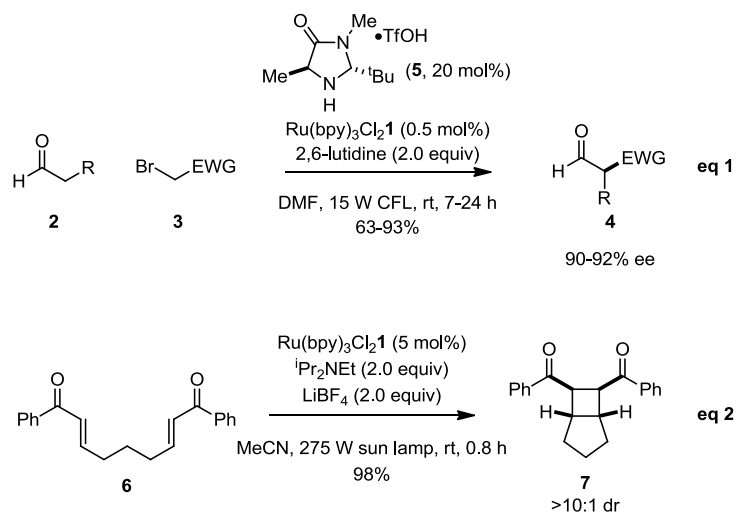
Pioneering research prior to 2008 by the groups of Deronzier,<sup>20</sup> Oda and Okada,<sup>21</sup> Kellogg<sup>22</sup> and Fukuzumi<sup>23</sup> identified some of the key reactivity of Ru(bpy)<sub>3</sub>Cl<sub>2</sub> that could be applied to organic synthesis. They demonstrated the ability of Ru(bpy)<sub>3</sub>Cl<sub>2</sub> to successfully reduce a variety of C–X bonds, N–O bonds, diazonium salts, and nitroarenes. However, these were often limited to isolated and sporadic examples, with the wider utility of Ru(bpy)<sub>3</sub>Cl<sub>2</sub> and related complexes predominantly overlooked by the broader synthetic chemistry community.

Two publications in 2008 initiated continued and directed interest in photoredox catalysis, primarily through novel application of known modes of Ru(bpy)<sub>3</sub>Cl<sub>2</sub> reactivity. Nicewicz and Macmillan reported an efficient merger of photoredox and organocatalysis to overcome the barriers associated with traditional two electron strategies for the asymmetric alkylation of aldehydes. They elegantly harnessed the ability of Ru(bpy)<sub>3</sub>Cl<sub>2</sub> to reduce C–Br bonds (such as in **3**), thus creating an electron deficient radical that may add to a chiral enamine. This transformation proceeded in typically excellent yield and ee for a range of alkyl aldehydes and activated alkyl bromides (Figure 1.4, equation 1).<sup>24</sup>

Independently, the group of Yoon demonstrated the ability to perform [2+2] cycloadditions, traditionally the realm of high-energy UV light, with a photoredox catalyst harnessing visible light. In this methodology a radical anion is generated from reduction of an activated enone by Ru(bpy)<sub>3</sub><sup>+</sup>, leading to intramolecular cyclization and ultimately the

cycloaddition products such as **7** (Figure 1.4, equation 2).<sup>25</sup> Following these publications the synthetic community began to appreciate the wider applicability of  $\text{Ru}(\text{bpy})_3\text{Cl}_2$  and related complexes, leading to an exponential increase in the quantity and diversity of publications. This renewed focus has transformed photoredox catalysis from a series of independent publications to a definable field of research.

Recent comprehensive reviews<sup>26</sup> and numerous perspective articles<sup>27</sup> on this topic have already appeared that serve as excellent resource texts. Overall, these reviews and perspectives reveal the choice of both photocatalyst, and how it is employed within the catalytic cycle, drove the discovery and optimization of a wide range of photoredox mediated processes.



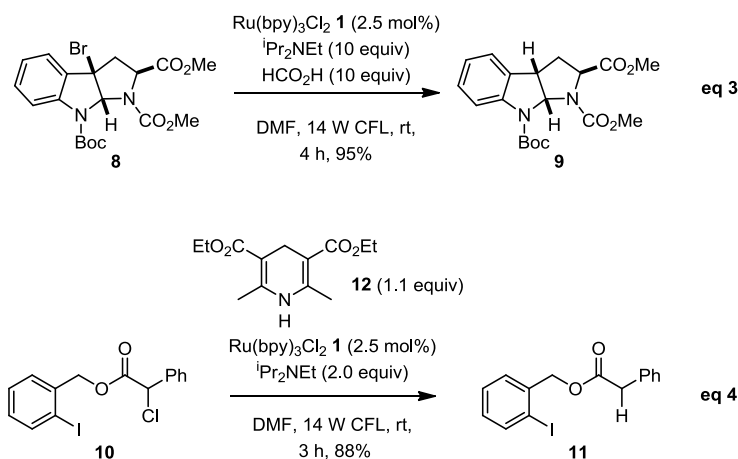
**Figure 1.4** Seminal 2008 photoredox publications.

## Reductive Quenching

### *Reductive Dehalogenation*

The endeavors of the Stephenson group in the field of photoredox catalysis were initiated during investigations aimed at the functionalization of bromopyrroloindolines such as **8**, and their subsequent use in complex molecule synthesis. The possibility of a radical dehalogenation

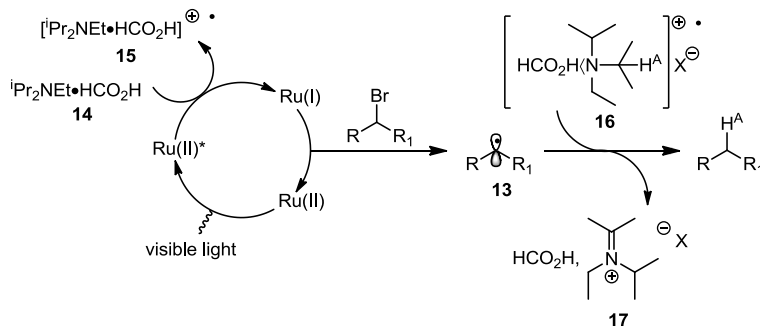
mediated by  $\text{Ru}(\text{bpy})_3\text{Cl}_2$  was hypothesized following the seminal publications of both the Macmillan and Yoon research groups in 2008. The Stephenson group initially focused on the reduction of activated C–Br bonds, reporting a generalized protocol to accompany pioneering initial studies by Fukuzumi and Tanaka,<sup>23,28</sup> Kellogg<sup>22</sup> and Kern and Sauvage.<sup>29</sup> This method allows the tin-free reductive dehalogenation of a range of both activated alkyl chlorides and bromides. Importantly, this approach displays excellent chemoselectivity with both aryl and alkenyl bromides and iodides tolerated without competing reduction, while proceeding with typical yields of 70-99%.<sup>30</sup> Two complementary sets of reaction conditions were developed for this transformation: **A**.  $\text{Ru}(\text{bpy})_3\text{Cl}_2$  (1.0 mol%),  $i\text{Pr}_2\text{NEt}$  (10 equiv) and formic acid ( $\text{HCO}_2\text{H}$ , 10 equiv) (Figure 1.5, eq 3); or **B**.  $\text{Ru}(\text{bpy})_3\text{Cl}_2$  (1.0 mol%),  $i\text{Pr}_2\text{NEt}$  (2.0 equiv) and Hantzsch Ester (1.1 equiv) (Figure 1.5, eq 4). Conditions **B** were shown to be particularly effective for substrates prone to undergoing competing displacement of the activated halogen with formate (such as **10**).



**Figure 1.5** Reductive dehalogenation of activated carbon-halogen bonds.

The proposed catalytic cycle is initiated by single electron transfer from the ammonium formate complex **14** to the excited  $\text{Ru}(\text{II})^*$ . The  $\text{Ru}(\text{I})$  complex formed then selectively reduces the carbon-halogen bond of the substrate, returning to the initial  $\text{Ru}(\text{II})$  photoactive ground state.

Deuterium labeling studies showed that the H-atom abstracted by alkyl radical **13** is primarily from one of the methine carbons belonging to the radical cation of  ${}^i\text{Pr}_2\text{NEt}$  (Figure 1.6).  $\text{Ru}(\text{bpy})_3\text{Cl}_2$  ( $E_{1/2}^{\text{II/I}} = -1.33 \text{ V vs. SCE}$ ) was initially chosen as the photocatalyst due to its commercial availability and previously demonstrated versatility. As a matter of fact, limited



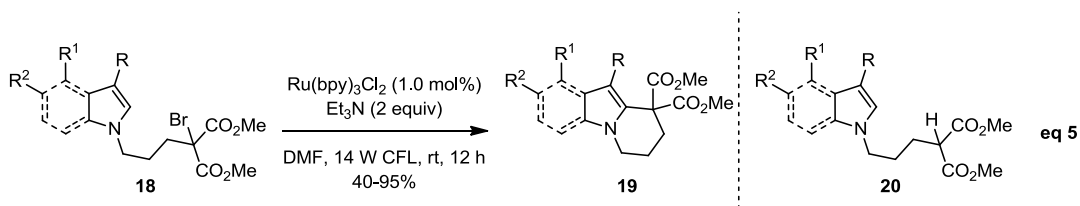
**Figure 1.6** Proposed catalytic cycle for reductive dehalogenation.

experience and knowledge in the field of organometallic chemistry rendered many organic groups slow to fully appreciate the number of well-described transition metal photocatalysts, their main use to this date being in inorganic and materials science. Recently, several groups have shown how a considered selection of photocatalysis has allowed the rapid expansion of methods that operate via both the reductive and oxidative quenching cycle (*vide infra*).

#### *Intramolecular Radical Additions*

Following the Stephenson group's initial report of dehalogenation, a subsequent report demonstrated that the radical formed via carbon-halogen bond reduction could efficiently participate in carbon-carbon bond forming processes.<sup>31</sup> By employing slightly modified conditions to that of the reductive dehalogenation, a range of bromomalonates (such as **18**) could be efficiently reduced and intramolecularly coupled to either indoles or pyrroles in good yield (typically >60%) (Figure 1.7). This approach provides a complementary alternative to previous

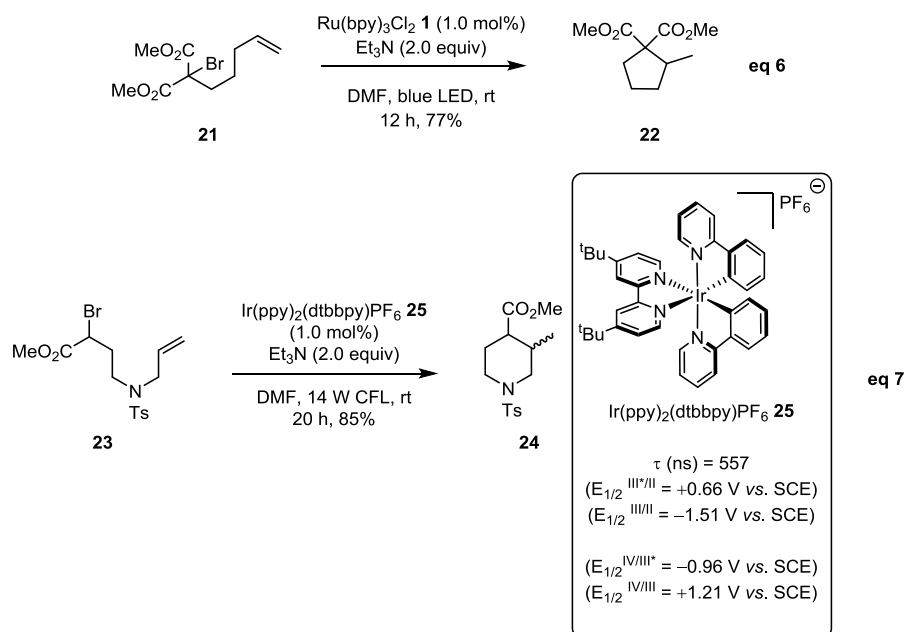
methods such as the oxidative  $\text{Mn}(\text{OAc})_3$  process<sup>32</sup> reported by Kerr and co-workers.<sup>33</sup> Formation of the reductive dehalogenation product from premature H-atom abstraction by the alkyl radical was minimized via the use of  $\text{Et}_3\text{N}$  as the reductive quencher. Other amine quenchers such as DABCO,  $\text{Me}_3\text{N}$  and  $(\text{HOCH}_2\text{CH}_2)_3\text{N}$  were efficient in generating the alkyl radical but resulted primarily in the formation of reduced indole **20**. Furthermore  $\text{Ph}_3\text{N}$  was completely selective for the desired product **19**, however it suffered from consistently low conversions (60%), even after prolonged reaction time (>48 h), presumably due to its increased oxidation potential when compared to trialkyl amines, limiting access to the  $\text{Ru}(\text{bpy})_3^+$  reductant.



**Figure 1.7** Intramolecular radical cyclization of electron rich heterocycles.

The reaction conditions developed for intramolecular radical coupling of electron rich heterocycles were directly applied for the analogous intramolecular addition to alkynes and alkenes.<sup>34</sup> A range of 5 or 6-exo cyclizations (Figure 1.8, eq 6) could be realized in good yield (69-99%) via initial reduction of the activated C–Br bond. Concurrent with the previous report of Macmillan,<sup>24</sup> it was found that the use of inexpensive, commercially available blue LEDs (1W,  $\lambda_{\text{max}} = 435 \text{ nm}$ ) greatly accelerated the reaction when employing  $\text{Ru}(\text{bpy})_3\text{Cl}_2$  as the photocatalyst. Although this method displays more mild initiation and greater functional group tolerance than typical radical processes, attempts to further improve the utility of this reaction by expanding the substrate scope to less activated bromides, such as  $\alpha$ -bromoesters, typically led only to recovery of starting material. Reasoning that a more strongly reducing photocatalyst was

required, I explored the use of  $\text{Ir}(\text{ppy})_2(\text{dtbbpy})\text{PF}_6^{24}$  ( $(E_{1/2}^{\text{III/II}} = -1.51 \text{ V vs. SCE})$ ) compared to  $\text{Ru}(\text{bpy})_3\text{Cl}_2$  ( $E_{1/2}^{\text{II/I}} = -1.33 \text{ V}$ ) and was now able to efficiently cyclize  $\alpha$ -bromo ester (such as **23**) and dibrominated cyclopropane substrates (Figure 1.8, eq 7) (*vide infra*). This was the first demonstration in the Stephenson group that judicious choice of photocatalyst can allow for altered reactivity and a broader substrate scope.



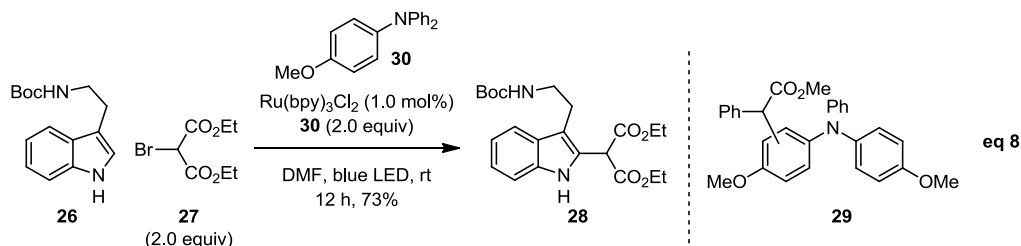
**Figure 1.8.** Expansion of intramolecular radical cyclization.

### *Intermolecular Radical Additions*

Attempts to apply this method to intermolecular coupling were consistently hampered by competitive H-atom abstraction from the trialkylamine by the malonyl radical, forming the reduced malonate. This pathway also leads to further reactive components derived from the amine, such as iminium ions and enamine species that, while detrimental to this reaction, were effectively utilized as discrete intermediates in other photochemical transformations (*vide infra*). This challenge was overcome by the use of 4-methoxy-*N,N*-diphenylaniline **30** as a reductive



quencher that cannot function as an efficient H-atom donor, showcasing the ability to drive selective reactivity through variation of either photocatalyst or quencher independently. Under the optimized conditions a range of electron-rich heterocycles, such as Boc-protected tryptamine **26** were efficiently coupled to diethylbromomalonate in good to excellent yield (typically 60-90%) (Figure 1.9).<sup>35</sup> However, significant challenges still remained as this methodology could not be applied to less activated C–Br bonds (such as methyl 2-bromo-2-phenylacetate) where typically only starting material was recovered. In this case, a postulated charge recombination between the triarylamine radical cation and the Ru(I) outcompetes C–Br bond reduction. Employing a more electron-rich triarylamine ((4-MeOPh)<sub>2</sub>NPh) successfully reactivated the reduction cycle. However, addition to the electron-rich amine (**29**), rather than the indole, dominated, highlighting the scope for further development of efficient photocatalyst quenchers. Ultimately the reduction of unactivated carbon-halogen bonds was accomplished by switching the photocatalyst to *fac*-Ir(ppy)<sub>3</sub>,<sup>4</sup> a strong excited state reductant ( $E_{1/2}^{IV/III*} = -1.73$  V vs. SCE) thus eliminating the requirement for an amine quencher.

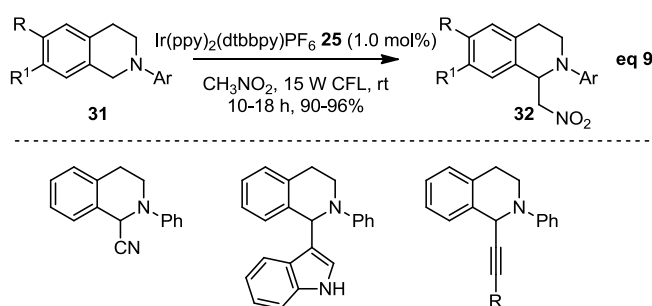


**Figure 1.9** Intermolecular radical coupling.

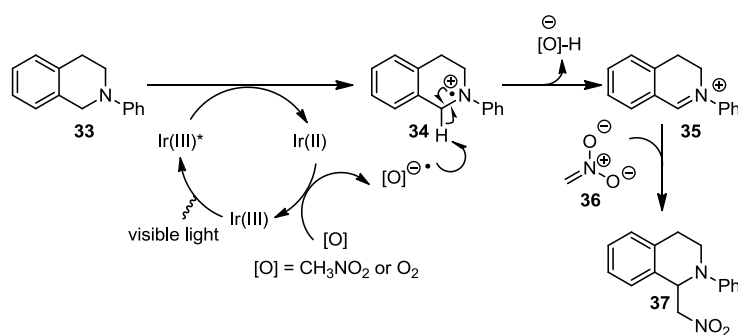
#### *Nucleophilic Addition to Iminium Ions Derived from Tetrahydroisoquinolines*

Seeking to harness iminium ions analogous to **17**, postulated as a detrimental side product in the debromination methodologies described above, the Stephenson group investigated their

competency as a reactive species in an oxidative aza-Henry process with nitroalkanes (Figure 1.10).<sup>36</sup> In this reaction manifold, the excited state of the photocatalyst (either  $\text{Ru}(\text{bpy})_3\text{Cl}_2$  or  $\text{Ir}(\text{ppy})_2(\text{dtbbpy})\text{PF}_6$ ) undergoes reductive quenching with a tetrahydroisoquinoline to generate the radical cation **34** and the reduced catalyst. Photocatalyst turnover is mediated by either adventitious oxygen and/or nitromethane to provide the ground state catalyst and a radical anion that may abstract a H-atom from the amine radical cation **34** to form the desired iminium **35** (Figure 1.11). Addition of the nitromethane-derived nitronate **36** to this iminium ion forms the observed product in good yield (90-96%) demonstrating this method comparable in efficiency to the analogous Cu-mediated process by Li and co-workers.<sup>37</sup>



**Figure 1.10** Aza-Henry and subsequent expansion to other nucleophiles.



**Figure 1.11** Proposed catalytic cycle for the aza-Henry reaction

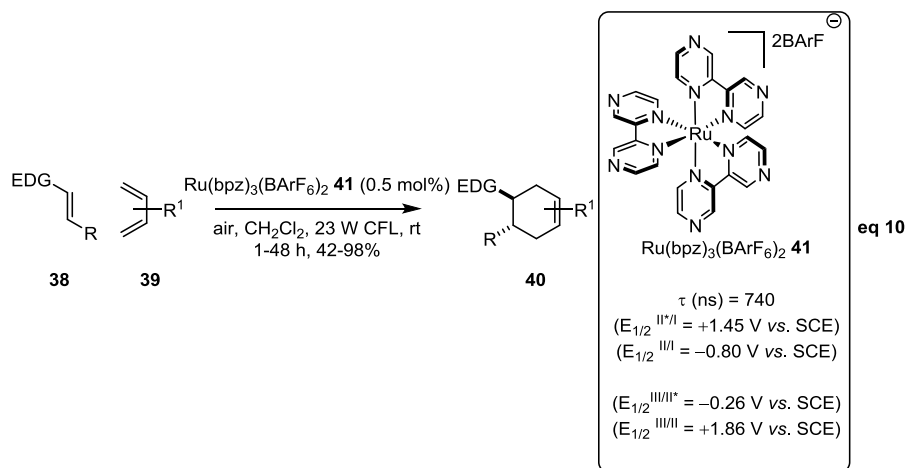
The general utility of this photoredox approach is exemplified by subsequent expansion by both the Stephenson group,<sup>38</sup> and numerous other research groups<sup>39</sup> to accomplish the

efficient addition of various nucleophiles such as, amongst others, cyanide, indole and alkynes.

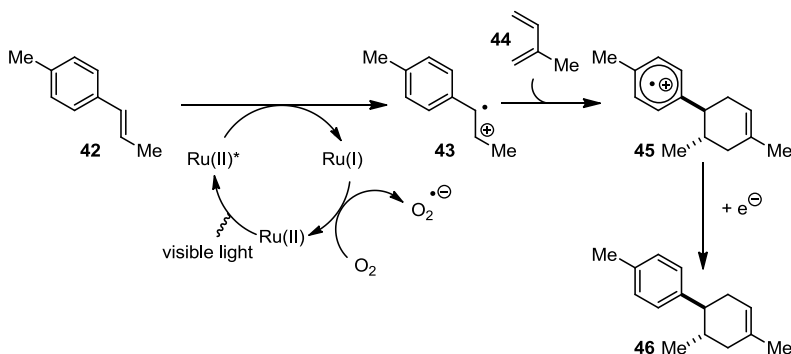
### *Radical Cation Diels-Alder Reactions*

The research group of Yoon has also studied the reactivity of tetrahydroisoquinolines under photoredox conditions, albeit in a formal reversal of polarity whereby an  $\alpha$ -amino radical adds efficiently to a range of  $\alpha,\beta$ -unsaturated ketones.<sup>40</sup> This report provides two notable conclusions, 1) the reaction is greatly enhanced by Brønsted acids, and 2) the primary operational mechanism is through radical propagation rather than photocatalyst turnover. The same group has also made significant contributions to the field via the development of a range of visible light-mediated cycloadditions,<sup>41</sup> perhaps the most striking example being the radical cation Diels-Alder cycloaddition.<sup>42</sup> In this methodology,  $\text{Ru}(\text{bpz})_3^{2+}$  ( $E_{1/2}^{\text{II}*/\text{I}} = +1.45 \text{ V vs. SCE}$ )<sup>43</sup> was employed as, unlike  $\text{Ru}(\text{bpy})_3\text{Cl}_2$  ( $E_{1/2}^{\text{II}*/\text{I}} = +0.77 \text{ V vs. SCE}$ ), it can directly oxidize **38** (+1.1 V) to the radical cation from its excited state. This important realization, coupled with the correct choice of counterion (BArF vs  $\text{PF}_6$ ) to allow solvation in less polar solvents, allowed a range of [4+2] cycloadditions to occur with low catalyst loadings (typically 0.5 mol%) and in good yield (typically 60-98%) (Figure 1.12). The mechanism is postulated to begin with excitation of  $\text{Ru}(\text{bpz})_3^{2+}$  ( $\lambda_{\text{max}} = 440 \text{ nm}$ ) to its excited state, which is capable of oxidizing **42** to its radical cation **43**. This species can then undergo intermolecular [4+2] cycloaddition and subsequently abstract an electron from **42** in a chain propagation sequence. Finally, the  $\text{Ru}(\text{bpz})_3^+$  is returned to the photoactive ground state  $\text{Ru}(\text{bpz})_3^{2+}$  by oxidation with oxygen (Figure 1.13). This elegant methodology displays both reversed intrinsic dienophile electronics, as well as overall regiochemical preference when compared to traditional Diels-Alder, making it highly complementary to previously reported methods. Equally impressive is the demonstration

of how effective photocatalyst selection and subsequent tuning of physical properties allows the realization of such a valuable method.



**Figure 1.12** Radical cation Diels-Alder.

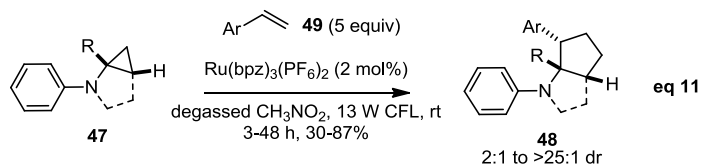


**Figure 1.13** Proposed catalytic cycle for radical cation Diels-Alder radical.

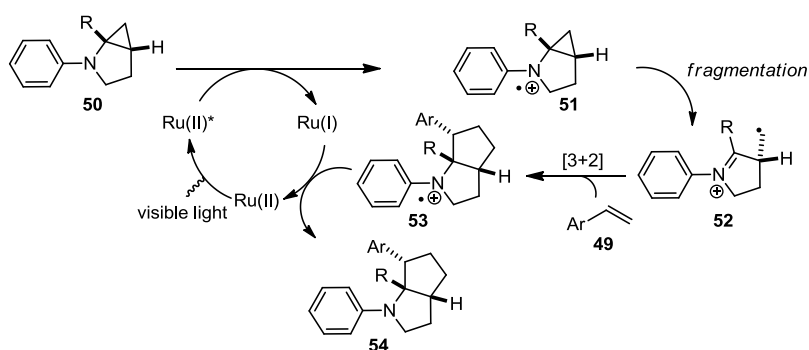
#### *Formal [3+2] Cycloadditions of Aminocyclopropanes*

Another methodology that successfully utilizes the strongly oxidizing  $\text{Ru}(\text{bpz})_3^{2+}$  excited state was recently reported by Zheng and co-workers for the intramolecular [3+2] cycloaddition of cyclopropylamines with alkenes.<sup>44</sup> In this system, concurrent with the tetrahydroisoquinoline methodology, the amine serves as the reactive species rather than the sacrificial quencher. The excited state photocatalyst initiates a cyclopropane ring opening by amine *N*-oxidation,

generating a  $\beta$ -carbon radical iminium ion that is competent in a formal [3+2] cycloaddition with a range of predominantly styrenyl alkenes (Figure 1.14 and 1.15). The authors postulate that the product following cycloaddition is reduced by Ru(I), returning the photocatalyst to the parent oxidation state and furnishing a range of cyclopentanes and fused bicyclic systems in good yield (typically >70% yield). The reaction scope with respect to the amine is limited to either secondary or tertiary amines bearing at least one aryl substituent. This method further showcases the ability to tune the reaction conditions via the choice of photocatalyst. The yield correlated well with the excited state oxidation potential with the weaker oxidants Ru(bpy)<sub>3</sub>Cl<sub>2</sub> ( $E_{1/2}^{\text{II}^*/\text{I}}$  +0.77 V vs. SCE) and Ir[(dtbbpy)(ppy)<sub>2</sub>](PF<sub>6</sub>)<sub>2</sub> ( $E_{1/2}^{\text{III}^*/\text{II}}$  +0.66 V vs. SCE) performing less efficiently than Ru(bpz)<sub>3</sub>Cl<sub>2</sub> ( $E_{1/2}^{\text{II}^*/\text{I}}$  +1.45 V vs. SCE).



**Figure 1.14** Formal [3+2] cycloaddition of amino cyclopropanes.

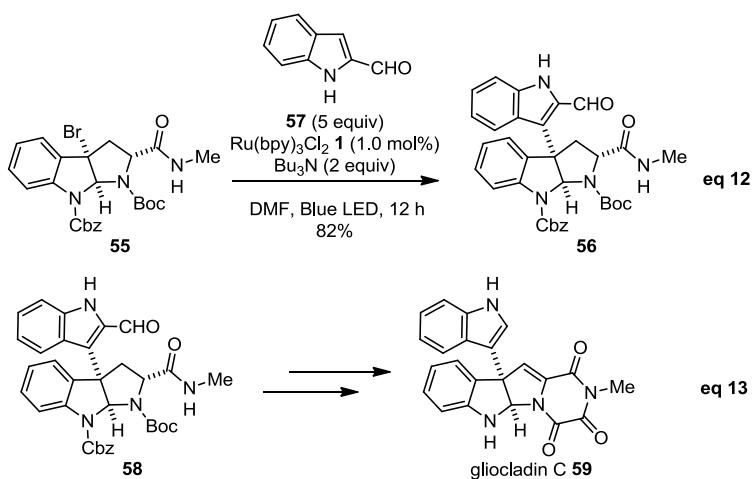


**Figure 1.15** Proposed mechanism of formal [3+2] cycloaddition of amino cyclopropanes.

### *Use of Reductive Quenching in Total Synthesis*

The use of the reductive quenching cycle within the Stephenson group returned to its

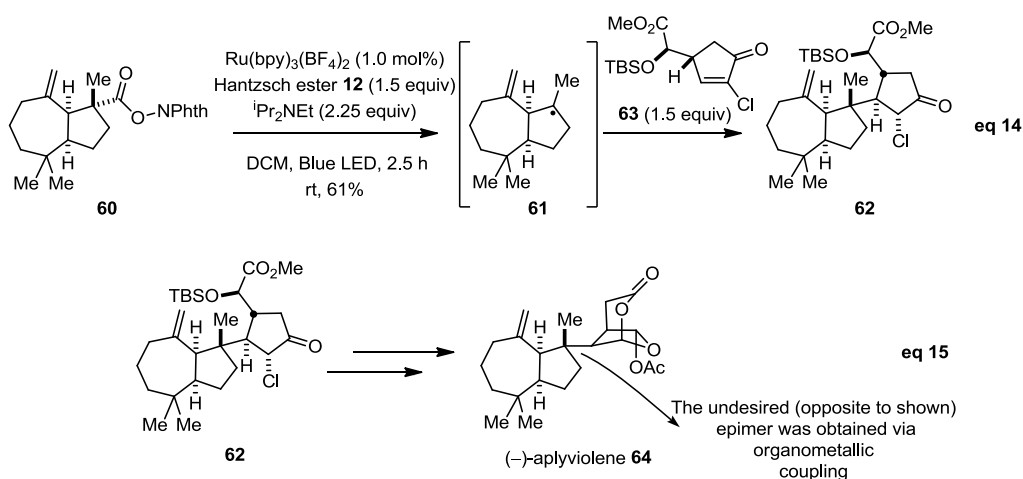
origins in complex molecule synthesis via its successful application to the synthesis of (+)-gliocladin C.<sup>45</sup> The key carbon-carbon bond was forged between the C-3 position of indole **57** and the elaborated bromopyrroloindoline radical generated by reductive dehalogenation of **55**. Ru(bpy)<sub>3</sub>Cl<sub>2</sub> was identified as the optimal photocatalyst in combination with Bu<sub>3</sub>N as the reductive quencher. Competing H-atom abstraction by the tertiary radical was minimized by the use of 5 equivalents of the readily available indole **57**, allowing the reaction to successfully operate on a multi gram scale in good yield (72%) with only 1 mol% of the photocatalyst (Figure 1.16). The efficiency of this reaction allowed the total synthesis of (+)-gliocladin C in 10 steps from commercially available Boc-D-tryptophan methyl ester in 30% yield and highlights the viability of photoredox catalysis to facilitate complex molecular synthesis.



**Figure 1.16** Key radical coupling en route to gliocladin C.

A similar strategy was elegantly employed by Schnerman and Overman in their concise second generation synthesis of (-)-aplyviolene.<sup>46</sup> The key transformation, diverging on the seminal work of Okada and Oda,<sup>21</sup> accomplishes the coupling of tertiary radical **61**, generated via decarboxylative reduction of a *N*-(acyloxy)phthalimide, to  $\alpha$ -chlorocyclopentenone **63** to

furnish adjacent quaternary and tertiary centers with high stereoselectivity. Optimization of this challenging transformation led to conditions reported by Gagné and coworkers for the reduction of glycosyl halides under anhydrous conditions.<sup>47</sup> Accordingly, 1 mol% of  $\text{Ru}(\text{bpy})_3(\text{BF}_4)_2$  with  $^i\text{Pr}_2\text{NEtN}$  (2.25 equiv) and Hantzsch ester **12** (1.5 equiv) in DCM provided **62** in 61% yield and importantly the opposite stereoselectivity to that obtained by means of an analogous organometallic coupling reaction (Figure 1.17). This method was later expanded to a general process for the synthesis of quaternary carbons from tertiary alcohols, with a range of electron deficient alkenes employed as the coupling partner.<sup>48</sup>



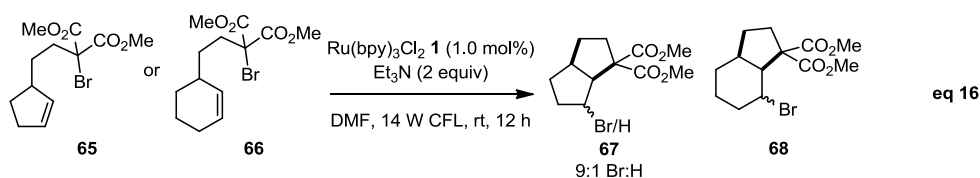
**Figure 1.17** Key radical coupling en route to aplyviolene.

## Oxidative Quenching

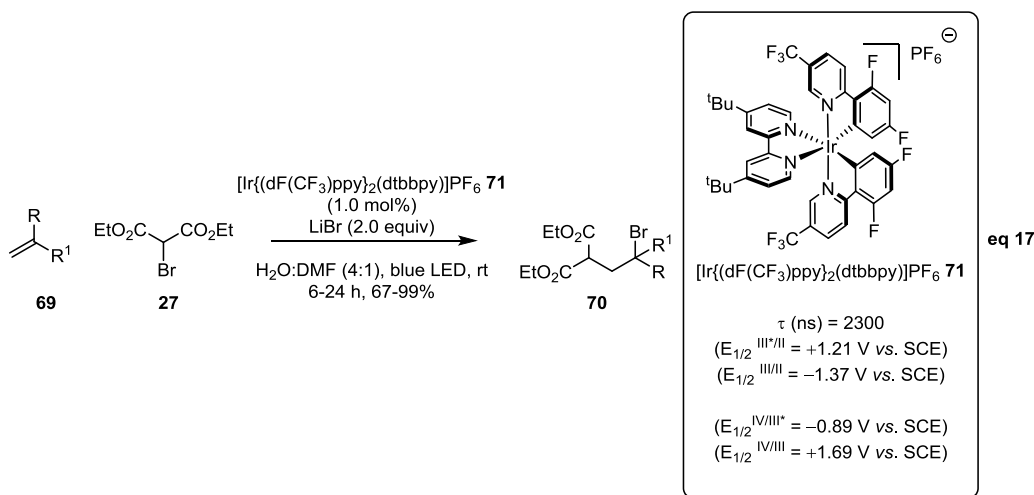
### Atom Transfer Radical Addition (ATRA)

The ability to efficiently utilize the oxidative quenching cycle was initially slower to develop than the corresponding reductive quenching pathway. During my investigation of reductive radical cyclizations I discovered that replacing terminal alkenes and alkynes for a tethered cyclopentene **65** or cyclohexene **66** provided atom transfer products (Figure 1.18).

Removal of the Et<sub>3</sub>N, which acts as both a reductive quencher and H-atom donor, provided exclusive atom transfer product.<sup>49</sup> Further optimization of this protocol, including the use of [Ir{dF(CF<sub>3</sub>)ppy}<sub>2</sub>(dtbbpy)]PF<sub>6</sub> as the photocatalyst greatly increased efficiency (Figure 1.19). It is postulated that [Ir{dF(CF<sub>3</sub>)ppy}<sub>2</sub>(dtbbpy)]PF<sub>6</sub> is optimal due to its extended excited state lifetime (2300 ns compared to 1100 ns for Ru(bpy)<sub>3</sub>Cl<sub>2</sub>) given their similar excited state reduction potentials ( $E_{1/2}^{IV/III^*} = -0.89$  V vs. SCE) compared to ( $E_{1/2}^{III/II^*} = -0.81$  V) for Ru(bpy)<sub>3</sub>Cl<sub>2</sub>.<sup>5</sup>



**Figure 1.18** Initial discovery of ATRA.



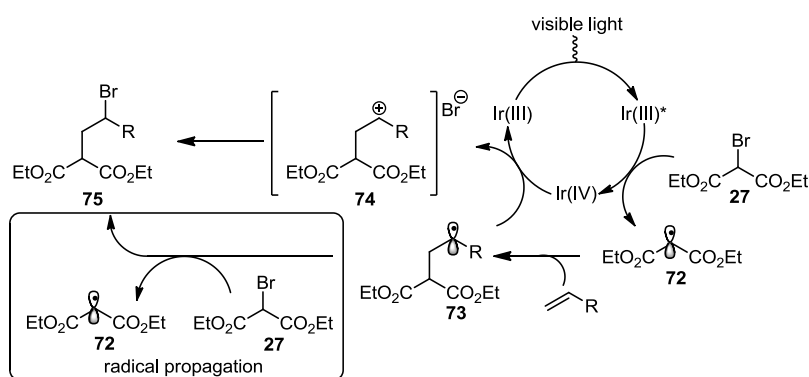
**Figure 1.19** Optimized ATRA protocol.

This optimized process now exclusively proceeds via oxidative quenching, whereby the excited state of the catalyst directly reduces the carbon-halogen bond of the substrate to produce the desired radical. Interestingly, mechanistic studies indicated it may further proceed via



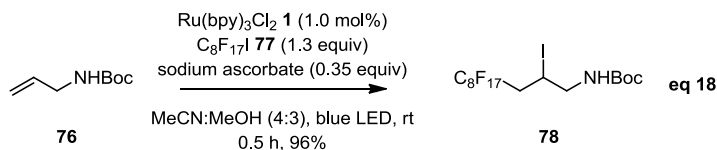
propagation, in a radical polar-crossover and/or via catalytic turnover to generate the same product (Figure 1.20). This mode of reactivity eliminates the requirement for a stoichiometric quencher and ultimately allowed the atom transfer radical addition (ATRA) coupling of a range of halogenated compounds to olefins under mild conditions, with typically excellent yields (Figure 1.20) (*vide infra*).

Although this methodology generally performed effectively for a range of halogenated substrates, it was not efficient for the addition of perfluoroalkyl iodides (such as **77**), a system



**Figure 1.20** Possible mechanisms for ATRA.

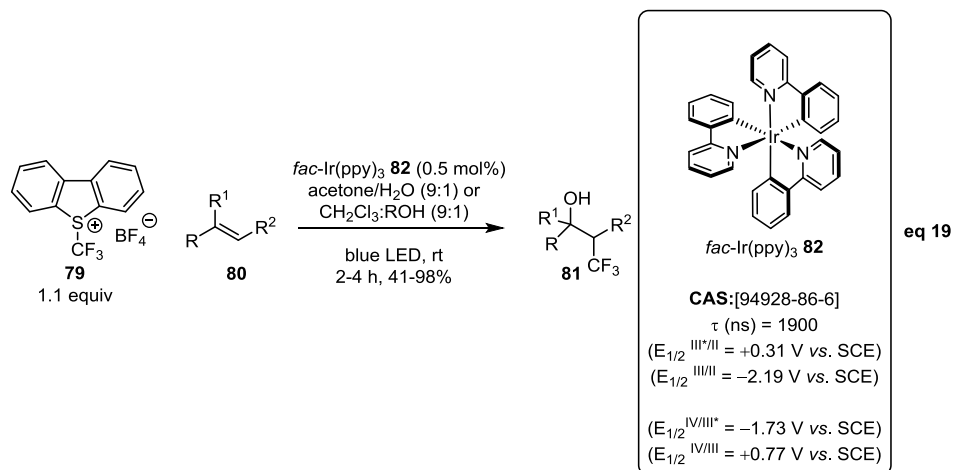
designed to achieve fluororous tagging. Therefore, I opted to return to reductive quenching of  $\text{Ru}(\text{bpy})_3\text{Cl}_2$ , but in this instance with sodium ascorbate as an electron donor instead of a tertiary amine. This effectively prevents the premature reduction of the perfluoroalkyl radical and allows the efficient ATRA tagging of a range of alkenes and alkynes such as **76** (Figure 1.21) (*vide infra*).<sup>50</sup>



**Figure 1.21** ATRA fluororous tagging.

## Oxytrifluoromethylation of Alkenes

Koike, Akita and co-workers recently published an elegant advancement of the ATRA methodology to oxytrifluoromethylation.<sup>51</sup> In this protocol, Unemoto's reagent is reduced by the excited state of the photocatalyst to generate the active CF<sub>3</sub> radical. Following radical addition and either oxidation or chain propagation, the carbocation intermediate (analogous to **74**) is trapped by a nucleophilic additive. The use of *fac*-Ir(ppy)<sub>3</sub>,<sup>4</sup> the strongest excited state reductant ( $E_{1/2}^{IV/III^*} = -1.73$  V vs. SCE) of the commonly employed photocatalysts, in combination with Unemoto's reagent ( $-0.25$  V vs. SCE)<sup>52</sup> proved critical for good reactivity. A range of styrenyl alkenes were efficiently trapped in good yield (typically >75% yield) by a range of alcohols, carboxylic acids, or water (Figure 1.22). Preliminary studies displayed moderate levels of diastereocontrol for the addition of simple alcohols to *trans*-stilbene (typically 5:1 dr), while the



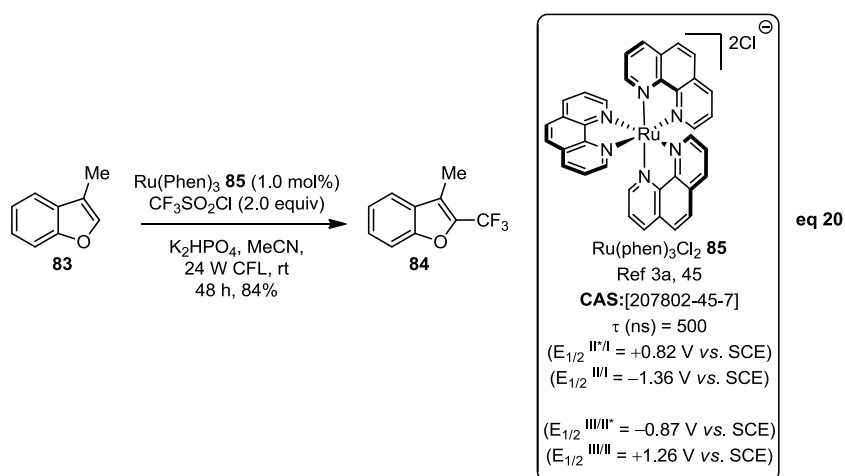
**Figure 1.22** Oxytrifluoromethylation of styrenyl alkenes.

application of this methodology to the synthesis of the antiestrogen drug Panomifene showcased its potential synthetic utility.

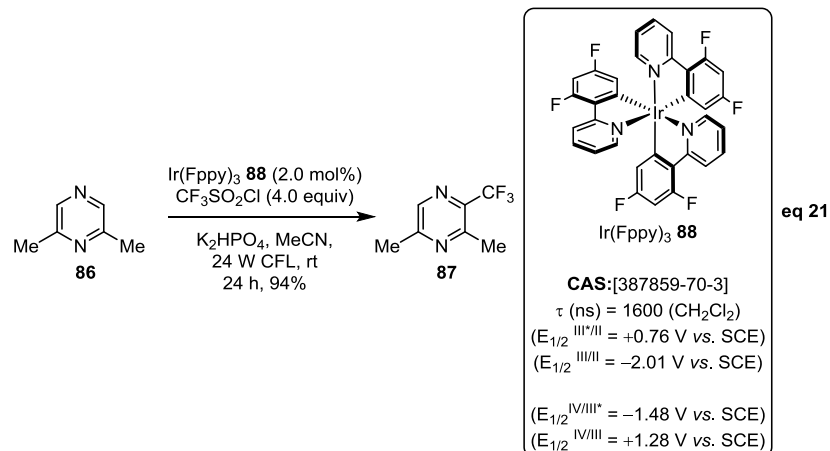
## Trifluoromethylation of Arene and Heteroarenes

Nagib and Macmillan developed an alternate method for the generation of the CF<sub>3</sub> radical

via photoredox catalysis, in this instance for the trifluoromethylation of arenes and heteroarenes.<sup>53</sup> Triflyl chloride (TfCl  $-0.18$  V vs. SCE), represents a comparatively cost effective and easily handled material when compared to other  $\text{CF}_3$  sources. In this protocol it was successfully employed to generate the  $\text{CF}_3$  radical via reduction by the excited state of the photoredox catalyst and fragmentation. Selective addition of this electron deficient radical to the most electron rich position of a range of arenes and heteroarenes provides, following rearomatization, pharmaceutically relevant building blocks in typically good yield ( $>30$



**Figure 1.23** Trifluoromethylation of electron rich heteroarenes using  $\text{Ru(phen)}_3\text{Cl}_2$ .

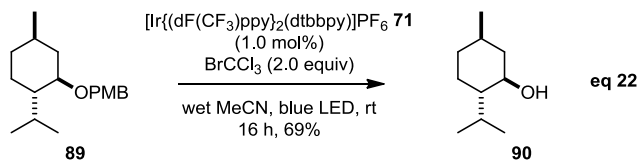


**Figure 1.24** Trifluoromethylation of electron poor heteroarenes using  $\text{Ir(Fppy)}_3$ .

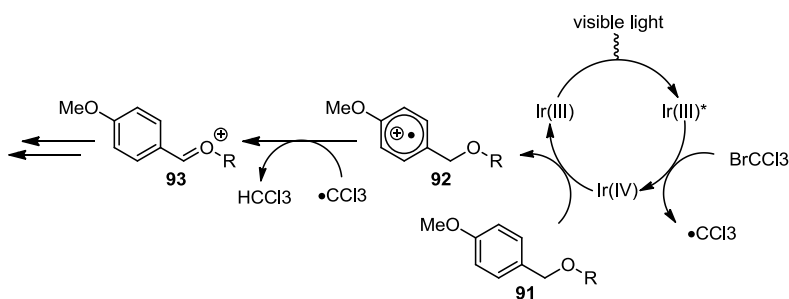
examples with >70% yield) and regiocontrol (Figure 1.23 and Figure 1.24). Ru(phen)<sub>3</sub> ( $E_{1/2}^{\text{III/II}^*} = -0.87 \text{ V vs. SCE}$ )<sup>54</sup> provided an optimal mix of reactivity and selectivity for electron rich heteroarenes, whereas Ir(Fppy)<sub>3</sub> (Fppy = (2,4-difluorophenyl)pyridine)<sup>55,56</sup> was employed for more difficult substrates, such as arenes and electron poor heteroarenes (such as **86**). The authors propose that the higher reactivity of Ir(Fppy)<sub>3</sub> is due to increased excited state lifetime when compared to Ru(phen)<sub>3</sub>.

### Deprotection of PMB Ethers

During the course of investigations into the functional group tolerance of the ATRA methodology my colleague, Dr. Joseph Tucker, discovered that PMB ethers (PMB = p-methoxybenzyl) were unstable to the reaction conditions, undergoing partial deprotection.



**Figure 1.25** Oxidative PMB deprotection.



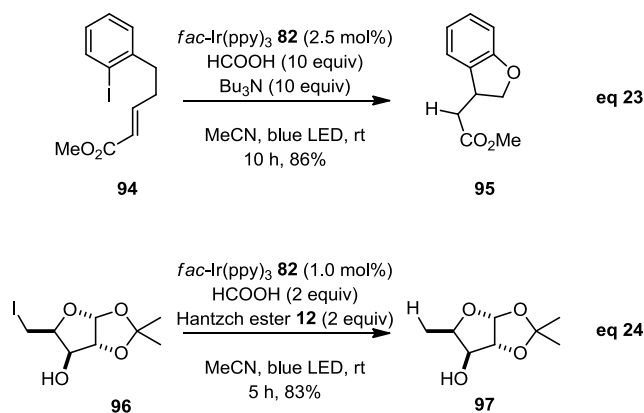
**Figure 1.26** Proposed catalytic cycle for the PMB deprotection.

Following optimization of reactions conditions, most notably running the reactions in wet acetonitrile with bromotrichloromethane, a range of PMB ethers could be selectively deprotected (Figure 1.25).<sup>57</sup> Functional group tolerance includes pivalate esters, substituted olefins, THP

acetals, Fmoc and Cbz groups. This mild catalytic PMB deprotection serves as an excellent alternative to typical methods that are performed with DDQ, CAN, SnCl<sub>4</sub>, AcOH, or Lewis acids. Similar to the mechanism for the photoredox catalyzed-ATRA reaction, BrCCl<sub>3</sub> oxidatively quenches \*Ir(III) to generate Ir(IV) and the trichloromethyl radical. Ir(IV) then oxidizes the PMB ether to generate a radical cation **92** and regenerate the ground state of the catalyst. The trichloromethyl radical may then abstract the benzylic H-atom of the PMB radical cation and produces an oxonium intermediate **93** that is intercepted by water and undergoes fragmentation to provide the free alcohol and anisaldehyde (Figure 1.26).

#### *Dehalogenation of Unactivated Alkyl, Alkenyl and Aryl Iodides*

The strong reductive power of *fac*-Ir(ppy)<sub>3</sub> from the excited state ( $E_{1/2}^{IV/III*} = -1.73$  V vs. SCE) returned me to earlier studies on reductive dehalogenation, considering the possibility of further expanding the scope to unactivated C–I bond reduction. By utilizing conditions similar to those employed by the Stephenson group during the initial entry into the area of photoredox catalysis, but harnessing the oxidative quenching cycle of *fac*-Ir(ppy)<sub>3</sub>, a range of unactivated alkyl, alkenyl and aryl iodides may be successfully reduced (Figure 1.27).<sup>58</sup> Consistent with the full suite of reductive protocols developed within the Stephenson group, the reaction displays excellent functional group compatibility, operational simplicity and proceeds in typically high yield (*vide infra*). It is important to note the reduction potentials of many of the substrates that are effectively reduced lie outside effective range of *fac*-Ir(ppy)<sub>3</sub>. This observation is of merit as it indicates that reduction potentials are an effective guide to available reactivity, but by no means the only defining factor. In this, and other instances,<sup>59</sup> the reaction seems to be driven by the rapid and irreversible C–H abstraction by the radical following C–I bond reduction.



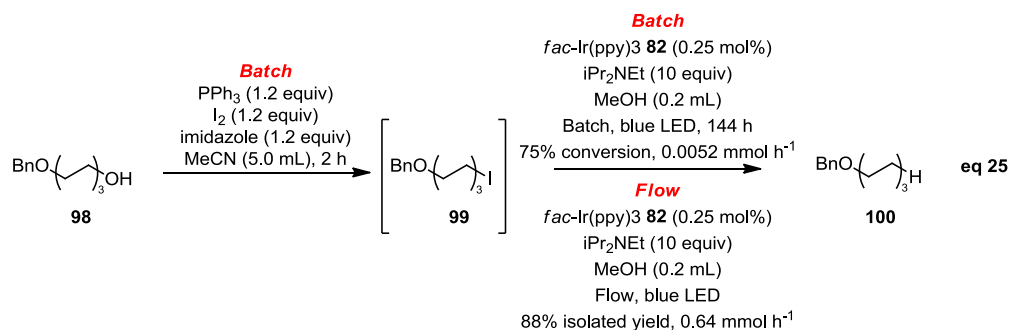
**Figure 1.27** Reduction of unactivated C–I bonds.

### *Batch to Flow Deoxygenation*

The efficiency of the dehalogenation described above, along with many other photoredox transformations, can be greatly improved by running the reaction in continuous flow. Seminal publications from Stephenson and Jamison,<sup>60</sup> Seeberger<sup>61</sup> and Gange<sup>62</sup> groups, demonstrated that by conducting photoredox reactions in flow, rather than in a batch setting, generally shorter reaction times, improved yields and lower catalyst loadings may be obtained. This is simplistically attributed to greater light penetration, owing to the increased surface-to-area ratio within a typical flow reactor when compared to a batch reaction.<sup>63</sup>

Attempts to merge the Stephenson group's photoredox method for the conversion of alcohols to halides<sup>64</sup> with the updated dehydroiodination protocol have, to this date, been largely unsuccessful. However, I have recently reported a batch to flow method for the efficient reduction of a range of primary and secondary alcohols.<sup>65</sup> This protocol proceeds by utilizing the Garegg-Samuelsson reaction<sup>66</sup> in batch, transforming the alcohol functionality to an iodide that then can be reduced in flow by the photocatalyst. The use of a flow system allows reduced  $\text{fac-Ir(ppy)}_3$  catalyst loading (0.25–0.5 mol% compared to 2.5 mol% in batch) and provides an

overall method that is competitive with deoxygenation strategies such as Barton-McCombie and others that typically employ tributyltinhydride or samarium diiodide (Figure 1.28).



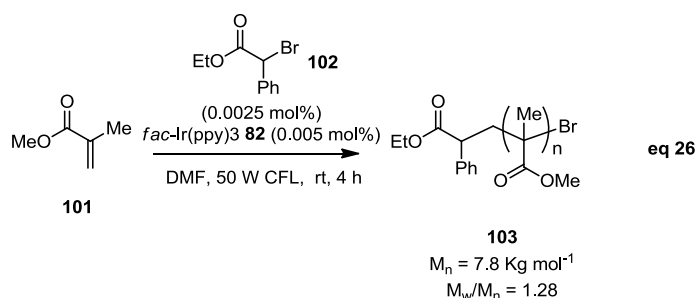
**Figure 1.28** Comparison of batch vs batch to flow deoxygenation.

### *Control of Living Polymerization*

An excellent application of the visible light-mediated ATRA reaction to living radical polymerization has recently been reported by Fors and Hawker.<sup>67</sup> In this system, atom transfer radical polymerization (ATRP) is initiated and controlled<sup>68</sup> via the use of *fac*-Ir(ppy)<sub>3</sub>. Reduction of alkyl bromide initiator **102**, by the excited state of the photocatalyst, and subsequent ATRA reaction with the monomer **101**, provides an overall cyclic process that can be turned on or off using visible light. This important feature allows excellent control over molecular weight, displaying low polydispersity while only employing between 0.005 and 0.13 mol% of *fac*-Ir(ppy)<sub>3</sub> (Figure 1.29). When compared to other traditional copper based ATRP processes this system displays excellent functional group tolerance, exemplified by the use of a free carboxylic acid monomer.

### **Conclusions and Future Prospects**

Building upon the pioneering investigations into the use of transition metal photoredox catalysts, others groups have successfully demonstrated their broader applicability in organic



**Figure 1.29** Application of visible light-mediated ATRA to living polymerization.

synthesis. While considerable research effort has been directed towards detailed investigations of previously reported transformations, many new modes of reactivity have also been outlined. This has in part been facilitated by leveraging the large number of reported transition metal photoredox catalysts, whose origins lie outside their direct use in organic synthesis. Concurrent with driving new reaction discovery, this review has highlighted that the breadth of available photocatalysts allow for astute reaction optimization, based on known photophysical properties. The ability for these photocatalysts to potentially operate as either strong oxidants or reductants, combined with the relatively large range of accessible potentials, is key to their expanded use in organic synthesis. This is particularly well illustrated by my continued research into the reduction of carbon-halogen bonds, where both modulation of the photocatalyst and mode of quenching has allowed reduction of increasingly more challenging substrates.

As the field continues to expand and mature, further novel applications that harness the versatile nature of this mode of single electron chemistry will undoubtedly be discovered. Equally important will be endeavors aimed at addressing some of the current limitations, for example the transition from one to two electron processes. Other areas with the potential for development include the further design and synthesis of catalysts with a similar range of electronic potentials, excited state lifetimes and chemical stability, which do not rely on costly



transition metals such as iridium and ruthenium. Another strategy to alleviate some of the cost pressures precluding wider use on scale may be analysis of catalyst recovery and re-use systems, particularly when coupled to the growing combination of photoredox and continuous processing methods. Given the frequent ambiguity over the precise mechanistic pathway for visible light mediated reactions, in depth mechanistic studies are also warranted, potentially providing insights into previous processes or directing new avenues for investigation.

## Chapter 2. Radical Reductive Dehalogenation and Reductive Cyclization

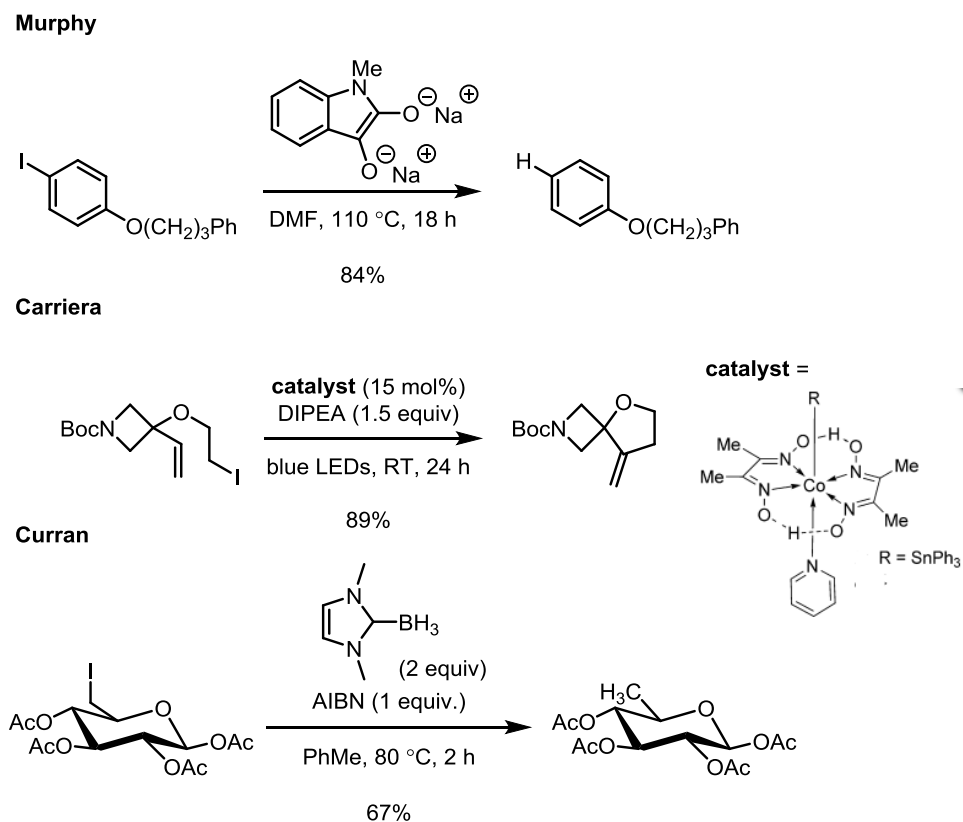
\*Portions of this chapter have been published in 1) Tucker, J. W.; Nguyen, J. D.; Narayanam, J. M. R.; Krabbe, S. W.; Stephenson, C. R. J. *Chem. Commun.* **2010**, 46, 4985; 2) Nguyen, J. D.; D'Amato, E. M.; Narayanam, J. M. R.; Stephenson, C. R. J. *Nature Chem.* **2012**, 4, 854; 3) Nguyen, J. D.; Reiss, B.; Dai, C.; Stephenson, C. R. J. *Chem. Commun.* **2013**, 49, 4352.

### Introduction

Free radicals are valuable reactive intermediates for synthetic chemists.<sup>69</sup> For instance, they provide a mechanism for the formation of C–C bonds which are difficult to synthesize via ionic mechanisms, including highly sterically encumbered bonds,<sup>70</sup> and, with thoughtful design of substrates, provide the potential for cascade reactions,<sup>71</sup> affording highly complex molecular structures in a single step.<sup>72</sup> However, many radical initiation systems require harsh reaction conditions, lack chemoselectivity and functional group tolerance, and are difficult to employ on preparative or industrial scales.<sup>73</sup> Formation of radical species often requires the use of stoichiometric amounts of toxic reagents, such as tributyltin hydride. Recently, the use of visible light-mediated photoredox catalysis to generate radical species has become popular, but the scope of radical precursors employed has been limited.

Conventional methods for reducing alkyl, alkenyl, and aryl iodide bonds<sup>74</sup> consist of metal-halogen exchange, a hydride source, or radical reductive dehalogenation. Reductions utilizing metal-halogen exchange<sup>75,76</sup> or a hydride source<sup>77</sup> commonly result in undesired side reactions, and are not functional group tolerant. This has led to the development of alternative

methods, which can be applied to the reductive dehalogenation of aryl halides and  $\alpha$ -halo carbonyls.<sup>78</sup> Radical reductive dehalogenation is by far the most commonly utilized method for the reduction of carbon-halogen bonds because the reaction conditions are typically mild and pH neutral, reactions times are short, and product yields are relatively high.<sup>74</sup> These characteristics have allowed radical chemistry to be utilized effectively for challenging bond constructions, such as those performed in the syntheses of hirsutene,<sup>79</sup> amaumomine,<sup>80</sup> and (+)-11,11'-dideoxyverticillin A.<sup>81</sup> However, the radical initiator or H-atom donor is typically toxic (organotin),<sup>82</sup> potentially explosive (azobisisobutyronitrile (AIBN) and peroxides),<sup>83</sup> unstable to air (samarium(II) iodide),<sup>84</sup> or pyrophoric (trialkylboranes).<sup>85,86</sup> In an attempt to avoid the toxicity associated with tributyltin hydride, other H-atom donors have been employed, such as



**Figure 2.1** Improved methods for radical reductive deiodination.

1,4-cyclohexadiene, triethylsilane, tris(trimethylsilyl)silane, triphenylgermane, thiols, and diphenylphosphine, but are less efficient, unstable, and/or expensive.

Recent efforts have been made to improve the process of radical reductive dehalogenation through replacement of the radical initiator and the development of new H-atom donors. Ground state neutral and charged electron donors utilized by Murphy<sup>87,88</sup> and the alkyl- and stannyl-cobaloxime catalysts developed by Careirra<sup>89</sup> have successfully generated alkyl radicals from alkyl iodides. In addition, several new H-atom donors have been introduced, such as *N*-heterocyclic carbene boranes by Curran<sup>90</sup> and water in the presence of Et<sub>3</sub>B<sup>91</sup> or Ti(III) salts.<sup>92</sup> Ultimately, the goal is to develop mild and efficient radical reductive dehalogenations protocol with broad functional group tolerance that utilizes an easy-to-handle catalyst along with an inexpensive and readily accessible H-atom donor.

## Background

During the last decade, several groups have illustrated the versatility of metal-based and organic photocatalysts<sup>93</sup> to carry out a variety of transformations<sup>26</sup> with beneficial applications in total synthesis.<sup>45</sup> A large portion of these reactions involve the generation of radical intermediates from activated carbon-halogen bonds including bromomalonates,<sup>31,35,49</sup> polyhalomethanes,<sup>38a,64,94</sup> electron-deficient benzyl bromides,<sup>19a</sup>  $\alpha$ -halo carbonyls,<sup>24,95</sup> and glycosyl bromides.<sup>47</sup> A major advantage of metal-based photocatalysts, such as [Ir{dF(CF<sub>3</sub>)ppy}<sub>2</sub>(dtbbpy)]PF<sub>6</sub> (**71**, Figure 1.19),<sup>3</sup> Ru(bpy)<sub>3</sub>Cl<sub>2</sub> (**1**, Figure 1.4),<sup>8</sup> Ir(dtbbpy)(ppy)<sub>2</sub>PF<sub>6</sub> (**25**, Figure 1.8),<sup>8</sup> and *fac*-Ir(ppy)<sub>3</sub> (**82**, Figure 1.22)<sup>4,8</sup> is the ease of tuning the complex to achieve desired redox potentials through modification of the ligands or replacement of the metal center.<sup>15</sup> These photocatalysts are capable of radical reductive cleavage of carbon-halogen bonds via direct reduction from the excited state of the catalyst (oxidative

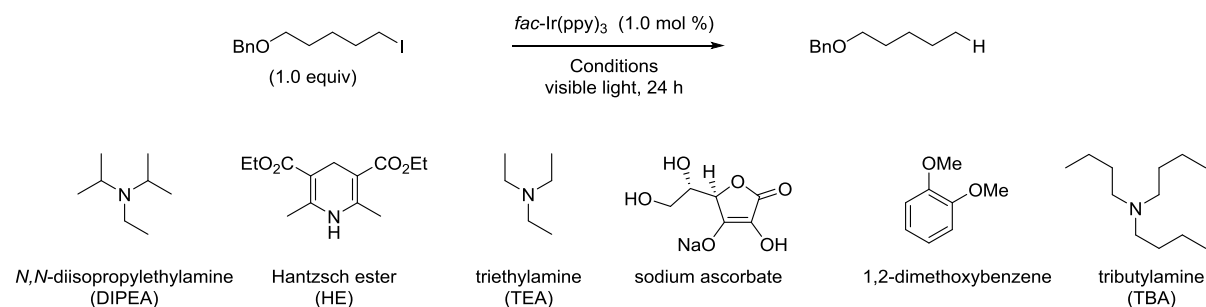
quenching), or via two single electron transfer (SET) processes, whereby the excited state is reduced by a sacrificial electron donor followed by reduction of the carbon-halogen bond (reductive quenching).

Previous work in the field of visible light-mediated photoredox catalysis has illustrated the advantages of being able to modify metal-based photocatalysts to achieve transformations initiated by SETs. For example, in previous studies I observed the intramolecular cyclization of bromomalonate-tethered  $\pi$ -systems via the reductive quenching of **1** (see Figure 1.4).<sup>34</sup> However,  $\alpha$ -bromoester analogs did not undergo cyclization using **1**, yet cyclized efficiently when the catalyst was replaced with **25** (see Figure 1.8). In this case, modification of the ligands and replacement of the metal center result in a more negative reduction potential for **25** (-1.51 V vs SCE)<sup>2</sup> than **1** (-1.31 V vs SCE),<sup>1</sup> which enabled the radical cyclization of  $\alpha$ -bromoesters onto  $\pi$ -systems. Another example of effective ligand substitution is seen when the 2-phenylpyridyl (ppy) ligands of **82** (see Figure 1.22) are replaced with 2-(2,4-difluorophenyl)-5-trifluoromethylpyridyl (dF(CF<sub>3</sub>)ppy) ligands to generate **71** (see Figure 1.19), a catalyst which has a more positive reduction potential ( $\text{Ir}^{4+} \rightarrow \text{Ir}^{3+}$ ) than **25** or **82**.<sup>21</sup> Although **1**, **25**, and **71** are calculated to have similar reductive abilities in their excited states via oxidative quenching, only **71** can efficiently produce atom transfer radical addition of CCl<sub>4</sub> onto olefins.<sup>50</sup> On the other hand, by replacing the 4,4'-di-*tert*-butyl-2,2'-dipyridyl (dtbbpy) ligand of **25** with another ppy ligand to make **82**, the reduction potentials of the catalyst become more negative. Specifically, the reduction potential for the  $\text{Ir}^{3+} \rightarrow \text{Ir}^{2+}$  couple changes from -1.51 V (vs SCE) for **25** to -2.19 V (vs SCE) for **82** and, likewise, the  $\text{Ir}^{4+} \rightarrow \text{Ir}^{3+*}$  couple becomes more negative (-0.93 V vs SCE for **25** to -1.73 V vs SCE for **82**).<sup>4</sup> The strong reduction potentials of **82** prompted my hypothesis that it could be utilized for a novel reductive dehalogenation protocol of alkyl, alkenyl, and aryl

iodides. I realized that the reduction of unactivated carbon-iodide bonds would be difficult to achieve with **82** due to the highly negative reduction potentials typical of alkyl, alkenyl, and aryl iodides (*e.g.* the reduction potential of *s*-butyl iodide has been measured to be between -1.61 V and -2.10 V vs SCE<sup>96,97</sup> and the reduction potential of iodobenzene has been measured to be between -1.59 V and -2.24 V vs SCE).<sup>98,99</sup> However, my investigation was encouraged by the successful utilization of the oxidative quenching of **82**<sup>100</sup> by MacMillan and co-workers to form benzyl radicals from electron-deficient benzyl bromides (Figure 1),<sup>22</sup> as well as by literature precedent indicating that **82** can be quenched by compounds with reduction potentials that have been measured to be more negative than -2.00 V (vs SCE).<sup>17</sup>

### **Reductive Hydrodeiodination**

My colleagues and I began our studies by screening conditions for the reduction of 5-iodopentyl benzyl ether, monitoring the conversion by <sup>1</sup>H NMR. Based on a previous protocol developed in the Stephenson group for the reductive dehalogenation of activated carbon-halogen bonds, I started optimization with *N,N*-diisopropylethylamine and Hantzsch ester in *N,N*-dimethylformamide (DMF).<sup>30</sup> A survey of solvents revealed that acetonitrile gave the best conversion over a 24 h reaction time, although the starting material was not fully consumed, even after increasing the equivalents of *N,N*-diisopropylethylamine and Hantzsch ester. Replacing *N,N*-diisopropylethylamine with other reductants, including triethylamine, sodium ascorbate, and 1,2-dimethoxybenzene, did not improve the conversion. However, tributylamine exhibited a significant increase in conversion, and upon exchanging the method of degassing from freeze-pump-thaw to argon sparging, full consumption of 5-iodopentyl benzyl ether was achieved in 24 h (Table 2.1).



entry	Conditions <sup>a</sup>	conversion (%) <sup>b</sup>	entry	Conditions <sup>a</sup>	conversion (%) <sup>b</sup>
1	DIPEA (1 equiv), HE (1 equiv), DMF	20	6	TEA (2 equiv), HE (2 equiv), MeCN	18
2	DIPEA (1 equiv), HE (1 equiv), DMSO	25	7	sodium ascorbate (2 equiv) HE (2 equiv), MeCN	40
3	DIPEA (1 equiv), HE (1 equiv), DCM	5	8	1,2-dimethoxybenzene (2 equiv) HE (2 equiv), MeCN	10
4	DIPEA (1 equiv), HE (1 equiv), MeCN,	33	9	TBA (2 equiv), HE (2 equiv), MeCN	90
5	DIPEA (2 equiv), HE (2 equiv), MeCN	45	<b>10<sup>c</sup></b>	<b>TBA (2 equiv), HE (2 equiv), MeCN</b>	<b>100</b>

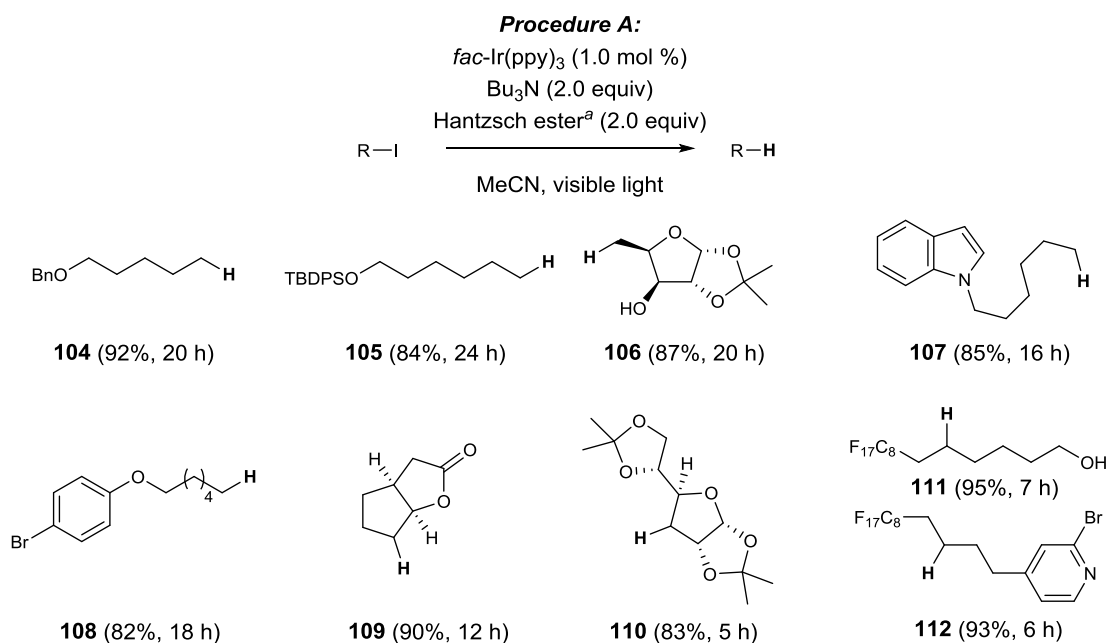
<sup>a</sup>Entries 1-9 were degassed by freeze-pump-thaw. <sup>b</sup>Conversion based upon <sup>1</sup>H NMR. <sup>c</sup>Reaction degassed for 0.5 h by sparging with Ar gas.

**Table 2.1** Optimization of hydrodeiodination of alkyl iodides.

The tributylamine and Hantzsch ester combination was employed with several primary and secondary iodides to give reduction products in good to excellent yields (Figure 2.2). This reduction protocol exhibits excellent functional group tolerance without affecting benzyl ethers, silyl ethers, acetals, lactones, or free alcohols. In addition, the chemoselective nature of the reaction allows for the reduction of alkyl iodides in the presence of aryl bromides.

Subsequently, I investigated the reactivity of aryl iodides. Reduction of *N*-(4-iodophenyl)-4-methylbenzenesulfonamide was successful with Procedure A, however, the reaction requires 52 h for full consumption of *N*-(4-iodophenyl)-4-methylbenzenesulfonamide. I

attempted to improve the reaction efficiency by replacing Hantzsch ester with formic acid, which is inexpensive and can be easily removed during work-up. Consequently, the reduction of *N*-(4-iodophenyl)-4-methylbenzenesulfonamide was complete in 20 h when five equivalents of tributylamine and five equivalents of formic acid were used. Erica D'Amato, an undergraduate

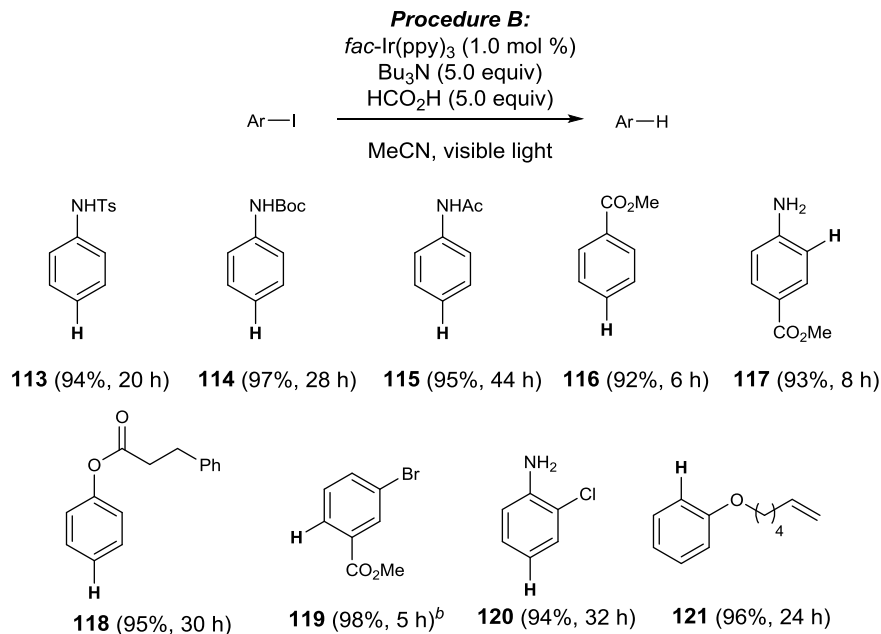


**Figure 2.2** Radical reductive hydrodeiodination of alkyl iodides.

student, and I tested these new conditions on several alkyl iodides, but all attempts led to low yields of the desired reduced compound. I discovered that employing Procedure B leads to a high degree of competitive substitution and elimination reactions with alkyl iodides that were not observed with Procedure A. In particular, secondary iodides provided substantial elimination product with Procedure B but is cleanly reduced with Procedure A. It is noteworthy that these reaction conditions afford the reduction of challenging electron-rich aryl iodides, making this a general protocol applicable to a wide range of substrates.

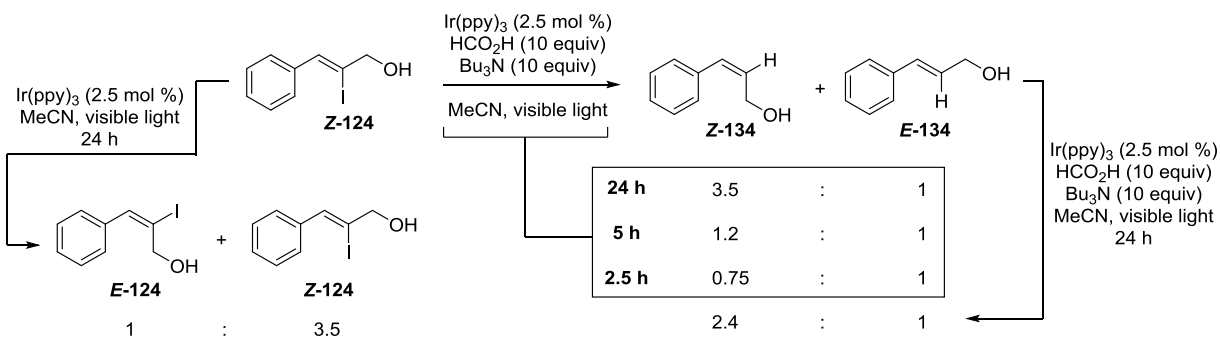
Procedure B was applied successfully to a diverse set of aryl iodides (Figure 2.3). The buffered reaction conditions were amenable to both acid and base labile groups, such as





**Figure 2.3** Radical reductive hydrodeiodination of aryl iodides.

carbamates, acetamides, and esters. Electron-rich and electron-deficient aryl iodides were all cleanly reduced, although electron-rich aryl iodides required longer reaction times. The reaction conditions also make it possible to reduce aryl iodides in the presence of aryl bromides, aryl chlorides, and distal olefins. To achieve the reduction of unactivated alkenyl iodides (Table 2.2, substrates **122** – **124**) in a reasonable timeframe, increasing the amounts of tributylamine and formic acid to 10 equivalents was required. Activated alkenyl iodides such as pure **Z-124**

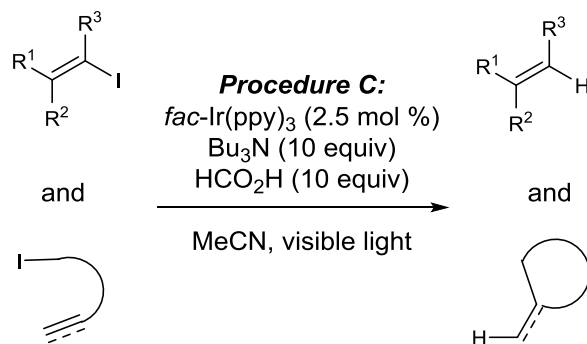


**Figure 2.4** *fac*-Ir(ppy)<sub>3</sub> mediated isomerization of cinnamyl alcohol substrates.

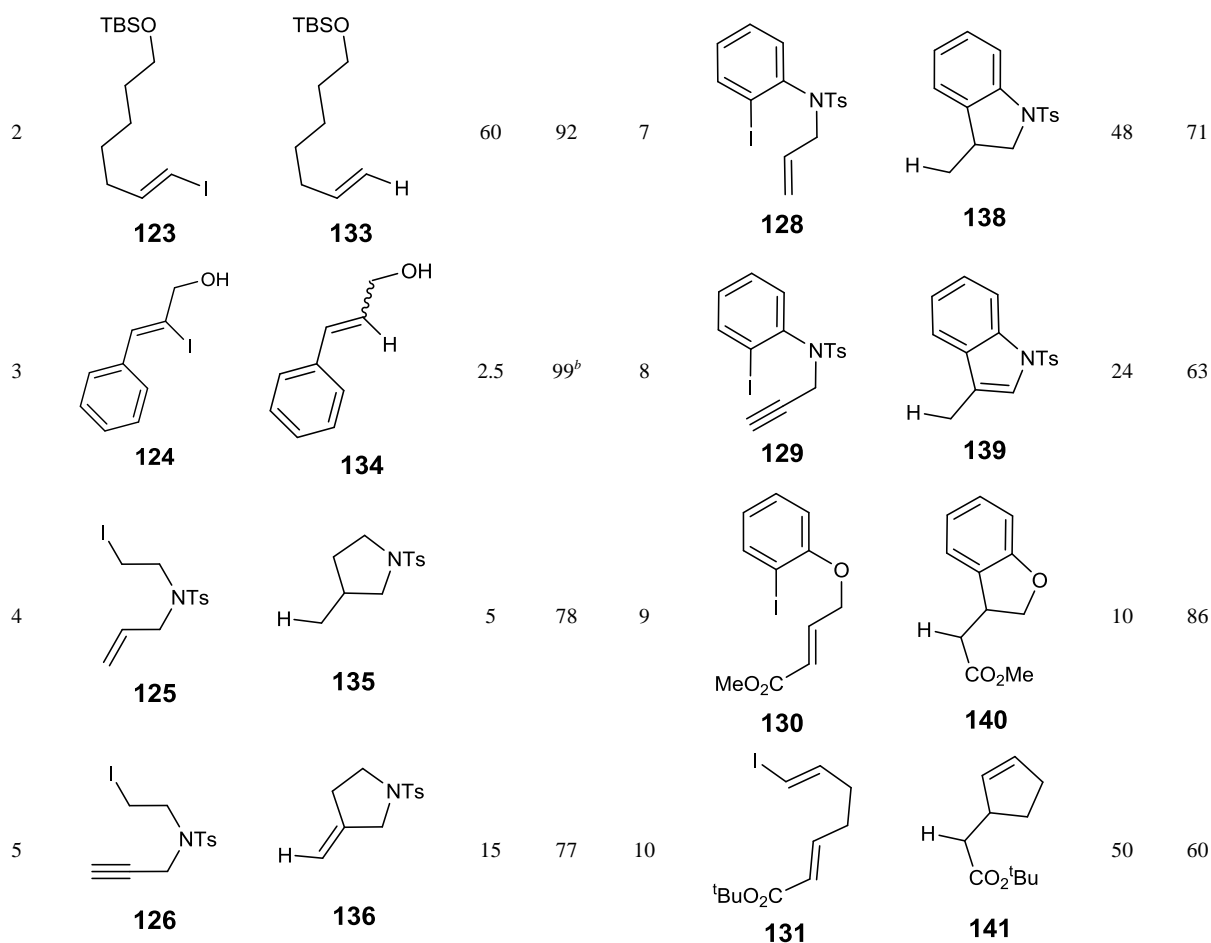
reduced very efficiently to produce a diastereomeric mixture of **134** with an *E/Z* ratio of 1:0.75 after 2.5 h.

In fact, I discovered that the *E/Z* ratio for the reduction of pure *Z*-**124** was dependent on the visible light irradiation time with longer reaction times favoring the *Z* isomer. The reduced product can undergo isomerization, which was observed when pure *E*-**134** was resubjected to the reaction conditions of Procedure C to give an *E/Z* ratio of 1:2.4 after 24 h. In addition, when the reaction is performed without the presence of tributylamine or Hantzsch ester, the isomerization of pure *Z*-**124** is observed to give an *E/Z* ratio of 1:3.5. Altogether, these results indicate that that *fac*-Ir(ppy)<sub>3</sub> is an excited state photosensitizer capable of isomerizing styrene derivatives.

In addition, Procedure C was found to be the most effective for intramolecular cyclizations of alkyl, alkenyl, and aryl iodide substrates (Table 2.2, substrates **125** – **131**). Surprisingly, all alkyl iodide substrates cyclized efficiently without any observable substitution



entry	substrate	product	time (h)	yield (%) <sup>a</sup>	entry	substrate	product	time (h)	yield (%) <sup>a</sup>
1			60	95	6			8	80 <sup>c</sup>
	<b>122</b>	<b>132</b>				<b>127</b>	<b>137</b>		



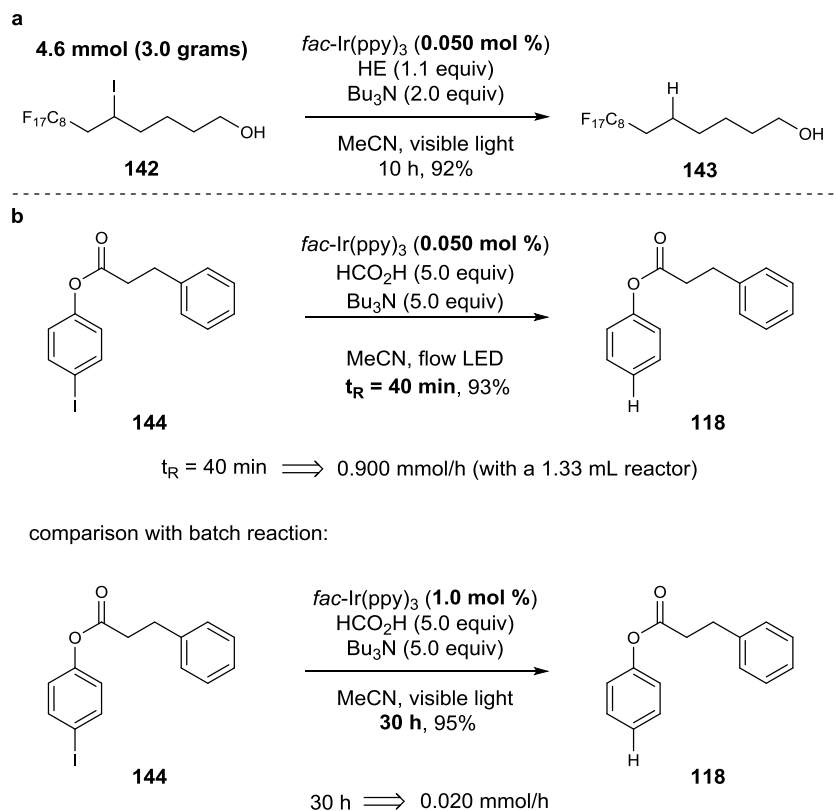
<sup>a</sup>Isolated yield after purification by chromatography on SiO<sub>2</sub>. <sup>b</sup>E/Z ratio = 1.3:1. <sup>c</sup>6.7:1 dr.

**Table 2.2** Reduction of alkenyl iodides and intramolecular reductive cyclizations.

or elimination products. These radical reductive cyclizations generated a wide scope of products, including pyrrolidines, tetrahydrofurans, indoles, indolines, dihydrobenzofurans, and carbocycles in moderate to high yields.

In order to demonstrate the efficacy of the reduction protocol on a preparative scale, the reduction of **142** (3.0 g, 4.6 mmol) was performed with lower catalyst loading and reduced amounts of Hantzsch ester. Gratifyingly, simultaneous scaling up of the reaction 750% and decreasing the catalyst loading by 2000% did not cause any significant loss of efficiency (Figure 2.5, top). Furthermore, when reductions are performed within a flow reactor, the reaction time

can be significantly shortened.<sup>60</sup> For example, the reduction of 0.60 mmol of **144** with 1.0 mol % of *fac*-Ir(ppy)<sub>3</sub> in a batch reactor required 30 h of light irradiation to afford 95% yield of **118** (Figure 2.5, bottom). However, by utilizing a 1.33 mL flow reactor with a residence time (*t*<sub>R</sub>) of



**Figure 2.5** Reductive hydrodeiodination utilizing flow chemistry.

40 min, the same scale reduction employing only 0.050 mol % of *fac*-Ir(ppy)<sub>3</sub> requires a 3 h reaction time to afford 93% yield of **118**, which indicates a turnover number (TON) of at least 1860.

### Deoxygenation Protocol

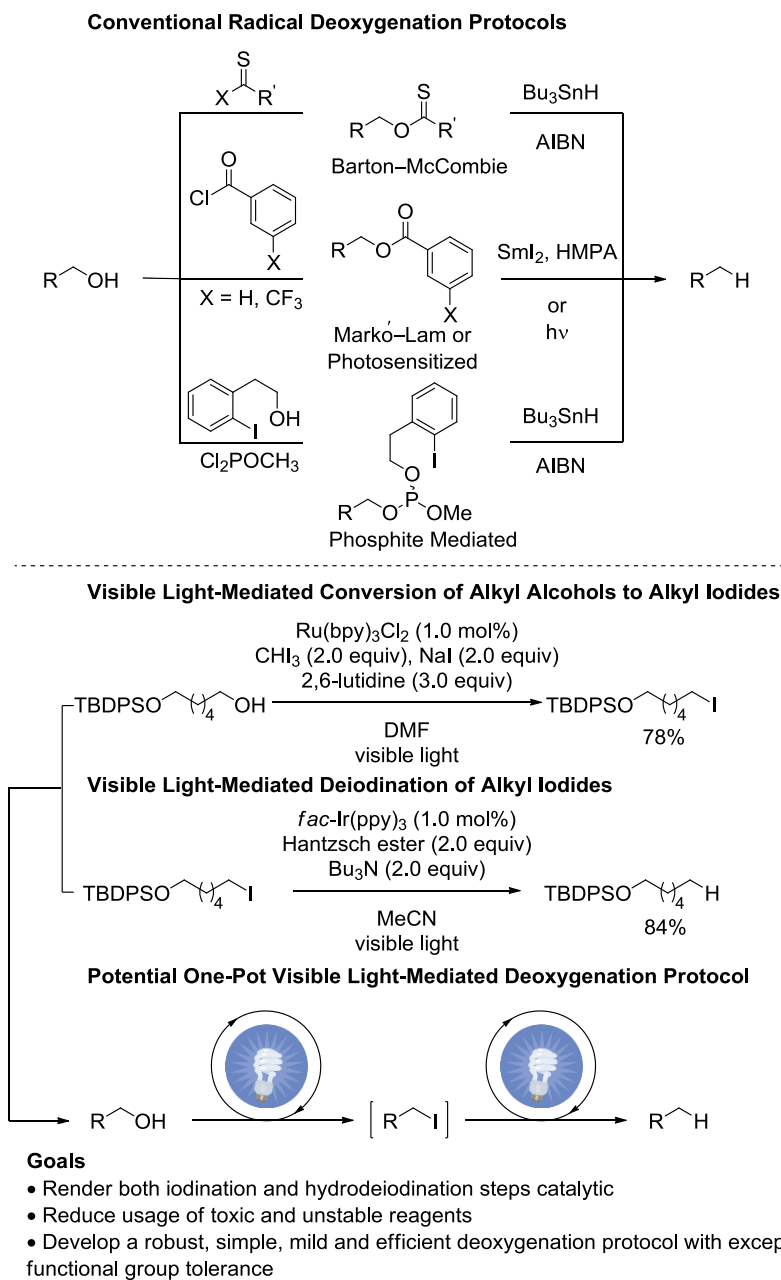
The deoxygenation of organic molecules is an important reaction in organic synthesis,<sup>101</sup> but remains one of the most difficult transformations due to the bond strength of the carbon-oxygen bond.<sup>102</sup> The most well-known and commonly utilized radical protocol for the removal of

hydroxyl groups from alkyl alcohols is the Barton–McCombie deoxygenation.<sup>103</sup> Alternative methods utilizing radical chemistry include benzoyl ester-mediated deoxygenations<sup>104</sup> and phosphite-mediated deoxygenations<sup>105</sup> (Figure 2.6, top). One aspect shared by all of the strategies mentioned above involve activation of the hydroxyl group to an intermediate, such as a xanthate, benzoate, or phosphite that can allow for a more facile cleavage of the carbon-oxygen bond. Recently, Miller has reported that phosphite-mediated deoxygenation can be utilized for molecular editing<sup>106</sup> via selective removal of hydroxyl groups from polyols such as erythromycin A.<sup>105b</sup> In an effort to develop a catalytic one-pot process for the removal of hydroxyl groups operating under mild conditions my colleagues and I investigated the possibility of utilizing visible light photoredox catalysis.<sup>107,108</sup>

Recently, the Stephenson group has developed a visible light-mediated technique for the conversion of primary and secondary alcohols to alkyl bromides and iodides<sup>64</sup> as well as a visible light-mediated method for the hydrodeiodination of alkyl, aryl, and alkenyl iodides (Figure 2.6, bottom).<sup>58</sup> In principle, the combination of these two reactions could be utilized to develop a visible light photoredox catalyzed one-pot deoxygenation in which the iodination and the reduction reactions occurred sequentially without an intermediate work-up or purification. Thus far attempts to achieve a streamlined “dual” photocatalytic deoxygenation in the Stephenson group have been unsuccessful largely due to the requirement for DMF in the iodination reaction, whereas the hydrodeiodination reaction is sluggish in DMF, and competitive reduction of iodoform requiring the use of much higher loading of electron donor/H-atom donor reagents.

However, the mild reaction conditions, functional group tolerance, and operational simplicity associated with photoredox catalysis bolstered my effort to design a novel strategy for deoxygenation. Due to the fact that the iodination procedure is more restricted in terms of the

reaction conditions, I explored alternative conditions for the conversion of alkyl alcohols to the alkyl iodides.

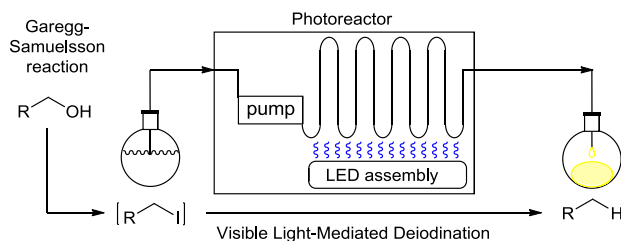


**Figure 2.6** Conceptual goal toward catalytic visible light-mediated deoxygenation.

By far the most common method for the conversion of alkyl alcohols to alkyl iodides is the Garegg–Samuelsson reaction.<sup>109</sup> In most cases, the addition of a primary or secondary alkyl

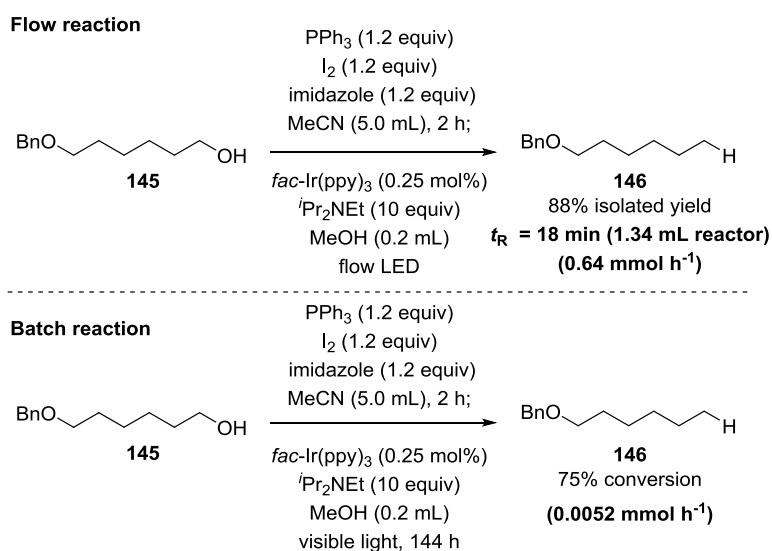
alcohol, triphenylphosphine, imidazole, and iodine in a variety of solvents efficiently converts alkyl alcohols to alkyl iodides with exceptional functional group tolerance. Therefore, my colleagues and I decided to investigate whether this reaction could be combined with the hydrodeiodination reaction that I had previously developed. I envisioned the overall transformation would involve the conversion the alkyl alcohol to the alkyl iodide and subsequent addition of the photocatalyst and electron-donor/H-atom donor reagents and light irradiation would cause reduction of the carbon-iodide bond.

The first step of this investigation involved finding a single solvent that could be applied to both reactions to avoid an intermediate work-up or solvent switch. Fortunately, the Garegg–Samuelsson reaction has been reported to be efficient in dichloromethane, DMF, tetrahydrofuran, acetonitrile (MeCN), and toluene,<sup>110</sup> while the visible light-mediated hydrodeiodination reaction is optimal in MeCN.<sup>58</sup> With a common solvent in hand I began to investigate the viability of developing a novel one-pot deoxygenation protocol. Substrate **145** is fully converted to an alkyl iodide in 2 h utilizing PPh<sub>3</sub>/I<sub>2</sub>/imidazole. The addition of Hantzsch ester (diethyl 1,4-dihydro-2,6-dimethyl-3,5-pyridinedicarboxylate) (2.0 equiv), tributylamine (2.0 equiv), and *fac*-Ir(ppy)<sub>3</sub> (1.0 mol%) is followed by 0.5 h of degassing with argon and light irradiation. After 72 h the reaction is incomplete and only a 50% conversion of the starting material to **146** is observed.



**Figure 2.7** Schematic for visible light-mediated one-pot deoxygenation protocol.

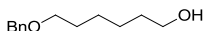
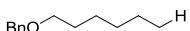
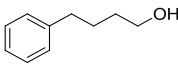
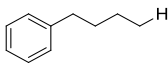


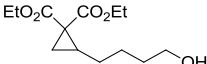
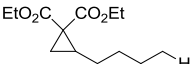
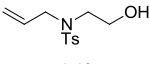
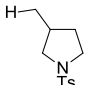
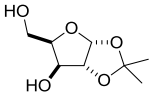
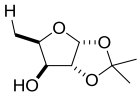
In order to increase the efficiency of the reduction step I decided to apply continuous flow chemistry based on the efficiency increase the Stephenson group has observed in previous reports.<sup>111</sup> Unfortunately, the presence of Hantzsch ester causes the reaction mixture to be heterogeneous and unsuitable for the flow reactor. Therefore, I decided to replace Hantzsch ester and tributylamine with *N,N*-diisopropylethylamine (*i*Pr<sub>2</sub>NEt) and include a small amount of MeOH to help the *i*Pr<sub>2</sub>NEt dissolve in the reaction mixture. A secondary advantage of flow processing was that catalyst loading could be lowered without loss of efficiency. Therefore, the design of this protocol involves the formation of an alkyl iodide in a batch reactor followed by the hydrodeiodination reaction performed in flow as shown in Scheme 2. Ultimately, a flow rate of 75  $\mu$ L/min in a 1.34 mL reactor (approximately an 18 minute residence time) with 0.25 mol% of *fac*-Ir(ppy)<sub>3</sub> (without degassing) gave full conversion of **145** to the reduced product **146** with an 88% isolated yield (Figure 2.8, top). This represents a 120 fold improvement to the conversion rate when compared to the same reaction in a batch reactor, which only provided 75% conversion of **145** to **146** after 144 h (Figure 2.8, bottom).

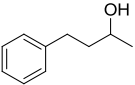
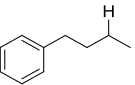

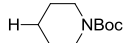
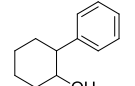
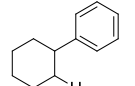
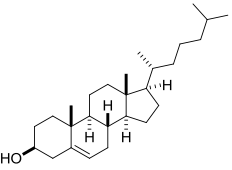
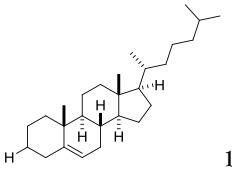


**Figure 2.8** Increased efficiency of deoxygenation in a flow reactor.



The combination of the Garegg–Samuelsson reaction, visible light-photoredox catalysis, and flow chemistry was applied successfully to the deoxygenation of a series of primary and secondary alcohols (Table 2.3). In case of substrate **153**, radical cyclization was observed rather than simple reduction due to the highly favorable *5-exo-trig* cyclization (entry 5). The functional group tolerance of this one-pot deoxygenation process is excellent with carbamates (entries 3 and 8), benzyl ethers (entry 1), esters (entry 4), acetals (entry 6), cyclopropanes (entry 4), and distal olefins (entry 10) unaffected throughout both steps. In addition, primary alcohols can be deoxygenated in the presence of secondary alcohols (entry 6) by selectively iodinating the primary alcohol over the secondary alcohol. Because the reduction step is tolerant of free alcohols, the secondary alcohol is maintained throughout the one-pot process. Overall, this strategy efficiently and mildly generates the desired product with distinct advantages over other

Entry <sup>a</sup>	substrate	product	yield <sup>b</sup>
1	 145	 146	88
2	 147	 148	74
3	 149	 150	81
4	 151	 152	87
5	 153	 154	85
6	 155	 156	70

7			78
	157	158	
8			76
	159	160	
9			67
	161	162	
10			72
	163	164	

---

<sup>a</sup>)Reaction Conditions: PPh<sub>3</sub> (1.2-2.5 equiv), I<sub>2</sub> (1.2-2.5 equiv), imidazole (1.2-5.0 equiv), MeCN (5.0-7.0 mL), *fac*-Ir(ppy)<sub>3</sub> (0.25-0.50 mol%), DIPEA (10-15 equiv), MeOH (0.2-0.5 mL), flow LED; <sup>b</sup>)% isolated yield after chromatography on SiO<sub>2</sub>; <sup>c</sup>)With toluene (2.0 mL).

**Table 2.3** One-pot deoxygenation of alkyl alcohols.

radical deoxygenation procedures resulting from the combination of photoredox catalysis and flow chemistry.

### Reductive Hydrodebromination

Although there has been progress toward the development of light-mediated methods for the reductive radical debromination of alkyl and aryl bromides from Lee,<sup>112</sup> Barriault,<sup>113</sup> and Jorgensen,<sup>114</sup> a general method that only relies upon visible light does not yet exist (Figure 2.9). My initial attempts toward the development of a method for reductive radical debromination focused on slightly heat the reaction to induce C–Br bond cleavage. This strategy seemed to work quite well for several substrates, but unfortunately was not a general solution (Figure 2.10). Jorgensen’s utilization of tris(trimethylsilyl)silane (TTMSS) and visible light was inefficient for the reductive radical debromination of aryl bromides and was only shown to be effective for a few examples of unactivated alkyl bromides. I hypothesized that it would be possible to increase



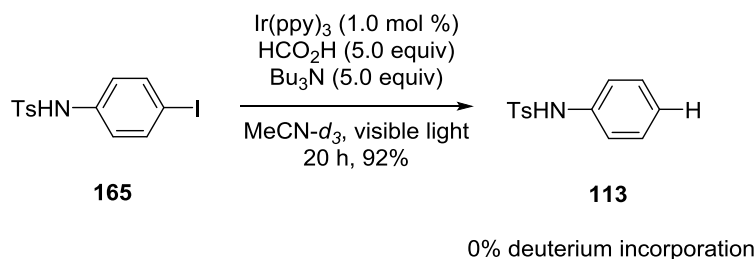
the efficiency of the TTMSS mediated reductive radical debromination of unactivated alkyl and aryl bromides in the presence of a photocatalyst such as Ir(ppy)<sub>2</sub>(dtbbpy)PF<sub>6</sub>. In fact, the presence of Ir(ppy)<sub>2</sub>(dtbbpy)PF<sub>6</sub> and reductive quencher (DIPEA) along with TTMSS has allowed for the efficient reductive radical debromination of unactivated alkyl and aryl bromides on a variety of substrates shown in Figure 2.11.

## Mechanism and Mechanistic Investigations

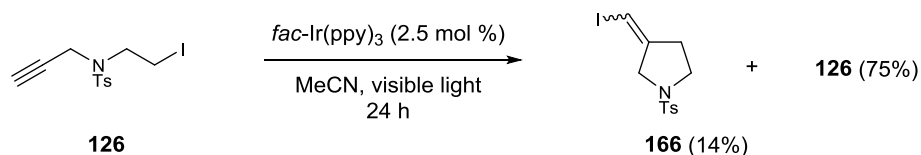
### Reductive Hydrodeiodination

The successful cyclization of substrates **125-131**, the more facile reduction of secondary alkyl iodides in comparison to primary alkyl iodides, and control reactions which reveal low conversions of the reduced products in the absence of *fac*-Ir(ppy)<sub>3</sub> and/or visible light irradiation strongly suggest a radical-based mechanism. In previous work,<sup>30</sup> the Stephenson group demonstrated that formic acid/trialkylamine and Hantzsch ester/trialkylamine combinations are effective electron donor/H-atom donor systems for the reductive dehalogenation of highly activated carbon-halogen bonds. The role of these reagents is likely unchanged for this protocol. However, to ensure that acetonitrile was not acting as an additional H-atom source, the reaction of compound **165** was performed in deuterated acetonitrile and no deuterium incorporation was observed (Figure 2.12).

Experimental evidence that the reaction was occurring through the oxidative quenching

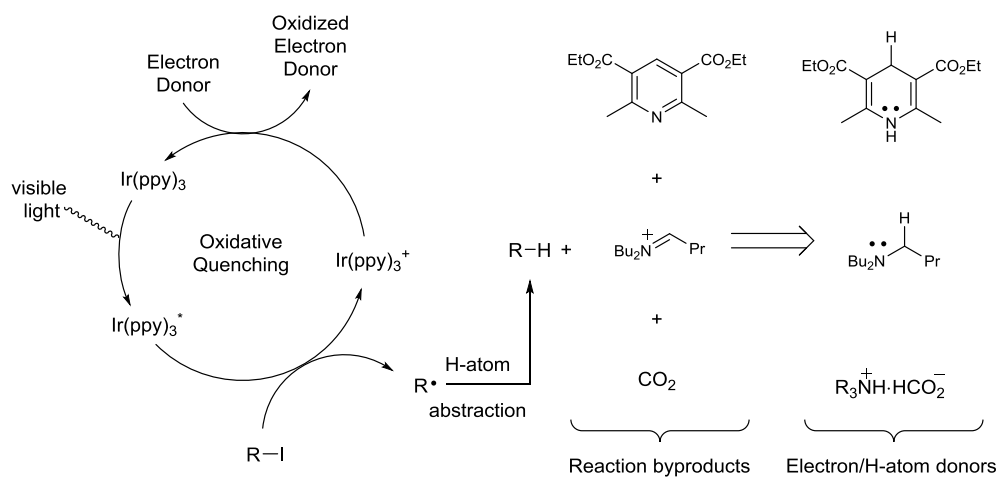


**Figure 2.12** Deuterium labeling study.



**Figure 2.13** Evidence for an operative oxidative quenching mechanism.

cycle of  $\text{fac-Ir(ppy)}_3$  was obtained when substrate **126** and 2.5 mol % of  $\text{fac-Ir(ppy)}_3$  in acetonitrile were subjected to visible light irradiation for 24 h to produce 14% of atom transfer product **166** along with 75% of recovered starting material (Figure 2.13). In the absence of tributylamine and formic acid, neither reductive quenching of  $\text{Ir(ppy)}_3^*$  nor the formation of **136** from **126** are possible, and oxidative quenching of  $\text{Ir(ppy)}_3^*$  leads to an atom transfer product via cyclization and I-atom abstraction by the vinyl radical. The low yield of **166** is most likely due to the fact that  $\text{fac-Ir(ppy)}_3$  only acts as an initiator for this reaction, because an electron donor is absent to effect catalyst turnover and the propagation chains are short-lived. Hence, the proposed mechanism of the reaction involves the oxidative quenching of  $\text{Ir(ppy)}_3^*$  by the alkyl, alkenyl, or



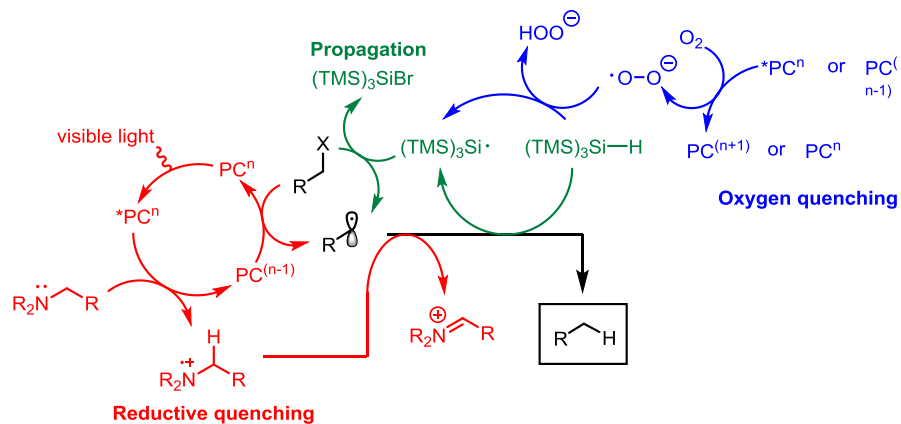
**Figure 2.14** Proposed mechanism for the radical reductive hydrodeiodination reaction.

aryl iodide. Reductive cleavage generates a carbon-centered radical that is capable of radical cyclization and/or H-atom abstraction from tributylamine, Hantzsch ester or formate. The

catalyst *fac*-Ir(ppy)<sub>3</sub> is regenerated from Ir(ppy)<sub>3</sub><sup>+</sup> by oxidation of tributylamine, Hantzsch ester, formate, or their oxidized forms (Figure 2.14).

### Reductive Hydrodebromination

My investigations regarding the radical reductive hydrodebromination reaction is currently in an early stage. Therefore, kinetic and mechanistic studies have not been fully developed in order to confidently propose a definitive mechanism. However, control studies have revealed that only partial substrate consumption is observed when any of the following components is absent: light irradiation, photocatalyst, TTMSS, DIPEA, or air. Based upon these results, the current proposed mechanism of the reaction relies upon a reductive quenching mechanism, a propagation mechanism, and an oxidative quenching mechanism that work cooperatively to provide a the same desired product.



**Figure 2.15** Proposed mechanism for the radical reductive hydrodebromination reaction.

### Conclusion

We initially developed a visible light photoredox-mediated radical reductive deiodination protocol capable of reducing alkyl, alkenyl, and aryl iodides utilizing the photocatalyst *fac*-tris[2-phenylpyridinato-C<sup>2</sup>,N]iridium(III) (*fac*-Ir(ppy)<sub>3</sub>) and tributylamine in combination with Hantzsch ester or formic acid. The generated radicals can also undergo intramolecular

cyclizations to provide a variety of cyclic scaffolds. The reaction protocol is characterized by mild conditions, low catalyst loading, high yields, and the utilization of inexpensive and accessible electron and H-atom donors. Functional group tolerance toward benzyl ethers, silyl ethers, free alcohols, acetals, lactones, esters, aryl bromides, aryl chlorides, carbamates, distal olefins, sulfonamides, tosylates, and acetamides is clearly illustrated. Moreover, the versatility and simplicity of the reduction protocol allows for easy scale-up, low catalyst loading, and short reaction times when the reaction is run in a flow reactor. These advancements signify the utility of photoredox catalysts in the area of radical chemistry, which has previously been dominated by tin,  $\text{SmI}_2$ , and trialkylboranes.<sup>115</sup> More recently, I have utilized TTMSS as an additive capable of efficiently reducing C–Br bonds of unactivated alkyl and aryl bromides. Altogether, these efforts clearly illustrate that the chemoselectivity of radical dehalogenation via photoredox catalysis can be controlled by careful choice of catalyst, solvent, and additives.

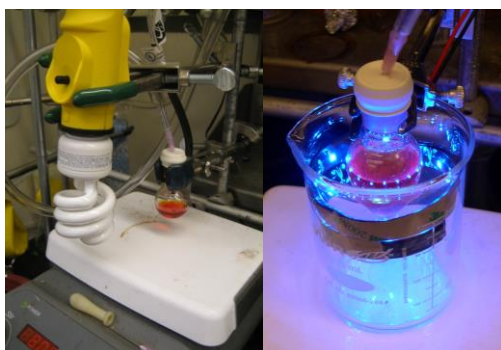
## Experimental

Chemicals were either used as received or purified according to *Purification of Common Laboratory Chemicals*. Glassware was dried in an oven at 150°C or flame dried and cooled under a dry atmosphere prior to use. All reactions were performed using common dry, inert atmosphere techniques unless otherwise noted. Reactions were monitored by TLC and visualized by a dual short wave/long wave UV lamp and stained with an ethanolic solution of potassium permanganate, *p*-anisaldehyde, or ceric ammonium molybdate. Column flash chromatography was performed using 230-400 mesh silica gel. NMR spectra were recorded on Varian Mercury 300, Varian Unity Plus 400, and Varian Mercury 400 spectrometers, Varian 500 spectrometers, and Varian 700. Chemical shifts for  $^1\text{H}$  NMR were reported as  $\delta$ , parts per million, relative to the signal of  $\text{CHCl}_3$  at 7.26 ppm. Chemical shifts for  $^{13}\text{C}$  NMR were reported as  $\delta$ , parts per million,

relative to the center line signal of the  $\text{CDCl}_3$  triplet at 77.0 ppm. Proton and carbon assignments were established using spectral data of similar compounds. The abbreviations s, br. s, d, dd, br. d, ddd, t, q, br. q, m, and br. m stand for the resonance multiplicity singlet, broad singlet, doublet, doublet of doublets, broad doublet, doublet of doublet of doublets, triplet, quartet, broad quartet, multiplet and broad multiplet, respectively. IR spectra were recorded on an Avatar 360 FT-IR or Perkin Elmer BX FT-IR spectrometers. Mass spectra were recorded at the Mass Spectrometry Facility at the Department of Chemistry of the Boston University in Boston, MA on a Waters Q-Tof API-US with ESI high resolution mass spectrometer or on a Waters® Micromass® AutoSpec Ultima™ with ESI high resolution mass spectrometer. Concentration refers to removal of solvent under reduced pressure (house vacuum at ca. 20 mmHg).

### Reaction Apparatus:

$\text{Ir}(\text{ppy})_2(\text{dtbbpy})\text{PF}_6$  catalyzed reactions were carried out under visible light irradiation by a 14W household compact fluorescent lamp (CFL) clamped ~15 cm from the reaction vessel.  $\text{Ru}(\text{bpy})_3\text{Cl}_2$  catalyzed reaction were carried out under irradiation by a 15 cm blue LED strip surrounding the reaction vessel. The  $\text{Ru}(\text{bpy})_3\text{Cl}_2$  photoredox system is also active under irradiation by the CFL.

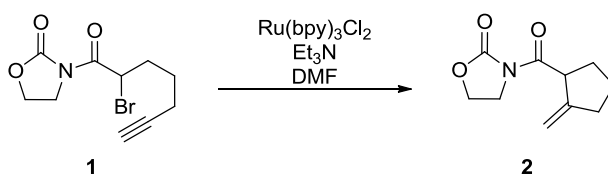


### General Procedure A: Photoredox Cyclization Reaction

A flame dried 10 mL round bottom flask is equipped with a rubber septum and magnetic stir bar



and is charged with photoredox catalyst (1.0  $\mu\text{mol}$ , 0.010 equiv), the corresponding halide (0.10 mmol, 1.0 equiv),  $\text{Et}_3\text{N}$  (0.20 mmol, 2.0 equiv) and DMF (5.0 mL). The mixture is degassed by the freeze-pump-thaw procedure, and placed in the respective irradiation apparatus. After the reaction is complete (as judged by TLC analysis), the mixture is poured into a separatory funnel containing 25 mL of  $\text{Et}_2\text{O}$  and 25 mL of  $\text{H}_2\text{O}$ . The layers are separated and the aqueous layer is extracted with  $\text{Et}_2\text{O}$  (2 X 50 mL). The combined organic layers are dried ( $\text{Na}_2\text{SO}_4$ ) and concentrated. The residue is purified by chromatography on silica gel, using the solvent system indicated, to afford the desired cyclized product.



**3-(2-methylenecyclopentanecarbonyl)oxazolidin-2-one, 2** (Scheme 1): According to General Procedure A, **1** (32 mg, 0.12 mmol),  $\text{Et}_3\text{N}$  (32  $\mu\text{L}$ , 0.23 mmol) and tris(2,2'-bipyridyl)ruthenium(II) chloride hexahydrate (0.90 mg, 1.2  $\mu\text{mol}$ ) in dry DMF (6.0 mL) afforded **2** (19 mg, 85%) as a colorless oil after purification by chromatography on  $\text{SiO}_2$  (15:85, AcOEt:hexane) (12 h reaction time).

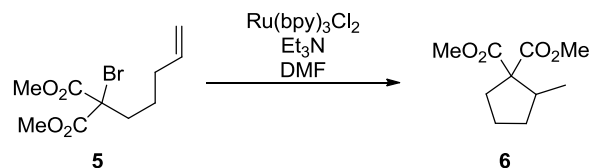
$R_f$  (AcOEt/hexane 30:70) 0.28;

IR (neat): 3363, 2958, 2922, 2355, 1776, 1697, 1479, 1386, 1222, 1106, 1041, 761  $\text{cm}^{-1}$ ;

$^1\text{H}$  NMR ( $\text{CDCl}_3$ , 500 MHz)  $\delta$  5.04 (dd,  $J = 4.2, 2.0$  Hz, 1 H), 4.90 (dd,  $J = 4.2, 2.0$  Hz, 1 H), 4.70 – 4.74 (m, 1 H), 4.21 (t,  $J = 8.0$  Hz, 2 H), 4.05 (dt,  $J = 8.0, 1.5$  Hz, 2 H), 2.37 – 2.49 (m, 2 H), 1.99 – 2.09 (m, 2 H), 1.86 – 1.73 (m, 1 H), 1.64 – 1.73 (m, 1 H);

$^{13}\text{C}$  NMR ( $\text{CDCl}_3$ , 75 MHz)  $\delta$  174.9, 153.4, 151.0, 108.1, 61.8, 47.1, 43.0, 33.8, 31.0, 25.1;

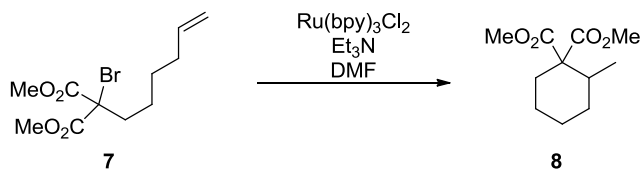
HRMS (ESI)  $m/z$  calculated for  $\text{C}_{10}\text{H}_{14}\text{NO}_3^+$  ( $[\text{M}+\text{H}]^+$ ) 196.0974, found 196.1053.



**Dimethyl 2-methylcyclopentane-1,1-dicarboxylate<sup>1</sup>, 6** (Table 1, Entry 1): According to General Procedure A, **5** (30 mg, 0.11 mmol), Et<sub>3</sub>N (31 μL, 0.22 mmol) and tris(2,2'-bipyridyl)ruthenium(II) chloride hexahydrate (0.80 mg, 1.1 μmol) in dry DMF (5.5 mL) afforded **6** (17 mg, 77%) as a colorless oil after purification by chromatography on SiO<sub>2</sub> (95:5, hexanes/EtOAc) (12 h reaction time).

*R<sub>f</sub>* (AcOEt/hexane 10:90) 0.31;

<sup>1</sup>H NMR (CDCl<sub>3</sub>, 500 MHz) δ 3.71 (s, 3 H), 3.70 (s, 3 H), 2.63 – 2.71 (m, 1 H), 2.40 – 2.46 (m, 1 H), 1.99 – 2.04 (m, 1 H), 1.88 – 1.94 (m, 1 H), 1.78 – 1.86 (m, 1 H), 1.51 – 1.59 (m, 1 H), 1.35 – 1.43 (m, 1 H), 0.97 (d, *J* = 7.0 Hz, 3 H).



**Dimethyl 2-methylcyclohexane-1,1-dicarboxylate<sup>2</sup>, 8** (Table 1, Entry 2): According to General Procedure A, **7** (89 mg, 0.30 mmol), Et<sub>3</sub>N (84 μL, 0.61 mmol) and tris(2,2'-bipyridyl)ruthenium(II) chloride hexahydrate (2.2 mg, 3.0 μmol) in dry DMF (15 mL) afforded **8** (45 mg, 69%) as a colorless oil after purification by chromatography on SiO<sub>2</sub> (50:50, DCM:Petroleum Ether) (12 h reaction time).

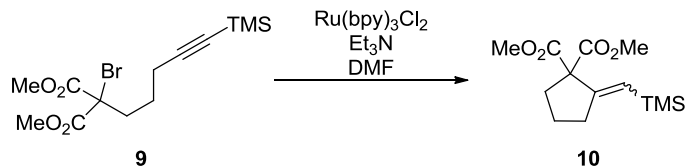
*R<sub>f</sub>* (AcOEt/hexane 15:85) 0.39;

<sup>1</sup>H NMR (CDCl<sub>3</sub>, 300 MHz) δ 3.73 (s, 3 H), 3.72 (s, 3 H), 2.29 – 2.35 (m, 1 H), 2.09 – 2.17 (m,

<sup>1</sup> *Chem. Commun.* **2008**, 2559.

<sup>2</sup> *Can. J. Chem.*, 1980, **67**, 555.

2 H), 1.89 – 1.97 (m, 1 H), 1.34 – 1.60 (br. m, 4 H), 1.01 (d,  $J = 7.2$  Hz, 3 H).



**Dimethyl 2-((trimethylsilyl)methylene)cyclopentane-1,1-dicarboxylate, 10** (Table 1, Entry 3):

According to General Procedure A, **9** (42 mg, 0.12 mmol), Et<sub>3</sub>N (33  $\mu$ L, 0.24 mmol) and tris(2,2'-bipyridyl)ruthenium(II) chloride hexahydrate (0.90 mg, 1.2  $\mu$ mol) in dry DMF (6.0 mL) afforded **10** (32 mg, quant.) as a colorless oil consisting of a 3:1 mixture of diastereoisomers after purification by chromatography on SiO<sub>2</sub> (99:1, Petroleum Ether:Et<sub>2</sub>O) (12 h reaction time).

Data for major diastereoisomer:

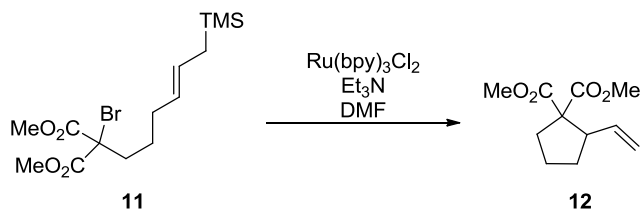
$R_f$  (AcOEt/hexane 5:95) 0.28;

IR (neat): 3077, 2954, 2861, 1747, 1436, 1255, 1133, 993, 915, 714  $\text{cm}^{-1}$ ;

<sup>1</sup>H NMR (CDCl<sub>3</sub>, 500 MHz)  $\delta$  5.76 (t,  $J = 2.0$  Hz, 1 H), 3.74 (s, 3 H), 3.73 (s, 3 H), 2.73 (t,  $J = 7.5$  Hz, 1 H), 2.56 (td,  $J = 7.5, 2.0$  Hz, 1 H), 2.48 (t,  $J = 7.0$  Hz, 1 H) 2.39 (t,  $J = 7.0$  Hz, 1 H), 1.69 – 1.76 (m, 2 H), 0.05 (s, 9 H);

<sup>13</sup>C NMR (CDCl<sub>3</sub>, 125 MHz)  $\delta$  171.4, 171.2, 170.2, 170.1, 154.7, 150.9, 133.9, 128.2, 125.8, 65.0, 63.3, 52.8, 52.6, 41.7, 41.0, 39.8, 39.7, 35.6, 32.9, 24.3, 24.0, 0.1, -0.3;

HRMS (ESI)  $m/z$  calculated for C<sub>13</sub>H<sub>22</sub>NaO<sub>4</sub>Si<sup>+</sup> ([M+Na]<sup>+</sup>) 293.1185, found 293.1217.



**Dimethyl 2-vinylcyclopentane-1,1-dicarboxylate, 12** (Table 1, Entry 4):

According to General Procedure A, **11** (40 mg, 0.11 mmol), Et<sub>3</sub>N (30  $\mu$ L, 0.22 mmol) and tris(2,2'-

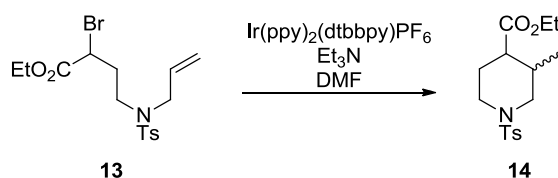
bipyridyl)ruthenium(II) chloride hexahydrate (0.80 mg, 1.1  $\mu\text{mol}$ ) in dry DMF (5.5 mL) afforded **12** (21 mg, 92%) as a colorless oil after purification by chromatography on  $\text{SiO}_2$  (99:1, Petroleum Ether: $\text{Et}_2\text{O}$ ) (12 h reaction time).

$R_f$  (AcOEt/hexane 5:95) 0.37;

IR (neat): 2887, 2861, 1747, 1443, 1255, 1223, 1082, 993, 876, 743, 682  $\text{cm}^{-1}$ ;

$^1\text{H}$  NMR ( $\text{CDCl}_3$ , 300 MHz)  $\delta$  5.72 – 5.84 (m, 1 H), 4.99 – 5.12 (m, 2 H), 3.73 (s, 3 H), 3.65 (s, 3 H), 3.24 (dt,  $J = 8.1, 7.5$  Hz, 1 H), 2.41 – 2.51 (m, 1 H), 2.04 – 2.13 (m, 1 H), 1.80 – 2.00 (m, 2 H), 1.60 – 1.73 (m, 2 H);

$^{13}\text{C}$  NMR ( $\text{CDCl}_3$ , 75 MHz)  $\delta$  172.6, 171.2, 137.6, 115.9, 64.3, 52.5, 52.1, 50.0, 33.9, 30.7, 23.1;



**Ethyl 3-methyl-1-tosylpiperidine-4-carboxylate, 14** (Table 1, Entry 5): According to General Procedure A, **13** (42.0 mg, 0.10 mmol),  $\text{Et}_3\text{N}$  (29  $\mu\text{L}$ , 0.20 mmol) and bis(2,2'-phenylpyridyl)(4,4'-ditertbutyl-2,2'-bipyridyl)iridium(III) hexafluorophosphate (0.90 mg, 1.0  $\mu\text{mol}$ ) in dry DMF (5.0 mL) afforded **14** (29 mg, 85%) as a colorless oil containing an inseparable mixture of diastereomers (1:1) after purification by chromatography on  $\text{SiO}_2$  (80:20, Hexanes: $\text{EtOAc}$ ) (20 h reaction time).

$R_f$  (AcOEt/hexane 80:20) 0.21;

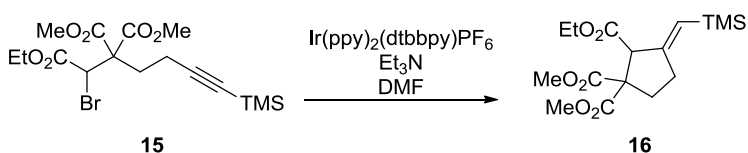
IR (neat): 2982, 2910, 1732, 1598, 1343, 1160, 1093, 757, 667  $\text{cm}^{-1}$ ;

$^1\text{H}$  NMR ( $\text{CDCl}_3$ , 400 MHz):  $\delta$  7.63 (d,  $J = 8.0$  Hz, 2 H), 7.62 (d,  $J = 8.0$  Hz, 2 H), 7.32 (d,  $J = 8.0$  Hz, 2 H), 7.31 (d,  $J = 8.0$  Hz, 2 H), 4.08 – 4.17 (m, 4 H), 3.80 (br. d,  $J = 10.4$  Hz, 1 H), 3.72 (ddd,  $J = 11.6, 4.0, 2.4$  Hz, 1 H), 3.54 (dd,  $J = 11.6, 5.6$  Hz, 1 H), 3.34 (dd,  $J = 10.4, 5.6$  Hz, 1

H), 2.51 (dd,  $J = 11.2, 3.2$  Hz, 1 H), 2.59 – 2.65 (m, 1 H), 2.47 (s, 3 H), 2.45 (s, 3 H), 2.25 – 2.31 (m, 1 H), 1.79 – 2.07 (m, 5 H), 1.23 – 1.29 (m, 10 H), 1.04 (d,  $J = 6.8$  Hz, 3 H), 0.93 (d,  $J = 6.0$  Hz, 3 H);

$^{13}\text{C}$  NMR ( $\text{CDCl}_3$ , 75 MHz):  $\delta$  174.2, 173.4, 143.7, 143.6, 133.4, 133.2, 129.8, 129.7, 127.8, 127.7, 127.1, 60.7, 60.5, 51.9, 51.1, 48.7, 45.5, 44.9, 43.5, 32.8, 31.0, 29.8, 28.3, 23.4, 21.7, 17.2, 14.3, 13.9;

HRMS (ESI)  $m/z$  calculated for  $\text{C}_{16}\text{H}_{23}\text{NaNO}_4\text{S}^+$  ( $[\text{M}+\text{Na}]^+$ ) 348.1245, found 348.1235.



**Dimethyl 2-vinylcyclopentane-1,1-dicarboxylate, 16** (Table 1, Entry 6): According to General Procedure A, **15** (82 mg, 0.19 mmol),  $\text{Et}_3\text{N}$  (54  $\mu\text{L}$ , 0.39 mmol) and bis(2,2'-phenylpyridyl)(4,4'-diterbutyl-2,2'-bipyridyl)iridium(III) hexafluorophosphate (1.7 mg, 2.0  $\mu\text{mol}$ ) in dry DMF (10 mL) afforded **16** (48 mg, 74%) as a colorless oil after purification by chromatography on  $\text{SiO}_2$  (95:5, Petroleum Ether: $\text{Et}_2\text{O}$ ) (12 h reaction time).

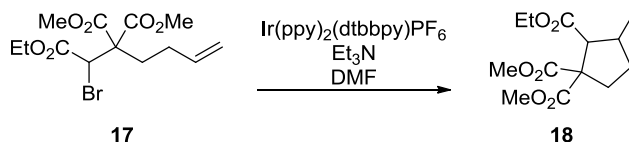
$R_f$  (AcOEt/hexane 10:90) 0.25;

IR (neat): 2954, 2360, 1736, 1628, 1434, 1246, 1220, 1152, 1110, 1029, 863, 842, 756 693  $\text{cm}^{-1}$ ;

$^1\text{H}$  NMR ( $\text{CDCl}_3$ , 400 MHz):  $\delta$  5.53 (s, 1 H), 4.06 – 4.15 (m, 3 H), 3.72 (s, 3 H), 3.70 (s, 3 H), 2.64 – 2.78 (m, 2 H), 2.33 – 2.45 (m, 2 H), 1.26 (t,  $J = 7.2$  Hz, 3 H), 0.13 (s, 9 H);

$^{13}\text{C}$  NMR ( $\text{CDCl}_3$ , 100 MHz):  $\delta$  171.0, 170.7, 169.9, 154.7, 126.3, 64.1, 61.1, 55.3, 53.1, 52.7, 33.6, 30.3, 14.0, -0.47;

HRMS (ESI)  $m/z$  calculated for  $\text{C}_{16}\text{H}_{27}\text{O}_6\text{Si}^+$  ( $[\text{M}+\text{H}]^+$ ) 343.1577, found 343.1583.



**2-ethyl 1,1-dimethyl 3-methylcyclopentane-1,1,2-tricarboxylate, 18** (Table 1, Entry 7):

According to General Procedure A, **17** (60 mg, 0.17 mmol), Et<sub>3</sub>N (48 μL, 0.34 mmol) and bis(2,2'-phenylpyridyl)(4,4'-ditertbutyl-2,2'-bipyridyl)iridium(III) hexafluorophosphate (1.6 mg, 2.0 μmol) in dry DMF (10 mL) afforded **18** (36 mg, 76 %) as a colorless oil containing an inseparable mixture of diastereomers (1:1) after purification by chromatography on SiO<sub>2</sub> (90:10), Hexanes:EtOAc (4 h reaction time).

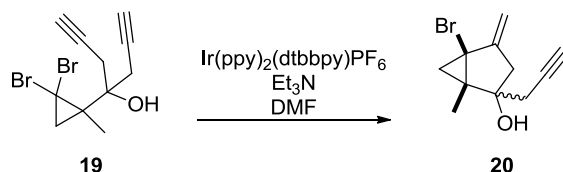
*R<sub>f</sub>* (AcOEt/hexane 10:90) 0.24;

IR (neat): 2982, 2955, 2909, 1736, 1642, 1436, 1374, 1275, 1201, 1030, 921, 720 cm<sup>-1</sup>;

<sup>1</sup>H NMR (CDCl<sub>3</sub>, 400 MHz): δ 4.09 – 4.16 (m, 4 H), 3.75 (s, 3 H), 3.72 (s, 3 H), 3.69 (s, 3 H), 3.67 (s, 3 H), 3.50 – 3.52 (d, *J* = 8 Hz, 1 H), 3.10 – 3.13 (d, *J* = 12 Hz, 1 H), 2.76 – 2.83 (m, 1 H), 2.43 – 2.55 (m, 2 H) 2.29 – 2.41 (m, 1 H), 2.13 – 2.21 (m, 2 H), 1.94 – 2.04 (m, 1 H), 1.83 – 1.91 (m, 1 H), 1.57 – 1.68 (m, 1 H), 1.22 – 1.27 (m, 8 H), 1.11 – 1.13 (d, *J* = 8 Hz, 3 H), 0.97 – 0.99 (d, *J* = 8 Hz, 3 H);

<sup>13</sup>C NMR (CDCl<sub>3</sub>, 100 MHz): δ 172.7, 172.0, 170.7, 63.8, 60.6, 57.7, 52.9, 52.5, 38.1, 34.5, 32.3, 19.4, 14.1.

HRMS (ESI) *m/z* calculated for C<sub>13</sub>H<sub>20</sub>NaO<sub>6</sub><sup>+</sup> ([M+Na]<sup>+</sup>) 295.1158, found 295.1167.



**5-bromo-1-methyl-4-methylene-2-(prop-2-yn-1-yl)bicyclo[3.1.0]hexan-2-ol,<sup>3</sup> 20** (Table 1,

Entry 8): According to General Procedure A, **19** (68 mg, 0.12 mmol), Et<sub>3</sub>N (33 μL, 0.24 mmol)

and bis(2,2'-phenylpyridyl)(4,4'-ditertbutyl-2,2'-bipyridyl)iridium(III) hexafluorophosphate (2.4 mg, 2.4  $\mu$ mol) in dry DMF (6.0 mL) afforded **20** (25 mg, 89 %) as a colorless oil containing a 1:1 mixture of diastereoisomers after purification by chromatography on SiO<sub>2</sub> (95:5, Petroleum Ether:Et<sub>2</sub>O) (12 h reaction time).

Diastereoisomer 1:

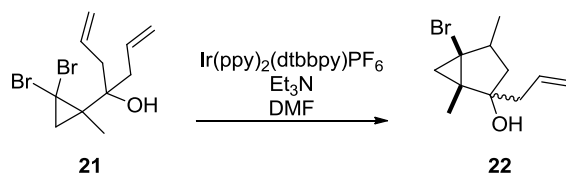
$R_f$  (AcOEt/hexane 10:90) 0.29;

<sup>1</sup>H NMR (CDCl<sub>3</sub>, 500 MHz):  $\delta$  5.15 (d,  $J = 2.5$  Hz, 1 H), 4.91 (d,  $J = 2.5$  Hz, 1 H), 2.67 (t,  $J = 15.5$  Hz, 2 H), 2.31 (dd,  $J = 16.5, 2.5$  Hz, 1 H), 2.09 – 2.17 (m, 3 H), 1.74 (d,  $J = 6.0$  Hz, 1 H), 1.34 (s, 3 H), 1.13 (d,  $J = 6.0$  Hz, 1 H);

Diastereoisomer 2:

$R_f$  (AcOEt/hexane 10:90) 0.25;

<sup>1</sup>H NMR (CDCl<sub>3</sub>, 500 MHz):  $\delta$  5.29 (s, 1 H), 5.01 (s, 1 H), 2.62 (dt,  $J = 17.0, 2.5$  Hz, 1 H), 2.45 (dt,  $J = 17.0, 2.5$  Hz, 1 H), 2.36 (s, 2 H), 2.07 (s, 1 H), 1.96 (s, 1 H), 1.45 (d,  $J = 6.5$  Hz, 1 H), 1.39 (s, 3 H), 1.19 (d,  $J = 6.5$  Hz, 1 H);



**2-allyl-5-bromo-1,4-dimethylbicyclo[3.1.0]hexan-2-ol**<sup>3</sup>, **22** (Table 1, Entry 9): According to General Procedure A, **21** (56 mg, 0.17 mmol), Et<sub>3</sub>N (49  $\mu$ L, 0.35 mmol) and bis(2,2'-phenylpyridyl)(4,4'-ditertbutyl-2,2'-bipyridyl)iridium(III) hexafluorophosphate (3.5 mg, 1.7  $\mu$ mol) in dry DMF (8.5 mL) afforded **22** (34 mg, 81 %) as a colorless oil after purification by chromatography on SiO<sub>2</sub> (99:1, Petroleum Ether:Et<sub>2</sub>O) (12 h reaction time).

<sup>3</sup>Chem. Lett. **1994**, 1757.

Diastereoisomer 1:

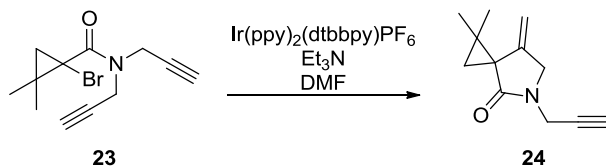
$R_f$  (AcOEt/hexane 5:95): 0.25;

$^1\text{H NMR}$  ( $\text{CDCl}_3$ , 300 MHz):  $\delta$  5.76 – 5.90 (m, 1 H), 5.11 – 5.15 (m, 2 H), 2.65 – 2.78 (m, 1 H), 2.38 (dd,  $J = 13.0, 7.4$  Hz, 1 H), 2.18 (dd,  $J = 13.0, 7.4$  Hz, 1 H), 1.58 – 1.66 (m, 2 H), 1.31 (s, 3 H), 1.07 (d,  $J = 6.3$  Hz, 3 H), 0.86 – 1.00 (m, 3 H), 0.69 (d,  $J = 6.6$  Hz, 1 H).

Diastereoisomer 2:

$R_f$  (AcOEt/hexane 5:95): 0.19;

$^1\text{H NMR}$  ( $\text{CDCl}_3$ , 500 MHz):  $\delta$  5.80 – 5.88 (m, 1 H), 5.14 – 5.18 (m, 2 H), 2.46 (dd,  $J = 14.0, 7.0$  Hz, 1 H), 2.35 – 2.41 (m, 1 H), 2.30 (dd,  $J = 14.0, 7.0$  Hz, 1 H); 1.85 (dd,  $J = 14.0, 8.0$  Hz, 1 H), 1.47 (s, 1 H), 1.29 – 1.31 (m, 4 H), 1.05 (d,  $J = 6.5$  Hz, 3 H), 0.85 (t,  $J = 12.0$  Hz, 1 H), 0.64 (d,  $J = 6.0$  Hz, 1 H).



**1,1-dimethyl-7-methylene-5-(prop-2-yn-1-yl)-5-azaspiro[2.4]heptan-4-one, 24** (Table 1, Entry 10): According to General Procedure A, **23** (0.13 g, 0.47 mmol), Et<sub>3</sub>N (0.13 mL, 0.94 mmol) and bis(2,2'-phenylpyridyl)(4,4'-ditertbutyl-2,2'-bipyridyl)iridium(III) hexafluorophosphate (4.5 mg, 5.0  $\mu\text{mol}$ ) in dry DMF (15 mL) afforded **24** (65 mg, 73%) as a colorless oil after purification by chromatography on SiO<sub>2</sub> (90:10, Petroleum Ether:Et<sub>2</sub>O) (12 h reaction time).

$R_f$  (AcOEt/hexane 20:80) 0.39;

IR (neat): 3301, 3236, 2924, 2872, 1691, 1659, 1428, 1247, 1108, 881, 639  $\text{cm}^{-1}$ ;

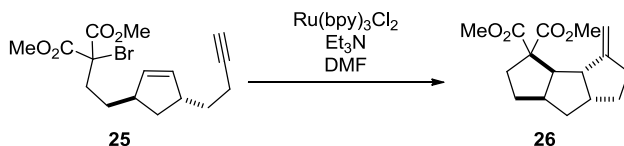
$^1\text{H NMR}$  ( $\text{CDCl}_3$ , 400 MHz):  $\delta$  5.00 (s, 1 H), 4.59, (s, 1 H), 4.19 (br s, 2 H), 4.12 (dt,  $J = 13.2$ ,



2.4 Hz, 1 H), 4.00 (d,  $J = 13.2$  Hz, 1 H), 2.23 (t,  $J = 2.4$  Hz, 1 H), 1.49 (d,  $J = 4.8$  Hz, 1 H), 1.35 (s, 3 H), 1.13 (s, 3 H), 0.99 (d,  $J = 4.8$  Hz, 1 H);

$^{13}\text{C}$  NMR ( $\text{CDCl}_3$ , 75 MHz):  $\delta$  173.2, 141.0, 104.8, 77.8, 72.2, 50.6, 37.7, 31.8, 31.4, 26.2, 20.4, 20.1;

HRMS (ESI)  $m/z$  calculated for  $\text{C}_{12}\text{H}_{16}\text{NO}^+$  ( $[\text{M}+\text{H}]^+$ ) 190.1232, found 190.1241.



**Dimethyl 4-methyleneoctahydro-1H-cyclopenta[a]pentalene-3,3(2H)-dicarboxylate, 26:**

According to General Procedure A, **25** (64 mg, 0.18 mmol),  $\text{Et}_3\text{N}$  (50  $\mu\text{L}$ , 0.36 mmol) and tris(2,2'-bipyridyl)ruthenium(II) chloride hexahydrate (1.4 mg, 1.8  $\mu\text{mol}$ ) in dry DMF (8.0 mL) afforded **26** (35 mg, 69%) as a colorless oil after purification by chromatography on  $\text{SiO}_2$  (95:5, Petroleum Ether: $\text{Et}_2\text{O}$ ) (4 h reaction time).

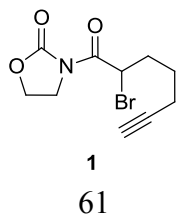
$R_f$  (AcOEt/hexane 10:90) 0.53;

IR (neat): 2949, 1732, 1650, 1434, 1272, 1244, 1142, 1079, 912, 736  $\text{cm}^{-1}$ ;

$^1\text{H}$  NMR ( $\text{CDCl}_3$ , 400 MHz):  $\delta$  4.88 (s, 1 H), 4.81 (s, 1 H), 3.72 (s, 3 H), 3.71 (s, 3 H), 3.10 (dd,  $J = 7.2, 3.6$  Hz, 1 H), 2.80 – 2.88 (m, 1 H), 2.51 – 2.59 (m, 1 H), 2.24 – 2.49 (m, 4 H), 2.07 (dd,  $J = 12.8, 6.8$  Hz, 1 H), 1.65 – 1.76 (m, 2 H), 1.36 – 1.56 (m, 4 H);

$^{13}\text{C}$  NMR ( $\text{CDCl}_3$ , 75 MHz):  $\delta$  172.6, 171.4, 157.2, 106.2, 65.9, 57.4, 52.6, 52.2, 52.1, 45.5, 44.9, 38.8, 33.5, 31.7, 30.3, 28.8;

HRMS (ESI)  $m/z$  calculated for  $\text{C}_{12}\text{H}_{23}\text{O}_4^+$  ( $[\text{M}+\text{H}]^+$ ) 279.1596, found 279.1586.



**3-(2-bromohept-6-ynoyl)oxazolidin-2-one, 1:** A flame dried 100 mL round bottom flask is equipped with a rubber septum and magnetic stir bar and is charged with a solution of 3-(hept-6-ynoyl)oxazolidin-2-one<sup>4</sup> (0.75 g, 3.8 mmol) in THF (40 mL) and cooled to -78 °C. A 1M solution of NaHMDS in THF (4.2 mL, 1.1 equiv) is added dropwise and the mixture allowed to stir at -78 °C for 30 min. NBS (0.75 g, 1.1 equiv) is then added and the mixture stirred at -78 °C until the reaction is complete (as judged by TLC analysis), the mixture is poured into a separatory funnel containing 50 mL of Et<sub>2</sub>O and 50 mL of H<sub>2</sub>O. The layers are separated and the aqueous layer is extracted with Et<sub>2</sub>O (2 X 75 mL). The combined organic layers are dried (Na<sub>2</sub>SO<sub>4</sub>) and concentrated to afford **1** (0.20 g, 20%) as a yellow oil after purification by chromatography on SiO<sub>2</sub> (30:70, AcOEt:hexane) (5.5 h reaction time).

$R_f$  (AcOEt/hexane 30:60) 0.25;

IR (neat): 3381, 3295, 2923, 2853, 2359, 1776, 1700, 1389, 1364, 1305, 1221, 1115, 1040, 908, 731, 631 cm<sup>-1</sup>;

<sup>1</sup>H NMR (CDCl<sub>3</sub>, 300 MHz): δ 5.64 (dd,  $J = 8.1, 6.6$  Hz, 1 H), 4.47 (t,  $J = 8.2$  Hz, 2 H), 4.08 (t,  $J = 8.2$  Hz, 2 H) 2.12 – 2.30 (m, 4 H), 1.98 (t,  $J = 3.0$  Hz, 1 H), 1.55 – 1.83 (m, 2 H);

<sup>13</sup>C NMR (CDCl<sub>3</sub>, 75 MHz): δ 169.1, 152.5, 83.2, 69.1, 62.1, 43.0, 42.8, 32.8, 26.0, 17.8;

HRMS (ESI)  $m/z$  calculated for C<sub>10</sub>H<sub>12</sub>BrNaNO<sub>3</sub><sup>+</sup> ([M+Na]<sup>+</sup>) 295.9898, found 295.9990.

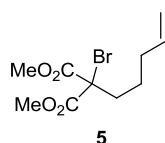
### General Procedure B: Bromination of Dimethyl Malonates

A flame dried 25 mL round bottom flask, equipped with a rubber septum and magnetic stir bar, is charged with the corresponding malonate (0.50 mmol, 1.0 equiv), and anhydrous THF (5 mL) and cooled to -78 °C. A 1.0 M solution of NaHMDS in THF (0.55 mL, 1.1 equiv.) is then added dropwise and the mixture allowed to stir for 15 min. NBS (0.55 mmol, 1.1 equiv) is then added

---

<sup>4</sup> *Med. Chem. Lett.* **2008**, *18*, 1768.

and the mixture allowed to slowly warm to 0 °C over 4 h. After the reaction is complete (as judged by TLC analysis), the mixture is poured into a separatory funnel containing 25 mL of Et<sub>2</sub>O and 25 mL of H<sub>2</sub>O. The layers are separated and the aqueous layer is extracted with Et<sub>2</sub>O (2 X 50 mL). The combined organic layers are dried (Na<sub>2</sub>SO<sub>4</sub>) and concentrated. The residue is purified by chromatography on silica gel, using the solvent system indicated, to afford the desired reduced product.



**Dimethyl 2-bromo-2-(pent-4-en-1-yl)malonate, 5:** According to General Procedure B, dimethyl 2-(pent-4-en-1-yl)malonate<sup>5</sup> (1.9 g, 9.5 mmol), 1 M NaHMDS solution (10 mL, 10 mmol) and NBS (1.9 g, 10 mmol) in dry THF (95 mL) afforded **5** (2.5 g, 93%) as a colorless oil after purification by chromatography on SiO<sub>2</sub> (95:5, hexane:AcOEt) (7.5 h reaction time).

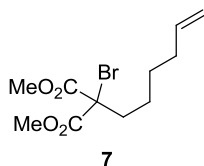
$R_f$  (AcOEt/hexane 5:95): 0.21;

IR (neat): 3457, 2956, 1743, 1641, 1436, 1255, 1132, 1101, 997, 925, 737 cm<sup>-1</sup>;

<sup>1</sup>H NMR (CDCl<sub>3</sub>, 300 MHz): δ 5.71 – 5.84 (m, 1 H), 4.97 – 5.06 (m, 2 H), 3.82 (s, 6 H), 2.28 (t,  $J = 7.8$  Hz, 2 H), 2.11 (q,  $J = 6.6$  Hz, 2 H), 1.46 – 1.56 (m, 2 H);

<sup>13</sup>C NMR (CDCl<sub>3</sub>, 75 MHz): δ 167.0, 137.2, 115.1, 62.3, 53.5, 37.4, 32.7, 24.2;

HRMS (ESI)  $m/z$  calculated for C<sub>10</sub>H<sub>16</sub>BrO<sub>4</sub><sup>+</sup> ([M+H]<sup>+</sup>) 279.0232, found 279.0234.



**Dimethyl 2-bromo-2-(hex-5-en-1-yl)malonate, 7:** According to General Procedure B, dimethyl

<sup>5</sup> *Org. Lett.* **2008**, *10*, 405.

2-(pent-4-en-1-yl)malonate<sup>6</sup> (1.0 g, 4.7 mmol), 1 M NaHMDS solution (5.1 mL, 5.1 mmol) and NBS (0.91 g, 5.1 mmol) in dry THF (47 mL) afforded **7** (1.3 g, 96%) as a colorless oil after purification by chromatography on SiO<sub>2</sub> (95:5, hexane:AcOEt) (7.5 h reaction time).

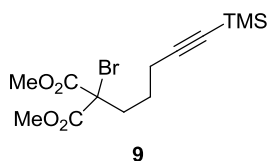
$R_f$  (AcOEt/hexane 15:85) 0.43;

IR (neat): 3077, 2931, 2859, 1744, 1640, 1436, 1251, 1133, 1102, 993, 913 cm<sup>-1</sup>;

<sup>1</sup>H NMR (CDCl<sub>3</sub>, 300 MHz):  $\delta$  5.71 – 5.85 (m, 1 H), 4.93 – 5.04 (m, 2 H), 3.82 (s, 6 H), 2.24 – 2.95 (m, 2 H), 2.04 – 2.08 (m, 2 H), 1.39 – 1.47 (m, 4 H);

<sup>13</sup>C NMR (CDCl<sub>3</sub>, 75 MHz):  $\delta$  167.3, 138.1, 114.7, 62.6, 53.8, 38.0, 33.2, 28.2, 24.6;

HRMS (ESI)  $m/z$  calculated for C<sub>11</sub>H<sub>18</sub>BrO<sub>4</sub><sup>+</sup> ([M+H]<sup>+</sup>) 293.0388, found 293.0396.



**Dimethyl 2-bromo-2-(5-(trimethylsilyl)pent-4-yn-1-yl)malonate, 9:** According to General Procedure B, dimethyl 2-(5-(trimethylsilyl)pent-4-yn-1-yl)malonate<sup>7</sup> (0.34 g, 1.3 mmol), 1 M NaHMDS solution (1.4 mL, 1.4 mmol) and NBS (0.25 g, 1.4 mmol) in dry THF (20 mL) afforded **9** (0.39 g, 89%) as a colorless oil after purification by chromatography on SiO<sub>2</sub> (95:5, hexane:AcOEt) (7.5 h reaction time).

$R_f$  (AcOEt/hexane 5:95): 0.25;

IR (neat): 2956, 2899, 2174, 1745, 1436, 1249, 1168, 840, 759, 639 cm<sup>-1</sup>;

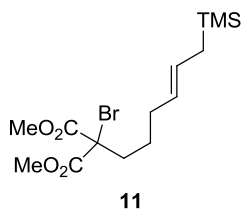
<sup>1</sup>H NMR (CDCl<sub>3</sub>, 300 MHz):  $\delta$  3.83 (s, 6 H), 2.35 – 2.40 (m, 2 H), 2.28 (t,  $J$  = 6.9 Hz, 2 H), 1.59 – 1.70 (m, 2 H), 0.15 (s, 9 H);

<sup>6</sup> *J. Org. Chem.* **2000**, *65*, 6819.

<sup>7</sup> *Tetrahedron* **1991**, *47*, 6293.

$^{13}\text{C}$  NMR ( $\text{CDCl}_3$ , 75 MHz):  $\delta$  167.0, 105.7, 85.3, 62.1, 53.7, 37.3, 24.6, 19.3, -0.1;

HRMS (ESI)  $m/z$  calculated for  $\text{C}_{13}\text{H}_{22}\text{BrO}_4\text{Si}^+$  ( $[\text{M}+\text{H}]^+$ ) 349.0471, found 349.0477.



**(E)-dimethyl 2-bromo-2-(6-(trimethylsilyl)hex-4-en-1-yl)malonate, 11:** A flame dried 10 mL round bottom flask is equipped with a reflux condenser and magnetic stir bar and is charged with Gubbs II catalysts (42.0 mg, 50  $\mu\text{mol}$ ). A solution of **4** (0.28 mg, 0.99 mmol) and allyl TMS (0.47 mL, 3.0 mmol) in degassed DCM (5 mL) is then added and the mixture heated to reflux. The reaction is cooled to rt and ethylvinylether is added and stirred for 30 min. The solvent is evaporated and the residue purified by chromatography on  $\text{SiO}_2$  (99:1, hexane:AcOEt) to afford **11** (0.13 mg, 35%) as a colorless oil.

$R_f$  (AcOEt/hexane 5:95): 0.36;

IR (neat): 3003, 2955, 1747, 1436, 1248, 1143, 912, 856, 736  $\text{cm}^{-1}$ ;

$^1\text{H}$  NMR ( $\text{CDCl}_3$ , 300 MHz):  $\delta$  5.36 – 5.48 (m, 1 H), 5.15 – 5.26 (m, 1 H), 3.82 (s, 6 H), 2.23 – 2.29 (m, 2 H), 2.04 (t,  $J = 6.6$  Hz, 2 H), 1.39 – 1.50 (m, 4 H), -0.01 (s, 9 H);

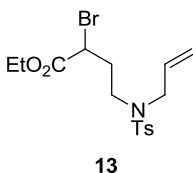
$^{13}\text{C}$  NMR ( $\text{CDCl}_3$ , 75 MHz):  $\delta$  167.5, 127.5, 127.3, 62.8, 53.8, 37.8 32.1, 25.5, 22.7, -1.9;

HRMS (ESI)  $m/z$  calculated for  $\text{C}_{14}\text{H}_{26}\text{BrO}_4\text{Si}^+$  ( $[\text{M}+\text{H}]^+$ ) 365.0784, found 365.0785.

### General Procedure C: $\alpha$ -Bromination of Esters

A flame dried 25 mL round bottom flask, equipped with a rubber septum and magnetic stir bar, is charged with the corresponding ester (0.50 mmol, 1.0 equiv), and anhydrous THF (5 mL) and cooled to -78  $^\circ\text{C}$ . A 1.0 M solution of NaHMDS in THF (0.55 mL, 1.1 equiv.) is then added dropwise and the mixture allowed to stir for 30 min. TMSCl (0.55 mmol, 1.1 equiv) is then

added and the mixture allowed to stir for 1 h. NBS (0.55 mmol, 1.1 equiv) is then added and the reaction allowed to stir at  $-78\text{ }^{\circ}\text{C}$ . After the reaction is complete (as judged by TLC analysis), the mixture is poured into a separatory funnel containing 25 mL of  $\text{Et}_2\text{O}$  and 25 mL of  $\text{H}_2\text{O}$ . The layers are separated and the aqueous layer is extracted with  $\text{Et}_2\text{O}$  (2 X 50 mL). The combined organic layers are dried ( $\text{Na}_2\text{SO}_4$ ) and concentrated. The residue is purified by chromatography on silica gel, using the solvent system indicated, to afford the desired reduced product.



**Ethyl 4-(N-allyl-4-methylphenylsulfonamido)-2-bromobutanoate, 13:** According to General Procedure C, ethyl 4-(N-allyl-4-methylphenylsulfonamido)butanoate (0.50 g, 1.5 mmol), NaHMDS (1.7 mL, 1.7 mmol), TMSCl (0.21 mL, 1.7 mmol) and NBS (0.30 g, 1.7 mmol) in dry THF (16 mL) afforded **13** (0.42 g, 62%) as a light yellow oil after purification by chromatography on  $\text{SiO}_2$  (90:10, hexanes:AcOEt) (8 h reaction time).

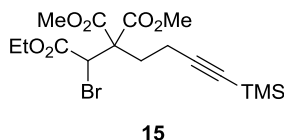
$R_f$  (AcOEt/hexane 20:80): 0.29;

IR (neat): 3083, 2983, 2873, 1735, 1598, 1494, 1372, 1155, 1092, 1019, 754, 662  $\text{cm}^{-1}$ ;

$^1\text{H}$  NMR ( $\text{CDCl}_3$ , 400 MHz):  $\delta$  7.68 (d,  $J = 8.4$  Hz, 2 H), 7.31 (d,  $J = 8.4$  Hz, 2 H), 5.57 – 5.67 (m, 1 H), 5.16 – 5.22 (m, 2 H), 4.35 (dd,  $J = 6.0, 8.0$  Hz, 1 H), 4.26 (q,  $J = 7.0$  Hz, 2 H), 3.81 (d,  $J = 6.4$  Hz, 2 H), 3.18 – 3.32 (m, 2 H), 2.46 (s, 3 H), 2.37 – 2.45 (m, 1 H), 2.18 – 2.27 (m, 1 H), 1.35 (t,  $J = 7.0$  Hz, 3 H);

$^{13}\text{C}$  NMR ( $\text{CDCl}_3$ , 75 MHz):  $\delta$  169.3, 143.5, 136.3, 132.7, 129.8, 127.2, 119.6, 62.1, 51.6, 45.2, 42.8, 33.8, 21.5, 13.9;

HRMS (ESI)  $m/z$  calculated for  $\text{C}_{16}\text{H}_{23}\text{BrNO}_4\text{S}^+$  ( $[\text{M}+\text{H}]^+$ ) 404.0531, found 404.0518.



**1-ethyl 2,2-dimethyl 1-bromo-6-(trimethylsilyl)hex-5-yne-1,2,2-tricarboxylate, 15:** A flame dried 50 mL round bottom flask, equipped with a rubber septum and magnetic stir bar, is charged with 1-ethyl 2,2-dimethyl hex-5-yne-1,2,2-tricarboxylate (1.0 g, 3.8 mmol), and anhydrous THF (40 mL) and cooled to -78 °C. A 1.0 M solution of NaHMDS in THF (7.9 mL, 7.9 mmol) is then added dropwise and the mixture allowed to stir for 30 min. TMSCl (1.0 mL, 7.9 mmol) is then added and the mixture allowed to stir for 2 h. NBS (0.67 g, 3.8 mmol) is then added and the reaction allowed to stir at -78 °C. After the reaction is complete (as judged by TLC analysis), the mixture is poured into a separatory funnel containing 50 mL of Et<sub>2</sub>O and 50 mL of H<sub>2</sub>O. The layers are separated and the aqueous layer is extracted with Et<sub>2</sub>O (2 X 75 mL). The combined organic layers are dried (Na<sub>2</sub>SO<sub>4</sub>) and concentrated. The residue is purified by chromatography on SiO<sub>2</sub> (90:10, hexanes:AcOEt) to afford **15** (0.91 g, 69%) as a colorless oil.

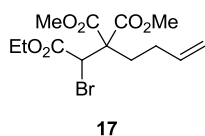
*R<sub>f</sub>* (AcOEt/hexane 10:90): 0.23 ;

IR (neat): 2957, 2177, 1736, 1435, 1370, 1249, 1206, 1180, 1067, 1027, 842 cm<sup>-1</sup>;

<sup>1</sup>H NMR (CDCl<sub>3</sub>, 400 MHz): δ 4.81 (s, 1 H), 4.23 (q, *J* = 7.2 Hz, 2 H), 3.78 (s, 3 H), 3.76 (s, 3 H), 2.32 – 2.54 (m, 4 H), 1.29 (t, *J* = 7.2 Hz, 3 H) 0.1 (s, 9 H);

<sup>13</sup>C NMR (CDCl<sub>3</sub>, 100 MHz): δ 168.4, 168.3, 167.3, 105.2, 85.3, 62.5, 60.1, 53.0, 53.0, 47.4, 32.7, 16.1, 13.8, 0.0;

HRMS (ESI) *m/z* calculated for C<sub>16</sub>H<sub>26</sub>BrO<sub>6</sub>Si<sup>+</sup> ([M+H]<sup>+</sup>) 421.0682, found 421.0673.



**1-ethyl 2,2-dimethyl 1-bromohex-5-ene-1,2,2-tricarboxylate, 17:** According to General Procedure C, 1-ethyl 2,2-dimethyl hex-5-ene-1,2,2-tricarboxylate (1.0 g, 3.7 mmol), NaHMDS (4.0 mL, 4.0 mmol), TMSCl (0.51 mL, 4.0 mmol) and NBS (0.72 g, 4.0 mmol) in dry THF (40 mL) afforded **17** (0.68 g, 53%) as a light yellow oil after purification by chromatography on SiO<sub>2</sub> (95:5, hexanes:AcOEt) (12 h reaction time).

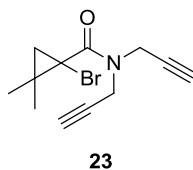
*R<sub>f</sub>* (AcOEt/hexane 20:80) 0.24;

IR (neat): 3075, 2982, 2955, 1743, 1642, 1435, 1337, 1264, 1212, 1154, 1027, 763 cm<sup>-1</sup>;

<sup>1</sup>H NMR (CDCl<sub>3</sub>, 400 MHz): δ 5.73 – 5.83 (m, 1 H), 4.98 – 5.08 (m, 2 H), 4.80 (s, 1 H), 4.25 (q, *J* = 7.2 Hz, 2 H), 3.81 (s, 3 H), 3.78 (s, 3 H), 2.90 – 2.35 (m, 1 H), 2.13 – 2.24 (m, 3 H), 1.33 (t, *J* = 7.2, 3 H);

<sup>13</sup>C NMR (CDCl<sub>3</sub>, 125 MHz): δ 168.8, 168.7, 167.5, 137.0, 115.5, 62.5, 60.3, 53.0, 52.9, 47.7, 33.5, 29.0, 13.9;

HRMS (ESI) *m/z* calculated for C<sub>13</sub>H<sub>19</sub>BrNaO<sub>6</sub><sup>+</sup> ([M+Na]<sup>+</sup>) 373.0263, found 373.0254.



**1-bromo-2,2-dimethyl-N,N-di(prop-2-yn-1-yl)cyclopropanecarboxamide (23):** A flame dried 25 mL round bottom flask, equipped with a rubber septum and magnetic stir bar, is charged with 1-bromo-2,2-dimethylcyclopropanecarboxylic acid<sup>8</sup> (10 mmol, 1.0 equiv) and DCM (12 mL) and cooled to 0 °C. Oxalyl chloride (15 mmol, 1.5 equiv), and DMF (5 drops) are then added and the mixture allowed to warm to rt. After stirring for 2.5 h, the solvent was removed and the crude acid chloride was used immediately. A separate flame dried 100 mL round bottom flask,

<sup>8</sup> *Angew. Chem.* **1982**, *94*, 79.



equipped with a rubber septum and magnetic stir bar is charged with dipropargyl ammonium trifluoroacetate<sup>9</sup> (15 mmol, 1.5 equiv), DMF (30 mL), and Et<sub>3</sub>N (31 mmol, 3.0 equiv). The crude acid chloride in DMF (10 mL) is then added and the mixture is allowed to stir at rt. After 12 h, the mixture is poured into a separatory funnel containing 25 mL of Et<sub>2</sub>O and 25 mL of H<sub>2</sub>O. The layers are separated and the aqueous layer is extracted with Et<sub>2</sub>O (2 X 50 mL). The combined organic layers are dried (Na<sub>2</sub>SO<sub>4</sub>) and concentrated. The residue is purified by chromatography on SiO<sub>2</sub> (95:5 to 90:10, hexanes:AcOEt) to afford **23** (2.0 g, 70%) as a pale yellow oil.

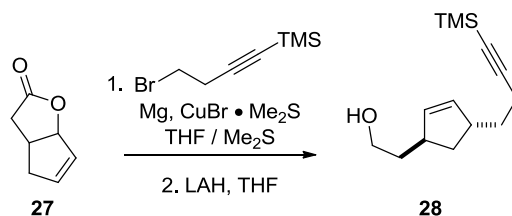
*R<sub>f</sub>* (AcOEt/hexane 15:85) 0.36;

IR (neat): 3295, 2956, 2928, 2121, 1651, 1414, 1337, 1234, 1180, 1022, 953, 656 cm<sup>-1</sup>;

<sup>1</sup>H NMR (CDCl<sub>3</sub>, 400 MHz): δ 4.38 – 4.46 (m, 2 H), 4.27 – 4.34 (m, 2 H), 2.35 (t, *J* = 2.4 Hz, 1 H), 2.21 (t, *J* = 2.4 Hz, 1 H), 1.61 (d, *J* = 6.6 Hz, 1 H), 1.44 (s, 3 H), 1.12 (s, 3 H), 1.02 (d, *J* = 6.6 Hz, 1 H);

<sup>13</sup>C NMR (CDCl<sub>3</sub>, 100 MHz): δ 166.9, 77.6, 77.2, 73.6, 72.1, 39.4, 37.2, 33.3, 27.0, 24.3, 23.6, 21.0;

HRMS (ESI) *m/z* calculated for C<sub>12</sub>H<sub>15</sub>BrNO<sup>+</sup> ([M+H]<sup>+</sup>) 268.0337, found 268.0342.



**2-(4-(4-(trimethylsilyl)but-3-yn-1-yl)cyclopent-2-en-1-yl)ethanol, 28:** A flame dried 50 mL round bottom flask, equipped with a rubber septum and magnetic stir bar, is charged with Mg (0.39 g, 2.0 equiv), THF (15 mL), I<sub>2</sub> (60 mg), and dibromoethane (45 μL). (4-bromobut-1-yn-1-

<sup>9</sup> *Chem. Commun.* **2002**, 22.

yl)trimethylsilane (2.5 g, 1.5 equiv) in THF (25 mL) is added over 1 h. The mixture is then allowed to stir at rt for 2 h. A separate flame dried 250 mL round bottom flask, equipped with a rubber septum and magnetic stir bar, is charged with CuBr•Me<sub>2</sub>S (3.3 g, 2.0 equiv), THF (20 mL), and Me<sub>2</sub>S (20 mL) and cooled to -10 °C. The Grignard solution is then added and the slurry and is allowed to stir at -10 °C for 20 min. **27**<sup>10</sup> (0.99 g, 8.0 mmol) in THF (5.0 mL) is added and the reaction allowed to stir at -10 °C for 4 h. The reaction mixture is partitioned between 1 N aq. HCl (50 mL) and Et<sub>2</sub>O (50 mL). The layers are separated and the aqueous layer is extracted with Et<sub>2</sub>O (2 X 50 mL). The combined organic layers are dried (Na<sub>2</sub>SO<sub>4</sub>) and concentrated. The residue is passed through a silica gel pad using 70:28:2 hexane:EtOAc:AcOH as the eluent affording the cyclopentenyl acetic acid which was used without further purification (1.6 g, 79% yield).

A flame dried 50 mL round bottom flask, equipped with a rubber septum and magnetic stir bar, is charged with the crude acid residue and THF (25 mL) and cooled to 0 °C. A 1.5 M solution of LAH in THF (6.4 mL, 1.5 equiv) is added dropwise and the reaction allowed to stir at 0 °C for 2 h. The reaction is then quenched by the slow addition of H<sub>2</sub>O (10 mL) The rxn is partitioned between 1 N aq. NaOH (50 mL) and Et<sub>2</sub>O (50 mL) The layers are separated and the aqueous layer is extracted with Et<sub>2</sub>O (2 X 50 mL). The combined organic layers are dried (Na<sub>2</sub>SO<sub>4</sub>) and concentrated. The residue is purified by chromatography on SiO<sub>2</sub> (90:10, hexanes:AcOEt) to afford **28** (1.3 g 85%) as a pale yellow oil.

*R<sub>f</sub>* (AcOEt/hexane 10:90) 0.13;

IR (neat): 3354, 2930, 2174, 1710, 1248, 1049, 839, 758, 736 cm<sup>-1</sup>;

<sup>1</sup>H NMR (CDCl<sub>3</sub>, 400 MHz): δ 5.70 (br s, 2 H), 3.64 – 3.72 (m, 2 H), 2.78 – 2.82 (m, 2 H), 2.21

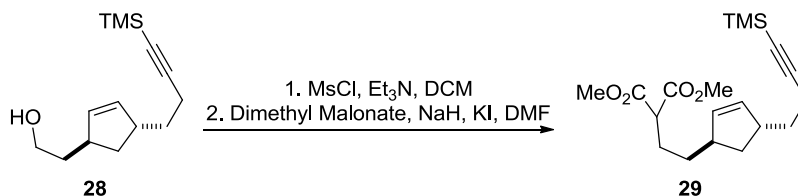
---

<sup>10</sup> *Angew. Chem., Int. Ed.* **2006**, *45*, 481.

– 2.26 (m, 2 H), 1.47 – 1.70 (m, 6 H), 0.14 (s, 9 H);

$^{13}\text{C}$  NMR ( $\text{CDCl}_3$ , 100 MHz):  $\delta$  134.6, 134.2, 107.4, 84.3, 61.5, 43.9, 41.2, 38.6, 36.0, 34.5, 18.2, 0.06.

HRMS (ESI)  $m/z$  calculated for  $\text{C}_{19}\text{H}_{30}\text{BrNO}^+$  ( $[\text{M}+\text{H}]^+$ ) 268.0337, found 268.0342.



**Dimethyl 2-(2-(4-(4-(trimethylsilyl)but-3-yn-1-yl)cyclopent-2-en-1-yl)ethyl)malonate (29):** A

flame dried 25 mL round bottom flask, equipped with a magnetic stir bar and rubber septum, is charged with **28** (0.74 g, 3.2 mmol), and DCM (11 mL) and cooled to 0 °C. The mixture is then treated with  $\text{Et}_3\text{N}$  (1.3 mL, 3.0 equiv) and  $\text{MsCl}$  (0.27 mL, 1.1 equiv). After 2 h at 0 °C the reaction is partitioned between sat. aq.  $\text{NH}_4\text{Cl}$  (50 mL) and  $\text{Et}_2\text{O}$  (50 mL). The layers are separated and the aqueous layer is extracted with  $\text{Et}_2\text{O}$  (2 x 50 mL). The combined organic layers are washed with  $\text{H}_2\text{O}$  and brine, dried ( $\text{Na}_2\text{SO}_4$ ), and concentrated. The crude mesylate is used without further purification.

A flame dried 25 mL round bottom flask, equipped with a rubber septum and a magnetic stir bar, is charged with a 60% dispersion of  $\text{NaH}$  in mineral oil (0.14 g, 1.1 equiv) and a 1:1 THF:DMF mixture (10 mL) and cooled to 0 °C. The slurry is then treated with  $\text{KI}$  (53 mg, 0.1 equiv) and dimethyl malonate (0.39 mL, 1.1 equiv). The mixture is then allowed to warm to rt and treated with the crude mesylate in 1:1 THF:DMF (5 mL) and heated to 70 °C. After 16 h the reaction is partitioned between  $\text{H}_2\text{O}$  (50 mL) and  $\text{Et}_2\text{O}$  (50 mL). The layers are separated and the aqueous layers are extracted with  $\text{Et}_2\text{O}$  (2 x 50 mL). The combined organic layers are washed with  $\text{H}_2\text{O}$  and brine, dried ( $\text{Na}_2\text{SO}_4$ ) and concentrated. The residue is purified by

chromatography on SiO<sub>2</sub> (95:5 hexane:EtOAc) to afford **29** (0.72 g, 65%) as a pale yellow oil.

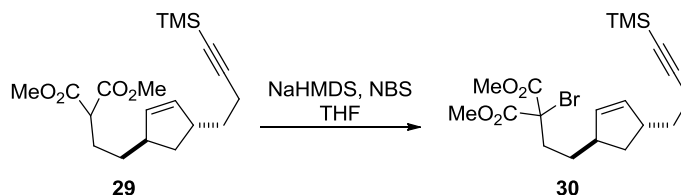
*R<sub>f</sub>* (AcOEt/hexane 15:85) 0.37;

IR (neat): 2954, 2857, 2173, 1736, 1435, 1248, 1148, 840, 759 cm<sup>-1</sup>;

<sup>1</sup>H NMR (CDCl<sub>3</sub>, 400 MHz): δ 5.67 – 5.69 (m, 1 H), 5.64 – 5.66 (m, 1 H), 3.73 (s, 6 H), 3.34 (t, *J* = 7.6 Hz, 1 H), 2.75 – 2.78 (m, 1 H), 2.66 – 2.69 (m, 1 H), 2.22 (td, *J* = 7.6, 2.0 Hz, 2 H), 1.87 – 1.94 (m, 2 H), 1.55 – 1.65 (m, 3 H), 1.46 – 1.52 (m, 1 H), 1.34 – 1.43 (m, 1 H), 1.22 – 1.31 (m, 1 H), 0.14 (s, 9 H);

<sup>13</sup>C NMR (CDCl<sub>3</sub>, 100 MHz): δ 169.5, 134.3, 134.2, 107.2, 84.1, 52.2, 51.6, 44.2, 43.8, 35.7, 34.5, 33.3, 26.9, 18.1, -0.06;

HRMS (ESI) *m/z* calculated for C<sub>14</sub>H<sub>25</sub>O<sub>5</sub>Si<sup>+</sup> ([M+H]<sup>+</sup>) 237.1675, found 237.1774.



**Dimethyl 2-bromo-2-(2-(4-(4-(trimethylsilyl)but-3-yn-1-yl)cyclopent-2-en-1-yl)ethyl)malonate (30)**: According to General Procedure B, **29** (0.70 g, 2.0 mmol), 1 M NaHMDS solution (2.2 mL, 2.2 mmol) and NBS (0.39 mg, 2.2 mmol) in dry THF (25 mL) afforded **30** (0.61 g, 71%) as a pale yellow oil after purification by chromatography on SiO<sub>2</sub> (95:5, hexane:AcOEt) (6 h reaction time).

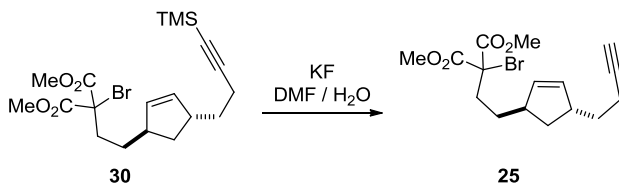
*R<sub>f</sub>* (AcOEt/hexane 5:95): 0.34;

IR (neat): 2955, 2173, 1745, 1436, 1249, 912, 840, 733 cm<sup>-1</sup>;

<sup>1</sup>H NMR (CDCl<sub>3</sub>, 400 MHz): δ 5.69 – 5.71 (m, 1 H), 5.63 – 5.65 (m, 1 H), 3.82 (s, 6 H), 2.77 – 2.80 (m, 1 H), 2.69 – 2.73 (m, 1 H), 2.21 – 2.30 (m, 4 H), 1.45 – 1.68 (m, 5 H), 1.31 – 1.39 (m, 1 H), 0.14 (s, 9 H);

$^{13}\text{C}$  NMR ( $\text{CDCl}_3$ , 100 MHz):  $\delta$  167.3, 134.7, 134.0, 107.3, 84.3, 62.6, 53.7, 44.1, 44.0, 36.4, 35.7, 34.5, 31.1, 18.2, 0.06.

HRMS (ESI)  $m/z$  calculated for  $\text{C}_{19}\text{H}_{30}\text{BrO}_4\text{Si}^+$  ( $[\text{M}+\text{H}]^+$ ) 429.1097, found 429.1078.



**Dimethyl 2-bromo-2-(2-(4-(but-3-yn-1-yl)cyclopent-2-en-1-yl)ethyl)malonate (25):** A 10 mL round bottom flask, equipped with a magnetic stir bar and rubber septum, is charged with **30** (0.20 g, 0.46 mmol), and DMF (4 mL). The mixture is then treated with KF (40 mg, 1.5 equiv) and  $\text{H}_2\text{O}$  (0.10 mL). After 12 h at rt the reaction is partitioned between  $\text{H}_2\text{O}$  (50 mL) and  $\text{Et}_2\text{O}$  (50 mL). The layers are separated and the aqueous layer is extracted with  $\text{Et}_2\text{O}$  (2 x 50 mL). The combined organic layers are washed with  $\text{H}_2\text{O}$  and brine, dried ( $\text{Na}_2\text{SO}_4$ ), and concentrated. The residue is purified by chromatography on  $\text{SiO}_2$  (95:5 hexane:EtOAc) to afford **30** (0.16 mg, 99%) as a pale yellow oil.

$R_f$  (AcOEt/hexane 10:90): 0.33;

IR (neat): 3294, 3043, 2930, 2858, 1744, 1436, 1258  $\text{cm}^{-1}$ ;

$^1\text{H}$  NMR ( $\text{CDCl}_3$ , 500 MHz):  $\delta$  5.70 – 5.72 (m, 1 H), 5.66 – 5.68 (m, 1 H), 3.84 (s, 6 H), 2.82 – 2.88 (m, 1 H), 2.71 – 2.77 (m, 1 H), 2.30 (ddd,  $J = 2.5, 2.5, 2.5$  Hz, 1 H), 2.20 – 2.25 (m, 1 H), 1.97 (t,  $J = 2.5$  Hz, 1 H), 1.70 (t,  $J = 6.5$  Hz, 1 H), 1.60 – 1.67 (m, 1 H), 1.49 – 1.55 (m, 1 H), 1.36 – 1.44 (m, 1 H);

$^{13}\text{C}$  NMR ( $\text{CDCl}_3$ , 75 MHz):  $\delta$  167.3, 134.5, 134.1, 84.4, 68.2, 62.6, 53.8, 44.1, 43.8, 36.5, 35.7, 34.4, 31.1, 16.7;

HRMS (ESI)  $m/z$  calculated for  $\text{C}_{16}\text{H}_{22}\text{BrO}_4^+$  ( $[\text{M}+\text{H}]^+$ ) 357.0701, found 357.2697.

### General Procedure A: Alkyl Iodide Reduction

A flame dried 10 mL round bottom flask with a rubber septum and magnetic stir bar was charged with the corresponding alkyl iodide (0.60 mmol, 1.0 equiv), MeCN (6.0 mL), Hantzsch ester (1.2 mmol, 2.0 equiv), tributylamine (1.2 mmol, 2.0 equiv), and *fac*-Ir(ppy)<sub>3</sub> (0.0060 mmol, 0.010 equiv). The heterogenous mixture was degassed by argon sparging for 30 min and placed in a 250 mL beaker with blue or white LEDs wrapped inside. The reaction mixture was stirred at 25–30 °C until it was complete (as judged by TLC analysis or GC/MS). The solvent was removed from the crude mixture *in vacuo* and was dissolved in EtOAc. The contents were poured into a separatory funnel containing 25 mL of EtOAc and 25 mL of 1 M HCl solution. The layers were separated and the aqueous layer was extracted with EtOAc (2 × 25 mL). The combined organic layers were washed with sat. NaHCO<sub>3</sub> solution, brine, dried (Na<sub>2</sub>SO<sub>4</sub>) and concentrated *in vacuo*. The residue was purified by chromatography on silica gel to afford the desired product.

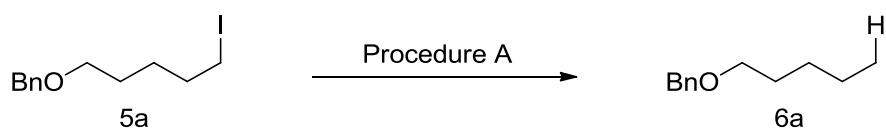
### General Procedure B: Aryl Iodide Reduction

A flame dried 10 mL round bottom flask with a rubber septum and magnetic stir bar was charged with the corresponding aryl iodide (0.60 mmol, 1.0 equiv), MeCN (6.0 mL), tributylamine (3.0 mmol, 5.0 equiv), formic acid (3.0 mmol, 5.0 equiv) and *fac*-Ir(ppy)<sub>3</sub> (0.0060 mmol, 0.010 equiv). The reaction mixture was degassed by argon sparging for 30 min and placed in a 250 mL beaker with blue or white LEDs wrapped inside. The reaction mixture was stirred at 25–30 °C until it was complete (as judged by TLC analysis or GC/MS). The solvent was removed from the crude mixture *in vacuo* and was dissolved in EtOAc. The contents were poured into a separatory funnel containing 25 mL of EtOAc and 25 mL of 2 M HCl solution. The layers were separated and the aqueous layer was extracted with EtOAc (2 × 25 mL). The combined organic layers were

washed with sat. NaHCO<sub>3</sub> solution, brine, dried (Na<sub>2</sub>SO<sub>4</sub>) and concentrated *in vacuo*. The residue was purified by chromatography on silica gel to afford the desired product.

### General Procedure C: Alkenyl Iodide Reduction and Radical Cyclizations

A flame dried 10 mL round bottom flask with a rubber septum and magnetic stir bar was charged with the corresponding aryl iodide (0.60 mmol, 1.0 equiv), MeCN (6.0 mL), tributylamine (6.0 mmol, 10 equiv), formic acid (6.0 mmol, 10 equiv) and *fac*-Ir(ppy)<sub>3</sub> (0.015 mmol, 0.025 equiv). The reaction mixture was degassed by argon sparging for 30 min and placed in a 250 mL beaker with blue or white LEDs wrapped inside. The reaction mixture was stirred at 25–30 °C until it was complete (as judged by TLC analysis or GC/MS). The solvent was removed from the crude mixture *in vacuo* and was dissolved in EtOAc. The contents were poured into a separatory funnel containing 25 mL of EtOAc and 25 mL of 2 M HCl solution. The layers were separated and the aqueous layer was extracted with EtOAc (2 × 25 mL). The combined organic layers were washed with 2 M HCl solution, sat. NaHCO<sub>3</sub> solution, brine, dried (Na<sub>2</sub>SO<sub>4</sub>) and concentrated *in vacuo*. The residue was purified by chromatography on silica gel to afford the desired product.



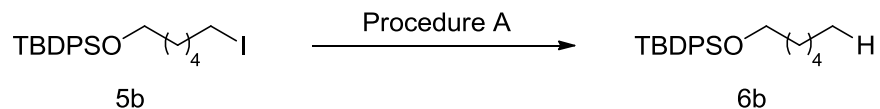
**Benzyl pentyl ether (Figure 2a):** According to General Procedure A, **5a**<sup>11</sup> (0.18 g, 0.60 mmol), tributylamine (0.29 mL, 0.22 g, 1.2 mmol), Hantzsch ester (0.30 g, 1.2 mmol) and *fac*-Ir(ppy)<sub>3</sub> (4.0 mg, 6.0 μmol) in MeCN (6.0 mL) afforded **6a**<sup>12</sup> (98 mg, 92%) after purification by chromatography on SiO<sub>2</sub> (98:2, petroleum ether/EtOAc).

*R<sub>f</sub>*(EtOAc/hexane 1:19): 0.50;

<sup>11</sup> *Biochemistry* **2001**, *40*, 12254.

<sup>12</sup> *Can. J. Chem.* **2001**, *77*, 258.

$^1\text{H}$  NMR ( $\text{CDCl}_3$ , 400 MHz):  $\delta$  7.34 – 7.25 (m, 5H), 4.50 (s, 2H), 3.46 (t,  $J = 6.6$  Hz, 2H), 1.64 – 1.57 (m, 2H), 1.35 – 1.29 (m, 4H), 0.89 (t,  $J = 7.0$  Hz, 3H).



***tert*-Butyl(hexyloxy)diphenylsilane (Figure 2a):** According to General Procedure A, **5b**<sup>13</sup> (0.28 g, 0.60 mmol), tributylamine (0.29 mL, 0.22 g, 1.2 mmol), Hantzsch ester (0.30 g, 1.2 mmol) and *fac*-Ir(ppy)<sub>3</sub> (4.0 mg, 6.0  $\mu\text{mol}$ ) in MeCN (6.0 mL) afforded **6b** (0.17 g, 84%) after purification by chromatography on  $\text{SiO}_2$  (99:1, petroleum ether/EtOAc).

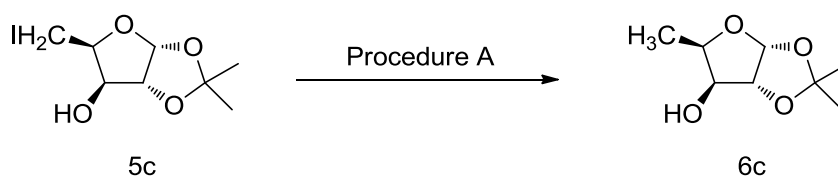
$R_f$  (EtOAc/petroleum ether 1:10): 0.38;

IR (neat): 3071, 3050, 2956, 2930, 2858, 1472, 1428, 1107, 823, 738, 700, 687  $\text{cm}^{-1}$ ;

$^1\text{H}$  NMR ( $\text{CDCl}_3$ , 500 MHz):  $\delta$  7.71 – 7.67 (m, 4H), 7.46 – 7.37 (m, 6H), 3.67 (t,  $J = 6.5$  Hz, 2H), 1.61 – 1.54 (m, 2H), 1.40 – 1.23 (m, 6H), 1.07 (s, 9H), 0.89 (t,  $J = 7.0$  Hz, 3H);

$^{13}\text{C}$  NMR ( $\text{CDCl}_3$ , 125 MHz):  $\delta$  135.6, 134.2, 129.5, 127.6, 64.0, 32.6, 31.6, 27.0, 25.5, 22.6, 19.2, 14.1;

HRMS (ESI)  $m/z$  calculated for  $\text{C}_{22}\text{H}_{32}\text{OSi}^+$  ( $[\text{M}+\text{H}]^+$ ) 341.2301, found 341.2300.



**1,2-*O*-Isopropylidene-5-deoxy- $\alpha$ -D-xylofuranose (Figure 2a):** According to General Procedure A, **5c**<sup>14</sup> (0.18 g, 0.60 mmol), tributylamine (0.29 mL, 0.22 g, 1.2 mmol), Hantzsch ester (0.30 g, 1.2 mmol) and *fac*-Ir(ppy)<sub>3</sub> (4.0 mg, 6.0  $\mu\text{mol}$ ) in MeCN (6.0 mL) afforded **6c**<sup>15</sup> (91 mg, 87%)

<sup>13</sup> *Nature Chem.* **2011**, 3, 140.

<sup>14</sup> *Russ. J. Org. Chem.* **2009**, 45, 762.

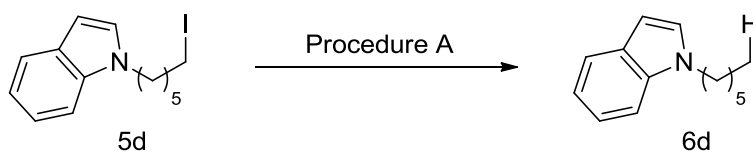
<sup>15</sup> *Org Lett.* **2005**, 7, 3187.



after purification by chromatography on SiO<sub>2</sub> (70:30, hexanes/EtOAc).

*R<sub>f</sub>*(EtOAc/hexane 2:3): 0.37;

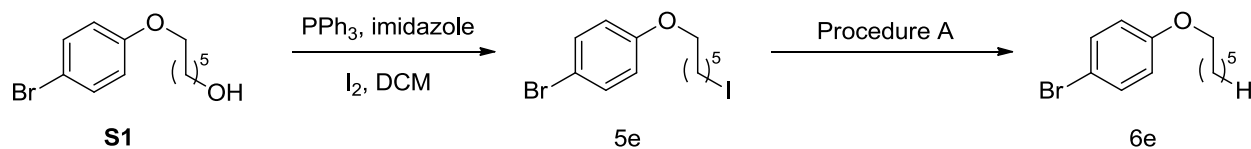
<sup>1</sup>H NMR (CDCl<sub>3</sub>, 400 MHz): δ 5.90 (d, *J* = 4.0 Hz, 1H), 4.53 (d, *J* = 4.0 Hz, 1H), 4.36 – 4.30 (m, 1H), 4.00 (d, *J* = 2.4 Hz, 1H), 1.65 – 1.57 (br s, 1H), 1.51 (s, 3H), 1.33–1.30 (m, 6H).



**1-Hexyl-1*H*-indole (Figure 2a)**: According to General Procedure A, **5d**<sup>16</sup> (0.20 g, 0.60 mmol), tributylamine (0.29 mL, 0.22 g, 1.2 mmol), Hantzsch ester (0.30 g, 1.2 mmol) and *fac*-Ir(ppy)<sub>3</sub> (4.0 mg, 6.0 μmol) in MeCN (6.0 mL) afforded **6d**<sup>6</sup> (0.10 g, 85%) after purification by chromatography on SiO<sub>2</sub> (petroleum ether).

*R<sub>f</sub>*(EtOAc/hexane 1:99): 0.30;

<sup>1</sup>H NMR (CDCl<sub>3</sub>, 500 MHz): δ 7.64 (d, *J* = 8.0 Hz, 1H), 7.35 (d, *J* = 8.2 Hz, 1H), 7.21 (t, *J* = 8.0 Hz, 1H), 7.12 – 7.08 (m, 2H), 6.49 (s, 1H), 4.12 (t, *J* = 7.2 Hz, 2H), 1.88 – 1.79 (m, 2H), 1.31 (s, 6H), 0.91 – 0.86 (m, 3H).



**1-Bromo-4-(hexyloxy)benzene (Figure 2a)**: According to General Procedure A, **5e** (0.23 g, 0.60 mmol), tributylamine (0.29 mL, 0.22 g, 1.2 mmol), Hantzsch ester (0.30 g, 1.2 mmol) and *fac*-Ir(ppy)<sub>3</sub> (4.0 mg, 6.0 μmol) in MeCN (6.0 mL) afforded **6e**<sup>17</sup> (0.13 g, 82%) after purification by chromatography on SiO<sub>2</sub> (99:1, petroleum ether/EtOAc).

*R<sub>f</sub>*(EtOAc/hexane 1:19): 0.68;

<sup>16</sup> *J. Org. Chem.* **2008**, *73*, 4638.

<sup>17</sup> *J. Chem. Soc. Perkin Trans. 2*, **1989**, 2041.

$^1\text{H}$  NMR ( $\text{CDCl}_3$ , 500 MHz):  $\delta$  7.35 (d,  $J = 9.0$  Hz, 2H), 6.76 (d,  $J = 9.0$  Hz, 2H), 3.90 (t,  $J = 6.6$  Hz, 2H), 1.77 – 1.75 (m, 2H), 1.45 – 1.43 (m, 2H), 1.34 – 1.31 (m, 4H), 0.90 (t,  $J = 6.9$  Hz, 3H).

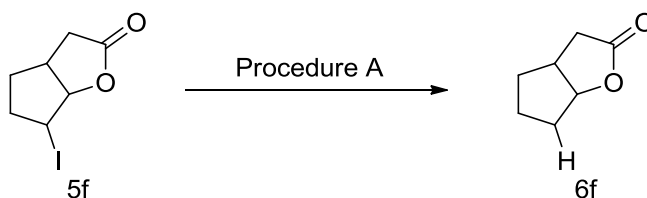
**1-Bromo-4-(6-iodohexyloxy)benzene (5e)**: To a solution of  $\text{PPh}_3$  (2.2 g, 8.4 mmol) and imidazole (0.57 g, 8.4 mmol) in  $\text{CH}_2\text{Cl}_2$  (20 mL) was carefully added iodine (2.1 g, 8.4 mmol) at  $0^\circ\text{C}$  (exothermic reaction). After 15 min, a solution of alcohol **S1**<sup>18</sup> (2.2 g, 8.0 mmol) in  $\text{CH}_2\text{Cl}_2$  (8 mL) was added dropwise (exothermic reaction). The ice bath was removed and the suspension was stirred overnight. The  $\text{CH}_2\text{Cl}_2$  was almost completely removed under reduced pressure (800 mbar,  $40^\circ\text{C}$ ) to provide an orange slurry which was then diluted with 40 mL pentane and filtered through a pad of celite. The solvents were removed under reduced pressure (800 mbar,  $40^\circ\text{C}$ ) and purification by chromatography on  $\text{SiO}_2$  (99:1, petroleum ether/EtOAc) afforded **5e** (2.3 g, 6.0 mmol, 75%).

$R_f$  (EtOAc/hexane 1:9): 0.71;

IR (neat): 2937, 2859, 1591, 1488, 1242, 1170, 905, 821, 727  $\text{cm}^{-1}$ ;

$^1\text{H}$  NMR ( $\text{CDCl}_3$ , 500 MHz):  $\delta$  7.37 (d,  $J = 9.1$  Hz, 2H), 6.78 (d,  $J = 9.1$  Hz, 2H), 3.93 (t,  $J = 6.4$  Hz, 2H), 3.21 (t,  $J = 7.0$  Hz, 2H), 1.91 – 1.83 (m, 2H), 1.83 – 1.76 (m, 2H), 1.53 – 1.45 (m, 4H);

$^{13}\text{C}$  NMR ( $\text{CDCl}_3$ , 125 MHz):  $\delta$  157.9, 131.9, 116.1, 112.4, 67.7, 33.1, 30.0, 28.8, 25.0, 6.9.



**Hexahydro-2H-cyclopenta[b]furan-2-one (Figure 2a)**: According to General Procedure A, **5f**<sup>19</sup> (0.15 g, 0.60 mmol), tributylamine (0.29 mL, 0.22 g, 1.2 mmol), Hantzsch ester (0.30 g, 1.2

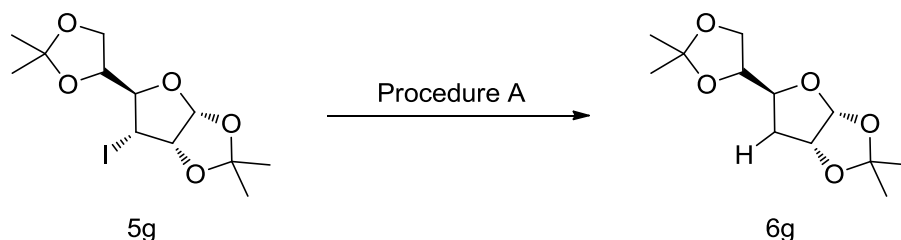
<sup>18</sup> *J. Am. Chem. Soc.* **2007**, *129*, 9366.

<sup>19</sup> *Adv. Synth. Catal.* **2004**, *346*, 1525.

mmol) and *fac*-Ir(ppy)<sub>3</sub> (4.0 mg, 6.0 μmol) in MeCN (6.0 mL) afforded **6f**<sup>20</sup> (68 mg, 90%) after purification by chromatography on SiO<sub>2</sub> (75:25, hexane/EtOAc).

*R<sub>f</sub>*(EtOAc/hexane 1:4): 0.16;

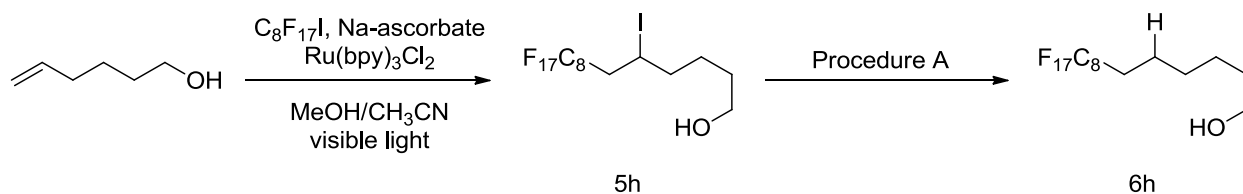
<sup>1</sup>H NMR (CDCl<sub>3</sub>, 500 MHz): δ 4.98 (t, *J* = 6.8 Hz, 1H), 2.91 – 2.83 (m, 1H), 2.82 (dd, *J* = 17, 1.0 Hz, 1H), 2.27 (dd, *J* = 17, 2.0 Hz, 1H), 2.06 – 2.02 (m, 1H), 1.89 – 1.80 (m, 1H), 1.78 – 1.64 (m, 3H), 1.55 – 1.49 (m, 1H).



**1,2:5,6-Di-*O*-isopropylidene-3-deoxy- $\alpha$ -D-glucofuranose (Figure 2a):** According to General Procedure A, **5g**<sup>21</sup> (0.22 g, 0.60 mmol), tributylamine (0.29 mL, 0.22 g, 1.2 mmol), Hantzsch ester (0.30 g, 1.2 mmol) and *fac*-Ir(ppy)<sub>3</sub> (4.0 mg, 6.0 μmol) in MeCN (6.0 mL) afforded **6g**<sup>11</sup> (0.12 g, 83%) after purification by chromatography on SiO<sub>2</sub> (75:25, hexane/EtOAc).

*R<sub>f</sub>*(EtOAc/hexane 1:4): 0.23;

<sup>1</sup>H NMR (CDCl<sub>3</sub>, 400 MHz): δ 5.82 (d, *J* = 3.7 Hz, 1H), 4.76 (t, *J* = 4.2 Hz, 1H), 4.21 – 4.07 (m, 3H), 3.87 – 3.79 (m, 1H), 2.19 (dd, *J* = 13.3, 4.2 Hz, 1H), 1.78 (ddd, *J* = 13.3, 9.6, 4.2 Hz, 1H), 1.52 (s, 3H), 1.43 (s, 3H), 1.36 (s, 3H), 1.32 (s, 3H).



<sup>20</sup> *J. Org. Chem.* **2011**, *76*, 7096.

<sup>21</sup> *Org. Biomol. Chem.* **2011**, *9*, 3415.

**Perfluorooctylhexan-1-ol (Figure 2a):** According to General Procedure A, **5h** (0.39 g, 0.60 mmol), tributylamine (0.29 mL, 0.22 g, 1.2 mmol), Hantzsch ester (0.30 g, 1.2 mmol) and *fac*-Ir(ppy)<sub>3</sub> (4.0 mg, 6.0 μmol) in MeCN (6.0 mL) afforded **6h** (0.30 g, 95%) after purification by chromatography on SiO<sub>2</sub> (80:20, hexane/EtOAc).

*R<sub>f</sub>* (EtOAc/hexane 1:4): 0.24;

IR (neat): 3363, 2936, 2861, 1238, 1201, 1146, 908, 732, 704 cm<sup>-1</sup>;

<sup>1</sup>H NMR (CDCl<sub>3</sub>, 400 MHz): δ 3.67 (t, *J* = 6.6 Hz, 2H), 2.14 – 2.00 (m, 2H), 1.67 – 1.55 (m, 5H), 1.48 – 1.38 (m, 4H);

<sup>13</sup>C NMR (CDCl<sub>3</sub>, 125 MHz): δ 62.5, 32.4, 30.7 (t, *J* = 22.0 Hz), 28.9, 25.4, 20.1.

**5-Iodo-6-perfluorooctylhexanol (5h):** A 0.5 L round bottom flask was equipped with a rubber septum and a magnetic stir bar and was charged with 5-hexen-1-ol (4.0 g, 4.8 mL, 40 mmol), MeCN (0.16 L), C<sub>8</sub>F<sub>17</sub>I (14 mL, 28 g, 52 mmol), MeOH (0.12 L), sodium L-ascorbate (2.8 g, 14 mmol), Ru(bpy)<sub>3</sub>Cl<sub>2</sub> (9.0 mg, 12 μmol). The mixture was then degassed by Ar sparging for 15 min. The mixture was then stirred under an Ar atmosphere and irradiated by blue LEDs. After the reaction was complete, as judged by TLC analysis (typically 30 min), celite was added to the mixture and solvents were removed *in vacuo*. Celite with adsorbed crude mixture was loaded onto a silica gel column afforded **5h** (25 g, 96%) after purification by chromatography on SiO<sub>2</sub> (70:30, hexanes/EtOAc).

*R<sub>f</sub>* (EtOAc/hexane 1:4): 0.13;

IR (neat): 3337, 2934, 1199, 1146, 1117, 1062, 656 cm<sup>-1</sup>;

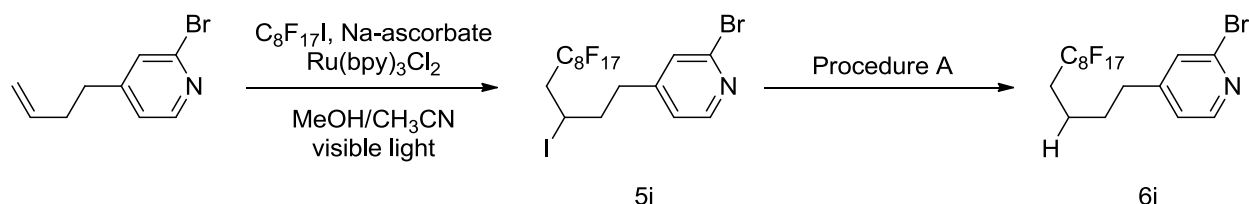
<sup>1</sup>H NMR (CDCl<sub>3</sub>, 500 MHz): δ 4.40 – 4.30 (m, 1H), 3.70 (t, *J* = 7.5 Hz, 2H), 3.04 – 2.70 (m, 2H), 1.95 – 1.77 (m, 2H), 1.73 – 1.45 (m, 4H), 1.41 – 1.23 (br s, 1H);

<sup>19</sup>F NMR (CDCl<sub>3</sub>, 376 MHz): δ -80.8 (t, *J* = 10 Hz, 3F), -111.3 – -112.2 (m, 1F), -114.2 – -115.2

(m, 1F), -121.5 – -121.7 (br s, 2F), -121.8 – -122.1 (br s, 4F), -122.6 – -122.9 (br s, 2F), -123.5 – -123.7 (br s, 2F), -126.0 – -126.2 (br s, 2F);

$^{13}\text{C}$  NMR ( $\text{CDCl}_3$ , 125 MHz):  $\delta$  62.5, 41.7 (t,  $J = 22$  Hz), 40.1, 31.5, 26.0, 20.4;

LRMS (ESI)  $m/z$  (relative intensity): 629 (100%), 367 (13%), 501 (13%), 630 (5%).



### 2-bromo-4-(5,5,6,6,7,7,8,8,9,9,10,10,11,11,12,12,12-heptafluorododecyl)pyridine

(Figure 2a): According to General Procedure A, **5i** (0.45 g, 0.60 mmol), tributylamine (0.29 mL, 0.22 g, 1.2 mmol), Hantzsch ester (0.30 g, 1.2 mmol) and *fac*-Ir(ppy)<sub>3</sub> (4.0 mg, 6.0  $\mu\text{mol}$ ) in MeCN (6.0 mL) afforded **6i** (0.35 g, 93%) after purification by chromatography on  $\text{SiO}_2$  (95:5, hexane/EtOAc).

$R_f$  (EtOAc/hexane 1:9): 0.34;

IR (neat): 2951, 1589, 1542, 1463, 1381, 1199, 1145, 1079, 703, 655  $\text{cm}^{-1}$ ;

$^1\text{H}$  NMR ( $\text{CDCl}_3$ , 400 MHz):  $\delta$  8.28 (d,  $J = 5.1$  Hz, 1H), 7.33 (t,  $J = 0.6$  Hz, 1H), 7.12 (dd,  $J = 5.0$  Hz, 0.6 Hz, 1H), 2.65 (t,  $J = 7.4$  Hz, 2H), 2.19 – 2.03 (m, 2H), 1.79 – 1.61 (m, 4H);

$^{13}\text{C}$  NMR ( $\text{CDCl}_3$ , 125 MHz):  $\delta$  153.7, 150.0, 142.4, 127.7, 122.8, 34.3, 30.4 (t,  $J = 22$  Hz), 29.4, 19.8;

HRMS (ESI)  $m/z$  calculated for  $\text{C}_{17}\text{H}_{11}\text{BrF}_{17}\text{N}^+$  ( $[\text{M}+\text{H}]^+$ ) 631.9882, found 631.9880.

### 2-bromo-4-(5,5,6,6,7,7,8,8,9,9,10,10,11,11,12,12,12-heptafluoro-3-iodododecyl)pyridine

(**5i**): A 0.25 L round bottom flask was equipped with a rubber septum and a magnetic stir bar and was charged with 2-bromo-4-(but-3-en-1-yl)pyridine (1.6 g, 7.5 mmol), MeCN (60 mL),  $\text{C}_8\text{F}_{17}\text{I}$  (2.6 mL, 5.4 g, 9.9 mmol), MeOH (45 mL), sodium L-ascorbate (0.51 g, 2.6 mmol),  $\text{Ru}(\text{bpy})_3\text{Cl}_2$

(5.7 mg, 7.5  $\mu\text{mol}$ ). The mixture was then degassed by Ar sparging for 15 min. The mixture was then stirred under an Ar atmosphere and irradiated by blue LEDs. After the reaction was complete, as judged by TLC analysis (typically 2.0 h), celite was added to the mixture and solvents were removed *in vacuo*. Celite with adsorbed crude mixture was loaded onto a silica gel column afforded **5i** (4.8 g, 85%) after purification by chromatography on  $\text{SiO}_2$  (90:10, hexane/EtOAc).

$R_f$  (EtOAc/hexane 1:4): 0.42;

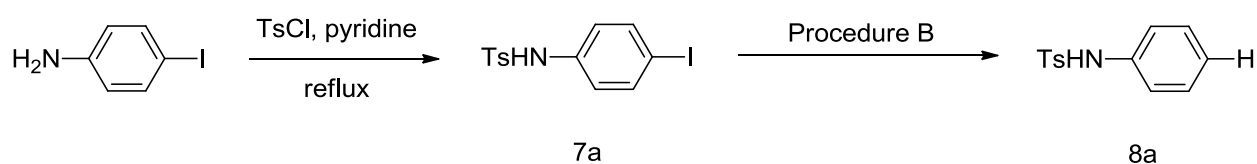
IR (neat): 2917, 2849, 1589, 1543, 1463, 1382, 1200, 1146, 1117, 1080, 723, 704, 656  $\text{cm}^{-1}$ ;

$^1\text{H}$  NMR ( $\text{CDCl}_3$ , 500 MHz):  $\delta$  8.30 (d,  $J = 5.0$  Hz, 1H), 7.37 (s, 1H), 7.12 (d,  $J = 5.0$  Hz, 1H), 4.31 – 4.22 (m, 1H), 3.07 – 2.68 (m, 4H), 2.17 – 2.06 (m, 2H);

$^{19}\text{F}$  NMR ( $\text{CDCl}_3$ , 282 MHz):  $\delta$  -80.7 (t,  $J = 8.0$  Hz, 3F), -110.5 – -111.5 (m, 1F), -114.1 – -115.1 (m, 1F), -121.4 – -121.7 (br s, 2F), -121.7 – -122.1 (br s, 4F), -122.6 – -122.9 (br s, 2F), -123.4 – -123.6 (br s, 2F), -126.0 – -126.3 (br s, 2F);

$^{13}\text{C}$  NMR ( $\text{CDCl}_3$ , 125 MHz):  $\delta$  152.0, 150.2, 142.7, 128.0, 122.9, 41.7 (t,  $J = 21$  Hz), 40.1, 34.8, 18.8.

HRMS (ESI)  $m/z$  calculated for  $\text{C}_{17}\text{H}_{10}\text{BrF}_{17}\text{IN}^+$  ( $[\text{M}+\text{H}]^+$ ) 757.8848, found 757.8860.



**4-methyl-N-phenylbenzenesulfonamide (Figure 2b):** According to General Procedure B, **7a** (0.22 g, 0.60 mmol), tributylamine (0.71 mL, 0.56 g, 3.0 mmol), formic acid (0.11 mL, 0.14 g, 3.0 mmol) and *fac*-Ir(ppy)<sub>3</sub> (4.0 mg, 6.0  $\mu\text{mol}$ ) in MeCN (6.0 mL) afforded **8a**<sup>22</sup> (0.14 g, 94%) after purification by chromatography on  $\text{SiO}_2$  (75:25, hexane/EtOAc).

<sup>22</sup> *Catal. Commun.* **2011**, *12*, 1477.

$R_f$  (EtOAc/hexane 1:3): 0.35;

$^1\text{H NMR}$  ( $\text{CDCl}_3$ , 500 MHz):  $\delta$  7.65 (d,  $J = 8.5$  Hz, 2H), 7.27 – 7.21 (m, 4H), 7.12 (t,  $J = 7.5$  Hz, 1H), 7.07 (d,  $J = 8.5$  Hz, 2H), 6.63 – 6.51 (br s, 1H), 2.39 (s, 3H).

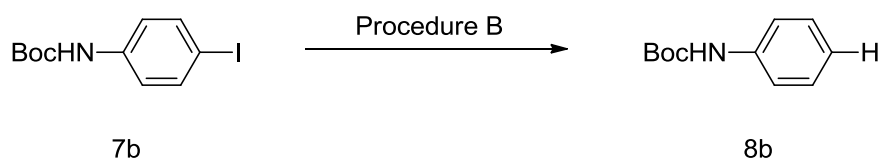
**N-(4-iodophenyl)-4-methylbenzenesulfonamide (7a)**: To a solution of the 4-iodoaniline<sup>23</sup> (0.22 g, 1.0 mmol) in pyridine (5 mL), *p*-toluenesulfonyl chloride (0.26 g, 1.35 mmol) was added and the mixture was heated at reflux for 16 h. The solvent was removed under reduced pressure and the crude residue was extracted with EtOAc and washed with HCl (1N), water and brine. The organic layer was dried over  $\text{MgSO}_4$  and the solvent was removed under reduced pressure. The crude residue was purified by flash chromatography on silica gel (90:10, hexane/EtOAc) to afford **7a** (0.36 g, 97%).

$R_f$  (EtOAc/hexane 1:9): 0.20;

IR (neat): 3254, 1484, 1383, 1325, 1290, 1156, 1090, 906, 812, 729, 662  $\text{cm}^{-1}$ ;

$^1\text{H NMR}$  ( $\text{CDCl}_3$ , 500 MHz):  $\delta$  7.65 (d,  $J = 8.2$  Hz, 2H), 7.55 (d,  $J = 8.9$  Hz, 2H), 7.25 (t,  $J = 7.5$  Hz, 2H), 6.83 (d,  $J = 8.9$  Hz, 2H), 6.51 – 6.44 (br s, 1H), 2.40 (s, 3H);

$^{13}\text{C NMR}$  ( $\text{CDCl}_3$ , 125 MHz):  $\delta$  144.1, 138.1, 136.4, 135.4, 129.7, 127.2, 122.8, 88.9, 21.5.



**tert-butyl phenylcarbamate (Figure 2b)**: According to General Procedure B, **7b**<sup>24</sup> (0.19 g, 0.60 mmol), tributylamine (0.71 mL, 0.56 g, 3.0 mmol), formic acid (0.11 mL, 0.14 g, 3.0 mmol) and *fac*- $\text{Ir}(\text{ppy})_3$  (4.0 mg, 6.0  $\mu\text{mol}$ ) in MeCN (6.0 mL) afforded **8b**<sup>25</sup> (0.11 g, 97%) after purification

<sup>23</sup> Commercially available from Sigma-Aldrich.

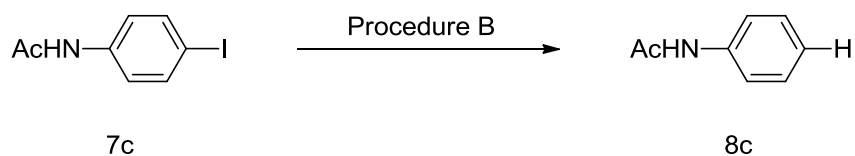
<sup>24</sup> *Org. Lett.* **2008**, *10*, 3207.

<sup>25</sup> *Tetrahedron Lett.* **2006**, *47*, 1087.

by chromatography on SiO<sub>2</sub> (95:5, hexane/EtOAc).

$R_f$  (EtOAc/hexane 3:17): 0.60;

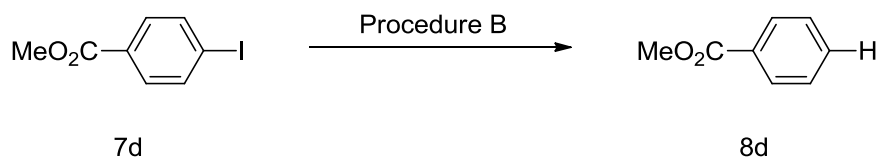
<sup>1</sup>H NMR (CDCl<sub>3</sub>, 400 MHz):  $\delta$  7.37 (d,  $J$  = 8.0 Hz, 2H), 7.32 – 7.27 (m, 2H), 7.07 – 7.01 (m, 1H), 6.55 – 6.45 (br s, 1H), 1.53 (s, 9H).



***N*-phenylacetamide (Figure 2b)**: According to General Procedure B, **7c**<sup>26</sup> (0.16 g, 0.60 mmol), tributylamine (0.71 mL, 0.56 g, 3.0 mmol), formic acid (0.11 mL, 0.14 g, 3.0 mmol) and *fac*-Ir(ppy)<sub>3</sub> (4.0 mg, 6.0  $\mu$ mol) in MeCN (6.0 mL) afforded **8c**<sup>27</sup> (77 mg, 95%) after purification by chromatography on SiO<sub>2</sub> (50:50, petroleum ether/EtOAc).

$R_f$  (EtOAc/ hexane 1:1): 0.24;

<sup>1</sup>H NMR (CDCl<sub>3</sub>, 400 MHz):  $\delta$  7.50 (d,  $J$  = 7.8 Hz, 2H), 7.32 (dd,  $J$  = 7.8 Hz, 7.3 Hz, 2H), 7.11 (t,  $J$  = 7.3 Hz, 1H), 2.18 (s, 3H).



**Methyl benzoate (Figure 2b)**: According to General Procedure B, methyl 4-iodobenzoate<sup>13</sup> (0.16 g, 0.60 mmol), tributylamine (0.71 mL, 0.56 g, 3.0 mmol), formic acid (0.11 mL, 0.14 g, 3.0 mmol) and *fac*-Ir(ppy)<sub>3</sub> (4.0 mg, 6.0  $\mu$ mol) in MeCN (6.0 mL) afforded **8d**<sup>28</sup> (75 mg, 92%) after purification by chromatography on SiO<sub>2</sub> (95:5, hexane/EtOAc).

$R_f$  (EtOAc/hexane 4:1): 0.50;

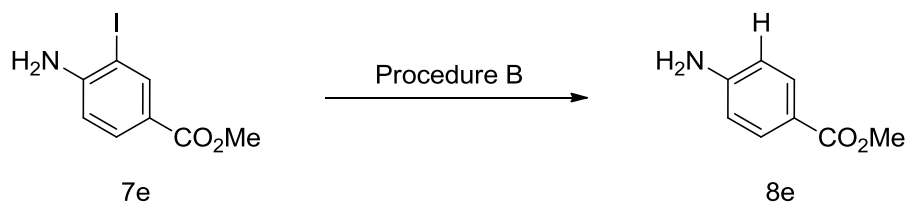
<sup>26</sup> *Tetrahedron Lett.* **2008**, *49*, 4742.

<sup>27</sup> *J. Comb. Chem.* **2006**, *8*, 289.

<sup>28</sup> *Org. Lett.* **2010**, *12*, 3645.



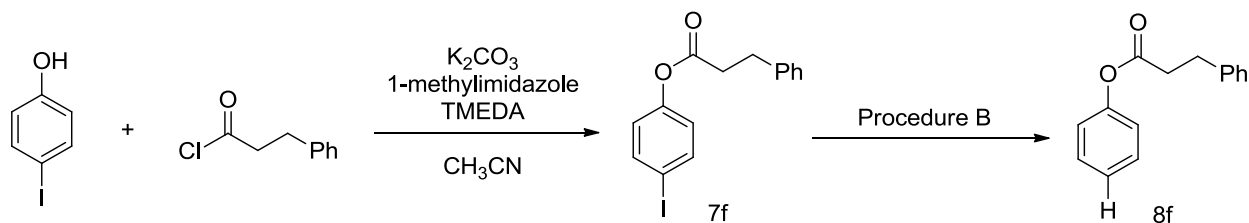
$^1\text{H}$  NMR ( $\text{CDCl}_3$ , 400 MHz):  $\delta$  8.05 (d,  $J = 8.4$  Hz, 2H), 7.56 (t,  $J = 7.3$  Hz, 1H), 7.44 (dd,  $J = 7.8$  Hz, 7.3 Hz, 2H), 3.93 (s, 3H).



**Methyl 4-aminobenzoate (Figure 2b):** According to General Procedure B, methyl 4-amino-3-iodobenzoate<sup>13</sup> (0.17 g, 0.60 mmol), tributylamine (0.71 mL, 0.56 g, 3.0 mmol), formic acid (0.11 mL, 0.14 g, 3.0 mmol) and *fac*- $\text{Ir}(\text{ppy})_3$  (4.0 mg, 6.0  $\mu\text{mol}$ ) in MeCN (6.0 mL) afforded **8e**<sup>29</sup> (84 mg, 93%) after purification by chromatography on  $\text{SiO}_2$  (50:50, hexane/EtOAc).

$R_f$  (EtOAc/hexane 2:3): 0.15;

$^1\text{H}$  NMR ( $\text{CDCl}_3$ , 400 MHz):  $\delta$  7.86 (d,  $J = 8.8$  Hz, 2H), 6.65 (d,  $J = 8.8$  Hz, 2H), 4.06 (br s, 2H), 3.86 (s, 3H).



**Phenyl 3-phenylpropanoate (Figure 2b):** According to General Procedure B, **7f** (0.21 g, 0.60 mmol), tributylamine (0.71 mL, 0.56 g, 3.0 mmol), formic acid (0.11 mL, 0.14 g, 3.0 mmol) and *fac*- $\text{Ir}(\text{ppy})_3$  (4.0 mg, 6.0  $\mu\text{mol}$ ) in MeCN (6.0 mL) afforded **8f**<sup>30</sup> (0.13 g, 95%) after purification by chromatography on  $\text{SiO}_2$  (95:5, hexane/EtOAc).

$R_f$  (EtOAc/hexane 1:4): 0.61;

$^1\text{H}$  NMR ( $\text{CDCl}_3$ , 400 MHz):  $\delta$  7.41 – 7.31 (m, 4H), 7.31 – 7.21 (m, 4H), 7.05 – 7.00 (m, 2H),

<sup>29</sup> *Tetrahedron* **2010**, *66*, 329.

<sup>30</sup> *Tetrahedron* **2010**, *66*, 7272.

3.10 (t,  $J = 7.6$  Hz, 2H), 2.91 (t,  $J = 7.6$  Hz, 2H).

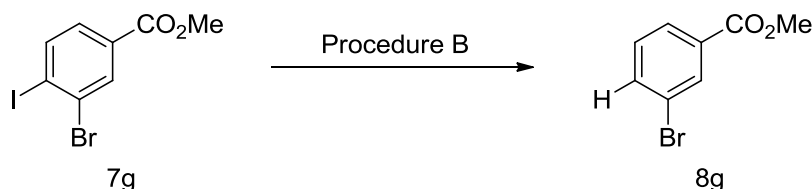
**4-iodophenyl 3-phenylpropanoate (7f):** PhCH<sub>2</sub>CH<sub>2</sub>COCl (2.5 g, 15 mmol) was added to a stirred suspension of 4-iodophenol<sup>13</sup> (2.2 g, 10 mmol), N-methylimidazole (1.23 g, 15 mmol), and TMEDA (1.74 g, 15 mmol) in CH<sub>3</sub>CN (45 mL) at 0 – 5 °C under an Ar atmosphere, and the mixture was stirred at the same temperature for 2 h. Water was added to the stirred mixture, which was extracted with EtOAc. The organic phase was washed with water and brine, dried (Na<sub>2</sub>SO<sub>4</sub>), and concentrated. The obtained crude product was purified by silica gel column chromatography (98:2, hexane/EtOAc) to give 4-iodophenyl 3-phenylpropanoate (3.0 g, 86%).

$R_f$  (EtOAc/hexane 1:20): 0.48;

IR (neat): 3087, 3062, 3029, 2922, 1753, 1479, 1195, 1166, 1123, 1054, 1007, 697 cm<sup>-1</sup>;

<sup>1</sup>H NMR (CDCl<sub>3</sub>, 400 MHz):  $\delta$  7.67 (d,  $J = 8.8$  Hz, 2H), 7.36 – 7.30 (m, 2H), 7.29 – 7.22 (m, 3H), 6.78 (d,  $J = 8.8$  Hz, 2H), 3.07 (t,  $J = 7.6$  Hz, 2H), 2.98 (t,  $J = 7.6$  Hz, 2H);

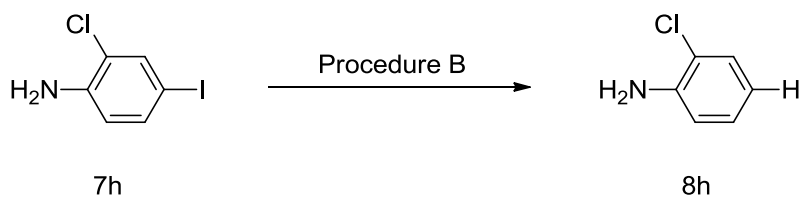
<sup>13</sup>C NMR (CDCl<sub>3</sub>, 125 MHz):  $\delta$  170.9, 150.4, 139.8, 138.3, 128.5, 128.3, 126.4, 123.7, 89.8, 35.8, 30.8.



**Methyl 3-bromobenzoate (Figure 2b):** According to General Procedure B, methyl 5-bromo-2-iodobenzoate<sup>13</sup> (0.20 g, 0.60 mmol), tributylamine (0.71 mL, 0.56 g, 3.0 mmol), formic acid (0.11 mL, 0.14 g, 3.0 mmol) and *fac*-Ir(ppy)<sub>3</sub> (4.0 mg, 6.0  $\mu$ mol) in MeCN (6.0 mL) afforded **8g**<sup>18</sup> (0.12 g, 95%) after purification by chromatography on SiO<sub>2</sub> (95:5, hexane/EtOAc).

$R_f$  (EtOAc/ hexane 1:4): 0.54;

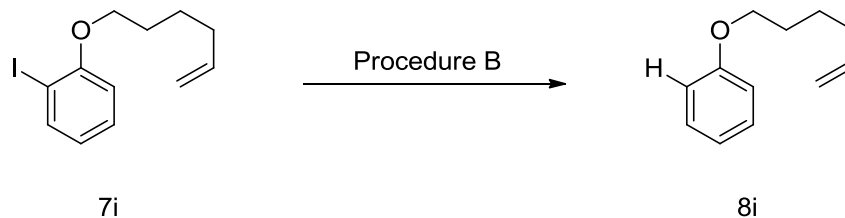
$^1\text{H}$  NMR ( $\text{CDCl}_3$ , 400 MHz):  $\delta$  8.18 (s, 1H), 7.97 (d,  $J = 7.8$  Hz, 1H), 7.68 (d,  $J = 7.8$  Hz, 1H), 7.32 (t,  $J = 7.9$  Hz, 1H), 3.92 (s, 3H).



**2-chloroaniline (Figure 2b):** According to General Procedure B, 2-chloro-4-iodoaniline<sup>13</sup> (0.20 g, 0.60 mmol), tributylamine (0.71 mL, 0.56 g, 3.0 mmol), formic acid (0.11 mL, 0.14 g, 3.0 mmol) and *fac*-Ir(ppy)<sub>3</sub> (4.0 mg, 6.0  $\mu\text{mol}$ ) in MeCN (6.0 mL) afforded **8h**<sup>31</sup> (75 mg, 98%) after purification by chromatography on  $\text{SiO}_2$  (90:10, hexane/EtOAc).

$R_f$  (EtOAc/hexane 1:4): 0.42;

$^1\text{H}$  NMR ( $\text{CDCl}_3$ , 400 MHz):  $\delta$  7.24 (d,  $J = 8.2$  Hz, 1H), 7.07 (m, 1H), 6.77 (d,  $J = 7.7$  Hz, 1H), 6.92 (m, 1H), 4.03 (br s, 2H).



**(Hex-5-en-1-yloxy)benzene (Figure 2b):** According to General Procedure B, **7i**<sup>32</sup> (0.18 g, 0.60 mmol), tributylamine (0.71 mL, 0.56 g, 3.0 mmol), formic acid (0.11 mL, 0.14 g, 3.0 mmol) and *fac*-Ir(ppy)<sub>3</sub> (4.0 mg, 6.0  $\mu\text{mol}$ ) in MeCN (6.0 mL) afforded **8i**<sup>33</sup> (0.10 g, 96%) after purification by chromatography on  $\text{SiO}_2$  (98:2, hexane/EtOAc).

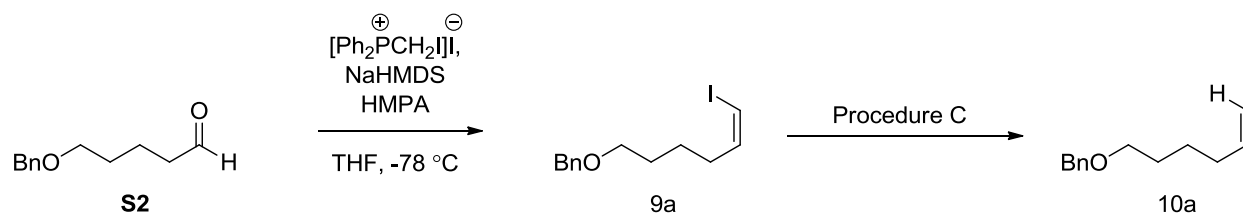
$R_f$  (EtOAc/hexane 1:19): 0.57;

<sup>31</sup> *Org. Lett.* **2008**, *10*, 1601.

<sup>32</sup> *J. Am. Chem. Soc.* **2011**, *133*, 5913.

<sup>33</sup> *J. Org. Chem.* **1991**, *56*, 1549.

$^1\text{H}$  NMR ( $\text{CDCl}_3$ , 400 MHz):  $\delta$  7.32 – 7.27 (m, 2H), 6.97 – 6.88 (m, 3H), 5.84, (ddt,  $J = 17.1$ , 10.3, 6.7 Hz, 1H), 5.08 – 4.97 (m, 2H), 3.98 (t,  $J = 6.5$ , 2H), 2.19 – 2.10 (m, 2H), 1.86 – 1.77 (m, 2H), 1.64 – 1.54 (m, 2H).



**((Hex-5-en-1-yloxy)methyl)benzene (Figure 3):** According to General Procedure C, **9a** (0.19 g, 0.60 mmol), tributylamine (1.4 mL, 1.1 g, 6.0 mmol), formic acid (0.22 mL, 0.28 g, 6.0 mmol) and *fac*-Ir(ppy)<sub>3</sub> (4.0 mg, 6.0  $\mu\text{mol}$ ) in MeCN (6.0 mL) afforded **10a**<sup>34</sup> (0.11 g, 95%) after purification by chromatography on SiO<sub>2</sub> (99:1, petroleum ether/EtOAc).

$R_f$  (hexane): 0.14;

$^1\text{H}$  NMR ( $\text{CDCl}_3$ , 400 MHz):  $\delta$  7.37 – 7.26 (m, 5H), 5.82 (ddt,  $J = 17.1$ , 10.3, 6.7 Hz, 1H), 5.05 – 4.93 (m, 2H), 4.52 (s, 2H), 3.49 (t,  $J = 6.5$ , 2H), 2.13 – 2.04 (m, 2H), 1.70 – 1.61 (m, 2H), 1.54 – 1.44 (m, 2H).

**(Z)-(((6-iodohex-5-en-1-yl)oxy)methyl)benzene (9a):** A slurry of iodo methyltriphenylphosphonium iodide<sup>35</sup> (0.57 g, 1.1 mmol) in THF (5 mL) at room temperature was treated, dropwise, with a 1.0 M solution of NaHMDS (1.1 mL, 1.1 mmol) in THF. The resultant red-orange solution was stirred for 30 min at room temperature, cooled to  $-78$   $^\circ\text{C}$ , and treated with HMPA (0.94 mL, 5.4 mmol) and a solution of **S2**<sup>36</sup> (0.21 g, 1.1 mmol) in THF (5 mL). After 3 h at  $-78$   $^\circ\text{C}$ , the mixture was quenched by saturated aqueous NaHCO<sub>3</sub> (1 mL) and diluted with Et<sub>2</sub>O (20 mL), and the resultant slurry was filtered through a pad of Celite. The

<sup>34</sup> *Synthesis* **2006**, 23, 4041.

<sup>35</sup> *Tetrahedron* **2003**, 59, 1719.

<sup>36</sup> *J. Org. Chem.* **2010**, 75, 8307.

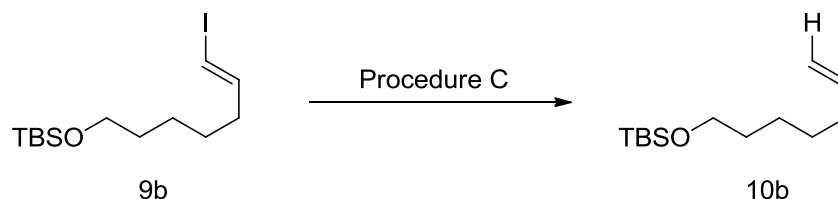
biphasic filtrate was separated, the organic phase was dried (Na<sub>2</sub>SO<sub>4</sub>) and concentrated, and the crude product was purified via column chromatography eluting with EtOAc/hexane (2:98) to give 0.21 g (60%) of **9a** as an inseparable mixture (1:8.5) of *E,Z*-vinyl iodide isomers, respectively.

*R<sub>f</sub>* (EtOAc/hexane 1:9): 0.66;

IR (neat): 3298, 3063, 3029, 2934, 2856, 1608, 1452, 1360, 1276, 1203, 1103, 1028, 733, 696 cm<sup>-1</sup>;

<sup>1</sup>H NMR (CDCl<sub>3</sub>, 400 MHz): δ 7.37 – 7.26 (m, 5H), 6.22 – 6.14 (m, 2H), 4.52 (s, 2H), 3.50 (t, *J* = 6.4, 2H), 2.21 – 2.14 (m, 2H), 1.72 – 1.62 (m, 2H), 1.59 – 1.50 (m, 2H);

<sup>13</sup>C NMR (CDCl<sub>3</sub>, 125 MHz): δ 141.0, 138.5, 128.3, 127.5, 127.4, 82.5, 72.8, 70.0, 34.4, 29.1, 24.6.



***tert*-butyl(hept-6-en-1-yloxy)dimethylsilane (Figure 3)**: According to General Procedure C, **9b**<sup>37</sup> (0.21 g, 0.60 mmol), tributylamine (1.4 mL, 1.1 g, 6.0 mmol), formic acid (0.22 mL, 0.28 g, 6.0 mmol) and *fac*-Ir(ppy)<sub>3</sub> (4.0 mg, 6.0 μmol) in MeCN (6.0 mL) afforded **10b** (0.13 g, 92%) after purification by chromatography on SiO<sub>2</sub> (petroleum ether).

*R<sub>f</sub>* (hexane): 0.26;

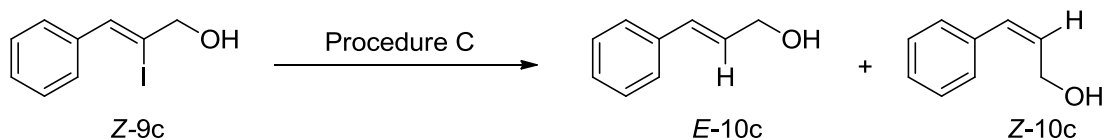
IR (neat): 2928, 2857, 1472, 1462, 1255, 1100, 908, 833, 773 cm<sup>-1</sup>;

<sup>1</sup>H NMR (CDCl<sub>3</sub>, 400 MHz): δ 5.82 (ddt, *J* = 17.0, 10.2, 6.7 Hz, 1H), 5.04 – 4.92 (m, 2H), 3.61 (t, *J* = 6.6, 2H), 2.10 – 2.02 (m, 2H), 1.56 – 1.28 (m, 2H), 1.45 – 1.29 (m, 4H), 0.90 (s, 9H), 0.06

<sup>37</sup> *Bioorg. Med. Chem. Lett.* **2010**, *20*, 4555.

(s, 6H);

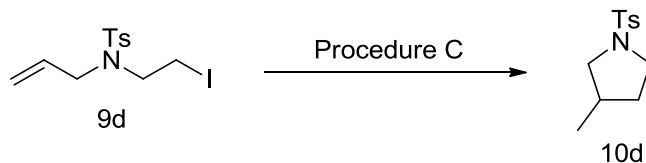
$^{13}\text{C}$  NMR ( $\text{CDCl}_3$ , 125 MHz):  $\delta$  138.9, 114.2, 63.2, 32.8, 32.7, 28.7, 26.0, 25.3, 18.3, -5.3.



**(E)-Cinnamyl alcohol (Figure 3):** According to General Procedure C, **(Z)-9c**<sup>38</sup> (0.16 g, 0.60 mmol), tributylamine (1.4 mL, 1.1 g, 6.0 mmol), formic acid (0.22 mL, 0.28 g, 6.0 mmol) and *fac*-Ir(ppy)<sub>3</sub> (4.0 mg, 6.0  $\mu\text{mol}$ ) in MeCN (6.0 mL) afforded **(E)-10c**<sup>39</sup> and **(Z)-10c**<sup>40</sup> in a 1:0.75 diastereomeric ratio<sup>41</sup> (81 mg, 99%) after purification by chromatography on SiO<sub>2</sub> (75:25, hexane/EtOAc).

$R_f$  (EtOAc/hexane 1:4): 0.14;

$^1\text{H}$  NMR ( $\text{CDCl}_3$ , 400 MHz):  $\delta$  7.44 – 7.38 (m, 2H), 7.37 – 7.31 (m, 2H), 7.30 – 7.24 (m, 1H), 6.62 (d,  $J$  = 15.9 Hz, 1H), 6.38 (dt,  $J$  = 15.9, 5.7 Hz, 1H), 4.32 (dd,  $J$  = 5.7, 1.5 Hz, 2H), 1.51 (br s, 1H).



**3-Methyl-1-tosylpyrrolidine (Figure 3):** According to General Procedure C, **9d**<sup>42</sup> (0.22 g, 0.60 mmol), tributylamine (1.4 mL, 1.1 g, 6.0 mmol), formic acid (0.22 mL, 0.28 g, 6.0 mmol) and *fac*-Ir(ppy)<sub>3</sub> (4.0 mg, 6.0  $\mu\text{mol}$ ) in MeCN (6.0 mL) afforded **10d**<sup>11</sup> (0.11 g, 78%) after purification by chromatography on SiO<sub>2</sub> (96:4, petroleum ether/EtOAc).

<sup>38</sup> *J. Org. Chem.* **2002**, *67*, 831.

<sup>39</sup> *J. Org. Chem.* **2005**, *70*, 4118.

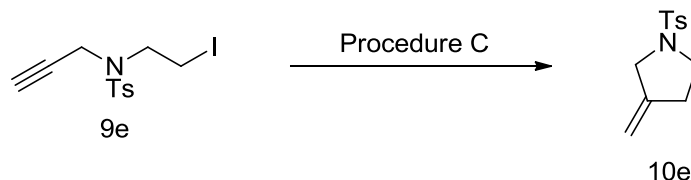
<sup>40</sup> *Chem. Commun.* **2010**, *46*, 568.

<sup>41</sup> Diastereomeric ratio is time dependent.

<sup>42</sup> *Tetrahedron* **2006**, *62*, 2207.

$R_f$  (EtOAc/hexane 1:9): 0.47;

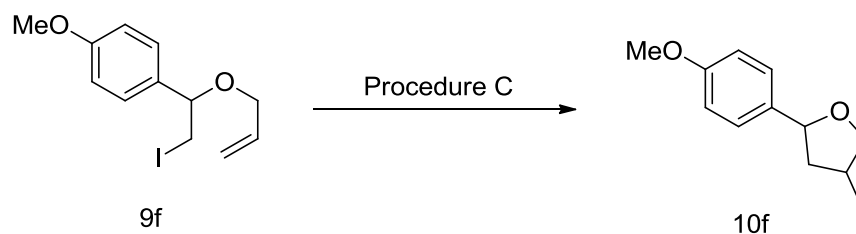
$^1\text{H NMR}$  ( $\text{CDCl}_3$ , 400 MHz):  $\delta$  7.72 (d,  $J = 8.4$  Hz, 2H), 7.33 (d,  $J = 8.4$  Hz, 2H), 3.43 (dd,  $J = 9.5, 7.1$  Hz, 1H), 3.35 (ddd,  $J = 9.8, 8.3, 4.2$  Hz, 1H), 3.27–3.19 (m, 1H), 2.76 (dd,  $J = 9.7, 7.7$  Hz, 1H), 2.44 (s, 3H), 2.19–2.07 (m, 1H), 1.96–1.86 (m, 1H), 1.42–1.31 (m, 1H), 0.93 (d,  $J = 6.7$  Hz, 3H).



**3-methylene-1-tosylpyrrolidine (Figure 3):** According to General Procedure C, **9e**<sup>43</sup> (0.22 g, and *fac*-Ir(ppy)<sub>3</sub> (4.0 mg, 6.0  $\mu\text{mol}$ ) in MeCN (6.0 mL) afforded **10e**<sup>44</sup> (0.11 g, 77%) after purification by chromatography on SiO<sub>2</sub> (90:10, petroleum ether/EtOAc).

$R_f$  (EtOAc/hexane 1:4): 0.35;

$^1\text{H NMR}$  ( $\text{CDCl}_3$ , 400 MHz):  $\delta$  7.72 (d,  $J = 8.3$  Hz, 2H), 7.34 (d,  $J = 8.3$  Hz, 2H), 4.95 – 4.89 (m, 2H), 3.80 – 3.76 (m, 2H), 3.29 (t,  $J = 7.1$  Hz, 2H), 2.52 – 2.45 (m, 2H), 2.44 (s, 3H).



**Tetrahydro-2-(4-methoxyphenyl)-4-methylfuran (Figure 3):** According to General Procedure C, **9f**<sup>45</sup> (0.19 g, 0.60 mmol), tributylamine (1.4 mL, 1.1 g, 6.0 mmol), formic acid (0.22 mL, 0.28 g, 6.0 mmol) and *fac*-Ir(ppy)<sub>3</sub> (4.0 mg, 6.0  $\mu\text{mol}$ ) in MeCN (6.0 mL) afforded **10f**<sup>35</sup> (92 mg,

<sup>43</sup> *Org. Lett.* **2011**, *13*, 2050.

<sup>44</sup> *J. Am. Chem. Soc.* **2007**, *129*, 12916.

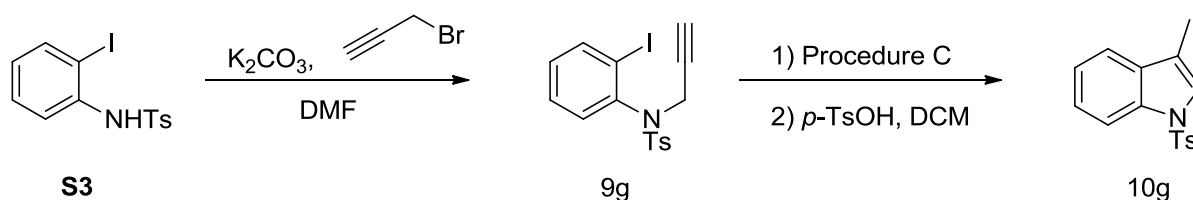
<sup>45</sup> *Angew. Chem., Int. Ed.* **2005**, *44*, 1356.

80%) as a mixture of diastereomers (6.7:1) after purification by chromatography on SiO<sub>2</sub> (90:10, hexane/EtOAc).

*R<sub>f</sub>* (EtOAc/hexane 1:4): 0.49;

Major isomer:

<sup>1</sup>H NMR (CDCl<sub>3</sub>, 400 MHz): δ 7.25 (d, *J* = 8.7 Hz, 2H), 6.87 (d, *J* = 8.7 Hz, 2H), 4.99 (t, *J* = 6.9 Hz, 1H), 4.21 (t, *J* = 7.6 Hz, 1H), 3.81 (s, 3H), 3.45 (t, *J* = 7.6 Hz, 1H), 2.51 – 2.38 (m, 1H), 2.04 – 1.87 (m, 2H) 1.10 (d, *J* = 6.7 Hz, 3H).



**3-methyl-1-tosyl-1H-indole (Figure 3):** According to General Procedure C, **9g** (0.19 g, 0.60 mmol), tributylamine (1.4 mL, 1.1 g, 6.0 mmol), formic acid (0.22 mL, 0.28 g, 6.0 mmol) and *fac*-Ir(ppy)<sub>3</sub> (4.0 mg, 6.0 μmol) in MeCN (6.0 mL) afforded **10g**<sup>46</sup> (0.11 g, 63%) after stirring the crude reaction mixture with *p*-TsOH (6.0 mmol) in DCM overnight and purification by chromatography on SiO<sub>2</sub> (95:5, petroleum ether/EtOAc).

*R<sub>f</sub>* (EtOAc/hexane 1:9): 0.33;

<sup>1</sup>H NMR (CDCl<sub>3</sub>, 400 MHz): δ 7.98 (d, *J* = 8.2 Hz, 1H), 7.74 (d, *J* = 8.3 Hz, 2H), 7.44 (d, *J* = 7.6 Hz, 1H), 7.28 – 7.33 (m, 2H), 7.20 – 7.26 (m, 1H), 7.19 (d, *J* = 8.3 Hz, 2H), 2.32 (s, 3H), 2.24 (d, *J* = 1.2 Hz, 3H).

**N-(2-iodophenyl)-4-methyl-N-(prop-2-yn-1-yl)benzenesulfonamide (9g):** To a solution of **S3**<sup>47</sup> (0.37 g, 1.0 mmol) in DMF (10 mL) at room temperature was added K<sub>2</sub>CO<sub>3</sub> (0.41 g, 3.0

<sup>46</sup> *Chin. J. Chem.* **2010**, *28*, 125.

<sup>47</sup> *J. Am. Chem. Soc.* **2005**, *127*, 13148.



mmol) and propargyl bromide (0.18 g, 1.5 mmol). The reaction mixture was stirred overnight, filtered, and partitioned between EtOAc and H<sub>2</sub>O. The organic phase was washed several times with water, washed once with brine, dried (Na<sub>2</sub>SO<sub>4</sub>) and concentrated. The crude product was purified via column chromatography eluting with EtOAc/hexane (10:90) to give 0.21 g (86%) of **9g**.

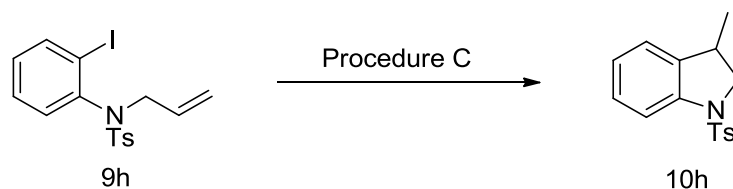
$R_f$  (EtOAc/hexane 1:9): 0.23;

IR (neat): 3294, 3061, 2922, 2254, 2120, 1465, 1351, 1160, 1092, 1020, 855, 733, 713, 658 cm<sup>-1</sup>;

<sup>1</sup>H NMR (CDCl<sub>3</sub>, 400 MHz):  $\delta$  7.94 – 7.90 (m, 1H), 7.72 (d,  $J$  = 8.2 Hz, 2H), 7.30 (d,  $J$  = 8.2 Hz, 2H), 7.31 – 7.27 (m, 1H), 7.17 – 7.12 (m, 1H), 7.10 – 7.07 (m, 1H), 4.78 (dd,  $J$  = 18.2, 2.3 Hz, 1H), 4.13 (dd,  $J$  = 18.2, 2.3 Hz, 1H), 2.46 (s, 3H), 2.17 (t,  $J$  = 2.3 Hz, 1H);

<sup>13</sup>C NMR (CDCl<sub>3</sub>, 125 MHz):  $\delta$  143.9, 140.5, 140.1, 136.5, 131.1, 130.4, 129.4, 128.7, 128.2, 102.5, 77.5, 74.1, 40.6, 21.5;

HRMS (ESI)  $m/z$  calculated for C<sub>16</sub>H<sub>14</sub>INO<sub>2</sub>S<sup>+</sup> ([M+H]<sup>+</sup>) 411.9868, found 411.9883.



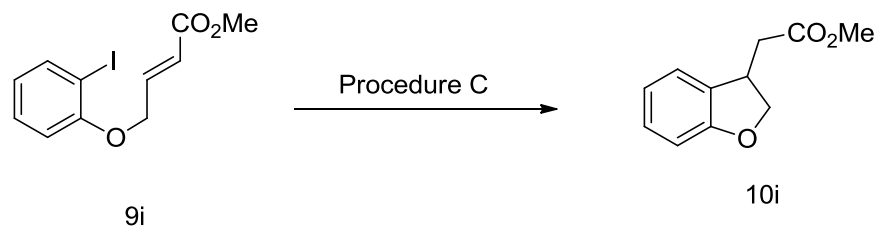
**3-methyl-1-tosylindoline (Figure 3)**: According to General Procedure C, **9h**<sup>48</sup> (0.25 g, 0.60 mmol), tributylamine (1.4 mL, 1.1 g, 6.0 mmol), formic acid (0.22 mL, 0.28 g, 6.0 mmol) and *fac*-Ir(ppy)<sub>3</sub> (4.0 mg, 6.0  $\mu$ mol) in MeCN (6.0 mL) afforded **10h**<sup>49</sup> (0.12 g, 71%) after purification by chromatography on SiO<sub>2</sub> (95:5, petroleum ether/EtOAc).

$R_f$  (EtOAc/hexane 1:9): 0.33;

<sup>48</sup> *Asia-Pac. J. Chem. Eng.* **2009**, *4*, 821.

<sup>49</sup> *Org. Lett.* **2004**, *6*, 2213.

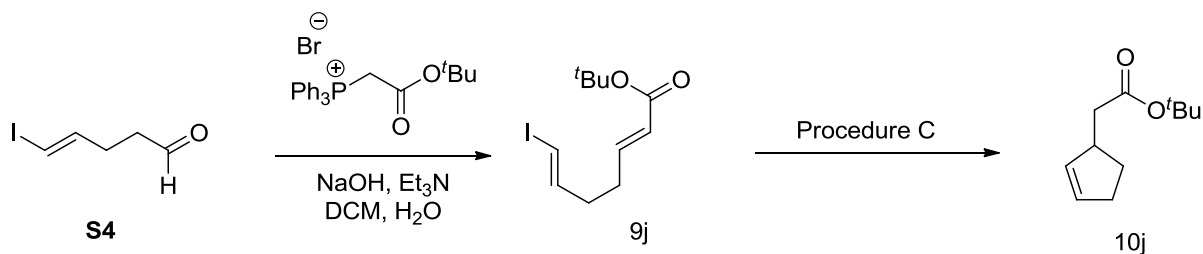
$^1\text{H}$  NMR ( $\text{CDCl}_3$ , 400 MHz):  $\delta$  7.68 (d,  $J = 8.4$  Hz, 2H), 7.64 (d,  $J = 8.4$  Hz, 1H), 7.26 – 7.16 (m, 3H), 7.08 – 6.96 (m, 2H), 4.08 (dd,  $J = 8.6, 10.4$  Hz, 1H), 3.42 (dd,  $J = 7.0, 10.4$  Hz, 1H), 3.19 (dq,  $J = 8.6, 7.0$  Hz, 1H), 2.36 (s, 3H), 1.11 (d,  $J = 7.0$  Hz, 3H).



**Methyl 2-(2,3-dihydrobenzofuran-3-yl)acetate (Figure 3):** According to General Procedure C, **9i**<sup>50</sup> (0.19 g, 0.60 mmol), tributylamine (1.4 mL, 1.1 g, 6.0 mmol), formic acid (0.22 mL, 0.28 g, 6.0 mmol) and *fac*-Ir(ppy)<sub>3</sub> (4.0 mg, 6.0  $\mu\text{mol}$ ) in MeCN (6.0 mL) afforded **10i**<sup>40</sup> (99 mg, 86%) after purification by chromatography on SiO<sub>2</sub> (90:10, hexane/EtOAc).

$R_f$  (EtOAc/hexane 1:4): 0.40;

$^1\text{H}$  NMR ( $\text{CDCl}_3$ , 400 MHz):  $\delta$  7.12 (t,  $J = 7.5$  Hz, 2H), 6.83 (t,  $J = 7.5$  Hz, 1H), 6.77 (d,  $J = 8.1$  Hz, 1H), 4.71 (t,  $J = 8.1$  Hz, 1H), 4.21 (dd,  $J = 9.2, 6.3$  Hz, 1H), 3.90 – 3.78 (m, 1H), 3.69 (s, 3H), 2.77 (dd,  $J = 16.4, 5.3$  Hz, 1H), 2.55 (dd,  $J = 16.4, 9.5$  Hz, 1H).



**tert-Butyl 2-(cyclopent-2-en-1-yl)acetate (Figure 3):** According to General Procedure C, **9j** (0.18 g, 0.60 mmol), tributylamine (1.4 mL, 1.1 g, 6.0 mmol), formic acid (0.22 mL, 0.28 g, 6.0 mmol) and *fac*-Ir(ppy)<sub>3</sub> (4.0 mg, 6.0  $\mu\text{mol}$ ) in MeCN (6.0 mL) afforded **10j** (66 mg, 60%) after

<sup>50</sup> *J. Am. Chem. Soc.* **1998**, *120*, 4934.

purification by chromatography on SiO<sub>2</sub> (98:2, petroleum ether/EtOAc).

*R<sub>f</sub>* (EtOAc/ hexane 1:49): 0.30;

IR (neat): 3051, 2977, 2934, 2853, 1729, 1367, 1260, 1161, 1141 cm<sup>-1</sup>;

<sup>1</sup>H NMR (CDCl<sub>3</sub>, 400 MHz): δ 5.78 – 5.73 (m, 1H), 5.69 – 5.65 (m, 1H), 3.11 – 2.98 (m, 1H), 2.43 – 2.04 (m, 6H), 1.46 (s, 9H).

<sup>13</sup>C NMR (CDCl<sub>3</sub>, 125 MHz): δ 172.3, 133.9, 131.2, 80.1, 42.3, 41.8, 31.8, 29.5, 28.1.

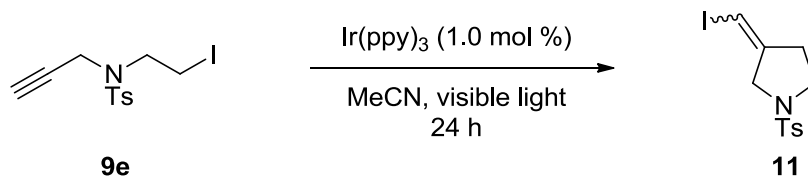
**(2*E*,6*E*)-tert-Butyl 7-iodohepta-2,6-dienoate (9j)**: To a solution of (*E*)-5-iodopent-4-enal (S4)<sup>51</sup> (0.83 g, 3.9 mmol) in CH<sub>2</sub>Cl<sub>2</sub> (32 mL) and H<sub>2</sub>O (16 mL) was added (*tert*-butoxycarbonylmethyl)triphenylphosphonium bromide (1.8 g, 4.0 mmol), NaOH (0.32 g, 7.9 mmol) and Et<sub>3</sub>N (1.7 mL, 11.9 mmol) at room temperature. After stirring at room temperature for 1 hr, the organic phase was separated and washed with 1 N HCl (30 mL) and saturated aqueous NaHCO<sub>3</sub> (30 mL). The organic phase was dried over Na<sub>2</sub>SO<sub>4</sub>, filtered, and concentrated to give a crude product, which was purified by flash column chromatography (99:1, petroleum ether/ether) to afford pure product **9j** (0.50 g, 41%).

*R<sub>f</sub>* (EtOAc/hexane 1:4): 0.79;

IR (neat): 2977, 2931, 1709, 1653, 1366, 1288, 1140, 976, 948, 850 cm<sup>-1</sup>;

<sup>1</sup>H NMR (CDCl<sub>3</sub>, 400 MHz): δ 6.82 (dt, *J* = 15.6, 6.6 Hz, 1H), 6.51 (dt, *J* = 14.6, 6.8 Hz, 1H), 6.08 (dt, *J* = 14.6, 1.3 Hz, 1H), 5.77 (dt, *J* = 15.6, 1.5 Hz, 1H), 2.33 – 2.17 (m, 4H), 1.49 (s, 9H).

<sup>13</sup>C NMR (CDCl<sub>3</sub>, 125 MHz): δ 165.7, 145.7, 144.7, 123.9, 80.2, 75.8, 34.4, 30.7, 28.1.



<sup>51</sup> *Org. Lett.*, **2010**, *12*, 340.

A flame dried 10 mL round bottom flask with a rubber septum and magnetic stir bar was charged with **9e** (0.22 g, 0.60 mmol), MeCN (6.0 mL), and *fac*-Ir(ppy)<sub>3</sub> (4.0 mg, 6.0 μmol). The heterogenous mixture was degassed by argon sparging for 30 min and placed in a 250 mL beaker with blue or white LEDs wrapped inside. The reaction mixture was stirred at 25–30 °C for 24 h. The solvent was removed from the crude mixture *in vacuo* and the residue was purified by chromatography on silica gel to afford **11** (99 mg, 86%) after purification by chromatography on SiO<sub>2</sub> (90:10, hexane/EtOAc).

Data for major isomer:

*R<sub>f</sub>* (EtOAc/ hexane 1:9): 0.15;

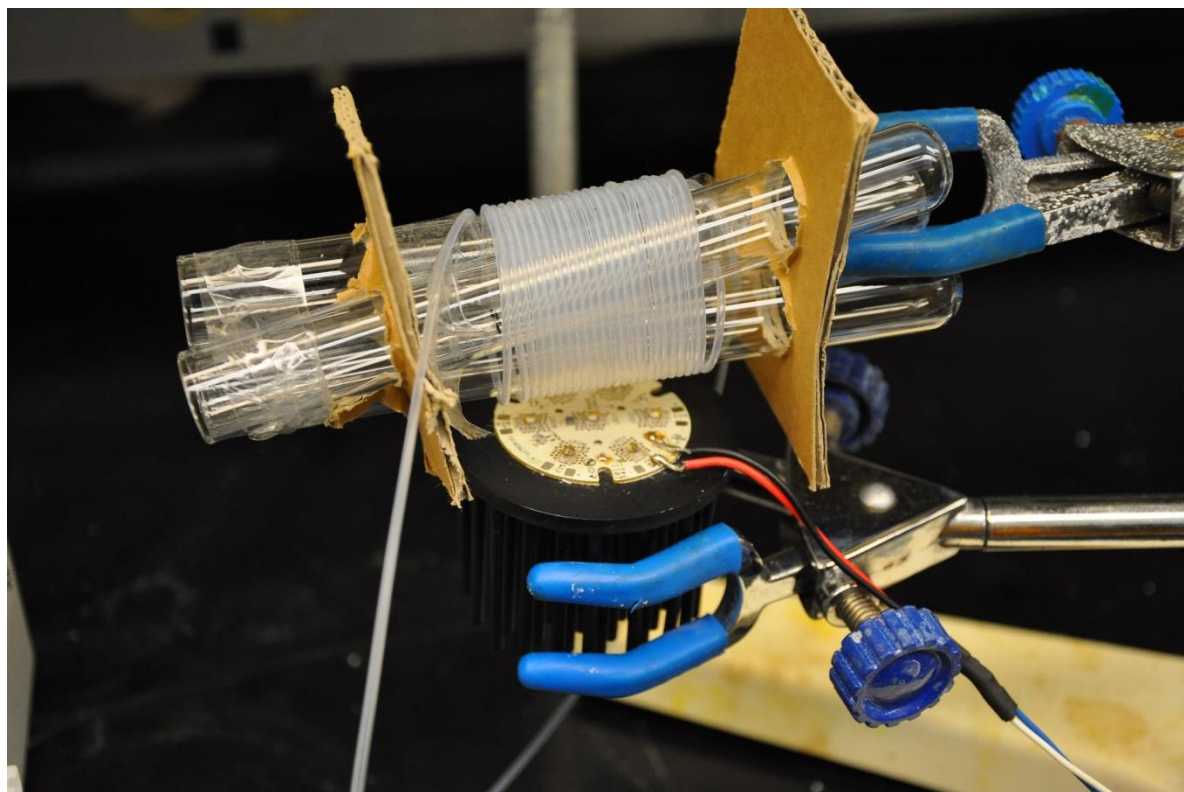
IR (neat): 3062, 2924, 2856, 1597, 1347, 1162, 1092, 1034, 662 cm<sup>-1</sup>;

<sup>1</sup>H NMR (CDCl<sub>3</sub>, 400 MHz): δ 7.74 (d, *J* = 8.2 Hz, 2H), 7.36 (d, *J* = 8.2 Hz, 2H), 6.03 – 5.99 (m, 1H), 3.73 (s, 2H), 3.42 (t, *J* = 6.9 Hz, 1H), 2.56 – 2.50 (m, 2H), 2.46 (s, 3H).

<sup>13</sup>C NMR (CDCl<sub>3</sub>, 125 MHz): δ 143.9, 140.5, 140.1, 136.5, 131.1, 130.4, 129.4, 128.7, 128.2, 102.5, 77.5, 74.1, 40.6, 21.5.

HRMS (ESI) *m/z* calculated for C<sub>12</sub>H<sub>14</sub>INO<sub>2</sub>S<sup>+</sup> ([M+H]<sup>+</sup>) 363.9868, found 363.9865.

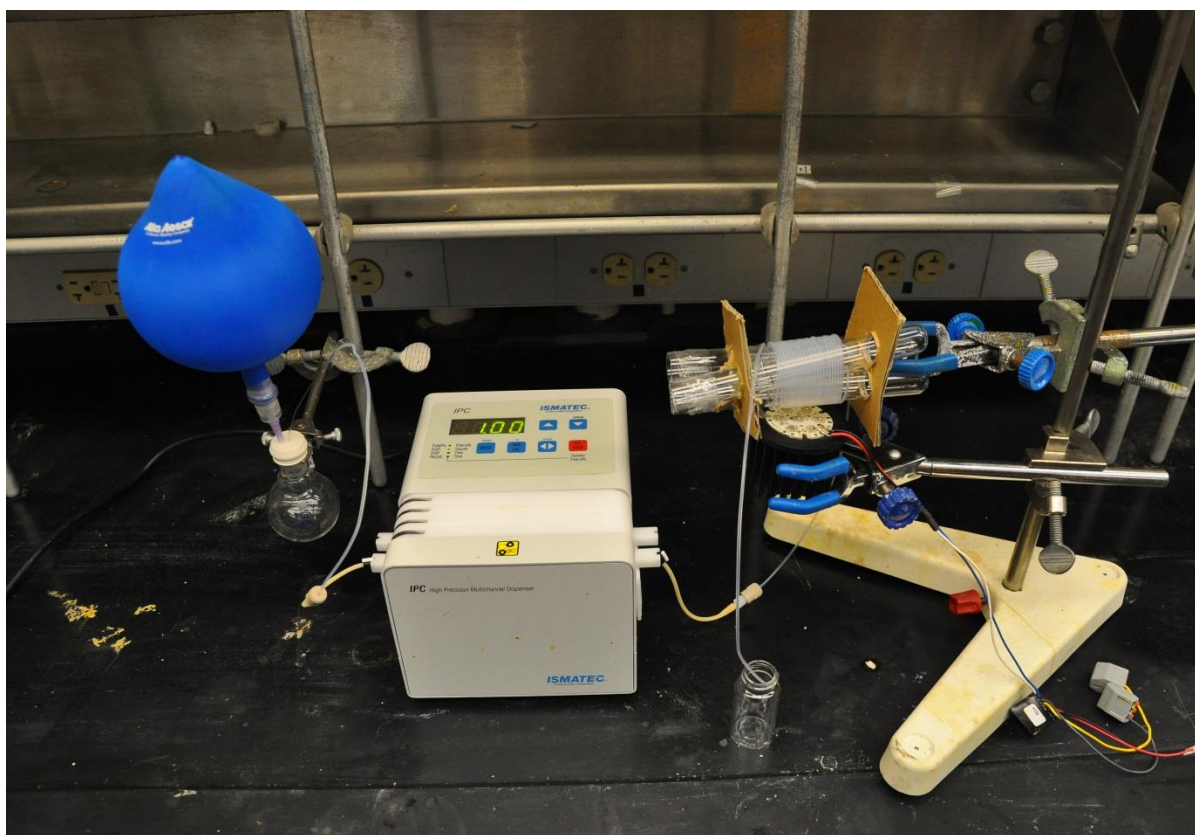
## Reaction Apparatus



A photograph of the assembled photoreactor is shown in Figure S-1. The LED assembly (5.88 W) consists of 7 prearranged Luxeon Rebel high power LEDs (royal blue color,  $\lambda_{\text{max}} = 447.5 \text{ nm}$ ) (<http://www.luxeonstar.com/Royal-Blue-447-5nm-7-LED-40mm-Round-Assembly-p/sr-02-r0425.htm>). This is mounted to a heat sink to dissipate any heat generated by the LEDs (<http://www.luxeonstar.com/60mm-Round-Alpha-Heat-Sink-p/cn60-45b.htm>) and powered by a 24V power supply (<http://www.ledsupply.com/24vdc17a.php>). To support the tubing, three flint glass test tubes were supported at both ends by small pieces of cardboard. The PFA Tubing (IDEX Health and Science, Part # 1514L) is wrapped around and between the tubes so that a total volume of 1.34 mL is placed on the test tubes. This is done so that the total length of the coils does not exceed the size of the LED apparatus (4.0 cm). The tubing is secured in place by a

small piece of tape. The coiled tubing is then suspended approximately 2 cm above the LED apparatus.

The photoreactor tubing is then connected to the peristaltic pump tubing (IDEX Health and Science, Part # SC0717) by means of a conical adapter (IDEX Health and Science, Part # P-797) which contains the appropriate female nut, ferrule and washer. Likewise another short piece of PFA tubing, for delivery of the reaction mixture, was connected to the other end of the peristaltic pump tubing and fitted with a 20 gauge needle to pierce the septum of the reaction flask. Figure S-2 depicts the assembled reactor. During the operation of the flow reactor a sheet of aluminum foil is placed around the reaction apparatus due to the brightness of the LEDs.



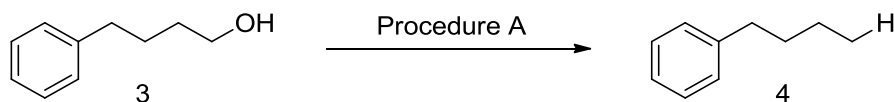
### General Procedure A

A flame dried 10 mL round bottom flask with a rubber septum and magnetic stir bar was charged with the corresponding alkyl alcohol (1.0 mmol, 1.0 equiv), MeCN (5.0 mL), triphenylphosphine (1.2 mmol, 1.2 equiv), and imidazole (1.2 mmol, 1.2 equiv). The reaction mixture is cooled in an ice bath to 0 °C and iodine (1.2 mmol, 1.2 equiv) is added in portions. After 0.5 h, the reaction is removed from the ice bath and stirred at room temperature until the alcohol is fully consumed (as judged by TLC analysis). *N,N*-Diisopropylethylamine (10 mmol, 10 equiv), methanol (0.2 mL), and *fac*-Ir(ppy)<sub>3</sub> (0.0025 mmol, 0.0025 equiv) are added to the reaction mixture and stirred until a homogenous solution is formed. The reaction mixture is then pumped through the photoreactor at a flow rate to achieve a residence time of 18 min. The solvent was removed from the crude mixture *in vacuo* and was dissolved in a minimal amount of EtOAc before being passed through a bed of silica gel and eluted with diethyl ether. The filtrate was concentrated and the crude product was purified by chromatography on silica gel, using the solvent system indicated, to afford the desired product.

### General Procedure B

A flame dried 10 mL round bottom flask with a rubber septum and magnetic stir bar was charged with the corresponding alkyl alcohol (1.0 mmol, 1.0 equiv), MeCN (5.0 mL), triphenylphosphine (1.5 mmol, 1.5 equiv), and imidazole (2.0 mmol, 2.0 equiv). The reaction mixture is cooled in an ice bath to 0 °C and iodine (1.5 mmol, 1.5 equiv) is added in portions. After 0.5 h, the reaction is removed from the ice bath and stirred at room temperature until the alcohol is fully consumed (as judged by TLC analysis). *N,N*-Diisopropylethylamine (10 mmol, 10 equiv), methanol (0.2 mL), and *fac*-Ir(ppy)<sub>3</sub> (0.0025 mmol, 0.0025 equiv) are added to the reaction mixture and stirred until a homogenous solution is formed. The reaction mixture is then pumped through the photoreactor

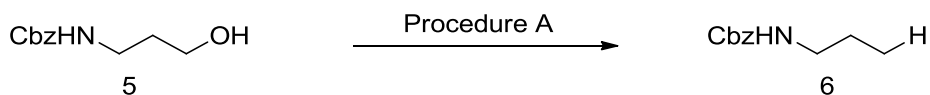
at a flow rate to achieve a residence time of 18 min. The solvent was removed from the crude mixture *in vacuo* and was dissolved in a minimal amount of EtOAc before being passed through a bed of silica gel and eluted with diethyl ether. The filtrate was concentrated and the crude product was purified by chromatography on silica gel, using the solvent system indicated, to afford the desired product.



**Butylbenzene:** According to General Procedure A, **3**<sup>52</sup> (0.15 g, 1.0 mmol), triphenylphosphine (0.32 g, 1.2 mmol), imidazole (82 mg, 1.2 mmol), and iodine (0.30 g, 1.2 mmol) in MeCN (5.0 mL) was stirred overnight. After full consumption of the alcohol *N,N*-Diisopropylethylamine (1.7 mL, 10 mmol), methanol (0.2 mL), and *fac*-Ir(ppy)<sub>3</sub> (1.6 mg, 0.0025 mmol) are added and the reaction mixture is pumped through the photoreactor at a flow rate to achieve a residence time of 18 min which afforded **4**<sup>53</sup> (99 mg, 74%) as a colorless oil after purification by chromatography on SiO<sub>2</sub> (petroleum ether).

*R<sub>f</sub>*(hexanes): 0.54;

<sup>1</sup>H NMR (CDCl<sub>3</sub>, 400 MHz): δ 7.33 – 7.29 (m, 2H), 7.23 – 7.18 (m, 3H), 2.65 (t, *J* = 8.0 Hz, 2H), 1.68 – 1.60 (m, 2H), 1.44 – 1.36 (m, 2H), 0.97 (t, *J* = 7.3 Hz, 3H).



**Benzyl propylcarbamate:** According to General Procedure A, **5**<sup>54</sup> (0.20 g, 1.0 mmol), triphenylphosphine (0.32 g, 1.2 mmol), imidazole (82 mg, 1.2 mmol), and iodine (0.30 g, 1.2

<sup>52</sup> Commercially available from Sigma Aldrich.

<sup>53</sup> *Tetrahedron* **2009**, *65*, 10637.

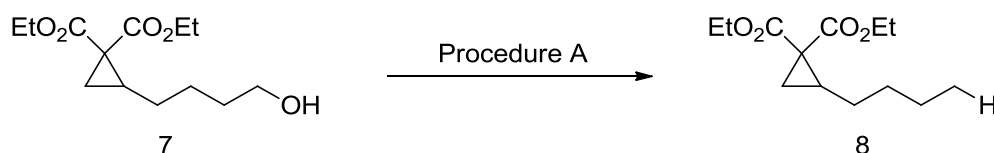
<sup>54</sup> Characterization and preparation of substrate **5** is reported in *Can. J. Chem.* **2009**, *87*, 393.



mmol) in MeCN (5.0 mL) was stirred overnight. After full consumption of the alcohol *N,N*-Diisopropylethylamine (1.7 mL, 10 mmol), methanol (0.2 mL), and *fac*-Ir(ppy)<sub>3</sub> (1.6 mg, 0.0025 mmol) are added and the reaction mixture is pumped through the photoreactor at a flow rate to achieve a residence time of 18 min which afforded **6**<sup>55</sup> (0.16 g, 81%) as a colorless oil after purification by chromatography on SiO<sub>2</sub> (95:5, hexanes/EtOAc).

*R<sub>f</sub>*(EtOAc/hexane 1:4): 0.42;

<sup>1</sup>H NMR (CDCl<sub>3</sub>, 400 MHz): δ 7.38 – 7.30 (m, 5H), 5.10 (s, 2H), 3.21 – 3.13 (m, 2H), 1.60 – 1.48 (m, 2H), 0.93 (t, *J* = 7.4 Hz, 3H).



**Diethyl 2-butylcyclopropane-1,1-dicarboxylate:** According to General Procedure A, **7**<sup>56</sup> (0.26 g, 1.0 mmol), triphenylphosphine (0.32 g, 1.2 mmol), imidazole (82 mg, 1.2 mmol), and iodine (0.30 g, 1.2 mmol) in MeCN (5.0 mL) was stirred overnight. After full consumption of the alcohol *N,N*-Diisopropylethylamine (1.7 mL, 10 mmol), methanol (0.2 mL), and *fac*-Ir(ppy)<sub>3</sub> (1.6 mg, 0.0025 mmol) are added and the reaction mixture is pumped through the photoreactor at a flow rate to achieve a residence time of 18 min which afforded **8**<sup>57</sup> (0.21 g, 87%) as a colorless oil after purification by chromatography on SiO<sub>2</sub> (95:5, hexanes/EtOAc).

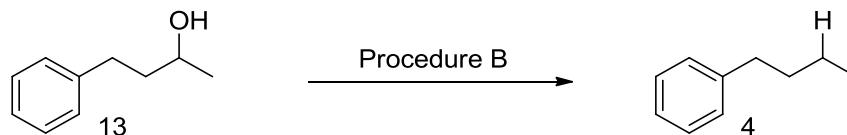
*R<sub>f</sub>*(EtOAc/hexanes 1:9): 0.50;

<sup>1</sup>H NMR (CDCl<sub>3</sub>, 400 MHz): δ 4.31 – 4.09 (m, 4H), 1.93 – 1.84 (m, 1H), 1.53 – 1.14 (m, 14H), 0.89 (t, *J* = 7.1 Hz, 3H).

<sup>55</sup> *Tetrahedron* **2000**, *56*, 8433.

<sup>56</sup> Characterization and preparation of substrate **7** is reported in *J. Am. Chem. Soc.* **2011**, *133*, 4160-4163.

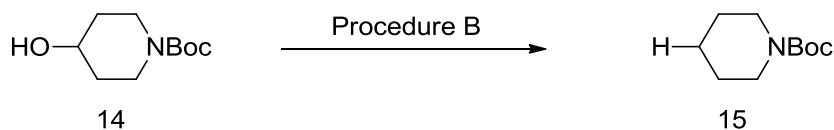
<sup>57</sup> *Eur. J. Med. Chem.* **2010**, *45*, 3818-3830.



**Butylbenzene:** According to General Procedure B, **13**<sup>52</sup> (0.15 g, 1.0 mmol), triphenylphosphine (0.39 g, 1.5 mmol), imidazole (0.14 g, 2.0 mmol), and iodine (0.38 g, 1.5 mmol) in MeCN (5.0 mL) was stirred overnight. After full consumption of the alcohol *N,N*-Diisopropylethylamine (1.7 mL, 10 mmol), methanol (0.2 mL), and *fac*-Ir(ppy)<sub>3</sub> (1.6 mg, 0.0025 mmol) are added and the reaction mixture is pumped through the photoreactor at a flow rate to achieve a residence time of 18 min which afforded **4** (0.10 g, 78%) as a colorless oil after purification by chromatography on SiO<sub>2</sub> (petroleum ether).

*R<sub>f</sub>*(hexanes): 0.54;

<sup>1</sup>H NMR (CDCl<sub>3</sub>, 400 MHz): δ 7.33 – 7.29 (m, 2H), 7.23 – 7.18 (m, 3H), 2.65 (t, *J* = 8.0 Hz, 2H), 1.68 – 1.60 (m, 2H), 1.44 – 1.36 (m, 2H), 0.97 (t, *J* = 7.3 Hz, 3H).

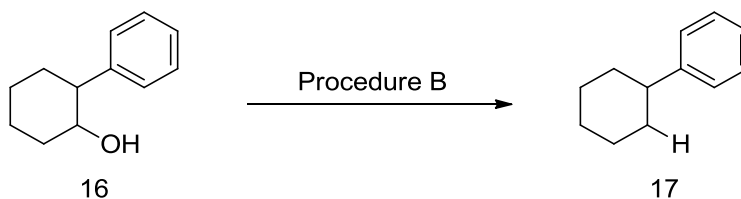


***tert*-Butyl piperidine-1-carboxylate:** According to General Procedure B, **14**<sup>52</sup> (0.20 g, 1.0 mmol), triphenylphosphine (0.39 g, 1.5 mmol), imidazole (0.14 g, 2.0 mmol), and iodine (0.38 g, 1.5 mmol) in MeCN (5.0 mL) was stirred overnight. After full consumption of the alcohol *N,N*-Diisopropylethylamine (1.7 mL, 10 mmol), methanol (0.2 mL), and *fac*-Ir(ppy)<sub>3</sub> (1.6 mg, 0.0025 mmol) are added and the reaction mixture is pumped through the photoreactor at a flow rate to achieve a residence time of 18 min which afforded **15**<sup>58</sup> (0.14 g, 76%) as a colorless oil after purification by chromatography on SiO<sub>2</sub> (95:5, hexanes/EtOAc).

<sup>58</sup> *Org. Lett.* **2010**, *12*, 4176.

$R_f$ (EtOAc/hexane 1:9): 0.32;

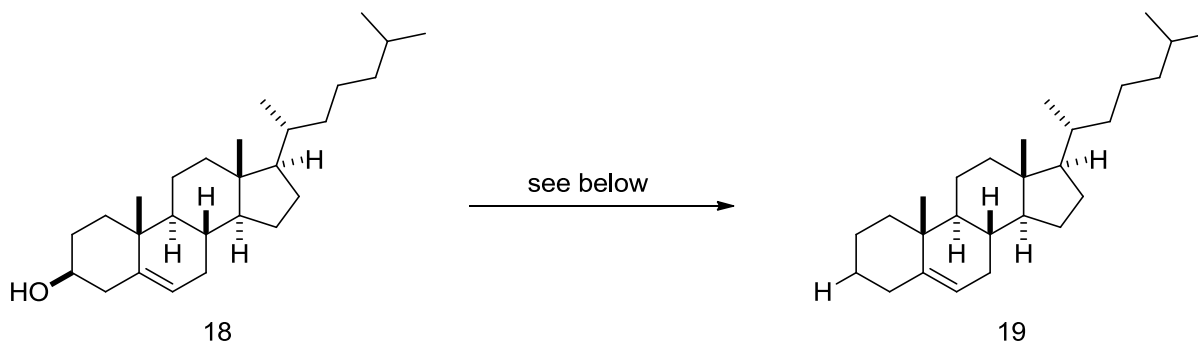
$^1\text{H NMR}$  ( $\text{CDCl}_3$ , 400 MHz):  $\delta$  3.37 – 3.33 (m, 4H), 1.59 – 1.53 (m, 2H), 1.53 – 1.46 (m, 4H), 1.45 (s, 9H).



**Cyclohexylbenzene:** According to General Procedure B, **16**<sup>59</sup> (0.18 g, 1.0 mmol), triphenylphosphine (0.39 g, 1.5 mmol), imidazole (0.14 g, 2.0 mmol), and iodine (0.38 g, 1.5 mmol) in MeCN (5.0 mL) was stirred overnight. After full consumption of the alcohol *N,N*-Diisopropylethylamine (1.7 mL, 10 mmol), methanol (0.2 mL), and *fac*-Ir(ppy)<sub>3</sub> (1.6 mg, 0.0025 mmol) are added and the reaction mixture is pumped through the photoreactor at a flow rate to achieve a residence time of 18 min which afforded **17**<sup>60</sup> (0.11 g, 67%) as a colorless oil after purification by chromatography on SiO<sub>2</sub> (petroleum ether).

$R_f$ (hexanes): 0.51;

$^1\text{H NMR}$  ( $\text{CDCl}_3$ , 400 MHz):  $\delta$  7.34 – 7.29 (m, 2H), 7.26 – 7.18 (m, 3H), 2.57 – 2.48 (m, 1H), 1.96 – 1.82 (m, 4H), 1.82 – 1.75 (m, 1H), 1.51 – 1.37 (m, 4H), 1.34 – 1.23 (m, 1H).



<sup>59</sup> Characterization and preparation of substrate **16** is reported in *Org. Lett.* **2009**, *11*, 3116.

<sup>60</sup> *J. Am. Chem. Soc.* **2004**, *126*, 7788.

**Cholest-5-ene:** A flame dried 10 mL round bottom flask with a rubber septum and magnetic stir bar was charged with the **18**<sup>52</sup> (0.39 g, 1.0 mmol), toluene (2.0 mL), MeCN (4.0 mL), triphenylphosphine (0.39 g, 1.5 mmol), and imidazole (0.14 g, 2.0 mmol). The reaction mixture is cooled in an ice bath to 0 °C and iodine (0.38 g, 1.5 mmol) is added in portions. After 0.5 h, the reaction is removed from the ice bath and stirred at room temperature until the alcohol is fully consumed (as judged by TLC analysis). *N,N*-Diisopropylethylamine (2.6 mL, 15 mmol), methanol (0.5 mL), and *fac*-Ir(ppy)<sub>3</sub> (1.6 mg, 0.0025 mmol) are added to the reaction mixture and stirred until a homogenous solution is formed. The reaction mixture is then pumped through the photoreactor at a flow rate to achieve a residence time of 38 min. The solvent was removed from the crude mixture *in vacuo* and was dissolved in a minimal amount of EtOAc before being passed through a bed of silica gel and eluted with diethyl ether. The filtrate was concentrated and the crude product was purified by chromatography on silica gel (petroleum ether) to afford **19**<sup>61</sup> (0.27 g, 72%) as a colorless solid.

*R<sub>f</sub>*(hexanes): 0.73;

<sup>1</sup>H NMR (CDCl<sub>3</sub>, 400 MHz): δ 5.27 (br dt, *J* = 5.2, 1.6 Hz, 1H), 2.29 – 2.18 (m, 1H), 2.03 – 1.91 (m, 3H), 1.87 – 1.78 (m, 2H), 1.76 – 1.69 (m, 1H), 1.00 (s, 3H), 1.62 – 0.92 (m, 23H), 0.92 (d, *J* = 6.8 Hz, 3H), 0.87 (d, *J* = 1.6 Hz, 3H), 0.86 (d, *J* = 2.0 Hz, 3H), 0.68 (s, 3H).

---

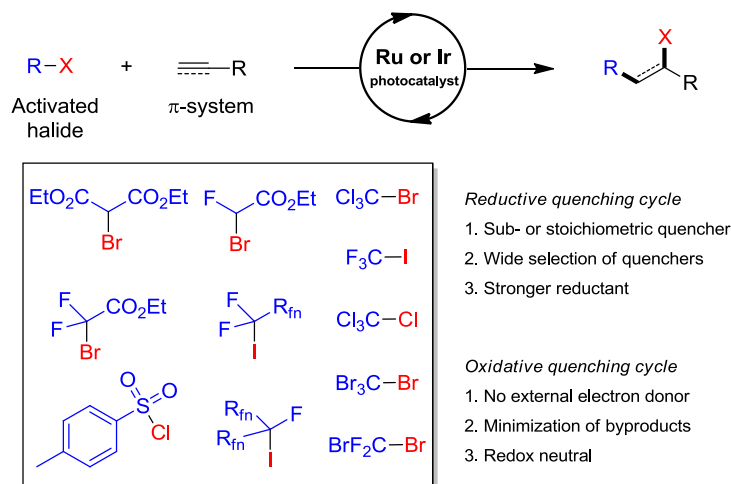
<sup>61</sup> *Org. Biomol. Chem.* **2004**, *2*, 585.

### Chapter 3. Radical Atom Transfer Radical Addition Reactions

\*Portions of this chapter have been published in 1) Nguyen, J. D.; Tucker, J. W.; Konieczynska, M. D.; Stephenson, C. R. J. *J. Am. Chem. Soc.* **2011**, *133*, 4160; 2) Wallentin, C.-J.; Nguyen, J. D.; Finkbeiner, P.; Stephenson, C. R. J. *J. Am. Chem. Soc.* **2012**, *134*, 8875.

#### Introduction

Atom transfer radical addition (ATRA) of haloalkanes and  $\alpha$ -halocarbonyls to olefins serves as an atom-economical<sup>116</sup> method of simultaneously forming C-C and C-X bonds. ATRA allows for efficient alkene or alkyne difunctionalization, typically through the use of radical initiators or transition metal catalysts.<sup>117</sup> Following Kharasch's seminal work,<sup>118</sup> Curran,<sup>119</sup> Oshima,<sup>120</sup> and others have developed ATRA into a useful tool in organic chemistry. Typical ATRA initiators include toxic and hazardous reagents, such as peroxides,<sup>118</sup> organotin

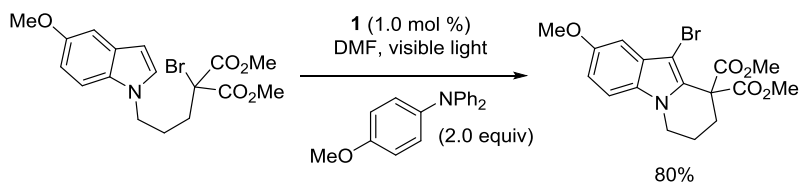


**Figure 3.1** Photoredox catalyzed ATRA.

reagents,<sup>119</sup> and triethylboron.<sup>120</sup> Other less common initiators have also been used, including *p*-methoxybenzene-diazonium tetrafluoroborate with TiCl<sub>3</sub>,<sup>121</sup> dimanganese decacarbonyl,<sup>122</sup> copper,<sup>123</sup> iron,<sup>124</sup> bimetallic Rh–Ru complexes,<sup>125</sup> and chromium(II) acetate,<sup>126</sup> but these methods employ harsh conditions and/or lack broad functional group tolerance. In this regard, I sought to develop a protocol capable of effecting ATRA with a broad scope under mild conditions and utilizing safer reagents using photoredox catalysis (Figure 3.1).<sup>108</sup>

## Background

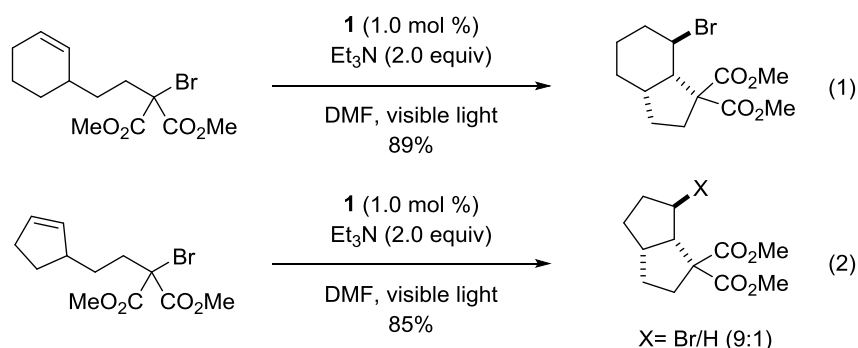
While investigating the use of 4-MeO-C<sub>6</sub>H<sub>4</sub>-NPh<sub>2</sub> as an electron donor, my colleague, Bryan Matsuura, isolated an ATRA product while performing a 6-*exo*-trig cyclization of a bromomalonate derivative onto a tethered indole moiety as depicted in Figure 3.2. Even though the mechanism for this transformation is still elusive, I realized that ATRA products could be obtained by means of the Stephenson group's photocatalytic approach toward general C–C coupling reactions.



**Figure 3.2** Initial observation of ATRA product under photoredox conditions.

My colleagues and I were pleased to find the exclusive formation of the ATRA product from an intramolecular cyclization that provided a bromo bicyclo[4.3.0]nonane derivative when visible light photoredox catalysis conditions mediated by reductive quenching were applied (Figure 3.3, eq 1). The reaction was found to be very substrate dependent and preferentially gave the cyclization-reduction product with terminal alkenes and alkynes. The strong substrate dependence is emphasized by the reaction of the closely related cyclopentene substrate that gave a 9:1 mixture of a bromo bicyclo[3.3.0]octane derivative and the cyclization-reduction product,

respectively (Figure 3.3 eq 2). Not surprisingly, all attempts to perform the intermolecular ATRA with these conditions resulted only in dehalogenation of starting material.



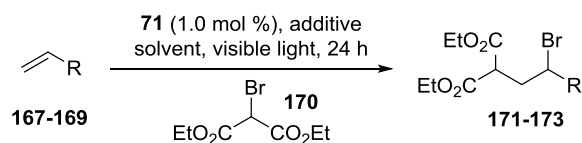
**Figure 3.3** Initial results for intramolecular ATRA.

### Atom Transfer Radical Addition via Oxidative Quenching

I reasoned that these side reactions could be suppressed by utilizing the substrate itself as the excited state quencher via an oxidative quenching pathway.<sup>127</sup> During a survey of photoredox catalysts, Jagan Narayanam, a former postdoctoral fellow, identified Ir[(dF(CF<sub>3</sub>)ppy)<sub>2</sub>(dtbbpy)]PF<sub>6</sub> (**71**, see Figure 1.19) as a complex capable of mediating intermolecular ATRA.<sup>3</sup> My goal was to successfully perform intermolecular ATRA reactions of haloalkanes and  $\alpha$ -halocarbonyls onto olefins under mild conditions that would be catalyzed by a visible light active photoredox catalyst.

My first attempt at intermolecular ATRA involved using tosylated allylamine (**167**), diethyl 2-bromomalonate (**170**, 2.0 equiv) and **71** (1.0 mol %) in DMF and gave 17% yield after 24 h (entry 1, Table 3.1). The addition of a Lewis acidic additive, LiBF<sub>4</sub>, resulted in an increased yield, but with incomplete conversion of starting material.<sup>11a,b</sup> Optimization of the additive and solvent led to increased yield along with greater conversion of the starting material (entries 3-5). However, increasing the nucleophilicity of the olefin, by utilizing Boc-protected allylamine (**168**)

and 5-hexen-1-ol (**169**), afforded complete consumption of the starting materials and nearly quantitative yield of the atom transfer products (entries 6 and 7).



entry	R	conditions <sup>a</sup>	yield <sup>b</sup>
1	CH <sub>2</sub> NHTs ( <b>167</b> )	170 (2.0 equiv), DMF	17
2	167	170 (2.0 equiv), LiBF <sub>4</sub> (2.0 equiv), DMF	25
3	167	170 (2.0 equiv), LiBr (2.0 equiv), DMF	45
4	167	170 (2.0 equiv), LiBr (2.0 equiv), DMF/H <sub>2</sub> O (4:1)	54
5	167	170 (2.0 equiv), LiBr (2.0 equiv), DMF/H <sub>2</sub> O (1:4)	67
6	CH <sub>2</sub> NHBoc ( <b>168</b> )	170 (2.0 equiv), LiBr (2.0 equiv), DMF/H <sub>2</sub> O (1:4)	99
7	(CH <sub>2</sub> ) <sub>4</sub> OH ( <b>169</b> )	170 (2.0 equiv), LiBr (2.0 equiv), DMF/H <sub>2</sub> O (1:4)	99
8	169	170 (2.0 equiv), LiBr (2.0 equiv), DMF/H <sub>2</sub> O (1:4), <i>no light</i>	0
9	169	<i>no catalyst</i> , 170 (2.0 equiv), LiBr (2.0 equiv), DMF/H <sub>2</sub> O (1:4)	0
10	169	170 (1.1 equiv), LiBr (1.1 equiv), DMF/H <sub>2</sub> O (1:4)	97
11	169	170 (0.95 equiv), LiBr (0.95 equiv), DMF/H <sub>2</sub> O (1:4)	95
12	169	170 (2.0 equiv), <i>no additive</i> , DMF/H <sub>2</sub> O (1:4)	72
13	169	170 (2.0 equiv), LiBr (2.0 equiv), DMF	46

<sup>a</sup>Entries 1-6 were degassed (freeze-pump-thaw). <sup>b</sup>Isolated yield (%) after purification on SiO<sub>2</sub>.

**Table 3.1** Optimization and control experiments for intermolecular ATRA.

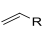
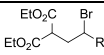
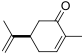
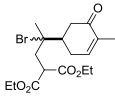
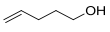
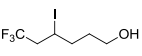
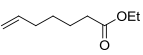
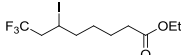
In order to evaluate the significance of each of the reaction parameters, additional control reactions were run. As expected, no conversion to product was observed in the absence of light or photocatalyst (entries 8 and 9). Furthermore, either component, olefin or **170**, can be used as the limiting reagent with no decrease in yield or reaction efficiency (entries 10 and 11). In addition, LiBr and H<sub>2</sub>O are required to allow the reaction to progress to completion in a 24 h timeframe (entries 12 and 13).<sup>128</sup>

With the optimized conditions in hand, the atom transfer of **170** with various olefins was examined (entries 1-9, Table 3.2). Several functional groups are well tolerated under the reaction



conditions including free alcohols, silyloxy ethers, benzyl ethers, alkyl bromides, esters, enones, carbamates, and aromatic rings. In addition, monosubstituted and 1,1-disubstituted olefins are competent reaction partners with **170**. All reactions are characterized by clean conversion to product within 24 h and can be isolated easily by column chromatography.

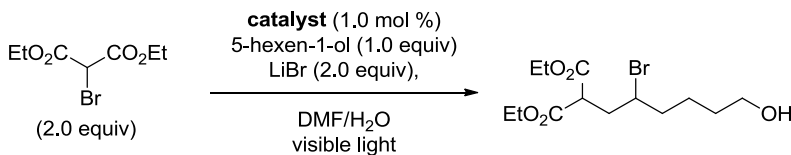
The success of the intermolecular atom transfer with **170** prompted the examination of other compounds containing activated C-X bonds (entries 10-16, Table 3.2). The optimized conditions worked well with a number of  $\alpha$ -halocarbonyls and haloalkanes. It is noteworthy that cyclohexene, which did not undergo coupling with **170**, underwent efficient ATRA with ethyl bromodifluoroacetate (entry 13).<sup>129</sup> Several fluorinated compounds are effective reaction partners, and demonstrate the applicability of this methodology to the synthesis of molecules that have particular value in medicinal chemistry,<sup>130</sup> agrochemicals<sup>131</sup> and material science.<sup>132</sup>

entry	substrate	olefin	product	yield <sup>b</sup>
				
1	<b>170</b>	R = CH <sub>2</sub> NHTs		67 <sup>c</sup>
2	<b>170</b>	R = CH <sub>2</sub> NHBoc		99
3	<b>170</b>	R = (CH <sub>2</sub> ) <sub>4</sub> OH		95
4	<b>170</b>	R = (CH <sub>2</sub> ) <sub>3</sub> OH		99
5	<b>170</b>	R = (CH <sub>2</sub> ) <sub>4</sub> OTBS		90
6	<b>170</b>	R = (CH <sub>2</sub> ) <sub>4</sub> OCH <sub>2</sub> Ph		92
7	<b>170</b>	R = (CH <sub>2</sub> ) <sub>3</sub> Br		92
8	<b>170</b>	R = (CH <sub>2</sub> ) <sub>4</sub> CO <sub>2</sub> Et		99
9	<b>170</b>			95 <sup>d</sup>
10	CF <sub>3</sub> I			90 <sup>ef</sup>
11	CF <sub>3</sub> I			81 <sup>ef</sup>



method to encompass a broader substrate scope.

The first attempt to improve the atom transfer protocol involved a more comprehensive screen of photocatalysts. Utilizing the conditions optimized for the intermolecular ATRA between diethyl bromomalonate and 5-hexen-1-ol with  $[\text{Ir}\{\text{dF}(\text{CF}_3)\text{ppy}\}_2(\text{dtbbpy})]\text{PF}_6$  (**71**, see Figure 1.19),  $[\text{Ru}(\text{bpy})_3]\text{Cl}_2$  (**1**, see Figure 1.4),  $[\text{Ir}(\text{ppy})_2(\text{dtbbpy})]\text{PF}_6$  (**25**, see Figure 1.8), and *fac*- $\text{Ir}(\text{ppy})_3$  (**82**, see Figure 1.22) were screened. The photocatalysts **1** and **71** both provided full conversion of starting material and high yields of the product after 24 h, although **1** provided slightly higher yields than **71**. On the contrary, the use of photocatalyst **82** resulted in incomplete conversion of the starting material, possibly due to the low solubility of **82** in the DMF/H<sub>2</sub>O solvent system (Table 3.3). For reasons associated with accessibility and lower cost of **1** as compared with **71**, further studies employed the use photocatalyst **1**.<sup>135</sup>



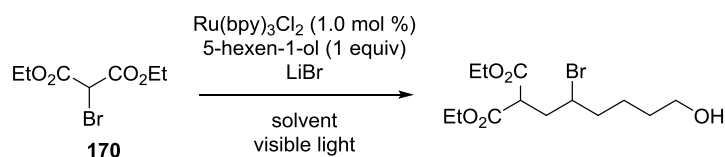
entry	catalyst	yield (%) <sup>b</sup>
1	none	0
2	$[\text{Ru}(\text{bpy})_3]\text{Cl}_2$	99
3	$[\text{Ir}\{\text{dF}(\text{CF}_3)\text{ppy}\}_2(\text{dtbbpy})]\text{PF}_6$	99
4	$[\text{Ir}(\text{ppy})_2(\text{dtbbpy})]\text{PF}_6$	93
5	<i>fac</i> - $\text{Ir}(\text{ppy})_3$	35

<sup>a</sup>24 h reaction time. <sup>b</sup>Isolated yield (%) after purification by chromatography on SiO<sub>2</sub>.

**Table 3.3** Catalyst screening.

The generality of the atom transfer protocol was then evaluated with respect to the solvent (Table 3.4). Highly polar solvents such as DMSO, hexafluoroisopropanol (HFIP), MeCN, and H<sub>2</sub>O all provided the atom transfer of diethyl bromomalonate onto 5-hexen-1-ol

cleanly and in high yields (Table 3.4, entries 1–5). In particular, DMSO afforded full conversion of the starting material in the shortest time frame (Table 3.4, entry 2). Although MeOH did provide the desired product, the crude reaction mixture gave partial transesterification of the product, which resulted in a lower isolated yield of the desired product (Table 3.4, entry 9). Less polar solvents such as THF, EtOAc and DCM typically gave complex reaction mixtures and lower yields, and longer reaction times did not increase the yields significantly (Table 3.4, entry 6–8). With DMSO as the solvent, I observed that lowering the loading of the halogenated coupling partner from 2.0 equivalents to 1.2 equivalents and LiBr from 200 mol % to 10 mol % only slightly increased the reaction time but did not lower the yield (Table 3.4, entry 14). These new optimized conditions offer several advantages when compared to the original conditions: a nearly equimolar ratio of alkene and atom transfer coupling partner, a photocatalyst that is commercially available and more cost efficient to synthesize, reduction of Lewis acid additive to sub-stoichiometric quantities, and a solvent system capable of overcoming most solubility issues. To evaluate the improved reaction conditions (1.0 equiv alkene, 1.2 equiv atom transfer agent, 10 mol % LiBr for  $\alpha$ -bromo carbonyls, 2 mL DMSO/mmol alkene, and 1.0 mol % **1**) in terms of the

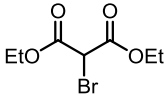
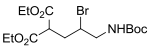
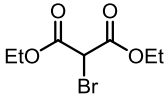
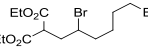
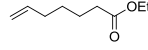
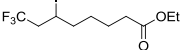
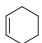
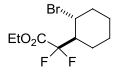
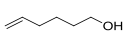
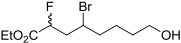
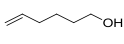
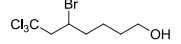


entry	solvent	<b>170</b> (equiv)	LiBr (mol %)	time (h)	yield <sup>a</sup> (%)
1	DMF/H <sub>2</sub> O	2.0	200	10	99
2	DMSO	2.0	200	6	99
3	HFIP	2.0	200	7	93
4	MeCN	2.0	200	20	95
5	H <sub>2</sub> O	2.0	200	7	95
6	THF	2.0	200	20	74

7	EtOAc	2.0	200	24	47 <sup>b</sup>
8	DCM	2.0	200	24	28 <sup>b</sup>
9	MeOH	2.0	200	12	72
10	DMSO	2.0	100	6	98
11	DMSO	2.0	50	6	96
12	DMSO	2.0	10	7	95
13	DMSO	1.5	10	7	94
<b>14</b>	<b>DMSO</b>	<b>1.2</b>	<b>10</b>	<b>8</b>	<b>98</b>

<sup>a</sup>Isolated yield (%) after purification by chromatography on SiO<sub>2</sub>. <sup>b</sup>Full conversion of starting material not observed.

**Table 3.4** Solvent screening.

entry	RX	olefin	product	yield(%) with <b>71</b> <sup>b,d</sup>	yield(%) with <b>1</b> <sup>c,d</sup>
1	<b>5</b>			99	99
2	<b>5</b>			92	94
3 <sup>e,f</sup>	<b>6</b>			81	90
4	<b>7</b>			75	88
5 <sup>g</sup>	<b>8</b>			99 <sup>c</sup>	99 <sup>c</sup>
6 <sup>e</sup>	<b>9</b>			87	95

<sup>a</sup>24 h reaction time unless otherwise noted. <sup>b</sup>Reactions conducted using 1.0 mol % **1**, 2.0 equiv of haloalkane or haloester, and 2.0 equiv of LiBr in H<sub>2</sub>O/DMF (4:1). <sup>c</sup>Reactions conducted using 1.0 mol % **2**, 1.2 equiv of haloalkane or haloester, and 10 mol % of LiBr in DMSO. <sup>d</sup>Isolated yield (%) after purification on SiO<sub>2</sub>. <sup>e</sup>No LiBr added. <sup>f</sup>48 h reaction time. <sup>g</sup>dr 1:1.

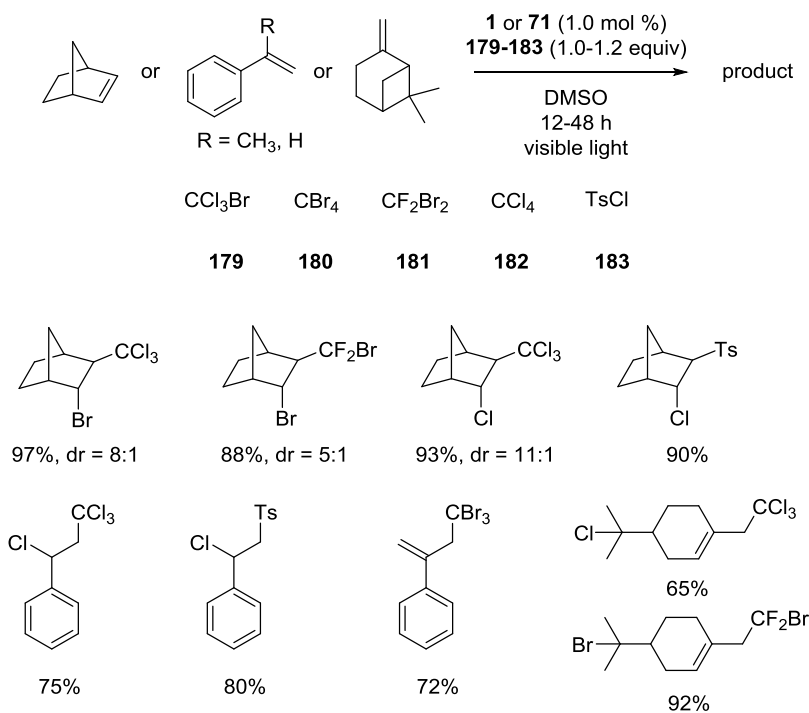
**Table 3.5** Newly optimized conditions for ATRA via oxidative quenching.

substrate scope, Calle-Johan Wallentin, a former postdoctoral associate, repeated several of my previously published coupling reactions. He observed that yields were comparable and, in some cases, even higher with the newly developed reaction conditions (Table 3.5).

In an effort to further broaden the substrate scope and thus achieve a high degree of generality of the ATRA protocol, I revisited substrates that were not compatible with the original conditions. Specifically, utilizing the oxidative quenching cycle of **71** (see Figure 1.19), the atom transfer onto styrene derivatives and 1,2-disubstituted alkenes (with the exception of cyclohexene) were unsuccessful. In addition, CCl<sub>4</sub> failed to couple efficiently to all olefin substrates, even though the excited state of **71** ( $\text{Ir}^{3+*}/\text{Ir}^{4+} = -0.89 \text{ V vs. SCE}$ ) should be sufficient to reduce CCl<sub>4</sub> ( $-0.78 \text{ V vs. SCE}$ ).<sup>136</sup> This portion of the investigation began with the use of norbornene and  $\beta$ -pinene, because these strained alkenes are known to be more reactive than cyclohexene.<sup>137</sup>

Utilizing the originally optimized conditions, the ATRA of CCl<sub>3</sub>Br to norbornene was sluggish, partly attributable to the low solubility of norbornene in DMF/H<sub>2</sub>O. However, the newly optimized conditions utilizing DMSO and **1** (see Figure 1.4) provided a homogeneous reaction mixture and the atom transfer addition product in high yield (Figure 3.5). Dibromodifluoromethane (CF<sub>2</sub>Br<sub>2</sub>)<sup>138</sup> and 4-toluenesulfonyl chloride (TsCl) with norbornene also provided the corresponding ATRA products in high yields, but the ATRA product of CCl<sub>4</sub> and norbornene could only be achieved in high yield when **71** was utilized in combination with the new conditions. My colleagues and I speculated that the successful atom transfer of CCl<sub>4</sub> onto norbornene was due to a combination of the inherent strain energy of norbornene and its increased solubility in DMSO. However, the successful coupling of CCl<sub>4</sub> and 5-hexen-1-ol with either **1** or **71** was observed in DMSO, whereas neither catalyst gave the ATRA product in the DMF/H<sub>2</sub>O solvent system in which solubility was not an issue. This indicates that DMSO is not only superior to the DMF/H<sub>2</sub>O solvent system with regard to solubility but also with regard to promoting the atom transfer radical addition process. In addition to norbornene,  $\beta$ -pinene,

styrene, and  $\alpha$ -methyl styrene were also successful coupling partners with several halogenated compounds; however, high yields for the ATRA of  $\text{CCl}_4$  required the use of **71** rather than **1** in all cases (Figure 3.5).



**Figure 3.5** Expansion of Photocatalytic ATRA via Oxidative Quenching.

Motivated by the successful enhancement of the ATRA protocol, I next sought to develop a fluorous tagging protocol of alkenes and alkynes utilizing perfluoroalkyl iodides that would rival known protocols in terms of efficiency (reaction time and yield), mild reaction conditions, and functional group tolerance.

### Atom Transfer Radical Addition via Reductive Quenching

The fluorous biphasic concept<sup>139</sup> was introduced to the field of organic synthesis in the mid 1990's, and since then, the special properties of perfluorinated carbons have been innovatively utilized for the synthesis of small molecules.<sup>140</sup> The introduction of perfluorinated tags in conjunction with solid phase extraction (F-SPE) by Curran and co-workers<sup>141</sup> made an

especially crucial impact on both industrial and academic research in the context of conventional, parallel and combinatorial syntheses.<sup>142,143</sup> By temporary attachment or permanent affixation of a perfluorinated alkyl chain to reagents or reactants, product isolation in reactions that typically have been tedious and laborious are now promptly performed by either multiphasic solvent systems or by SPE techniques, utilizing either heavy (>60% fluorine by weight) or light (<40% fluorine by weight) perfluorinated molecules, respectively. Even though several perfluorinated compounds of various sizes are commercially available, the development of novel methods for efficient and selective introduction of fluorinated motifs is a growing area of interest because of the expansion of its applications within the research fields of medicinal, synthetic, industrial, and agricultural chemistry.<sup>144</sup>

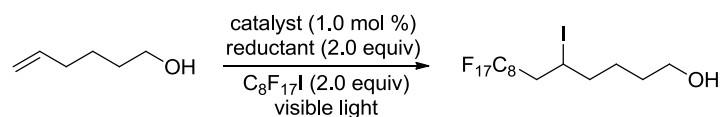
Perfluorinated motifs can be incorporated both under stoichiometric<sup>145</sup> and catalytic<sup>146</sup> conditions. Addition reactions of perfluoroalkyl iodides to alkenes and alkynes represent one of the most common means to synthesize fluorinated compounds. This type of transformation can be accomplished photochemically (UV), thermally (>200 °C), electrochemically, or through a redox active system.<sup>147</sup> During the investigation of visible light-mediated ATRA of activated halides across double bonds utilizing the oxidative quenching catalytic cycle of **71**, I managed to access trifluoromethylated alkanes in high yields. However, a large excess of CF<sub>3</sub>I, high boiling solvents (DMF or DMSO), and long irradiation times (48 h) were required for high conversions. These disadvantages encouraged my colleagues and I to further develop and expand the ATRA protocol within the field of fluorinated chemistry.

Initially, I sought to apply the optimized conditions for the ATRA, mediated by the oxidative quenching of **1** (see Figure 1.4) or **71** (see Figure 1.19), to the ATRA of a variety of perfluoroalkyl iodides. It is well known that longer chain perfluoroalkyl iodides are more easily



reduced (less negative reduction potentials) than  $\text{CF}_3\text{I}$ .<sup>148</sup> Therefore, I reasoned that the oxidative quenching of **1** and **71** would promote the ATRA of perfluoroalkyl iodides such as  $\text{C}_8\text{F}_{17}\text{I}$  with high efficiency. Surprisingly, no conversion was observed after 24 h when  $\text{C}_8\text{F}_{17}\text{I}$  ( $-1.32$  V vs. SCE) and 5-hexen-1-ol were reacted with photocatalyst **71** (Table 3.6, entry 1). I then turned to the newly improved conditions utilizing **1** in DMSO, which generated the desired product in 95% yield within 5 h (Table 3.6, entry 2). However, Calle continued screening conditions with the expectation that the reaction time could be lowered while maintaining high yields by using a catalyst with a stronger reducing capacity. When employing photocatalyst **82** (see Figure 1.22), which has a much stronger excited state reduction potential ( $-1.72$  V vs. SCE) than **1** or **71**,<sup>149</sup> the desired product was isolated in only 43% yield after 9 days (Table 3.6, entry 3). These unsatisfactory results led to the revisitation of the reductive quenching cycle of **1**.<sup>107,108</sup> Initially, Calle and I were uncertain about relying on the reductive quenching cycle due to the issues related to prominent side reactions (*vide supra*). Nevertheless, the advantages of using **1** as the photocatalyst include its low cost and the relatively strong reduction potential of  $[\text{Ru}(\text{bpy})_3]^+$  ( $-1.33$  V vs. SCE).<sup>150</sup>

Prompted by this reassessment, I screened various stoichiometric reductants for **1** (Table 3.6, entries 4–7), and the desired product was isolated in yields ranging from 10% to 73% after 5 h of irradiation. I observed low solubility of sodium ascorbate in acetonitrile and consequently found that the addition of either a phase transfer catalyst such as hexadecyltrimethylammonium bromide or the use of MeOH as co-solvent led to significant improvements in both yield and reaction time (Table 3.6, entries 8–9). Thorough optimization of the reaction conditions by Calle provided a 99% yield in just 0.5 h (Table 3.6, entry 10). The efficiency of the reaction was preserved in other polar solvents and was diminished in less polar solvents. No product



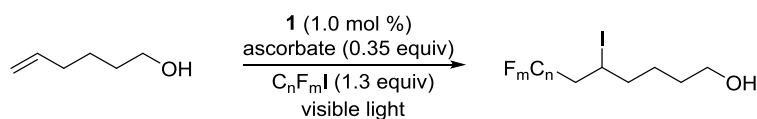
entry	cat.	solvent	reductant	time (h)	yield <sup>g</sup> (%)
1	<b>71</b>	DMF	-----	24	N.R.
2 <sup>a</sup>	<b>1</b>	DMSO	-----	5	95
3	<b>82</b>	DMF	-----	216	43
4	<b>1</b>	MeCN	H.E. <sup>f</sup>	5	10
5	<b>1</b>	MeCN	<sup>i</sup> Pr <sub>2</sub> NEt	5	73
6	<b>1</b>	MeCN	Bu <sub>3</sub> N	5	58
7	<b>1</b>	MeCN	Na-ascorbate	5	25
8 <sup>b</sup>	<b>1</b>	MeCN	Na-ascorbate	1.5	99
9	<b>1</b>	MeCN/MeOH <sup>c</sup>	Na-ascorbate	0.5	91
10 <sup>c</sup>	<b>1</b>	MeCN/MeOH <sup>c</sup>	Na-ascorbate	0.5	99
11 <sup>d</sup>	<b>1</b>	MeCN/MeOH <sup>c</sup>	Na-ascorbate	0.5	67

<sup>a</sup>Reaction conducted using C<sub>8</sub>F<sub>17</sub>I (1.2 equiv). <sup>b</sup>Hexadecyltrimethylammonium bromide used as an additive. <sup>c</sup>1.3 equiv of perfluoroalkyl iodide and 0.35 equiv of sodium ascorbate were used. <sup>d</sup>1.3 equiv of perfluoroalkyl iodide and 0.05 equiv of sodium ascorbate were used. <sup>e</sup>4:3 mixture. <sup>f</sup>H.E. = Hantzsch ester (Diethyl 1,4-dihydro-2,6-dimethyl-3,5-pyridinedicarboxylate). <sup>g</sup>Isolated yield (%) after purification by chromatography on SiO<sub>2</sub>.

**Table 3.6** Optimization of ATRA of C<sub>8</sub>F<sub>17</sub>I onto 5-hexen-1-ol.

formation was observed in the absence of catalyst or a visible light irradiation source.

After the successful intermolecular ATRA of C<sub>8</sub>F<sub>17</sub>I onto 5-hexen-1-ol, the reaction scope toward structurally diverse perfluoroalkyl iodides was examined. As expected, high to excellent yields were obtained for various perfluoroalkyl iodides (Table 3.7) with a small decrease in yield for shorter C<sub>6</sub>F<sub>13</sub>I (Table 3.7, entry 2) and branched (CF<sub>3</sub>)<sub>2</sub>CFI (Table 3.7, entry 5). A plausible explanation for this drop in yield for C<sub>6</sub>F<sub>13</sub>I is that shorter perfluoroalkyl iodides have a more negative reduction potential. In the case of (CF<sub>3</sub>)<sub>2</sub>CFI, the drop in yield probably stems from steric effects rather than redox properties.<sup>151</sup>



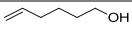
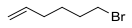
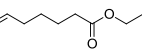
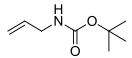
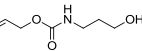
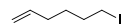
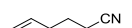
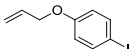
entry	substrate	time (h)	yield (%) <sup>c</sup>
1 <sup>a</sup>	CF <sub>3</sub> I	48	90
2 <sup>b</sup>	C <sub>6</sub> F <sub>13</sub> I	0.5	81
3	C <sub>8</sub> F <sub>17</sub> I	0.5	99
4	C <sub>10</sub> F <sub>21</sub> I	0.5	97
5	(CF <sub>3</sub> ) <sub>2</sub> CFI	0.5	81

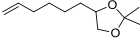
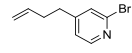
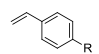
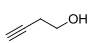
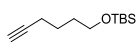
<sup>a</sup>See eq 8. <sup>b</sup>2.0 equiv of both perfluoroalkyl iodide and reductant were used. <sup>c</sup>Isolated yield (%) after purification by chromatography on SiO<sub>2</sub>.

**Table 3.7** ATRA of Various Perfluoroalkyl Iodides.

The scope and functional group compatibility of the optimized conditions of the intermolecular ATRA between C<sub>8</sub>F<sub>17</sub>I and various terminal alkenes and alkynes were also evaluated (Table 3.8). In general, yields were high to excellent for a wide variety of substrates with the exception of styrene derivatives. Although the addition of perfluoroalkyl radicals onto styrene derivatives has been performed using radical initiators,<sup>152</sup> electron neutral, poor and rich styrenes all produced complex reaction mixtures from which the corresponding product could not be isolated (Table 3.8, entry 11). Side reactions, such as polymerization, might arise from reduction or oxidation of either product or alkene starting material by the catalyst. However, non-conjugated alkenes substituted with electron-deficient aromatics, such as 2-bromo-4-(but-3-en-1-yl)pyridine (Table 3.8, entry 10), as well as alkenes substituted with non-conjugated electron-rich aromatics (Table 3.8, entry 8) afforded the product in high yields. Of significant importance is that both aromatic and alkyl bromides and iodides are compatible with these mild

reaction conditions (Table 3.8, entries 2, 6, 8 and 10). Alkenes containing allylic *N*- and *O*-carbamate functionalities, frequently utilized as fluorous-tagged protecting groups for amines and alcohols, gave high to excellent yields, as did acetals (Table 3.8, entries 4, 5 and 9). Multi-gram scale reactions were performed without significant decrease in yields within the optimized reaction time of 0.5 h (Table 3.8, entries 1 and 10). Furthermore, on large scale (40 mmol) only 0.01 mol % of **1** was needed to obtain a yield of 96% in ATRA with C<sub>8</sub>F<sub>17</sub>I and 5-hexen-1-ol.<sup>153</sup> Alkynes are also suitable partners in this ATRA protocol. However, the optimized conditions that provided exclusive ATRA products for alkenes gave significant quantities of reduced byproducts for all alkynes investigated. This problem was successfully addressed by changing the solvent system from MeCN/MeOH to *t*-BuOH/H<sub>2</sub>O providing the corresponding perfluorovinyl iodides in high yields (Table 3.8, entries 12 and 13). Assuming that propagation is a non-active mechanistic component (*vide infra*), the turnover number (TON) of the catalyst is  $\sim 10^4$  and the turnover frequency (TOF) is  $> 5.3 \text{ s}^{-1}$ .

entry	substrate	t (h)	yield (%) <sup>a</sup>
1		0.5	99 (96%) <sup>a</sup>
2		0.5	93
3		0.5	94
4		0.5	96
5		0.5	79
6		0.5	94
7		0.5	90
8		4	99

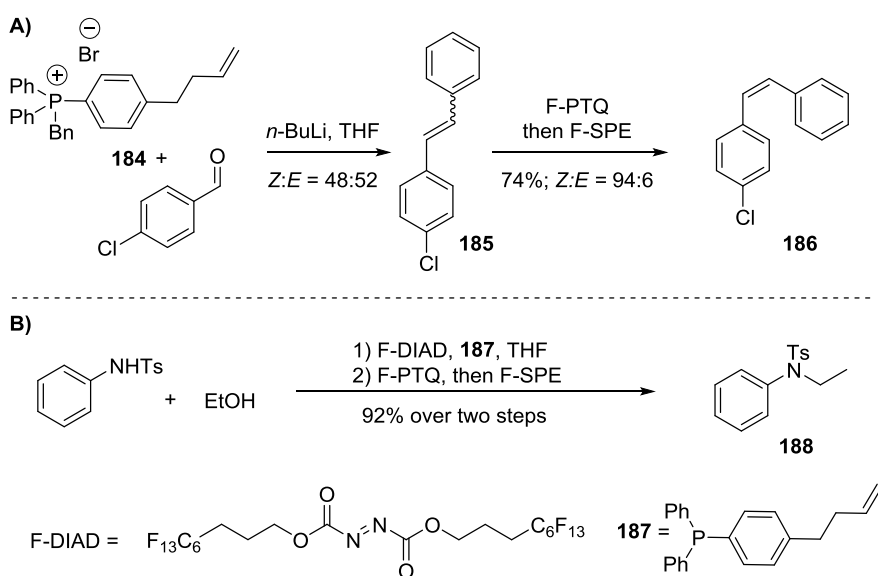
9		0.5	91 <sup>b</sup>
10		2	88 (85%) <sup>c</sup>
11	 R = H, OMe, C(O)OEt, PPh <sub>2</sub> , POPh <sub>2</sub>	0.5 - 24	0 <sup>d</sup>
12		0.5	96 <sup>e</sup>
13		0.5	94 <sup>f</sup>

<sup>a</sup>Yield in parentheses is for a preparative reaction (4.0 g, 40 mmol) using 0.01 mol % catalyst. <sup>b</sup>1:1 dr. <sup>c</sup>Yield in parentheses is for a preparative reaction (1.6 g, 7.5 mmol) using 0.1 mol % catalyst. <sup>d</sup>Partial conversion of starting material. For all substrates, a complex reaction mixture was obtained or the targeted product was unstable and thus not successfully isolated. <sup>e</sup>1.8:1 dr. <sup>f</sup>2:1 dr. <sup>g</sup>Isolated yield (%) after purification by chromatography on SiO<sub>2</sub>.

**Table 3.8** Substrate scope for iodoperfluoroalkylation of alkenes and alkynes.

The high efficiency and broad functional group compatibility of this system prompted an investigation of its potential for the strategic introduction of perfluorinated tags in the synthesis of structurally complex molecules. Curran and co-workers introduced the concept of fluororous scavenging to facilitate small molecule synthesis in terms of a general strategy for product isolation.<sup>154</sup> Similarly, post-transformational introduction of perfluorinated tags to alkene-functionalized protecting groups or reagents via the present protocol would circumvent possible solubility issues and/or other impeding properties imposed by perfluorinated tags. In addition, this method also provides the possibility to tune the fluororous nature of substrates and catalysts. The validity of this hypothesis was evaluated by fluororous post-transformational quenching (F-PTQ) of alkene-functionalized phosphine reagents in both Wittig (Figure 3.6, top) and Mitsunobu reactions (Figure 3.6, bottom). Both transformations are known to produce byproducts that are problematic during product isolation. Several strategies have been employed to address this issue,<sup>155</sup> including fluororous techniques,<sup>156</sup> which suggested that they would be

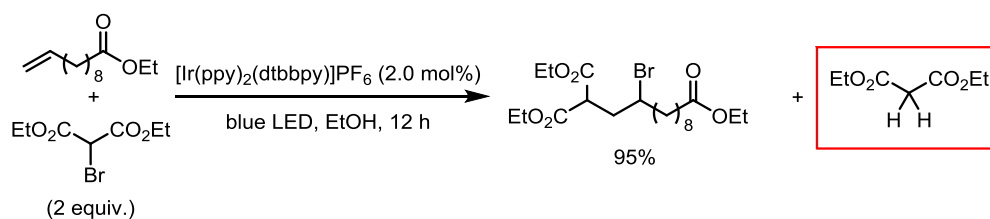
suitable test systems for the evaluation of the general applicability of this protocol. For the Wittig reaction, phosphonium salt **184** was treated with *n*-BuLi, followed by *p*-chlorobenzaldehyde, providing a crude reaction mixture consisting of stilbene derivative **185** and a phosphine oxide functionalized with a terminal alkene. Subjecting the crude reaction mixture to F-PTQ with a prolonged irradiation time, followed by F-SPE, allowed for the isolation of the pure product **186** in 74% yield (94:6 dr). As a consequence of excited state quenching (energy transfer) of the catalyst by the stilbene derivative, a longer reaction time was needed for full conversion of the phosphine oxide. (*E*)-stilbene has a smaller HOMO-LUMO gap than (*Z*)-stilbene which explains the enrichment of the (*E*)-diastereoisomer during the photocatalyzed reaction.<sup>157</sup> For the Mitsunobu reaction, *N*-tosylaniline and EtOH were treated with phosphine **187** and fluororous tagged DIAD (F-DIAD) providing a crude reaction mixture consisting of product **188**, excess phosphine **187**, phosphine oxide from **187**, excess F-DIAD, and fluororous tagged hydrazine. The crude mixture was once again subjected to F-PTQ to tag the excess phosphine and phosphine oxide. After 2.5 h the reaction was subjected to F-SPE to provide the pure product in 92% yield.



**Figure 3.6** Post-transformational fluororous quenching.

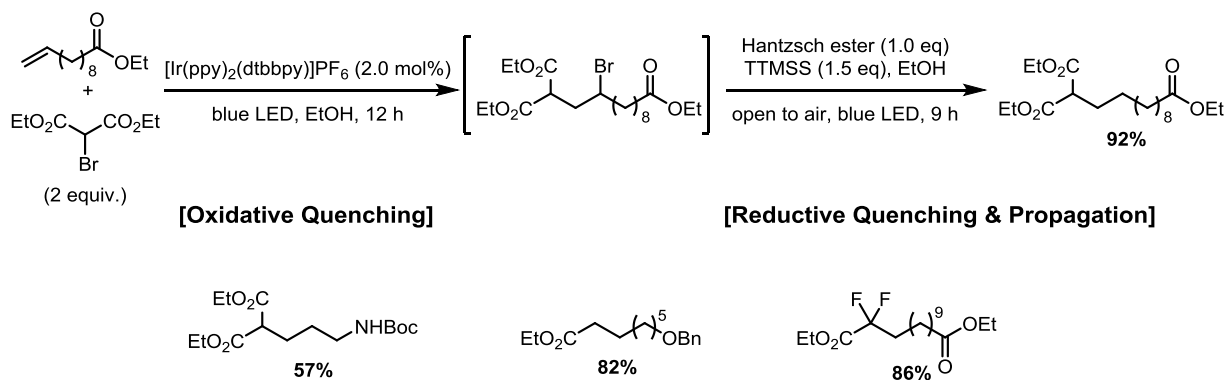
## One-Pot Reductive Coupling

During an independent study of new reaction conditions for ATRA via oxidative quenching it was discovered that ethanol could act as an H-atom donor. This H-atom donating ability of ethanol is best suited for highly activated carbon radicals, but is slow enough not to interfere with the ATRA process. For example, the atom transfer of diethyl bromomalonate onto ethyl 10-undecenoate in ethanol provides the desired product in high yield, but prolonged reaction time shows full conversion of excess diethyl bromomalonate to diethyl malonate (Figure 3.7).



**Figure 3.7** Discovery that ethanol is an efficient H-atom source.

This serendipitous observation has allowed for the development of a one-pot reductive coupling. The first step involves the atom transfer of a halogenated substrate onto an alkene subsequently followed quenching of excess halogenated substrate by ethanol. The second step involves telescoping the reaction with the addition of Hantzsch ester and TTMS (a modified



**Figure 3.8** One-pot reductive coupling protocol.

reductive radical hydrodebromination procedure described in Chapter 2) to provide the reductive coupling product in moderate to high yields (Figure 3.8).

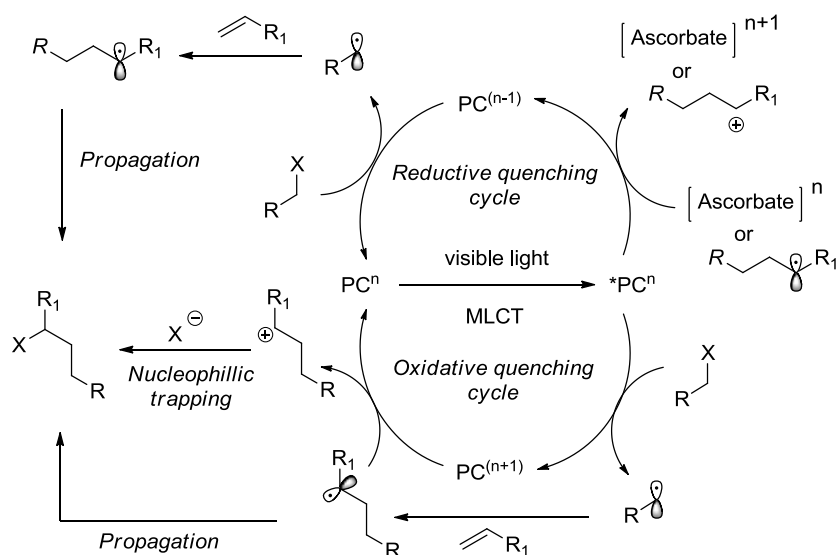
### **Mechanism and Mechanistic Studies**

Both the reductive and oxidative quenching cycles are initiated by activation of the photocatalyst by visible light absorption to produce the  $^3\text{MLCT}$  state of the catalyst (Figure 3.9). In the presence of a stoichiometric electron donor, the excited state is reductively quenched providing a reduced catalyst ( $^*\text{PC}^n/\text{PC}^{n-1}$ , PC = photocatalyst). For the fluororous tagging protocol,  $^*[\text{Ru}(\text{bpy})_3]^{2+}$  is reduced to  $[\text{Ru}(\text{bpy})_3]^+$  using sodium ascorbate as the electron donor.  $[\text{Ru}(\text{bpy})_3]^+$  has a sufficiently low reduction potential ( $-1.33$  V vs. SCE) to effectively convert perfluoroalkyl iodides ( $-1.0$  to  $-1.5$  V vs. SCE) to electrophilic free radicals. The radical then undergoes addition to the alkene or alkyne. The ATRA product can subsequently be formed via two different routes: either by propagation or by oxidation to the cation followed by nucleophilic trapping in accordance with the oxidative quenching pathway as outlined in Figure 3.9. The reduction potential of secondary radicals ( $0.47$  V vs. SCE)<sup>158</sup> renders them prone to oxidation by the photocatalyst, consequently initiating another catalytic cycle. Nucleophilic trapping with iodide, possibly pre-associated as a counterion to the catalyst, provides the ATRA product. For ATRA using classical radical initiators, propagation has been shown to be an operative mechanism and can also be a viable mechanistic component in this catalytic system. For either route, sodium ascorbate acts only as an initiator to provide the initial  $[\text{Ru}(\text{bpy})_3]^+$  species. This is corroborated by the fact that only small amounts of sodium ascorbate (0.05 mol %) are needed for high conversion of the starting material.

In the redox neutral oxidative quenching pathway, the photocatalyst reduces the halogenated substrate directly from its excited state to produce an oxidized photocatalyst



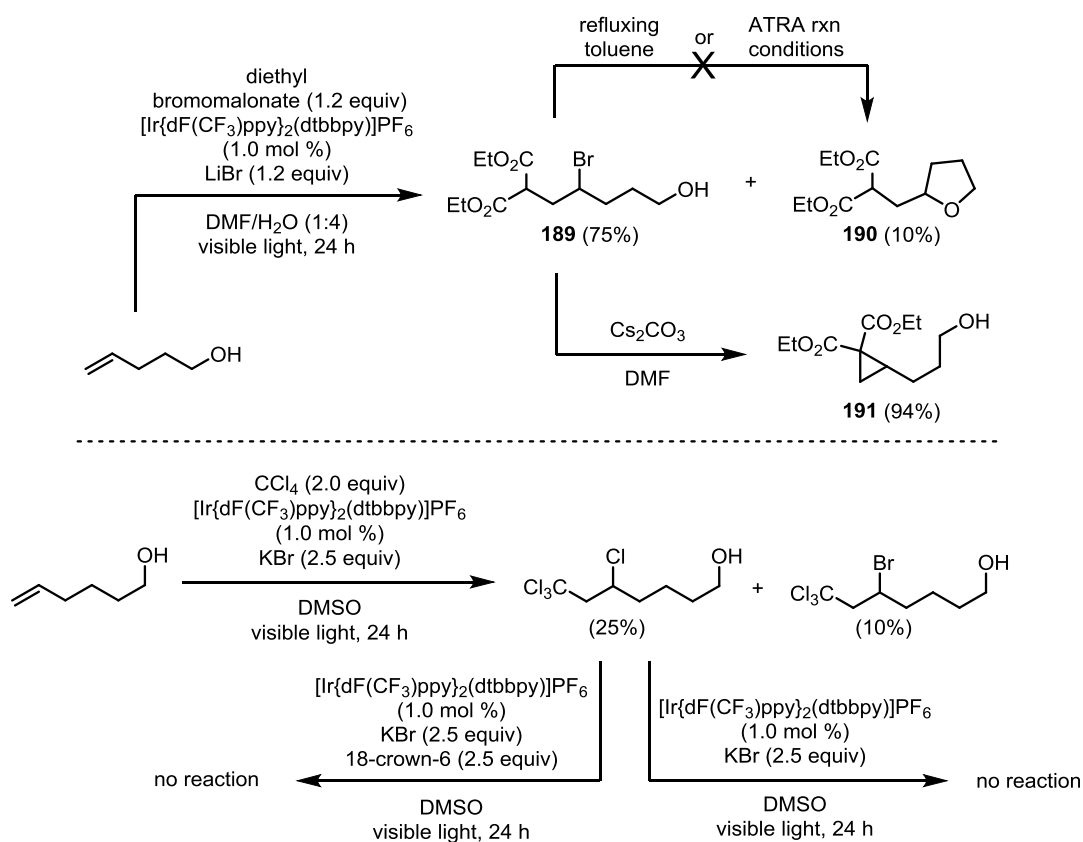
(\*PC<sup>n</sup>/PC<sup>n+1</sup>) and an electrophilic radical that undergoes addition to an alkene. The addition produces a radical that can be oxidized to a carbocation by the catalyst to complete the catalytic cycle and subsequently generate the product by nucleophilic trapping of a halide, or the radical can participate in a propagation chain to also produce the ATRA product.



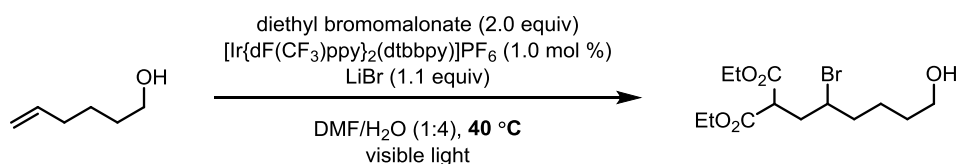
**Figure 3.9** Proposed mechanisms for photoredox-catalyzed ATRA.

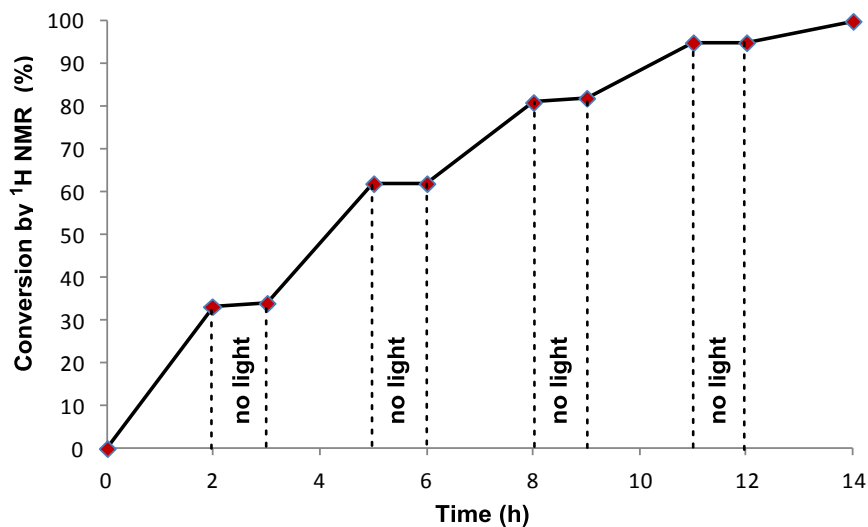
Experimental evidence indicates a radical-polar crossover mechanisms proposed above and evidence that light is a necessary component of the reaction (Scheme 5). When the ATRA of diethyl bromomalonate (1.2 equiv) was performed with 4-penten-1-ol, LiBr (1.2 equiv), and [Ir{dF(CF<sub>3</sub>)ppy}<sub>2</sub>(dtbbpy)]PF<sub>6</sub> (1.0 mol %) in DMF/H<sub>2</sub>O, the tetrahydrofuran byproduct **190** is isolated in 10% yield. When the atom transfer product **189** is resubjected to the reaction conditions or refluxed in toluene, the formation of **190** is not observed. In addition, the treatment of **189** with base exclusively generated cyclopropane **191**. This indicates that **190** is not generated from **189** but rather from the nucleophilic trapping of a carbocation intermediate by the tethered alcohol (Figure 3.10, top). In addition, an experiment to verify the necessity of light for the ATRA protocol was performed using diethyl bromomalonate (2.0 equiv), 5-hexen-1-ol, LiBr (2.0 equiv), and [Ir{dF(CF<sub>3</sub>)ppy}<sub>2</sub>(dtbbpy)]PF<sub>6</sub> (1.0 mol %) in DMF/H<sub>2</sub>O (Figure 3.10,

bottom). The progress of the reaction was measured in terms of conversion of starting material and monitored by  $^1\text{H}$  NMR. After 2.5 h of visible light irradiation, conversion was measured to be 50% and the light source was removed. The reaction was stirred for 6 h in the dark with no detectable reaction progression. The light source was then reintroduced to reactivate the catalyst, and after an additional 4.5 h the conversion of 5-hexen-1-ol was judged to be complete. The results of this experiment neither definitively confirm a radical-polar crossover mechanism nor definitively negate a radical chain propagation mechanism, although it is clear that visible light is a necessary component of the reaction.



**Figure 3.10** Evidence for radical polar crossover mechanism.

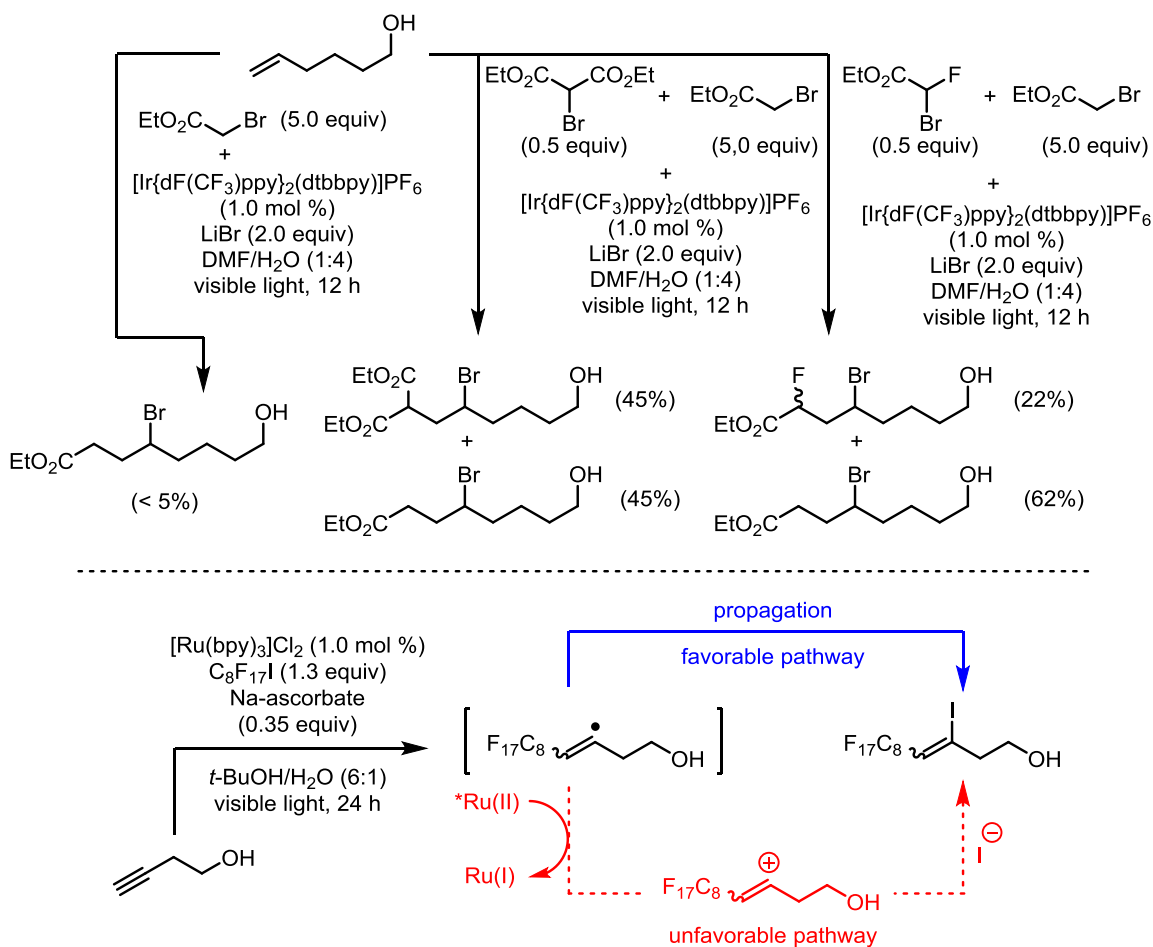




**Figure 3.11** Light/dark experiment.

However, the successful ATRA of perfluoroalkyl iodides onto alkynes indicates that chain propagation is operational to some extent for photocatalytic ATRA when utilizing the reductive quenching of **1**. A plausible mechanistic rationale for the oxidative quenching of **1** and **71** involves visible light-mediated initiation of the chain propagation that provides the ATRA product. Termination of the propagation via oxidation of the radical to the carbocation by the catalyst provides the ATRA product by nucleophilic trapping, and also regenerates the ground state catalyst (PC<sup>hν</sup>), completing the catalytic cycle. Therefore, the use of a photocatalyst as an initiator for ATRA contrasts traditional radical initiators in that the termination process is actually productive.

Although both quenching pathways lead to the same product, there are essential differences worth noting. The reduction potentials for  $^*[\text{Ir}\{\text{dF}(\text{CF}_3)\text{ppy}\}_2(\text{dtbbpy})]^+$  and  $^*[\text{Ru}(\text{bpy})_3]^{2+}$  are  $-0.89\text{ V}$  and  $-0.86\text{ V}$  vs. SCE, respectively, for oxidative quenching, whereas the reduction potential of  $[\text{Ir}\{\text{dF}(\text{CF}_3)\text{ppy}\}_2(\text{dtbbpy})]$  is  $-1.37\text{ V}$  vs. SCE and  $-1.33\text{ V}$  vs. SCE for  $[\text{Ru}(\text{bpy})_3]^+$  for reductive quenching. Due to the nature of these metal-centered complexes,



**Figure 3.12** Evidence for propagation mechanism.

the reduction potential for a photocatalyst when applying the oxidative quenching pathway is less negative than when utilizing the reductive quenching pathway. This is illustrated by the longer reaction times and the requirement of using Lewis acid additives (i.e. LiBr) when  $\alpha$ -bromo carbonyls are used for ATRA via oxidative quenching. In this case, the Lewis acid coordination makes the carbon-halogen bond more prone to reduction and, therefore, to free radical formation. In contrast, the reductive quenching cycle utilizes a reductive quencher to access a stronger reductant ( $\text{PC}^{\text{n-1}}$ ) to achieve the reduction of the carbon-halogen bond without the need for a Lewis acid. This ability to effect the same transformation by carefully optimizing

the reaction conditions for either oxidative or reductive quenching of a photocatalyst illustrates the complementary nature of the two quenching pathways.

## Conclusion

During the pursuit to develop efficient reductive cyclization and intermolecular coupling reactions by means of visible light photocatalysis, the formation of ATRA products was observed in several cases. As a consequence of these observations I realized that redox neutral coupling products might be obtained by utilizing a photocatalytic approach towards general C–C coupling reactions. The reductive quenching conditions optimized for reductive coupling and cyclization reactions with tertiary amines as stoichiometric electron donors did not produce efficient and general ATRA transformations. I consequently turned to the oxidative quenching pathway and successfully employed  $[\text{Ir}\{\text{dF}(\text{CF}_3)\text{ppy}\}_2(\text{dtbbpy})]\text{PF}_6$  in the photocatalytic ATRA between various activated halides and alkenes. Even though this protocol efficiently mediated the ATRA between terminal alkenes and activated alkyl bromides and iodides, the reaction conditions were not amenable to activated alkyl chlorides, 1,2-disubstituted alkenes, or styrene derivatives. However, these limitations were resolved by utilizing  $[\text{Ru}(\text{bpy})_3]\text{Cl}_2$  or  $[\text{Ir}\{\text{dF}(\text{CF}_3)\text{ppy}\}_2(\text{dtbbpy})]\text{PF}_6$  in DMSO instead of a DMF/H<sub>2</sub>O mixture.

By utilizing the oxidative quenching cycle of the photocatalyst, reactions originating from sacrificial electron donors are avoided. However, this somewhat restricts the reductive ability of the catalyst and limits the substrate scope. These shortcomings were addressed successfully during the development of a highly efficient and mild protocol to effect fluorine tagging of both alkenes and alkynes. By utilizing sodium ascorbate as an inexpensive substoichiometric electron donor, I managed to bypass shortcomings associated with the use of tertiary amines as electron donors. The ATRA reaction has a broad functional group tolerance

and is competent with structurally diverse perfluorinated alkyl iodides. Yields are high to excellent and reaction times are typically 0.5 h. Furthermore, the capability of the protocol in post-transformational quenching was illustrated by fluororous tagging of an alkene-functionalized triphenylphosphine derivative in both a Wittig and a Mitsunobu reaction.

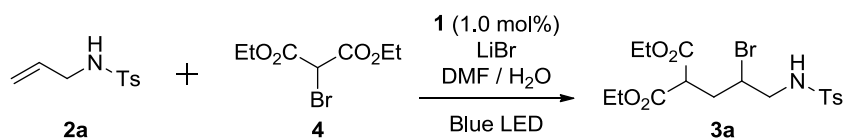
The development of ATRA via the oxidative and reductive quenching of photocatalysts has been firmly established as a reliable and versatile methodology. In particular, the ability to predictably direct the reaction outcome by careful selection and modification of the catalysts, additives, and solvents has been presented.

## Experimental

### General Procedure A: Typical Photoredox Catalyzed Atom Transfer Radical Addition

A 10 mL round bottom flask was equipped with a rubber septum and magnetic stir bar and was charged with olefin (1.0 mmol, 1.0 equiv), atom transfer agent (2.0 mmol, 2.0 equiv), additive (2.0 mmol, 2.0 equiv), DMF (0.20 mL), H<sub>2</sub>O (0.80 mL), Ir(dF(CF<sub>3</sub>)ppy)<sub>2</sub>(dtbbpy)PF<sub>6</sub>, **1**, (0.010 mmol, 0.010 equiv). The flask was evacuated and backfilled with argon. The heterogeneous mixture was then irradiated by a 1 W blue LED strip under an atmosphere of Ar for 6 – 24h. After the reaction was complete (as judged by TLC analysis), the mixture was poured into a separatory funnel containing 25 mL of EtOAc and 25 mL of H<sub>2</sub>O. The layers were separated and the aqueous layer was extracted with EtOAc (2 X 50 mL). The combined organic layers were dried (Na<sub>2</sub>SO<sub>4</sub>) and concentrated. The residue was purified by chromatography on silica gel, using the solvent system indicated, to afford the desired atom transfer product.

Diethyl 2-(2-bromo-3-(4-methylphenylsulfonamido)propyl)malonate, **3a** (Table 2, entry 1):



According to General Procedure A, **2a** (0.19 g, 0.90 mmol), **4** (0.43 g, 1.8 mmol), LiBr (0.16 g, 1.8 mmol), and **1** (10 mg, 9.0  $\mu$ mol) in DMF (0.20 mL) and H<sub>2</sub>O (0.80 mL) afforded **3a** (0.27 g, 67%) as a colorless oil after purification by chromatography on SiO<sub>2</sub> (4:1 to 6:4, hexanes/EtOAc) (48 h reaction time).

$R_f$  (EtOAc/hexane 1:4): 0.16;

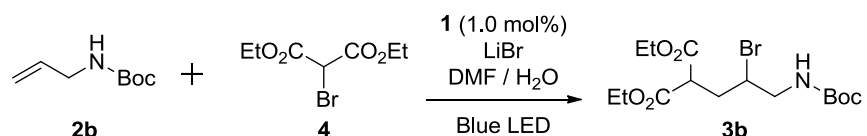
IR (neat): 3282, 2984, 2925, 1730, 1445, 1334, 1304, 1159, 1093, 1026, 815, 665 cm<sup>-1</sup>;

<sup>1</sup>H NMR (CDCl<sub>3</sub>, 400 MHz):  $\delta$  7.74 (d,  $J$  = 8.0 Hz, 2 H), 7.31 (d,  $J$  = 8.0 Hz, 2 H), 4.92 (t,  $J$  = 6.3 Hz, 1 H), 4.27 – 4.15 (m, 4 H), 4.10 – 4.04 (m, 1 H), 3.65 (dd,  $J$  = 9.4, 4.8 Hz, 1 H), 3.37 – 3.22 (m, 2 H), 2.47 – 2.40 (m, 4 H), 2.30 – 2.23 (m, 1 H), 1.29 – 1.24 (m, 6 H);

<sup>13</sup>C NMR (CDCl<sub>3</sub>, 100 MHz):  $\delta$  168.6, 168.3, 143.7, 136.7, 129.8, 127.0, 61.8, 61.7, 51.7, 49.9, 49.4, 34.5, 21.5, 13.9, 13.9;

HRMS (ESI)  $m/z$  calculated for C<sub>17</sub>H<sub>24</sub>BrNNaO<sub>6</sub>S<sup>+</sup> ([M+Na]<sup>+</sup>) 472.0405, found 472.0403.

Diethyl 2-(2-bromo-3-((tert-butoxycarbonyl)amino)propyl)malonate, **3b** (Table 2, entry 2):



According to General Procedure A, **2b** (0.17 g, 1.1 mmol), **4** (0.52 g, 2.2 mmol), LiBr (0.19 g, 2.2 mmol), and **1** (12 mg, 11  $\mu$ mol) in DMF (0.20 mL) and H<sub>2</sub>O (0.80 mL) afforded **3b** (0.43 g, 99%) as a colorless oil after purification by chromatography on SiO<sub>2</sub> (4:1, hexanes/EtOAc) (24 h reaction time).

$R_f$  (EtOAc/hexane 3:7): 0.48;

IR (neat): 3388, 2979, 2935, 1728, 1511, 1367, 1249, 1159, 1095, 1028, 860 cm<sup>-1</sup>;

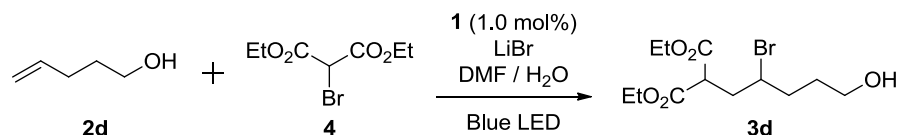
<sup>1</sup>H NMR (CDCl<sub>3</sub>, 400 MHz):  $\delta$  4.96 (br. s, 1 H), 4.26 – 4.18 (m, 4 H), 4.14 – 4.10 (m, 1 H), 3.74 (dd,  $J$  = 9.6, 4.8 Hz, 1 H), 3.54 – 3.48 (m, 2 H), 2.51 – 2.44 (m, 1 H), 2.30 – 2.23 (m, 1 H), 1.45

(s, 9 H), 1.30 – 1.25 (m, 6 H);

$^{13}\text{C}$  NMR ( $\text{CDCl}_3$ , 125 MHz):  $\delta$  168.8, 168.4, 155.6, 79.8, 61.7, 61.7, 53.2, 50.1, 47.1, 34.6, 28.3, 14.0, 14.0;

HRMS (ESI)  $m/z$  calculated for  $\text{C}_{15}\text{H}_{26}\text{BrNO}_6^+$  ( $[\text{M}+\text{H}]^+$ ) 395.0943, found 395.0941.

Diethyl 2-(2-bromo-5-hydroxypentyl)malonate, **3d** (Table 2, entry 4):



According to General Procedure A, **2d** (0.17 g, 2.0 mmol), **4** (0.95 g, 4.0 mmol), LiBr (0.34 g, 4.0 mmol), and **1** (22mg, 12  $\mu\text{mol}$ ) in DMF (0.40 mL) and H<sub>2</sub>O (1.6 mL) afforded **3d** (0.62 g, 95%) as a colorless oil after purification by chromatography on SiO<sub>2</sub> (4:1, hexanes/EtOAc) (24 h reaction time).

$R_f$  (EtOAc/hexane 30:70): 0.23;

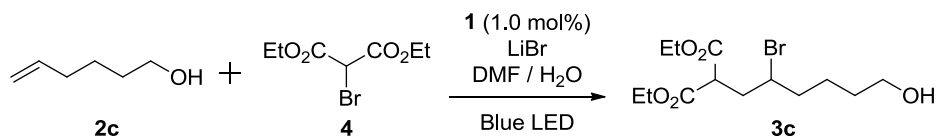
IR (neat): 3442, 2981, 2939, 1729, 1445, 1369, 1264, 1150, 1028  $\text{cm}^{-1}$ ;

$^1\text{H}$  NMR ( $\text{CDCl}_3$ , 300 MHz):  $\delta$  4.27 – 4.15 (m, 4 H), 4.09 – 4.00 (m, 1 H), 3.78 (dd,  $J = 10.2, 4.5$  Hz, 1 H), 3.69 (t,  $J = 6.0$  Hz, 2 H), 2.48 (ddd,  $J = 15.0, 10.2, 3.6$  Hz, 1 H), 2.27 (ddd,  $J = 15.0, 10.5, 4.5$  Hz, 1 H), 2.03 – 1.67 (m, 4 H), 1.48 (br. s, 1 H), 1.31 – 1.25 (m, 6 H);

$^{13}\text{C}$  NMR ( $\text{CDCl}_3$ , 75 MHz):  $\delta$  168.7, 168.6, 61.5, 61.4, 54.4, 50.3, 37.6, 35.5, 30.2, 13.8, 13.8;

HRMS (ESI)  $m/z$  calculated for  $\text{C}_{12}\text{H}_{22}\text{BrO}_5^+$  ( $[\text{M}+\text{H}]^+$ ) 325.0651, found 325.0679.

Diethyl 2-(2-bromo-6-hydroxyhexyl)malonate, **3c** (Table 2, entry 3):



According to General Procedure A, **2c** (0.10 g, 1.0 mmol), **4** (0.48 g, 2.0 mmol), LiBr (0.17 g, 2.0 mmol), and **1** (11 mg, 10  $\mu\text{mol}$ ) in DMF (0.20 mL) and H<sub>2</sub>O (0.80 mL) afforded **3c** (0.34 g,



99%) as a yellow oil after purification by chromatography on SiO<sub>2</sub> (4:1, hexanes/EtOAc) (24 h reaction time).

$R_f$  (EtOAc/hexane 30:70): 0.23;

IR (neat): 3395, 2982, 2938, 2360, 1728, 1369, 1261, 1151, 1030, 913, 731 cm<sup>-1</sup>;

<sup>1</sup>H NMR (CDCl<sub>3</sub>, 500 MHz):  $\delta$  4.29 – 4.18 (m, 4 H), 4.05 – 4.00 (m, 1 H), 3.79 (dd,  $J = 11.6, 4.4$  Hz, 1 H), 3.67 (t,  $J = 6.3$  Hz, 2 H), 2.49 (ddd,  $J = 15.0, 10.5, 3.3$  Hz, 1 H), 2.28 (ddd,  $J = 14.7, 10.5, 4.1$  Hz, 1 H) 1.94 – 1.89 (m, 2 H), 1.69 – 1.50 (m, 5 H), 1.32 – 1.28 (m, 6 H);

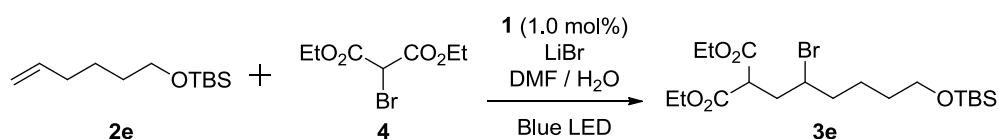
<sup>13</sup>C NMR (CDCl<sub>3</sub>, 125 MHz):  $\delta$  168.9, 168.7, 62.4, 61.7, 61.6, 54.6, 50.5, 39.1, 37.8, 31.8, 23.7, 14.0, 14.0;

HRMS (ESI)  $m/z$  calculated for C<sub>13</sub>H<sub>23</sub>BrO<sub>5</sub><sup>+</sup> ([M+H]<sup>+</sup>) 339.0807, found 339.0800.

Preparative Scale with Low Catalyst Loading:

According to General Procedure A, **S7** (1.5 g, 15 mmol), **4** (7.1 g, 30 mmol), LiBr (2.6 g, 30 mmol), and **1** (3.3 mg, 3.0  $\mu$ mol) in DMF (6.1 mL) and H<sub>2</sub>O (25 mL) afforded **S8** (4.7 g, 97%) as a yellow oil after purification by chromatography on SiO<sub>2</sub> (4:1, hexanes/EtOAc) (24 h reaction time).

Diethyl 2-(2-bromo-6-((tert-butyldimethylsilyl)oxy)hexyl)malonate, **3e** (Table 2, entry 5):



According to General Procedure A, **2e** (0.13 g, 0.61 mmol), **4** (0.20 g, 1.2 mmol), LiBr (0.11 g, 1.2 mmol), and **1** (6.8 mg, 6.1  $\mu$ mol) in DMF (0.20 mL) and H<sub>2</sub>O (0.80 mL) afforded **3e** (0.25 g, 90%) as a yellow oil after purification by chromatography on SiO<sub>2</sub> (95:5, hexanes/EtOAc) (24 h reaction time).

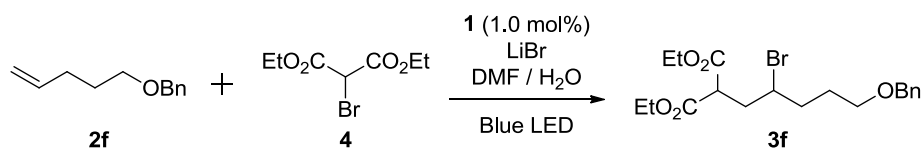
$R_f$  (EtOAc/hexane 5:95): 0.13;

IR (neat): 2931, 2857, 1732, 1471, 1255, 1205, 1096, 835, 775  $\text{cm}^{-1}$ ;

$^1\text{H}$  NMR ( $\text{CDCl}_3$ , 400 MHz):  $\delta$  4.27 – 4.17 (m, 4 H), 4.03 – 3.97 (m, 1 H), 3.78 (dd,  $J = 10.4$ , 4.0 Hz, 1 H), 3.61 (t,  $J = 5.6$  Hz, 2 H), 2.46 (ddd,  $J = 14.0$ , 10.5, 3.2 Hz, 1 H), 2.25 (ddd,  $J = 14.8$ , 10.5, 4.4 Hz, 1 H), 1.90 – 1.84 (m, 2 H), 1.61 – 1.17 (m, 6 H), 1.30 – 1.25 (m, 6 H), 0.89 (s, 9 H), 0.05 (s, 6 H);

$^{13}\text{C}$  NMR ( $\text{CDCl}_3$ , 125 MHz):  $\delta$  168.9, 168.7, 62.7, 61.6, 61.5, 54.7, 50.5, 39.1, 37.8, 31.9, 25.9, 23.8, 14.0, 13.9, -5.4.

Diethyl 2-(6-(benzyloxy)-2-bromohexyl)malonate, **3f** (Table 2, entry 6):



According to General Procedure A, **2f** (0.50 g, 2.8 mmol), **4** (1.4 g, 5.7 mmol), LiBr (0.49 g, 5.7 mmol), and **1** (16 mg, 28  $\mu\text{mol}$ ) in DMF (0.40 mL) and H<sub>2</sub>O (1.6 mL) afforded **3f** (1.1 g, 92%) as a colorless oil after purification by chromatography on SiO<sub>2</sub> (85:15, hexanes/EtOAc) (24 h reaction time).

$R_f$  (EtOAc/hexane 15:85): 0.25;

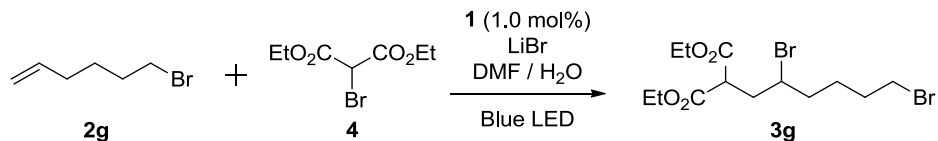
IR (neat): 2981, 2859, 1730, 1453, 1368, 1262, 1150, 1096, 1028, 737  $\text{cm}^{-1}$ ;

$^1\text{H}$  NMR ( $\text{CDCl}_3$ , 400 MHz):  $\delta$  7.30 – 7.19 (m, 5 H), 4.43 (s, 2 H), 4.19 – 4.10 (m, 4 H), 4.00 – 3.94 (m, 1 H), 3.71 (dd,  $J = 10.4$ , 4.4 Hz, 1 H), 3.43 (t,  $J = 6.0$  Hz, 2 H), 2.40 (ddd,  $J = 14.8$ , 10.4, 3.2 Hz, 1 H), 2.21 (ddd,  $J = 14.8$ , 10.4, 4.0 Hz, 1 H), 1.99 – 1.78 (m, 3 H), 1.74 – 1.64 (m, 1 H) 1.22 – 1.18 (m, 6 H);

$^{13}\text{C}$  NMR ( $\text{CDCl}_3$ , 75 MHz):  $\delta$  168.8, 168.6, 138.3, 128.3, 127.5, 127.5, 72.8, 69.2, 61.6, 61.5, 54.7, 50.5, 37.8, 36.1, 27.7, 14.0, 13.9;

HRMS (ESI)  $m/z$  calculated for  $\text{C}_{19}\text{H}_{27}\text{BrNaO}_5^+$  ( $[\text{M}+\text{Na}]^+$ ) 437.0940, found 437.0938.

Diethyl 2-(2,6-dibromohexyl)malonate, **3g** (Table 2, entry 7):



According to General Procedure A, **2g** (0.10 g, 0.61 mmol), **4** (0.29 g, 1.2 mmol), LiBr (0.11 g, 1.2 mmol), and **1** (6.9 mg, 6.1  $\mu$ mol) in DMF (0.20 mL) and H<sub>2</sub>O (0.80 mL) afforded **3g** (0.23 g, 94%) as a colorless oil after purification by chromatography on SiO<sub>2</sub> (9:1, hexanes/Et<sub>2</sub>O) (24 h reaction time).

*R<sub>f</sub>* (EtOAc/hexane 8:92): 0.29;

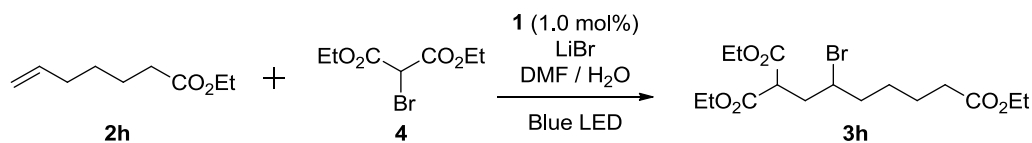
IR (neat): 2981, 2938, 1729, 1445, 1261, 1150, 1096, 1029, 857 cm<sup>-1</sup>;

<sup>1</sup>H NMR (CDCl<sub>3</sub>, 500 MHz):  $\delta$  4.27 – 4.19 (m, 4 H), 4.04 – 3.99 (m, 1 H), 3.80 (dd, *J* = 10.5, 4.5 Hz, 1 H), 3.43 (t, *J* = 7.0 Hz, 2 H), 2.48 (ddd, *J* = 15.0, 10.5, 3.0 Hz, 1 H), 2.28 (ddd, *J* = 14.5, 10.5, 4.0 Hz, 1 H), 1.95 – 1.88 (m, 4 H), 1.78 – 1.73 (m, 1 H), 1.68 – 1.60 (m, 1 H), 1.59 (s, 1 H), 1.33 – 1.29 (m, 6 H);

<sup>13</sup>C NMR (CDCl<sub>3</sub>, 100 MHz):  $\delta$  168.9, 168.7, 61.7, 61.6, 54.2, 50.5, 38.4, 37.8, 33.2, 31.9, 26.1, 14.0, 14.0;

HRMS (ESI) *m/z* calculated for C<sub>13</sub>H<sub>23</sub>Br<sub>2</sub>O<sub>4</sub><sup>+</sup> ([M+H]<sup>+</sup>) 400.9963, found 400.9958

Triethyl 3-bromoheptane-1,1,7-tricarboxylate, **3h** (Table 2, entry 8):



According to General Procedure A, **2g** (0.19 g, 1.2 mmol), **4** (0.58 g, 2.4 mmol), LiBr (0.21 g, 2.4 mmol), and **1** (13 mg, 12  $\mu$ mol) in DMF (0.20 mL) and H<sub>2</sub>O (0.80 mL) afforded **3h** (480 mg, 99%) as a colorless oil after purification by chromatography on SiO<sub>2</sub> (9:1, hexanes/Et<sub>2</sub>O) (24 h reaction time).

$R_f$  (EtOAc/hexane 1:4): 0.33;

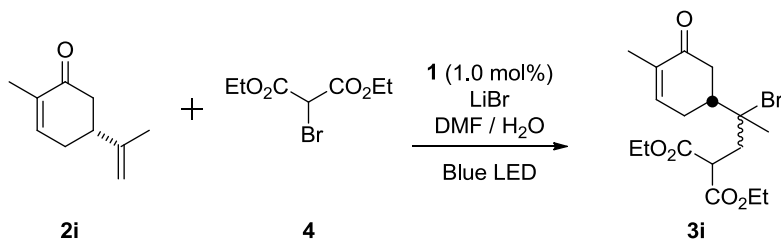
IR (neat): 2981, 2939, 1729, 1446, 1369, 1258, 1178, 1150, 1029  $\text{cm}^{-1}$ ;

$^1\text{H}$  NMR ( $\text{CDCl}_3$ , 500 MHz):  $\delta$  4.27 – 4.16 (m, 4 H), 4.13 (q,  $J = 9.0$  Hz, 2 H), 4.03 – 3.96 (m, 1 H), 3.77 (dd,  $J = 13.0, 5.5$  Hz, 1 H), 2.45 (ddd,  $J = 18.5, 13.0, 4.0$  Hz, 1 H), 2.31 (t,  $J = 8.5$  Hz, 2 H), 2.25 (ddd,  $J = 18.5, 13.0, 5.0$  Hz, 1 H), 1.89 – 1.84 (m, 2 H), 1.70 – 1.56 (m, 3 H), 1.53 – 1.44 (m, 1 H), 1.30 – 1.24 (m, 9 H);

$^{13}\text{C}$  NMR ( $\text{CDCl}_3$ , 75 MHz):  $\delta$  173.4, 168.9, 168.7, 61.7, 61.6, 60.2, 54.2, 50.2, 39.0, 37.8, 34.0, 26.9, 24.2, 14.2, 14.0, 14.0;

HRMS (ESI)  $m/z$  calculated for  $\text{C}_{16}\text{H}_{28}\text{BrO}_6^+$  ( $[\text{M}+\text{H}]^+$ ) 395.1069, found 395.1064.

Diethyl 2-(2-bromo-2-(4-methyl-5-oxocyclohex-3-en-1-yl)propyl)malonate, **3i** (Table 2, entry 9):



According to General Procedure A, **2i** (0.10 g, 0.66 mmol), **4** (0.32 g, 1.3 mmol), LiBr (0.12 g, 1.3 mmol), and **1** (7.5 mg, 6.6  $\mu\text{mol}$ ) in DMF (0.20 mL) and H<sub>2</sub>O (0.80 mL) afforded **3i** (0.25 g, 95%) as a colorless oil and an inseparable mixture of diastereoisomers after purification by chromatography on SiO<sub>2</sub> (4:1, hexanes/EtOAc) (24 h reaction time).

$R_f$  (EtOAc/hexane 1:4): 0.26;

IR (neat): 2981, 2935, 1730, 1673, 1447, 1268, 1254, 1149, 1109, 1026  $\text{cm}^{-1}$ ;

$^1\text{H}$  NMR ( $\text{CDCl}_3$ , 500 MHz):  $\delta$  6.74 (t,  $J = 7.0$  Hz, 1 H), 4.24 – 4.18 (m, 4 H), 3.71 – 3.68 (m, 1 H), 2.83 – 2.52 (m, 3 H), 2.49 – 2.37 (m, 3 H), 2.25 – 2.14 (m, 1 H), 1.78 (s, 3 H), 1.66 (s, 3 H);

$^{13}\text{C}$  NMR ( $\text{CDCl}_3$ , 125 MHz):  $\delta$  198.6, 198.5, 171.1, 169.4, 169.4, 169.0, 144.0, 143.7, 135.4,

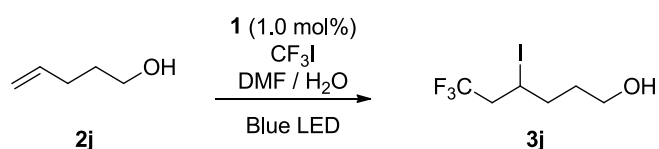
135.3, 72.9, 72.9, 62.0, 61.9, 61.9, 60.4, 49.7, 49.6, 47.1, 46.8, 41.0, 40.9, 40.7, 40.7, 28.9, 28.6, 28.1, 28.1, 21.0, 15.5, 14.2, 13.9;

HRMS (ESI)  $m/z$  calculated for  $C_{17}H_{23}BrNaO_4^+$  ( $[M+Na]^+$ ) 389.0964, found 389.0982

### General Procedure B: Photoredox Atom Transfer Radical Additions of $CF_3I$

A 15 mL pressure vessel was equipped with a rubber septum and magnetic stir bar and was charged with olefin (1.0 mmol, 1.0 equiv), DMF (0.20 mL),  $H_2O$  (0.80 mL),  $Ir(dF(CF_3)ppy)_2(dtbbpy)PF_6$  (0.01 mmol, 0.01 equiv) and degassed (3 x freeze/pump/thaw). The mixture was then cooled to  $-78\text{ }^\circ\text{C}$  and  $CF_3I$  was condensed in. The vessel was then sealed and allowed to warm to room temperature while under irradiation by a 1 W blue LED strip. After 48 h, the mixture was cooled to  $-78\text{ }^\circ\text{C}$ , the vessel was opened and the mixture was allowed to warm to room temperature. The mixture was then poured into a separatory funnel containing 25 mL of EtOAc and 25 mL of  $H_2O$ . The layers were separated and the aqueous layer was extracted with EtOAc (2 X 50 mL). The combined organic layers were dried ( $Na_2SO_4$ ) and concentrated. The residue was purified by chromatography on silica gel, using the solvent system indicated, to afford the desired atom transfer product.

6,6-Trifluoro-4-iodohexan-1-ol, **3j** (Table 2, entry 10):



According to General Procedure B **2j** (0.25 g, 2.9 mmol),  $CF_3I$ , and **1** (16 mg, 15  $\mu\text{mol}$ ) in DMF (1.2 mL) and  $H_2O$  (4.8 mL) afforded **3j** (0.74 g, 90%) as a colorless oil after purification by chromatography on  $SiO_2$  (4:1, hexanes/EtOAc) (48 h reaction time).

$R_f$  (EtOAc/hexane 1:4): 0.23;

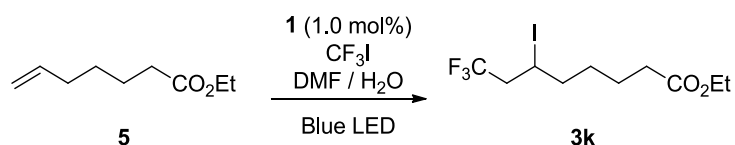
IR (neat): 3346, 2944, 1434, 1367, 1252, 1142, 1109, 1057, 1030  $\text{cm}^{-1}$ ;

$^1\text{H}$  NMR ( $\text{CDCl}_3$ , 500 MHz):  $\delta$  4.28 – 4.23 (m, 1 H), 3.73 (t,  $J = 6.5$  Hz, 2 H), 3.00 – 2.90 (m, 1 H), 2.87 – 2.77 (m, 1 H), 1.95 – 1.81 (m, 3 H), 1.75 – 1.68 (m, 1 H), 1.38 (br. s, 1 H);

$^{13}\text{C}$  NMR ( $\text{CDCl}_3$ , 100 MHz):  $\delta$  125.5 (q,  $^1J_{\text{C-F}} = 277.3$  Hz), 61.5, 44.8 (q,  $^2J_{\text{C-F}} = 28.2$  Hz), 36.1, 32.4, 21.3 (q,  $^2J_{\text{C-F}} = 3.0$  Hz);

LRMS (ESI)  $m/z$  (relative intensity): 337 (100%), 305 (5%), 277 (5%), 261 (37%), 258 (10%), 233 (11%), 130 (6%).

Ethyl 8,8,8-trifluoro-6-iodooctanoate, **3k** (Table 2, entry 11):



According to General Procedure B, **5** (0.15 g, 0.96 mmol),  $\text{CF}_3\text{I}$ , and **1** (11 mg, 9.6  $\mu\text{mol}$ ) in DMF (0.40 mL) and  $\text{H}_2\text{O}$  (1.6 mL) afforded **3k** (0.27 g, 81%) as a yellow oil after purification by chromatography on  $\text{SiO}_2$  (19:1, hexanes/EtOAc) (48 h reaction time).

$R_f$  (EtOAc/hexane 5:95): 0.32;

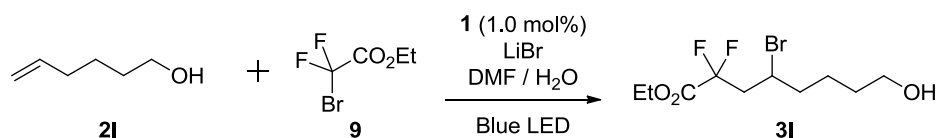
IR (neat): 2981, 2940, 1731, 1433, 1372, 1252, 1144, 1109, 1029  $\text{cm}^{-1}$ ;

$^1\text{H}$  NMR ( $\text{CDCl}_3$ , 500 MHz):  $\delta$  4.23 – 4.18 (m, 1 H), 4.15 (q,  $J = 7.0$  Hz, 2 H), 2.98 – 2.87 (m, 1 H), 2.85 – 2.71 (m, 1 H), 2.35 (t,  $J = 7.0$  Hz, 2 H), 1.88 – 1.57 (m, 5 H), 1.51 – 1.43 (m, 1 H), 1.29 (t,  $J = 7.0$  Hz, 3 H);

$^{13}\text{C}$  NMR ( $\text{CDCl}_3$ , 100 MHz):  $\delta$  173.2, 125.5 (q,  $^1J_{\text{C-F}} = 277.4$  Hz), 60.2, 44.8 (q,  $^2J_{\text{C-F}} = 28.3$  Hz), 39.2, 33.9, 28.9, 23.8, 21.0 (q,  $^3J_{\text{C-F}} = 2.2$  Hz), 14.2;

LRMS (ESI)  $m/z$  (relative intensity): 353 (100%), 344 (57%), 329 (42%), 301 (36%), 243 (29%), 197 (22%), 149 (33%).

Ethyl 4-bromo-2,2-difluoro-8-hydroxyoctanoate, **3l** (Table 2, entry 12):



According to General Procedure A, **21** (0.15 g, 1.5 mmol), **9** (0.61 g, 3.0 mmol), LiBr (0.26 g, 3.0 mmol), and **1** (17 mg, 15  $\mu$ mol) in DMF (0.70 mL) and H<sub>2</sub>O (2.5 mL) afforded **31** (0.42 g, 93%) as a colorless oil after purification by chromatography on SiO<sub>2</sub> (70:30, hexanes/EtOAc) (24 h reaction time)

$R_f$  (EtOAc/hexane 30:70): 0.20;

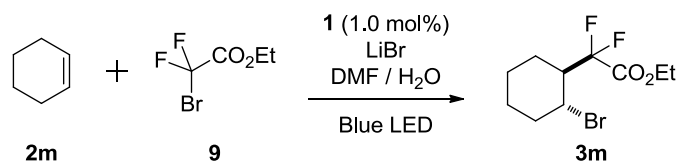
IR (neat): 3369, 2985, 2942, 2874, 1762, 1372, 1339, 1306, 1192, 1071, 851, 775 cm<sup>-1</sup>;

<sup>1</sup>H NMR (CDCl<sub>3</sub>, 500 MHz):  $\delta$  4.36 (q,  $J$  = 7.5 Hz, 2 H), 4.22 – 4.17 (m, 1 H), 3.69 (t,  $J$  = 6.0 Hz, 2 H), 2.90 – 2.79 (m, 1 H), 2.72 – 2.62 (m, 1 H), 1.98 – 1.88 (m, 2 H), 1.72 – 1.54 (m, 4 H), 1.40 (t,  $J$  = 7.5 Hz, 3 H);

<sup>13</sup>C NMR (CDCl<sub>3</sub>, 125 MHz):  $\delta$  163.5 (t, <sup>2</sup> $J_{C-F}$  = 39.3 Hz), 114.7 (dd, <sup>1</sup> $J_{C-F}$  = 251.8, 249.0 Hz) 63.2, 62.5, 46.0 (dd, <sup>3</sup> $J_{C-F}$  = 6.0, 3.75 Hz), 43.5 (t, <sup>2</sup> $J_{C-F}$  = 23.6, 22.6 Hz), 38.8, 31.6, 23.5, 13.8;

LRMS (ESI)  $m/z$  (relative intensity): 425 (100%), 403 (29%), 329 (22%), 305 (10%), 303 (10%), 287 (34%), 285 (34%), 205 (43%), 177 (13%).

Ethyl 2-(2-bromocyclohexyl)-2,2-difluoroacetate<sup>62</sup>, **3m** (Table 2, entry 13):



According to General Procedure A, **2m** (0.15 g, 1.8 mmol), **9** (0.74 g, 3.6 mmol), LiBr (0.32 g, 3.6 mmol), and **1** (20 mg, 18  $\mu$ mol) in DMF (0.40 mL) and H<sub>2</sub>O (1.6 mL) afforded **3m** (0.39 g, 75%) as a colorless oil after purification by chromatography on SiO<sub>2</sub> (99:1, petroleum

<sup>62</sup> *J. Fluorine Chem.* **2008**, *129*, 986.

ether/Et<sub>2</sub>O) (24 h reaction time).

*R<sub>f</sub>* (Et<sub>2</sub>O/Petroleum Ether 2:98): 0.35;

<sup>1</sup>H NMR (CDCl<sub>3</sub>, 300 MHz): δ 4.34 (q, *J* = 7.0 Hz, 2 H), 4.07 (ddd, *J* = 9.9, 9.9, 3.9 Hz, 1 H), 2.79 – 2.63 (m, 1 H), 2.39 – 2.34 (m, 1 H), 2.16 – 2.11 (m, 1 H), 1.95 – 1.72 (m, 4 H) 1.37 (t, *J* = 7.0 Hz, 3 H).

5-Bromo-7,7,7-trichloroheptan-1-ol, **3n** (Table 2, entry 14):



According to General Procedure A, **3n** (0.20 g, 2.0 mmol), **10** (0.79 g, 4.0 mmol), and **1** (22 mg, 20 μmol) in DMF (0.82 mL) and H<sub>2</sub>O (3.3 mL) afforded **3n** (0.51 g, 87%) as a colorless oil after purification by chromatography on SiO<sub>2</sub> (70:30, hexanes/EtOAc) (17 h reaction time).

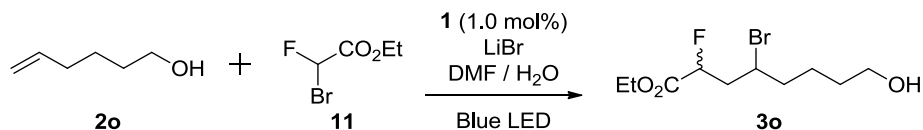
*R<sub>f</sub>* (EtOAc/hexane 30:70): 0.32;

IR (neat): 3344, 2939, 2865, 1457, 1423, 1188, 1053, 785, 699 cm<sup>-1</sup>;

<sup>1</sup>H NMR (CDCl<sub>3</sub>, 500 MHz): δ 4.38 – 4.33 (m, 1 H), 3.70 (t, *J* = 6.0 Hz, 2 H), 3.48 (dd, *J* = 15.5, 5.0 Hz, 1 H), 3.25 (dd, *J* = 15.5, 5.5 Hz, 1 H), 2.14 – 2.07 (m, 1 H), 2.04 – 1.97 (m, 1 H), 1.76 – 1.59 (m, 4 H), 1.36 (br. s, 1 H);

<sup>13</sup>C NMR (CDCl<sub>3</sub>, 125 MHz): δ 97.1, 62.5, 62.5, 48.9, 39.2, 31.7, 23.6.

Ethyl 4-bromo-2-fluoro-8-hydroxyoctanoate, **3o** (Table 2, entry 14):



According to General Procedure A, **2o** (0.15 g, 1.5 mmol), **11** (0.55 g, 3.0 mmol), LiBr (0.26 g, 3.0 mmol), and **1** (17 mg, 15 μmol) in DMF (0.70 mL) and H<sub>2</sub>O (2.5 mL) afforded **3o** (0.42 g, 99%) as a colorless oil and an inseparable mixture of diastereoisomers after purification by



chromatography on SiO<sub>2</sub> (13:7, hexanes/EtOAc) (24 h reaction time).

*R<sub>f</sub>* (EtOAc/hexane 30:70): 0.13;

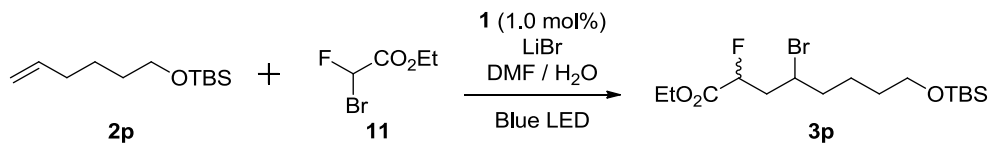
IR (neat): 3368, 2939, 1752, 1457, 1372, 1214, 1100, 1026, 909, 729 cm<sup>-1</sup>;

<sup>1</sup>H NMR (CDCl<sub>3</sub>, 500 MHz): δ 5.30 – 5.07 (m, 1 H), 4.31 – 4.26 (m, 2 H), 4.24 – 4.18 (m, 1 H), 3.69 (t, *J* = 6.0 Hz, 2 H), 2.56 – 2.44 (m, 1 H), 2.39 – 2.25 (m, 1 H), 1.98 – 1.88 (m, 2 H), 1.73 – 1.52 (m, 4 H), 1.37 – 1.33 (m, 4 H);

<sup>13</sup>C NMR (CDCl<sub>3</sub>, 100 MHz): δ 169.2 (d, <sup>2</sup>*J*<sub>C-F</sub> = 23.0 Hz), 168.9 (d, <sup>2</sup>*J*<sub>C-F</sub> = 23.0 Hz), 87.0 (d, <sup>1</sup>*J*<sub>C-F</sub> = 183.7 Hz), 86.7 (d, <sup>1</sup>*J*<sub>C-F</sub> = 183.7 Hz), 61.9, 61.6, 51.6, 51.6, 50.6, 50.5, 41.35 (d, <sup>2</sup>*J*<sub>C-F</sub> = 20.1 Hz), 41.0 (d, <sup>2</sup>*J*<sub>C-F</sub> = 21.6 Hz), 38.7, 37.8, 31.5, 31.5, 23.5, 23.4, 13.8, 13.8;

HRMS (ESI) *m/z* calculated for C<sub>10</sub>H<sub>19</sub>BrFO<sub>3</sub><sup>+</sup> ([M+H]<sup>+</sup>) 285.0502, found 285.0497.

Ethyl 4-bromo-8-((tert-butyldimethylsilyl)oxy)-2-fluorooctanoate, **3p** (Table 2, entry 16):



According to General Procedure A, **2p** (0.31 g, 1.4 mmol), **11** (0.53 g, 2.9 mmol), LiBr (0.25 g, 2.9 mmol), and **1** (16 mg, 14 μmol) in DMF (0.80 mL) and H<sub>2</sub>O (2.6 mL) afforded **3p** (480 mg, 84%) as a colorless oil and an inseparable mixture of diastereoisomers after purification by chromatography on SiO<sub>2</sub> (93:7, hexanes/EtOAc) (24 h reaction time).

*R<sub>f</sub>* (EtOAc/hexane 5:95): 0.33;

IR (neat): 2953, 2930, 1857, 1763, 1742, 1471, 1254, 1097, 835, 775, 733 cm<sup>-1</sup>;

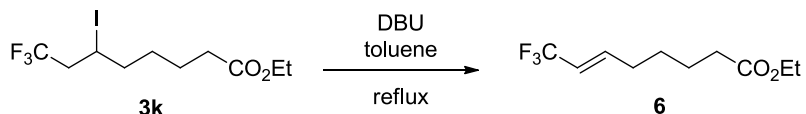
<sup>1</sup>H NMR (CDCl<sub>3</sub>, 500 MHz): δ 5.30 – 5.07 (m, 1 H), 4.31 – 4.26 (m, 2 H), 4.24 – 4.17 (m, 1 H), 3.64 (t, *J* = 6.0 Hz, 2 H), 2.53 – 2.44 (m, 1 H), 2.38 – 2.26 (m, 1 H), 1.95 – 1.88 (m, 2 H), 1.68 – 1.49 (m, 4 H), 1.37 – 1.33 (m, 3 H), 0.92 (s, 9 H), 0.08 (s, 6 H);

<sup>13</sup>C NMR (CDCl<sub>3</sub>, 100 MHz): δ 169.1 (d, <sup>2</sup>*J*<sub>C-F</sub> = 23.1 Hz), 168.8 (d, <sup>2</sup>*J*<sub>C-F</sub> = 23.8 Hz), 87.1 (d,

$^1J_{\text{C-F}} = 183.7$  Hz), 86.8 (d,  $^1J_{\text{C-F}} = 183.7$  Hz), 62.5, 61.5, 61.4, 51.6, 51.6, 50.6, 50.5, 41.6 (d,  $^2J_{\text{C-F}} = 20.9$  Hz), 41.2 (d,  $^2J_{\text{C-F}} = 21.6$  Hz), 38.9, 38.0, 31.8, 31.8, 25.8, 23.7, 23.6, 18.1, 13.9, 13.9, -5.5;

HRMS (ESI)  $m/z$  calculated for  $\text{C}_{10}\text{H}_{33}\text{BrFO}_3\text{Si}^+$  ( $[\text{M}+\text{H}]^+$ ) 399.1366, found 399.1367.

Ethyl 8,8,8-trifluorooct-6-enoate, **6**:



A flame dried 10 mL round bottom flask, equipped with a magnetic stir bar and fitted with a reflux condenser, was charged with **3k** (81 mg, 0.23 mmol), dry toluene (2.5 mL) and DBU (0.10 g, 0.46 mmol) and heated to reflux. Upon completion, the mixture was cooled to room temperature and poured into a separatory funnel containing 25 mL of Et<sub>2</sub>O and 25 mL of H<sub>2</sub>O. The layers were separated and the aqueous layer was extracted with Et<sub>2</sub>O (2 x 30 mL). The combined organic layers were dried (Na<sub>2</sub>SO<sub>4</sub>) and concentrated. The residue was purified by chromatography on silica gel (95:5, hexanes/EtOAc) to afford **6** (48 mg, 94%) as a colorless oil along with a small amount of (*E*) isomer (2 h reaction time).

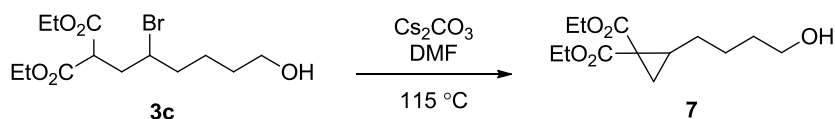
$R_f$  (EtOAc/hexane 5:95): 0.35;

IR (neat): 2934, 2865, 1735, 1274, 1173, 1119, 1088, 974  $\text{cm}^{-1}$ ;

$^1\text{H}$  NMR ( $\text{CDCl}_3$ , 400 MHz):  $\delta$  6.40 – 6.32 (m, 1 H), 5.66 – 5.57 (m, 1 H), 4.13 (q,  $J = 7.0$  Hz, 2 H), 2.31 (t,  $J = 8.0$  Hz, 2 H), 2.19 – 2.15 (m, 2 H), 1.69 – 1.62 (m, 2 H), 1.52 – 1.44 (m, 2 H), 1.26 (t,  $J = 7.0$  Hz, 3 H);

$^{13}\text{C}$  NMR ( $\text{CDCl}_3$ , 75 MHz):  $\delta$  173.3, 140.1 (q,  $^3J_{\text{C-F}} = 6.6$  Hz) 123.0 (q,  $^1J_{\text{C-F}} = 265.7$  Hz), 118.7, (q,  $^2J_{\text{C-F}} = 32.9$  Hz), 60.0, 33.6, 30.8, 27.1, 24.1, 13.8.

Diethyl 2-(4-hydroxybutyl)cyclopropane-1,1-dicarboxylate, **7**:



A flame dried 25 mL round bottom flask, equipped with a magnetic stir bar and fitted with a reflux condenser, was charged with **3c** (0.21 g, 0.62 mmol), dry DMF (6.0 mL) and Cs<sub>2</sub>CO<sub>3</sub> (0.22 g, 0.68 mmol) and heated to 115 °C. The mixture was poured into a separatory funnel containing 25 mL of Et<sub>2</sub>O and 25 mL of H<sub>2</sub>O. The layers were separated and the aqueous layer was extracted with Et<sub>2</sub>O (2 x 30 mL). The combined organic layers were dried (Na<sub>2</sub>SO<sub>4</sub>) and concentrated. The residue was purified by chromatography on silica gel (13:7, hexanes/EtOAc) to afford **7** (0.15 g, 94%) as a colorless oil (24 h reaction time).

*R<sub>f</sub>* (EtOAc/hexane 30:70): 0.21;

IR (neat): 3435, 2982, 2937, 2865, 1720, 1446, 1393, 1281, 1204, 1131, 1024, 861 cm<sup>-1</sup>;

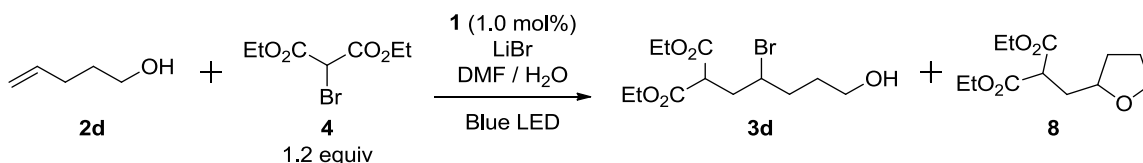
<sup>1</sup>H NMR (CDCl<sub>3</sub>, 500 MHz): δ 4.30 – 4.20 (m, 4 H), 3.64 (t, *J* = 6.0 Hz, 2 H), 1.94 – 1.88 (m, 1 H), 1.67 – 1.50 (m, 6 H), 1.42 – 1.35 (m, 3 H), 1.33 – 1.26 (m, 7 H);

<sup>13</sup>C NMR (CDCl<sub>3</sub>, 100 MHz): δ 170.4, 168.2, 62.3, 61.2, 61.2, 34.0, 32.1, 28.3, 28.0, 24.9, 20.8, 14.0, 13.9;

HRMS (ESI) *m/z* calculated for C<sub>13</sub>H<sub>23</sub>BrO<sub>5</sub><sup>+</sup> ([M+H]<sup>+</sup>) 259.1545, found 259.1556.

### Isolation of THF byproduct, **8**:

Diethyl 2-((tetrahydrofuran-2-yl)methyl)malonate, **8**<sup>63</sup> (*eq 1*):



<sup>63</sup> Tetrahydrofuran side product, **8**, was confirmed by <sup>1</sup>H and <sup>13</sup>C NMR, see: *J. Am. Chem. Soc.* **2005**, *127*, 12180.

A 10 mL round bottom flask was equipped with a rubber septum and magnetic stir bar and was charged with **2d** (100 mg, 1.2 mmol), **4** (330 mg, 1.4 mmol), LiBr (200 mg, 2.3 mmol), DMF (0.40 mL), H<sub>2</sub>O (1.60 mL), and Ir(dF(CF<sub>3</sub>)ppy)<sub>2</sub>(dtbbpy)PF<sub>6</sub>, **1**, (13 mg, 1.2 μmol). The flask was evacuated and backfilled with argon. The heterogeneous mixture was then irradiated by a 1 W blue LED strip under an atmosphere of Ar. The mixture was poured into a separatory funnel containing 25 mL of Et<sub>2</sub>O and 25 mL of H<sub>2</sub>O. The layers were separated and the aqueous layer was extracted with Et<sub>2</sub>O (2 x 30 mL). The combined organic layers were dried (Na<sub>2</sub>SO<sub>4</sub>) and concentrated. The residue was purified by chromatography on silica gel (4:1, hexanes/EtOAc) to afford **3d** (280 mg, 73%) as a colorless oil and **8** (29 mg, 10%) as a colorless oil (12 h reaction time).

*R<sub>f</sub>* (EtOAc/hexane 30:70): 0.34;

<sup>1</sup>H NMR (CDCl<sub>3</sub>, 300 MHz): δ 4.23 - 4.15 (m, 4 H), 3.90 – 3.85 (m, 1 H), 3.80 (t, *J* = 7.5 Hz, 1 H), 3.74 – 3.66 (m, 1 H), 3.56 (dd, *J* = 8.7, 6.0 Hz, 1 H), 2.11 (dd, *J* = 9.3, 4.8 Hz, 1 H), 2.07 – 1.96 (m, 2 H), 1.91 – 1.82 (m, 2 H), 1.56 – 1.45 (m, 1 H), 1.29 – 1.23 (m, 6 H);

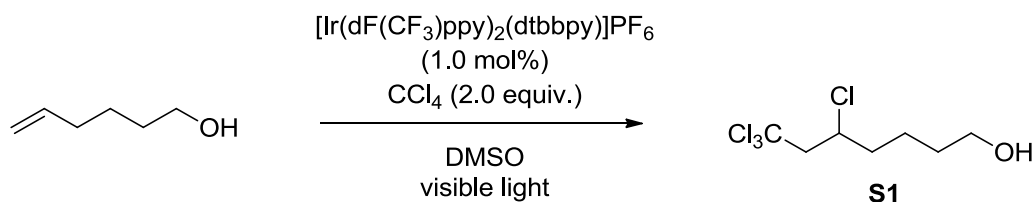
<sup>13</sup>C NMR (CDCl<sub>3</sub>, 75 MHz): δ 169.5, 169.3, 76.4, 67.6, 61.2, 49.3, 34.5, 31.3, 25.5, 13.9, 13.9.

**General Procedure A: ATRA via Oxidative Quenching of Ru(bpy)<sub>3</sub>Cl<sub>2</sub> or [Ir{dF(CF<sub>3</sub>)ppy}<sub>2</sub>(dtbbpy)]PF<sub>6</sub>**

A 10 mL round bottom flask (or Schlenk flask) was equipped with a rubber septum and a magnetic stir bar and was charged with alkene (1.0 mmol, 1.0 equiv.), DMSO (2.0 mL), halogenated atom transfer compound (1.2 – 2.0 equiv.), Ru(bpy)<sub>3</sub>Cl<sub>2</sub> or [Ir{dF(CF<sub>3</sub>)ppy}<sub>2</sub>(dtbbpy)]PF<sub>6</sub> (0.010 mmol, 0.010 equiv.). The mixture was then degassed by Ar sparging for 15 min. Alternatively, volatile alkenes and halogenated atom transfer agents are degassed separately and added to a degassed solution of Ru(bpy)<sub>3</sub>Cl<sub>2</sub> or

[Ir{dF(CF<sub>3</sub>)ppy}<sub>2</sub>(dtbbpy)]PF<sub>6</sub> in DMSO. The mixture was then stirred under an Ar atmosphere and irradiated by blue LEDs. After the reaction was complete, as judged by TLC analysis, the reaction mixture was diluted with EtOAc and washed with water. The organic layer was then washed with brine and dried with sodium sulfate. Organic solvents are removed *in vacuo* and the crude product was purified according to the indicated method.

5,7,7,7-Tetrachloroheptan-1-ol,<sup>64</sup> **S1**, (Eq. 10)

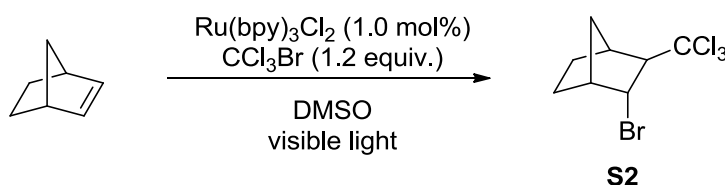


According to General Procedure A, 5-hexen-1-ol (0.10 g, 0.12 mL, 1.0 mmol), CCl<sub>4</sub> (0.30 g, 0.20 mL, 2.0 mmol), and [Ir(dF(CF<sub>3</sub>)ppy)<sub>2</sub>(dtbbpy)]PF<sub>6</sub> (12 mg, 10 μmol) in DMSO (2.0 mL) afforded **S1** (0.21 g, 82%) after purification by chromatography on SiO<sub>2</sub> (75:25, hexanes/EtOAc).

*R<sub>f</sub>* (EtOAc/hexanes 1:3): 0.22;

<sup>1</sup>H NMR (CDCl<sub>3</sub>, 500 MHz): δ 4.27 (m, 1H), 3.67 (t, *J* = 6.0 Hz, 2H), 3.26 (ABX system, *J*<sub>AB</sub> = 15.7 Hz, *J*<sub>BX</sub> = 10.6 Hz, 1H), 3.12 (ABX system, *J*<sub>AB</sub> = 15.7 Hz, *J*<sub>AX</sub> = 7.9 Hz, 1H), 2.05 (s, 1H), 2.05 – 1.53 (m, 6H).

2-bromo-3-(trichloromethyl)bicyclo[2.2.1]heptane,<sup>65</sup> **S2**, (Scheme 2)



<sup>64</sup> *Monatshefte für Chemie*, **2000**, *131*, 1091.

<sup>65</sup> *Angew. Chem., Int. Ed.* **2011**, *50*, 5532.

According to General Procedure A, 2-norbornene (94 mg, 1.0 mmol), CCl<sub>3</sub>Br (0.24 g, 0.12 mL, 1.2 mmol), and Ru(bpy)<sub>3</sub>Cl<sub>2</sub> (7.5 mg, 10 μmol) in DMSO (2.0 mL) afforded **S2** as an 8:1 mixture of two diastereoisomers (0.28 g, 97%) after purification by chromatography on SiO<sub>2</sub> (99:1, hexanes/EtOAc).

*R<sub>f</sub>* (EtOAc/hexanes 1:19): 0.79;

major diastereoisomer (*endo*-bromo, *exo*-trichloromethyl): <sup>1</sup>H NMR (CD<sub>3</sub>CN, 500 MHz): δ 4.33 (ddd, *J* = 6.0, 3.7, 1.4 Hz, 1H), 2.77 (d, *J* = 6.0 Hz, 1H), 2.59 (br. s, 1H), 2.55 (br. s, 1H), 2.10 (d, *J* = 11.0 Hz, 1H), 1.96 (d, *J* = 11.0 Hz, 1H), 1.72 – 1.56 (m, 2H), 1.50 – 1.29 (m, 2H).

2-bromo-3-(bromodifluoromethyl)bicyclo[2.2.1]heptane,<sup>66</sup> **S3**, (Scheme 2)



According to General Procedure A, 2-norbornene (94 mg, 1.0 mmol), CF<sub>2</sub>Br<sub>2</sub> (0.25 g, 0.11 mL, 1.2 mmol), and Ru(bpy)<sub>3</sub>Cl<sub>2</sub> (7.5 mg, 10 μmol) in DMSO (2.0 mL) afforded **S3** as a 5:1 mixture of two diastereoisomers (0.27 g, 88%) after purification by chromatography on SiO<sub>2</sub> (hexanes).

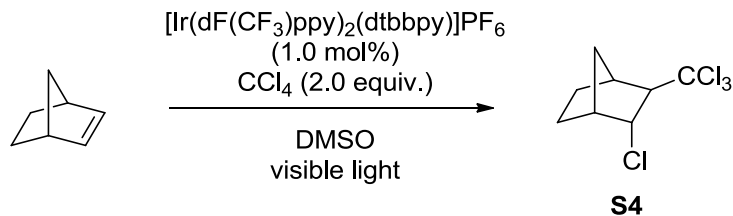
*R<sub>f</sub>* (EtOAc/hexanes 1:19): 0.87;

major diastereoisomer (*endo*-bromo, *exo*-monobromodifluoromethyl): <sup>1</sup>H NMR (CDCl<sub>3</sub>, 400 MHz): δ 4.16 (t, *J* = 5.0 Hz, 1H), 2.90 – 2.30 (m, 3H), 2.10 – 1.90 (m, 1H), 1.80 – 1.50 (m, 3H), 1.40 – 1.20 (m, 2H).

2-chloro-3-(trichloromethyl)bicyclo[2.2.1]heptane,<sup>67</sup> **S4**, (Scheme 2)

<sup>66</sup> *J. Org. Chem.* **1989**, *54*, 3992.

<sup>67</sup> *Adv. Synth. Catal.* **2008**, *350*, 1771.

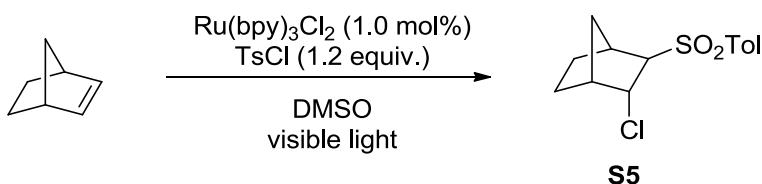


According to General Procedure A, 2-norbornene (94 mg, 1.0 mmol),  $\text{CCl}_4$  (0.30 g, 0.20 mL, 2.0 mmol), and  $[\text{Ir}(\text{dF}(\text{CF}_3)\text{ppy})_2(\text{dtbbpy})]\text{PF}_6$  (12 mg, 10  $\mu\text{mol}$ ) in DMSO (2.0 mL) afforded **S4** as a 11:1 mixture of two diastereoisomers (0.23 g, 93%) after purification by chromatography on  $\text{SiO}_2$  (99:1, hexanes/EtOAc).

$R_f$  (EtOAc/hexanes 1:19): 0.79;

major diastereoisomer (*endo*-chloro, *exo*-trichloromethyl):  $^1\text{H NMR}$  ( $\text{CDCl}_3$ , 400 MHz):  $\delta$  4.24 (m, 1H), 2.65 – 2.61 (m, 2H), 2.53 (s, 1H), 2.11 – 2.02 (m, 2H), 1.74 – 1.34 (m, 4H).

3-Chlorobicyclo[2.2.1] hept-2-yl 4-methylphenyl sulfone,<sup>68</sup> **S5**, (Scheme 2)

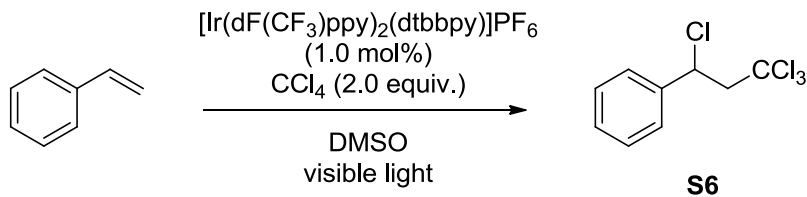


According to General Procedure A, 2-norbornene (94 mg, 1.0 mmol),  $\text{TsCl}$  (0.23 g, 1.2 mmol), and  $\text{Ru}(\text{bpy})_3\text{Cl}_2$  (7.5 mg, 10  $\mu\text{mol}$ ) in DMSO (2.0 mL) afforded **S5** as a single diastereoisomer (0.26 g, 90%) after the crude product was treated with chloroform, the solution obtained was passed through a bed of silica gel 0.5 cm thick, the chloroform was removed *in vacuo*, and the residue was recrystallized from ethanol.

$^1\text{H NMR}$  ( $\text{CDCl}_3$ , 400 MHz):  $\delta$  7.78 (d,  $J = 8.0$  Hz, 2H), 7.37 (d,  $J = 8.0$  Hz, 2H), 4.42 (m, 1H), 2.90 – 2.85 (m, 2H), 2.53 (br. s, 1H), 2.46 (s, 3H), 2.05 – 1.28 (m, 6H).

1,1,1,3-tetrachloro-3-phenylpropane,<sup>69</sup> **S6**, (Scheme 2)

<sup>68</sup> *Russ. J. Org. Chem.* **2006**, *42*, 1142.

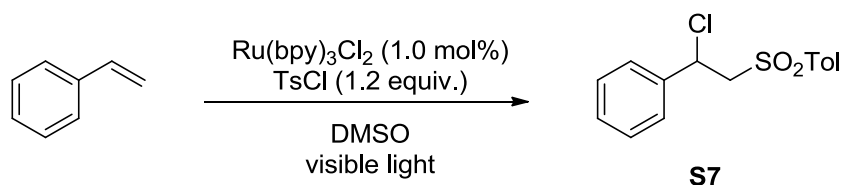


According to General Procedure A, styrene (0.10 g, 0.11 mL, 1.0 mmol),  $\text{CCl}_4$  (0.30 g, 0.20 mL, 2.0 mmol), and  $[\text{Ir}(\text{dF}(\text{CF}_3)\text{ppy})_2(\text{dtbbpy})]\text{PF}_6$  (12 mg, 10  $\mu\text{mol}$ ) in DMSO (2.0 mL) afforded **S6** (0.19 g, 75%) after purification by chromatography on  $\text{SiO}_2$  (hexanes).

$R_f$  (hexanes): 0.42;

$^1\text{H NMR}$  ( $\text{CDCl}_3$ , 400 MHz):  $\delta$  7.43 – 7.30 (m, 5H), 5.29 (t,  $J = 5.8$  Hz, 1H), 3.62 – 3.50 (m, 2H).

2-Chloro-2-phenylethyl *p*-tolyl sulfone,<sup>70</sup> **S7**, (Scheme 2)



According to General Procedure A, styrene (0.10 g, 0.11 mL, 1.0 mmol), TsCl (0.23 g, 1.2 mmol), and  $\text{Ru}(\text{bpy})_3\text{Cl}_2$  (7.5 mg, 10  $\mu\text{mol}$ ) in DMSO (2.0 mL) afforded **S7** (0.24 g, 80%) after purification by chromatography on  $\text{SiO}_2$  (70:30, petroleum ether/ether).

$R_f$  (ether/petroleum ether 1:2): 0.56;

$^1\text{H NMR}$  ( $\text{CDCl}_3$ , 400 MHz):  $\delta$  7.60 (d,  $J = 8.0$  Hz, 2H), 7.24 – 7.20 (m, 7H), 5.30 (t,  $J = 7.0$  Hz, 1H), 3.93 – 3.78 (m, 2H), 2.38 (s, 3H).

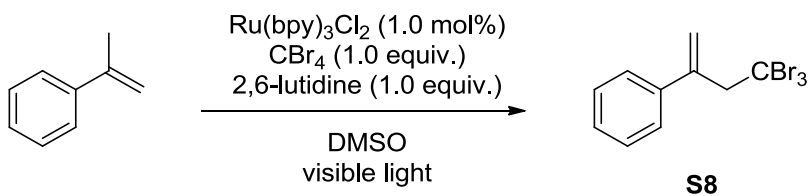
(4,4,4-tribromobut-1-en-2-yl)benzene,<sup>71</sup> **S8**, (Scheme 2)

<sup>69</sup> See ref. 66

<sup>70</sup> See ref. 66

<sup>71</sup> *Nature Chem.* **2011**, 3, 140.



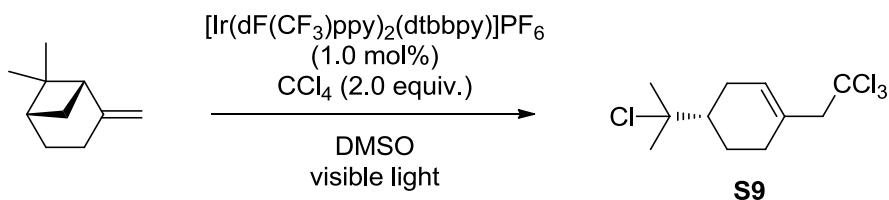


According to General Procedure A,  $\alpha$ -methylstyrene (0.12 g, 0.13 mL, 1.0 mmol),  $\text{CBr}_4$  (0.33 g, 1.0 mmol), 2,6-lutidine (0.11 g, 0.12 mL, 1.0 mmol) and  $\text{Ru}(\text{bpy})_3\text{Cl}_2$  (7.5 mg, 10  $\mu\text{mol}$ ) in DMSO (2.0 mL) afforded **S8** (0.27 g, 72%) after purification by chromatography on  $\text{SiO}_2$  (petroleum ether).

$R_f$  (hexanes): 0.65;

$^1\text{H}$  NMR ( $\text{CDCl}_3$ , 400 MHz):  $\delta$  7.44 – 7.25 (m, 5H), 5.68 (s, 1H), 5.58 (s, 1H), 4.26 (s, 2H).

1-(2,2,2-Trichloroethyl)-4-(2-chloroisopropyl)cyclohex-1-ene,<sup>72</sup> **S9**, (Scheme 2)



According to General Procedure A,  $\beta$ -pinene (0.14 g, 0.16 mL, 1.0 mmol),  $\text{CCl}_4$  (0.30 g, 0.20 mL, 2.0 mmol), and  $[\text{Ir}(\text{dF}(\text{CF}_3)\text{ppy})_2(\text{dtbbpy})]\text{PF}_6$  (12 mg, 10  $\mu\text{mol}$ ) in DMSO (2.0 mL) afforded **S9** (0.19 g, 65%) after purification by chromatography on  $\text{SiO}_2$  (hexanes).

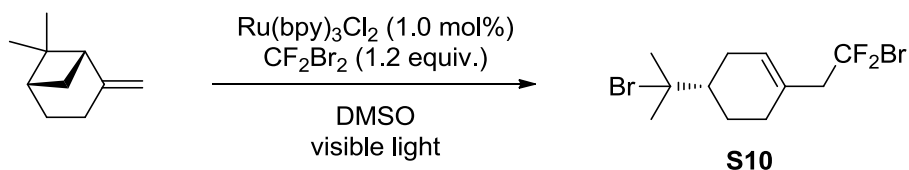
$R_f$  (hexanes): 0.55;

$^1\text{H}$  NMR ( $\text{CDCl}_3$ , 400 MHz):  $\delta$  5.81 (m, 1H), 3.35 (s, 2H), 2.40 (m, 2H), 2.00 (m, 4H), 1.88 (m, 1H), 1.60 (s, 3H), 1.56 (s, 3H).

1-(2-Bromo-2,2-difluoroethyl)-4-(2-bromoisopropyl)-cyclohexene,<sup>73</sup> **S10**, (Scheme 2)

<sup>72</sup> *J. Chem. Soc. Perkin Trans. I.* **1987**, 1515.

<sup>73</sup> *J. Fluorine Chem.* **2007**, 128, 1431.

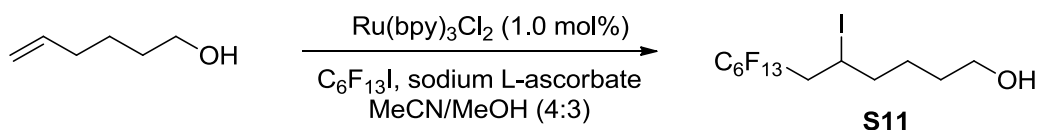


According to General Procedure A,  $\beta$ -pinene (0.14 g, 0.16 mL, 1.0 mmol),  $\text{CF}_2\text{Br}_2$  (0.25 g, 0.11 mL, 1.2 mmol), and  $\text{Ru(bpy)}_3\text{Cl}_2$  (7.5 mg, 10  $\mu\text{mol}$ ) in DMSO (2.0 mL) afforded **S10** (0.32 g, 92%) after crude product was diluted with water (5 ml), placed in a refrigerator for 1 h to produce colorless crystals, which were filtered off, washed several times with cold water and dried over  $\text{P}_4\text{O}_{10}$  under reduced pressure.

$^1\text{H NMR}$  ( $\text{CDCl}_3$ , 500 MHz):  $\delta$  5.70 (m, 1H), 3.04 (AB system,  $J_{\text{AB}} = 3.0$ ,  $^3J_{\text{HH}} = 15.5, 12.8$ , 2H), 2.35 – 2.00 (m, 5H), 1.80 (s, 3H), 1.75 (s, 3H), 1.65 (tdd,  $J = 11.5, 5.0, 2.3$ , 1H), 1.44 (ddd,  $J = 12.3, 11.8, 5.6$ , 1H).

### General Procedure B: Visible Light-Mediated Fluorous Tagging of Alkenes

A 10 mL round bottom flask was equipped with a rubber septum and a magnetic stir bar and was charged with alkene (0.25 mmol, 1.0 equiv.), MeCN (2.0 mL), perfluoroiodide (1.3 – 2.0 equiv.), MeOH (1.5 mL), sodium L-ascorbate (0.088 mmol, 0.35 equiv.),  $\text{Ru(bpy)}_3\text{Cl}_2$  (0.0025 mmol, 0.010 equiv.). The mixture was then degassed by Ar sparging for 15 min. The mixture was then stirred under an Ar atmosphere and irradiated by blue LEDs. After the reaction was complete, as judged by TLC analysis (typically 30 min), celite was added to the mixture and solvents were removed *in vacuo*. Celite with adsorbed crude mixture was loaded onto a silica gel column and purified, using the solvent system indicated, to afford the desired product. 5-Iodo-6-perfluorohexylhexanol, **S11**, (Table 5, entry 2)



According to General Procedure B, 5-hexen-1-ol (25 mg, 30  $\mu$ L, 0.25 mmol), C<sub>6</sub>F<sub>13</sub>I (0.11 mL, 0.22 g, 0.50 mmol), sodium L-ascorbate (0.10 g, 0.50 mmol), and Ru(bpy)<sub>3</sub>Cl<sub>2</sub> (1.9 mg, 2.5  $\mu$ mol) in MeOH (1.5 mL) and MeCN (2.0 mL) afforded **S11** (0.11 g, 81%) after purification by chromatography on SiO<sub>2</sub> (80:20, hexanes/EtOAc) (0.5 h reaction time).

$R_f$  (EtOAc/hexane 1:4): 0.22;

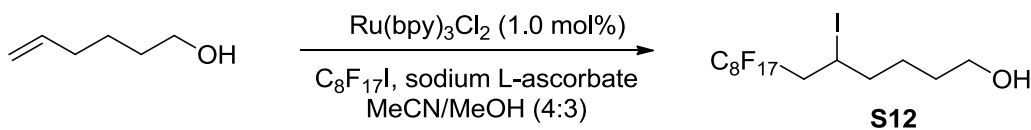
IR (neat): 3350, 2938, 2866, 1234, 1192, 1144, 1123, 1059 cm<sup>-1</sup>;

<sup>1</sup>H NMR (CDCl<sub>3</sub>, 500 MHz):  $\delta$  4.37 – 4.32 (m, 1H), 3.68 (t,  $J$  = 6.0 Hz, 2H), 2.99 – 2.87 (m, 1H), 2.85 – 2.73 (m, 1H), 1.91 – 1.79 (m, 2H), 1.60 – 1.48 (m, 4H);

<sup>19</sup>F NMR (CDCl<sub>3</sub>, 376 MHz):  $\delta$  -81.2 (t,  $J$  = 8.0 Hz, 3F), -111.1 – -111.7 (m, 1F), -113.9 – -114.6 (m, 1F), -121.1 – -121.4 (br s, 2F), -122.1 – -122.4 (br s, 2F), -122.9 – -123.1 (br s, 2F), -125.4 – -125.6 (br s, 2F);

<sup>13</sup>C NMR (CDCl<sub>3</sub>, 125 MHz):  $\delta$  62.5, 41.6 (t,  $J$  = 21 Hz), 40.0, 31.5, 26.0, 20.4.

5-Iodo-6-perfluorooctylhexanol, **S12**, (Table 5, entry 3)



According to General Procedure B, 5-hexen-1-ol (25 mg, 30  $\mu$ L, 0.25 mmol), C<sub>8</sub>F<sub>17</sub>I (88  $\mu$ L, 0.18 g, 0.33 mmol), sodium L-ascorbate (17 mg, 0.088 mmol), and Ru(bpy)<sub>3</sub>Cl<sub>2</sub> (1.9 mg, 2.5  $\mu$ mol) in MeOH (1.5 mL) and MeCN (2.0 mL) afforded **S12** (0.16 g, 99%) after purification by chromatography on SiO<sub>2</sub> (80:20, hexanes/EtOAc) (0.5 h reaction time).

Preparative Scale with Low Catalyst Loading:

5-hexen-1-ol (4.0 g, 4.8 mL, 40 mmol), C<sub>8</sub>F<sub>17</sub>I (14 mL, 28 g, 52 mmol), sodium L-ascorbate (2.8 g, 14 mmol), and Ru(bpy)<sub>3</sub>Cl<sub>2</sub> (3.0 mg, 4.0  $\mu$ mol) in MeOH (0.12 L) and MeCN (0.16 L) afforded **S12** (25 g, 96%) after purification by chromatography on SiO<sub>2</sub> (80:20, hexanes/EtOAc)

(0.5 h reaction time).

$R_f$  (EtOAc/hexane 1:4): 0.13;

IR (neat): 3337, 2934, 1199, 1146, 1117, 1062, 656  $\text{cm}^{-1}$ ;

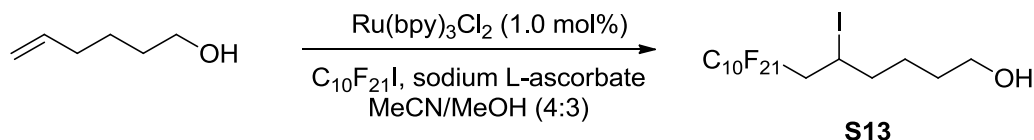
$^1\text{H}$  NMR ( $\text{CDCl}_3$ , 500 MHz):  $\delta$  4.40 – 4.30 (m, 1H), 3.70 (t,  $J = 7.5$  Hz, 2H), 3.04 – 2.70 (m, 2H), 1.95 – 1.77 (m, 2H), 1.73 – 1.45 (m, 4H), 1.41 – 1.23 (br s, 1H);

$^{19}\text{F}$  NMR ( $\text{CDCl}_3$ , 376 MHz):  $\delta$  -80.8 (t,  $J = 10$  Hz, 3F), -111.3 – -112.2 (m, 1F), -114.2 – -115.2 (m, 1F), -121.5 – -121.7 (br s, 2F), -121.8 – -122.1 (br s, 4F), -122.6 – -122.9 (br s, 2F), -123.5 – -123.7 (br s, 2F), -126.0 – -126.2 (br s, 2F);

$^{13}\text{C}$  NMR ( $\text{CDCl}_3$ , 125 MHz):  $\delta$  62.5, 41.7 (t,  $J = 22$  Hz), 40.1, 31.5, 26.0, 20.4;

LRMS (ESI)  $m/z$  (relative intensity): 629 (100%), 367 (13%), 501 (13%), 630 (5%).

5-Iodo-6-perfluorodecylhexanol, **S13**, (Table 5, entry 4)



According to General Procedure B, 5-hexen-1-ol (25 mg, 30  $\mu\text{L}$ , 0.25 mmol),  $\text{C}_{10}\text{F}_{21}\text{I}$  (0.19 g, 0.33 mmol), sodium L-ascorbate (17 mg, 0.088 mmol), and  $\text{Ru}(\text{bpy})_3\text{Cl}_2$  (1.9 mg, 2.5  $\mu\text{mol}$ ) in MeOH (1.5 mL) and MeCN (2.0 mL) afforded **S13** (0.18 g, 97%) after purification by chromatography on  $\text{SiO}_2$  (80:20, hexanes/EtOAc) (0.5 h reaction time).

$R_f$  (EtOAc/hexane 1:4): 0.25;

IR (neat): 3341, 2940, 2913, 2868, 1203, 1150, 1128, 1073, 650  $\text{cm}^{-1}$ ;

$^1\text{H}$  NMR ( $\text{CDCl}_3$ , 400 MHz):  $\delta$  4.39 – 4.32 (m, 1H), 3.72 – 3.67 (m, 2H), 3.03 – 2.71 (m, 2H), 1.95 – 1.77 (m, 2H), 1.73 – 1.47 (m, 4H), 1.31 – 1.26 (t,  $J = 5.2$  Hz, 1H);

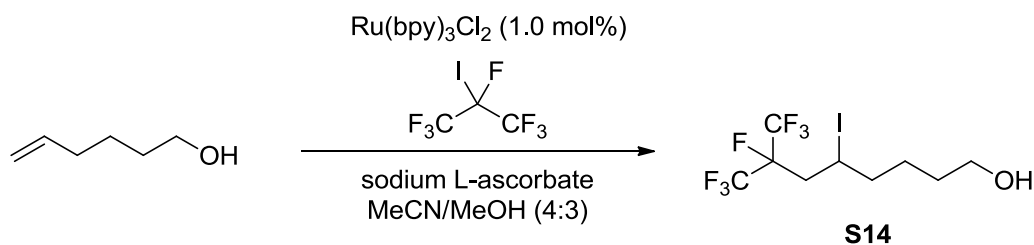
$^{19}\text{F}$  NMR ( $\text{CDCl}_3$ , 376 MHz):  $\delta$  -80.7 (t,  $J = 10$  Hz, 3F), -111.2 – -112.3 (m, 1F), -114.1 – -115.2 (m, 1F), -121.4 – -122.2 (br s, 10F), -122.6 – -122.9 (br s, 2F), -123.5 – -123.7 (br s, 2F), -126.0

-126.3 (br s, 2F);

$^{13}\text{C}$  NMR ( $\text{CDCl}_3$ , 100 MHz):  $\delta$  62.5, 41.6 (t,  $J = 20$  Hz), 40.0, 31.5, 26.0, 20.5;

HRMS (ESI)  $m/z$  calculated for  $\text{C}_{16}\text{H}_{10}\text{F}_{21}\text{I}$  ( $[\text{M} - \text{H}_2\text{O}]$ ) 728.9570, found 728.9572.

7,8,8,8-tetrafluoro-5-iodo-7-(trifluoromethyl)octan-1-ol, **S14**, (Table 5, entry 5)



According to General Procedure B, 5-hexen-1-ol (25 mg, 30  $\mu\text{L}$ , 0.25 mmol),  $(\text{CF}_3)_2\text{CFI}$  (47  $\mu\text{L}$ , 98 mg, 0.33 mmol), sodium L-ascorbate (17 mg, 0.088 mmol), and  $\text{Ru}(\text{bpy})_3\text{Cl}_2$  (1.9 mg, 2.5  $\mu\text{mol}$ ) in MeOH (1.5 mL) and MeCN (2.0 mL) afforded **S14** (80 mg, 81%) after purification by chromatography on  $\text{SiO}_2$  (80:20, hexanes/EtOAc) (0.5 h reaction time).

$R_f$  (EtOAc/hexane 3:17): 0.15;

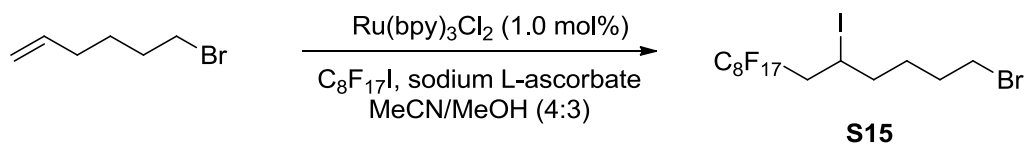
IR (neat): 3362, 2942, 2867, 1295, 1224, 1149, 1057, 953, 727  $\text{cm}^{-1}$ ;

$^1\text{H}$  NMR ( $\text{CDCl}_3$ , 500 MHz):  $\delta$  4.37 – 4.30 (m, 1H), 3.67 (t,  $J = 6.0$  Hz, 2H), 2.99 – 2.79 (m, 2H), 1.89 – 1.74 (m, 2H), 1.69 – 1.44 (m, 5H);

$^{19}\text{F}$  NMR ( $\text{CDCl}_3$ , 376 MHz):  $\delta$  -76.1 (qi,  $J = 8$  Hz, 3F), -77.5 (qi,  $J = 8$  Hz, 3F), -185.4 – -185.7 (m, 1F);

$^{13}\text{C}$  NMR ( $\text{CDCl}_3$ , 100 MHz):  $\delta$  62.4, 40.5, 39.7, 39.6, 31.5, 26.0, 22.4.

1-bromo-5-iodo-6-perfluorooctylhexane, **S15**, (Table 6, entry 2)



According to General Procedure B, 6-bromo-1-hexene (41 mg, 33  $\mu\text{L}$ , 0.25 mmol),  $\text{C}_8\text{F}_{17}\text{I}$  (88

$\mu\text{L}$ , 0.18 g, 0.33 mmol), sodium L-ascorbate (17 mg, 0.088 mmol), and  $\text{Ru}(\text{bpy})_3\text{Cl}_2$  (1.9 mg, 2.5  $\mu\text{mol}$ ) in MeOH (1.5 mL) and MeCN (2.0 mL) afforded **S15** (0.16 g, 93%) after purification by chromatography on  $\text{SiO}_2$  (hexanes) (0.5 h reaction time).

$R_f$  (hexane): 0.44;

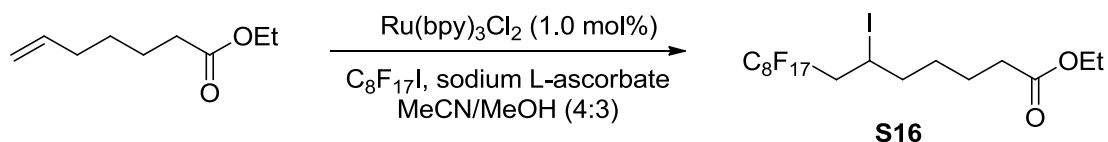
IR (neat): 2944, 2866, 1243, 1207, 1152, 1136, 736, 705, 658  $\text{cm}^{-1}$ ;

$^1\text{H}$  NMR ( $\text{CDCl}_3$ , 500 MHz):  $\delta$  4.38 – 4.30 (m, 1H), 3.43 (t,  $J = 7.0$  Hz, 2H), 3.02 – 2.87 (m, 1H), 2.86 – 2.71 (m, 1H), 2.01 – 1.68 (m, 5H), 1.65 – 1.54 (m, 1H);

$^{19}\text{F}$  NMR ( $\text{CDCl}_3$ , 376 MHz):  $\delta$  -81.4 (t,  $J = 10$  Hz, 3F), -110.8 – -111.8 (m, 1F), -113.8 – -113.8 (m, 1F), -120.9 – -121.2 (br s, 2F), -121.2 – -121.6 (br s, 4F), -122.1 – -122.4 (br s, 2F), -122.9 – -123.2 (br s, 2F), -125.2 – -125.7 (br s, 2F);

$^{13}\text{C}$  NMR ( $\text{CDCl}_3$ , 125 MHz):  $\delta$  41.7 (t,  $J = 20$  Hz), 39.3, 32.9, 31.6, 28.3, 19.8.

Ethyl 6-iodo-7-perfluorooctylheptanoate, **S16**, (Table 6, entry 3)



According to General Procedure B, ethyl 6-heptenoate (39 mg, 44  $\mu\text{L}$ , 0.25 mmol),  $\text{C}_8\text{F}_{17}\text{I}$  (88  $\mu\text{L}$ , 0.18 g, 0.33 mmol), sodium L-ascorbate (17 mg, 0.088 mmol), and  $\text{Ru}(\text{bpy})_3\text{Cl}_2$  (1.9 mg, 2.5  $\mu\text{mol}$ ) in MeOH (1.5 mL) and MeCN (2.0 mL) afforded **S16** (0.16 g, 94%) after purification by chromatography on  $\text{SiO}_2$  (94:6, hexanes/EtOAc) (0.5 h reaction time).

$R_f$  (EtOAc/hexane 1:3): 0.64;

IR (neat): 2986, 2942, 1737, 1372, 1243, 1208, 1152, 1135, 737, 705, 656  $\text{cm}^{-1}$ ;

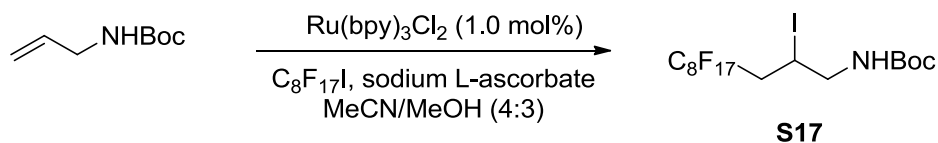
$^1\text{H}$  NMR ( $\text{CDCl}_3$ , 500 MHz):  $\delta$  4.36 – 4.29 (m, 1H), 4.14 (q,  $J = 7.0$  Hz, 2H), 2.99 – 2.85 (m, 1H), 2.84 – 2.70 (m, 1H), 2.33 (t,  $J = 7.0$  Hz, 2H), 1.90 – 1.76 (m, 2H), 1.76 – 1.55 (m, 3H), 1.52 – 1.42 (m, 1H), 1.26 (t,  $J = 7.0$  Hz, 3H);

$^{19}\text{F}$  NMR ( $\text{CDCl}_3$ , 376 MHz):  $\delta$  -81.0 (t,  $J$  = 9 Hz, 3F), -111.3 – -112.3 (m, 1F), -114.3 – -115.3 (m, 1F), -121.6 – -121.8 (br s, 2F), -121.9 – -122.2 (br s, 4F), -122.7 – -123.0 (br s, 2F), -123.6 – -123.9 (br s, 2F), -126.2 – -126.4 (br s, 2F);

$^{13}\text{C}$  NMR ( $\text{CDCl}_3$ , 125 MHz):  $\delta$  173.3, 60.3, 41.7 (t,  $J$  = 21 Hz), 39.9, 33.4, 29.1, 23.9, 20.1, 14.2;

HRMS (ESI)  $m/z$  calculated for  $\text{C}_{17}\text{H}_{16}\text{F}_{17}\text{IO}_2^+$  ( $[\text{M}+\text{H}]^+$ ) 703.0002, found 702.9994.

*tert*-butyl (4,4,5,5,6,6,7,7,8,8,9,9,10,10,11,11,11-heptadecafluoro-2-iodoundecyl)carbamate, **S17**,  
(Table 6, entry 4)



According to General Procedure B, *tert*-butyl allylcarbamate (39 mg, 0.25 mmol),  $\text{C}_8\text{F}_{17}\text{I}$  (88  $\mu\text{L}$ , 0.18 g, 0.33 mmol), sodium L-ascorbate (17 mg, 0.088 mmol), and  $\text{Ru}(\text{bpy})_3\text{Cl}_2$  (1.9 mg, 2.5  $\mu\text{mol}$ ) in MeOH (1.5 mL) and MeCN (2.0 mL) afforded **S17** (0.17 g, 96%) after purification by chromatography on  $\text{SiO}_2$  (95:5, hexanes/EtOAc) (0.5 h reaction time).

$R_f$  (EtOAc/hexane 1:4): 0.42;

IR (neat): 3376, 2983, 2938, 1688, 1515, 1370, 1240, 1202, 1148, 1117, 658  $\text{cm}^{-1}$ ;

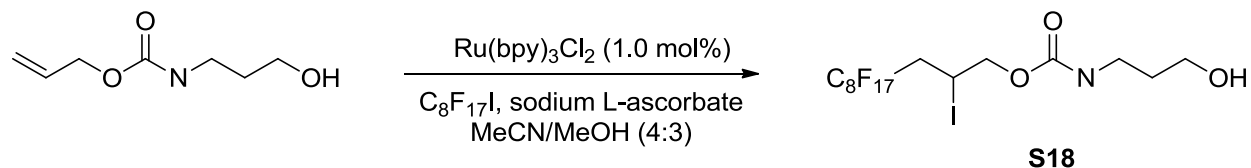
$^1\text{H}$  NMR ( $\text{CDCl}_3$ , 500 MHz):  $\delta$  5.08 – 4.86 (br s, 1H), 4.42 – 4.35 (m, 1H), 3.66 – 3.34 (m, 2H), 2.94 – 2.71 (m, 2H), 1.46 (s, 9H)

$^{19}\text{F}$  NMR ( $\text{CDCl}_3$ , 376 MHz):  $\delta$  -81.0 (t,  $J$  = 9 Hz, 3F), -111.7 – -114.8 (m, 2F), -121.5 – -121.8 (m, 2F), -121.9 – -122.3 (br s, 4F), -122.7 – -123.0 (br s, 2F), -123.6 – -123.9 (br s, 2F), -126.2 – -126.4 (br s, 2F);

$^{13}\text{C}$  NMR ( $\text{CDCl}_3$ , 125 MHz):  $\delta$  155.6, 80.2, 49.0, 38.6 (t,  $J$  = 21 Hz), 28.2, 18.5.

4,4,5,5,6,6,7,7,8,8,9,9,10,10,11,11,11-heptadecafluoro-2-iodoundecyl (3-hydroxypropyl)

carbamate, **S18**, (Table 6, entry 5)



According to General Procedure B, allyl (3-hydroxypropyl)carbamate (40 mg, 0.25 mmol),  $\text{C}_8\text{F}_{17}\text{I}$  (88  $\mu\text{L}$ , 0.18 g, 0.33 mmol), sodium L-ascorbate (17 mg, 0.088 mmol), and  $\text{Ru}(\text{bpy})_3\text{Cl}_2$  (1.9 mg, 2.5  $\mu\text{mol}$ ) in MeOH (1.5 mL) and MeCN (2.0 mL) afforded **S18** (0.14 g, 79%) after purification by chromatography on  $\text{SiO}_2$  (60:40, hexanes/EtOAc) (0.5 h reaction time).

$R_f$ (EtOAc/hexane 2:3): 0.17;

IR (neat): 3436, 3344, 2933, 2861, 1707, 1524, 1242, 1204, 1150, 907, 730, 650  $\text{cm}^{-1}$ ;

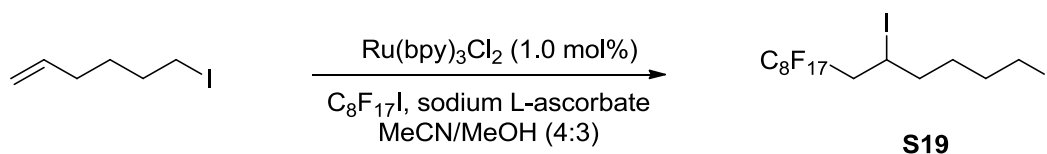
$^1\text{H}$  NMR ( $\text{CDCl}_3$ , 500 MHz):  $\delta$  5.33 – 5.12 (br s, 1H), 4.50 – 4.33 (m, 2H), 4.33 – 4.24 (m, 1H), 3.75 – 3.66 (m, 2H), 3.41 – 3.29 (m, 2H), 3.00 – 2.84 (m, 1H), 2.84 – 2.69 (m, 1H), 2.59 – 2.49 (br s, 1H), 1.80 – 1.70 (m, 2H);

$^{19}\text{F}$  NMR ( $\text{CDCl}_3$ , 376 MHz):  $\delta$  -81.6 (t,  $J = 9.0$  Hz, 3F), -112.0 – -113.0 (m, 1F), -113.4 – -114.4 (m, 1F), -121.0 – -121.3 (br s, 2F), -121.3 – -121.7 (br s, 4F), -122.0 – -122.5 (br s, 2F), -122.8 – -123.2 (br s, 2F), -125.4 – -125.8 (br s, 2F);

$^{13}\text{C}$  NMR ( $\text{CDCl}_3$ , 125 MHz):  $\delta$  156.2, 68.9, 59.7, 38.0 (t,  $J = 21$  Hz), 38.0, 32.3, 12.8;

HRMS (ESI)  $m/z$  calculated for  $\text{C}_{15}\text{H}_{13}\text{F}_{17}\text{INO}_3^+$  ( $[\text{M}+\text{H}]^+$ ) 705.9747, found 705.9720.

1,5-diiido-6-perfluorooctylhexane, **S19**, (Table 6, entry 6)



According to General Procedure B, 6-iodohexene (53 mg, 0.25 mmol),  $\text{C}_8\text{F}_{17}\text{I}$  (88  $\mu\text{L}$ , 0.18 g, 0.33 mmol), sodium L-ascorbate (17 mg, 0.088 mmol), and  $\text{Ru}(\text{bpy})_3\text{Cl}_2$  (1.9 mg, 2.5  $\mu\text{mol}$ ) in



MeOH (1.5 mL) and MeCN (2.0 mL) afforded **S19** (0.18 g, 94%) after purification by chromatography on SiO<sub>2</sub> (petroleum ether) (0.5 h reaction time).

*R<sub>f</sub>* (petroleum ether): 0.36;

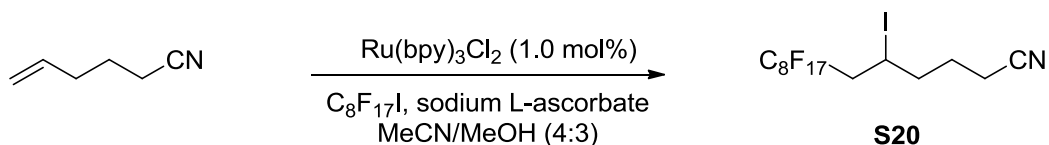
IR (neat): 2981, 2937, 2860, 1242, 1207, 1151, 736, 705, 668 cm<sup>-1</sup>;

<sup>1</sup>H NMR (CDCl<sub>3</sub>, 500 MHz): δ 4.38 – 4.28 (m, 1H), 3.26 – 3.17 (m, 2H), 3.02 – 2.87 (m, 1H), 2.87 – 2.70 (m, 1H), 1.98 – 1.77 (m, 4H), 1.75 – 1.65 (m, 1H), 1.62 – 1.51 (m, 1H);

<sup>19</sup>F NMR (CDCl<sub>3</sub>, 376 MHz): δ -80.8 (t, *J* = 10 Hz, 3F), -111.1 – -112.1 (m, 1F), -114.2 – -115.2 (m, 1F), -121.5 – -121.8 (br s, 2F), -121.8 – -122.2 (br s, 4F), -122.6 – -122.9 (br s, 2F), -123.5 – -123.6 (br s, 2F), -126.1 – -126.3 (br s, 2F);

<sup>13</sup>C NMR (CDCl<sub>3</sub>, 125 MHz): δ 41.7 (t, *J* = 20 Hz), 39.1, 32.3, 30.6, 19.8, 5.7.

5-iodo-6-perfluorooctylhexanenitrile, **S20**, (Table 6, entry 7)



According to General Procedure B, 5-hexenenitrile (29 μL, 24 mg, 0.25 mmol), C<sub>8</sub>F<sub>17</sub>I (88 μL, 0.18 g, 0.33 mmol), sodium L-ascorbate (17 mg, 0.088 mmol), and Ru(bpy)<sub>3</sub>Cl<sub>2</sub> (1.9 mg, 2.5 μmol) in MeOH (1.5 mL) and MeCN (2.0 mL) afforded **S20** (0.14 g, 90%) after purification by chromatography on SiO<sub>2</sub> (90:10, petroleum ether/ether) (0.5 h reaction time).

*R<sub>f</sub>* (ether/petroleum ether 1:9): 0.22;

IR (neat): 2941, 2249, 1242, 1206, 1151, 1118, 911, 738, 706, 668 cm<sup>-1</sup>;

<sup>1</sup>H NMR (CDCl<sub>3</sub>, 400 MHz): δ 4.38 – 4.28 (m, 1H), 3.06 – 2.89 (m, 1H), 2.88 – 2.71 (m, 1H), 2.47 – 2.40 (m, 2H), 2.06 – 1.93 (m, 3H), 1.89 – 1.75 (m, 1H);

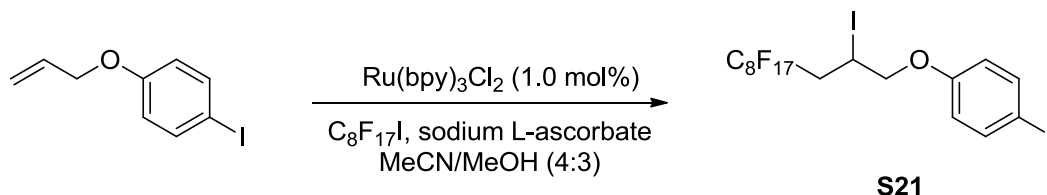
<sup>19</sup>F NMR (CDCl<sub>3</sub>, 376 MHz): δ -80.7 (t, *J* = 10 Hz, 3F), -111.0 – -112.0 (m, 1F), -114.1 – -115.1

(m, 1F), -121.4 – -121.7 (br s, 2F), -121.7 – -122.1 (br s, 4F), -122.6 – -122.9 (br s, 2F), -123.4 – -123.7 (br s, 2F), -126.0 – -126.3 (br s, 2F);

$^{13}\text{C}$  NMR ( $\text{CDCl}_3$ , 125 MHz):  $\delta$  118.8, 41.6 (t,  $J = 21$  Hz), 38.7, 25.8, 17.9, 16.2.

1-((4,4,5,5,6,6,7,7,8,8,9,9,10,10,11,11,11-heptadecafluoro-2-iodoundecyl)oxy)-4-iodobenzene<sup>74</sup>,

**S21**, (Table 6, entry 8)

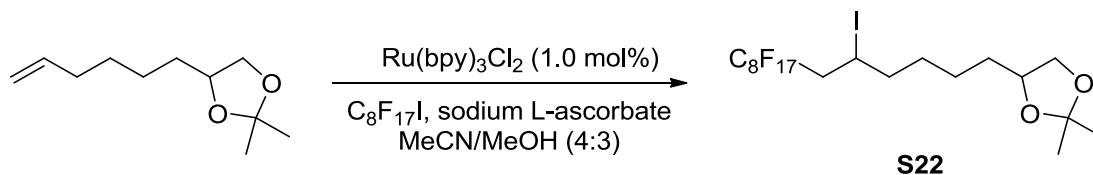


According to General Procedure B, 1-(allyloxy)-4-iodobenzene (65 mg, 0.25 mmol),  $\text{C}_8\text{F}_{17}\text{I}$  (88  $\mu\text{L}$ , 0.18 g, 0.33 mmol), sodium L-ascorbate (17 mg, 0.088 mmol), and  $\text{Ru}(\text{bpy})_3\text{Cl}_2$  (1.9 mg, 2.5  $\mu\text{mol}$ ) in MeOH (1.5 mL) and MeCN (2.0 mL) afforded **S21** (0.20 g, 99%) after purification by chromatography on  $\text{SiO}_2$  (petroleum ether) (4.0 h reaction time).

$R_f$ (petroleum ether): 0.27;

$^1\text{H}$  NMR ( $\text{CDCl}_3$ , 400 MHz):  $\delta$  7.59 (d,  $J = 9$  Hz, 2H), 6.70 (d,  $J = 9$  Hz, 2H), 4.56 – 4.46 (m, 1H), 4.26 (dd,  $J = 10.4, 4.8$  Hz, 1H), 4.16 (dd,  $J = 10.4, 6.4$  Hz, 1H), 3.24 – 3.06 (m, 1H), 2.90 – 2.72 (m, 1H).

4-(7,7,8,8,9,9,10,10,11,11,12,12,13,13,14,14,14-heptadecafluoro-5-iodotetradecyl)-2,2-dimethyl-1,3-dioxolane, **S22**, (Table 6, entry 9)



<sup>74</sup> *J. Fluorine Chem.* **2004**, *125*, 1909.

According to General Procedure B, 4-(hex-5-en-1-yl)-2,2-dimethyl-1,3-dioxolane (46 mg, 0.25 mmol), C<sub>8</sub>F<sub>17</sub>I (88 μL, 0.18 g, 0.33 mmol), sodium L-ascorbate (17 mg, 0.088 mmol), and Ru(bpy)<sub>3</sub>Cl<sub>2</sub> (1.9 mg, 2.5 μmol) in MeOH (1.5 mL) and MeCN (2.0 mL) afforded **S22** (0.17 g, 91%) after purification by chromatography on SiO<sub>2</sub> (95:5, hexanes/EtOAc) (0.5 h reaction time).

*R<sub>f</sub>* (EtOAc/ hexanes 1:19): 0.19;

IR (neat): 2988, 2940, 2867, 1371, 1243, 1209, 1152, 1066 cm<sup>-1</sup>;

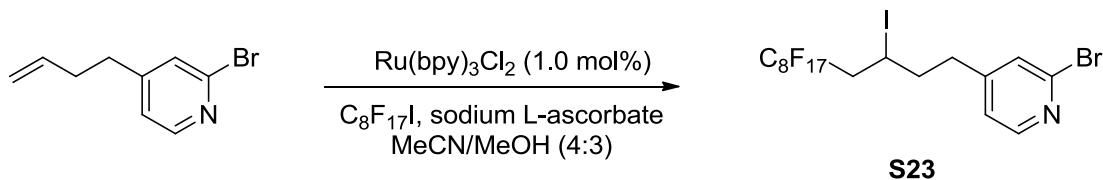
<sup>1</sup>H NMR (CDCl<sub>3</sub>, 400 MHz): δ 4.39 – 4.29 (m, 1H), 4.14 – 4.04 (m, 1H), 4.05 (t, *J* = 6.8 Hz, 1H), 3.52 (t, *J* = 6.8 Hz, 1H), 3.03 – 2.69 (m, 2H), 1.92 – 1.74 (m, 2H), 1.72 – 1.20 (m, 6H), 1.42 (s, 3H), 1.37 (s, 3H);

<sup>19</sup>F NMR (CDCl<sub>3</sub>, 376 MHz): δ -81.2 (t, *J* = 10 Hz, 3F), -110.8 – -111.9 (m, 1F), -113.7 – -114.7 (m, 1F), -120.8 – -121.1 (br s, 2F), -121.1 – -121.5 (br s, 4F), -122.0 – -122.2 (br s, 2F), -122.8 – -123.1 (br s, 2F), -125.3 – -125.6 (br s, 2F);

<sup>13</sup>C NMR (CDCl<sub>3</sub>, 125 MHz): δ 108.8, 69.4, 41.7 (t, *J* = 19 Hz), 40.1, 33.3, 29.6, 26.9, 25.7, 24.8, 20.4.

HRMS (ESI) *m/z* calculated for C<sub>19</sub>H<sub>20</sub>F<sub>17</sub>IO<sub>2</sub><sup>+</sup> ([M+H]<sup>+</sup>) 731.0315, found 731.0309.

2-bromo-4-(5,5,6,6,7,7,8,8,9,9,10,10,11,11,12,12,12-heptafluoro-3-iodododecyl)pyridine, **S23**, (Table 6, entry 10)



According to General Procedure B, 2-bromo-4-(but-3-en-1-yl)pyridine (53 mg, 0.25 mmol), C<sub>8</sub>F<sub>17</sub>I (88 μL, 0.18 g, 0.33 mmol), sodium L-ascorbate (17 mg, 0.088 mmol), and Ru(bpy)<sub>3</sub>Cl<sub>2</sub> (1.9 mg, 2.5 μmol) in MeOH (1.5 mL) and MeCN (2.0 mL) afforded **S23** (0.17 g, 88%) after

purification by chromatography on SiO<sub>2</sub> (90:10, hexanes/EtOAc) (2.0 h reaction time).

Preparative Scale with Low Catalyst Loading:

2-bromo-4-(but-3-en-1-yl)pyridine (1.6 g, 7.5 mmol), C<sub>8</sub>F<sub>17</sub>I (2.6 mL, 5.4 g, 9.9 mmol), sodium L-ascorbate (0.51 g, 2.6 mmol), and Ru(bpy)<sub>3</sub>Cl<sub>2</sub> (5.7 mg, 7.5 μmol) in MeOH (45 mL) and MeCN (60 mL) afforded **S23** (4.8 g, 85%) after purification by chromatography on SiO<sub>2</sub> (90:10, hexanes/EtOAc) (2.0 h reaction time).

*R<sub>f</sub>* (hexanes/EtOAc 4:1): 0.42;

IR (neat): 2917, 2849, 1589, 1543, 1463, 1382, 1200, 1146, 1117, 1080, 723, 704, 656 cm<sup>-1</sup>;

<sup>1</sup>H NMR (CDCl<sub>3</sub>, 500 MHz): δ 8.30 (d, *J* = 5.0 Hz, 1H), 7.37 (s, 1H), 7.12 (d, *J* = 5.0 Hz, 1H), 4.31 – 4.22 (m, 1H), 3.07 – 2.68 (m, 4H), 2.17 – 2.06 (m, 2H);

<sup>19</sup>F NMR (CDCl<sub>3</sub>, 282 MHz): δ -80.7 (t, *J* = 8.0 Hz, 3F), -110.5 – -111.5 (m, 1F), -114.1 – -115.1 (m, 1F), -121.4 – -121.7 (br s, 2F), -121.7 – -122.1 (br s, 4F), -122.6 – -122.9 (br s, 2F), -123.4 – -123.6 (br s, 2F), -126.0 – -126.3 (br s, 2F);

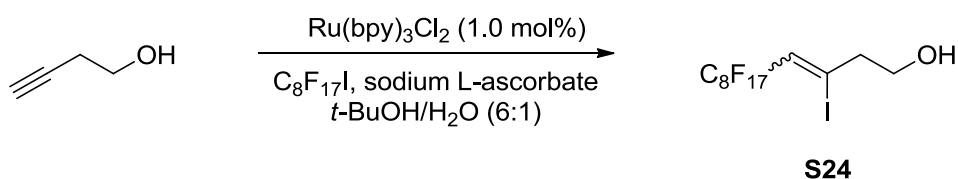
<sup>13</sup>C NMR (CDCl<sub>3</sub>, 125 MHz): δ 152.0, 150.2, 142.7, 128.0, 122.9, 41.7 (t, *J* = 21 Hz), 40.1, 34.8, 18.8.

HRMS (ESI) *m/z* calculated for C<sub>17</sub>H<sub>10</sub>BrF<sub>17</sub>IN<sup>+</sup> ([M+H]<sup>+</sup>) 757.8848, found 757.8860.

### General Procedure C: Visible Light-Mediated Fluorous Tagging of Alkynes

A 10 mL round bottom flask was equipped with a rubber septum and magnetic stir bar and was charged with alkyne (0.50 mmol, 1.0 equiv.), *t*-BuOH (3.0 mL), C<sub>8</sub>F<sub>17</sub>I (1.3 equiv.), H<sub>2</sub>O (0.50 mL), sodium L-ascorbate (0.18 mmol, 0.35 equiv.), Ru(bpy)<sub>3</sub>Cl<sub>2</sub> (0.0050 mmol, 0.010 equiv.). The mixture was then degassed by Ar sparging for 15 min. The mixture was then irradiated by blue LEDs. After the reaction was complete, as judged by TLC analysis (typically 30 min), *t*-BuOH was removed *in vacuo* and EtOAc (10 mL) and H<sub>2</sub>O (10 mL) were added to the residue.

The mixture was poured into a separatory funnel and the layers were separated and the aqueous layer was extracted with EtOAc (2 X 15 mL). The combined organic layers were washed with brine (20 mL), dried (Na<sub>2</sub>SO<sub>4</sub>) and concentrated *in vacuo*. The residue was purified by chromatography on silica gel, using the solvent system indicated, to afford the desired product. 5,5,6,6,7,7,8,8,9,9,10,10,11,11,12,12,12-heptafluoro-3-iodododec-3-en-1-ol, **S24**, (Table 6, entry 12)



According to General Procedure C, but-3-yn-1-ol (39  $\mu$ L, 36 mg, 0.50 mmol), C<sub>8</sub>F<sub>17</sub>I (0.17 mL, 0.36 g, 0.66 mmol), sodium L-ascorbate (34 mg, 0.18 mmol), and Ru(bpy)<sub>3</sub>Cl<sub>2</sub> (3.8 mg, 5.0  $\mu$ mol) in *t*-BuOH (3.0 mL) and H<sub>2</sub>O (0.50 mL) afforded **S24** (0.17 g, 96%) as a 1.8:1 mixture of diastereoisomers after purification by chromatography on SiO<sub>2</sub> (90:10, hexanes/EtOAc) (0.5 h reaction time).

Data for major isomer of compound **S24**:

*R<sub>f</sub>* (hexanes/EtOAc 17:3): 0.24;

<sup>1</sup>H NMR (CDCl<sub>3</sub>, 500 MHz):  $\delta$  6.50 (t, *J* = 15 Hz, 1H), 3.87 (t, *J* = 6.0 Hz, 2H), 2.97 – 2.93 (m, 2H), 1.62 (s, 1H);

<sup>19</sup>F NMR (CDCl<sub>3</sub>, 376 MHz):  $\delta$  -80.9 (t, *J* = 10 Hz, 3F), -105.2 – -105.5 (m, 2F), -121.4 – -121.7 (br s, 2F), -121.8 – -122.2 (br s, 4F), -122.7 – -123.0 (br s, 2F), -123.1 – -123.3 (br s, 2F), -126.1 – -126.4 (br s, 2F);

Data for minor isomer of compound **S24**:

*R<sub>f</sub>* (hexanes/EtOAc 17:3): 0.14;

$^1\text{H}$  NMR ( $\text{CDCl}_3$ , 500 MHz):  $\delta$  6.41 (t,  $J = 14$  Hz, 1H), 3.85 (t,  $J = 6.0$  Hz, 2H), 2.95 – 2.90 (m, 2H), 1.62 (s, 1H);

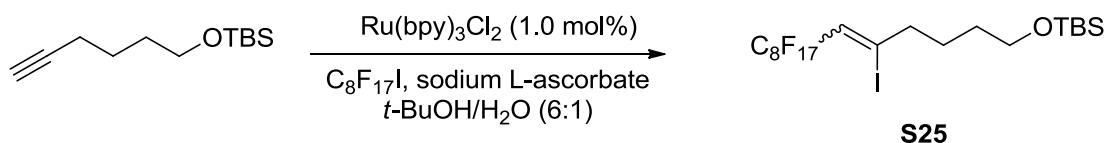
$^{19}\text{F}$  NMR ( $\text{CDCl}_3$ , 376 MHz):  $\delta$  -80.9 (t,  $J = 10$  Hz, 3F), -108.8 – -109.0 (m, 2F), -121.4 – -121.7 (br s, 2F), -121.8 – -122.2 (br s, 4F), -122.7 – -122.9 (br s, 4F), -126.1 – -126.4 (br s, 2F);

Data for mixture of isomers:

IR (neat): 3450, 2941, 2891, 1637, 1242, 1214, 1152, 905, 727, 651  $\text{cm}^{-1}$ ;

$^{13}\text{C}$  NMR ( $\text{CDCl}_3$ , 125 MHz):  $\delta$  129.0 (t,  $J = 24$  Hz), 124.3 (t,  $J = 24$  Hz), 117.0 (t,  $J = 6.1$  Hz), 111.5 (t,  $J = 5.5$  Hz), 61.9, 60.6, 50.9, 43.6.

*tert*-butyl((7,7,8,8,9,9,10,10,11,11,12,12,13,13,14,14,14-heptafluoro-5-iodotetradec-5-en-1-yl)oxy)dimethylsilane, **S25**, (Table 6, entry 13)



According to General Procedure C, *tert*-butyl(hex-5-yn-1-yloxy)dimethylsilane (0.11 mg, 0.50 mmol),  $\text{C}_8\text{F}_{17}\text{I}$  (0.17 mL, 0.36 g, 0.66 mmol), sodium L-ascorbate (34 mg, 0.18 mmol), and  $\text{Ru}(\text{bpy})_3\text{Cl}_2$  (3.8 mg, 5.0  $\mu\text{mol}$ ) in *t*-BuOH (3.0 mL) and  $\text{H}_2\text{O}$  (0.50 mL) afforded **S25** (0.36 g, 94%) as a 2:1 mixture of diastereoisomers after purification by chromatography on  $\text{SiO}_2$  (98:2, hexanes/EtOAc) (0.5 h reaction time).

Data for major isomer of compound **S25**:

$R_f$  (hexanes/EtOAc 19:1): 0.62;

$^1\text{H}$  NMR ( $\text{CDCl}_3$ , 400 MHz):  $\delta$  6.34 (t,  $J = 14$  Hz, 1H), 3.64 (t,  $J = 6.0$  Hz, 2H), 2.67 (t,  $J = 7.2$  Hz, 2H), 1.72 – 1.62 (m, 2H), 1.59 – 1.49 (m, 2H), 0.91 (s, 9H), 0.06 (s, 6H);

$^{19}\text{F}$  NMR ( $\text{CDCl}_3$ , 376 MHz):  $\delta$  -80.8 (t,  $J = 10$  Hz, 3F), -105.5 – -105.2 (m, 2F), -121.3 – -121.6 (br s, 2F), -121.7 – -122.1 (br s, 4F), -122.6 – -122.8 (br s, 2F), -123.1 – -123.4 (br s, 2F), -126.0

- -126.3 (br s, 2F);

Data for minor isomer of compound **S25**:

$R_f$  (hexanes/EtOAc 19:1): 0.53;

$^1\text{H}$  NMR ( $\text{CDCl}_3$ , 400 MHz):  $\delta$  6.26 (t,  $J = 14$  Hz, 1H), 3.64 (t,  $J = 6.0$  Hz, 2H), 2.71 (t,  $J = 7.2$  Hz, 2H), 1.72 – 1.62 (m, 2H), 1.59 – 1.49 (m, 2H), 0.91 (s, 9H), 0.06 (s, 6H);

$^{19}\text{F}$  NMR ( $\text{CDCl}_3$ , 376 MHz):  $\delta$  -80.8 (t,  $J = 10$  Hz, 3F), -108.4 – -108.6 (m, 2F), -121.3 – -121.6 (br s, 2F), -121.7 – -122.1 (br s, 4F), -122.6 – -122.8 (br s, 2F), -122.9 – -123.0 (br s, 2F), -126.0 – -126.3 (br s, 2F);

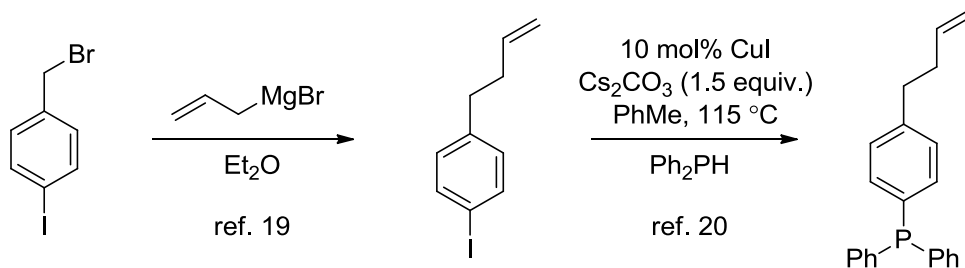
Data for mixture of isomers:

IR (neat): 2956, 2888, 2862, 1636, 1473, 1245, 1215, 1153, 1135, 1112, 838, 777, 668  $\text{cm}^{-1}$ ;

$^{13}\text{C}$  NMR ( $\text{CDCl}_3$ , 125 MHz):  $\delta$  126.7 (t,  $J = 24$  Hz), 122.8 (t,  $J = 6.0$  Hz), 121.8 (t,  $J = 24$  Hz), 62.5, 62.5, 48.2, 40.9, 40.8, 31.5, 32.0, 26.6, 25.9, 25.9, 18.3, 18.3, -5.4, -5.4.

HRMS (ESI)  $m/z$  calculated for  $\text{C}_{20}\text{H}_{24}\text{F}_{17}\text{IOSi}^+$  ( $[\text{M}+\text{H}]^+$ ) 759.0448, found 759.0479.

(4-(but-3-en-1-yl)phenyl)diphenylphosphine, **17**



In accordance with literature precedents<sup>75,76</sup> phosphine **17** was prepared and obtained in 55% yield after purification by chromatography on  $\text{SiO}_2$  (95:5, hexanes/DCM).

$R_f$  (petroleum ether/ether 19:1): 0.57;

IR (neat): 3069, 3053, 3028, 3013, 3001, 2927, 2854, 1640, 1598, 1585, 1433, 1187, 1117, 1091,

<sup>75</sup> *Chem. Commun.* **2011**, 47, 1494.

<sup>76</sup> *J. Org. Chem.* **2003**, 68, 4590.

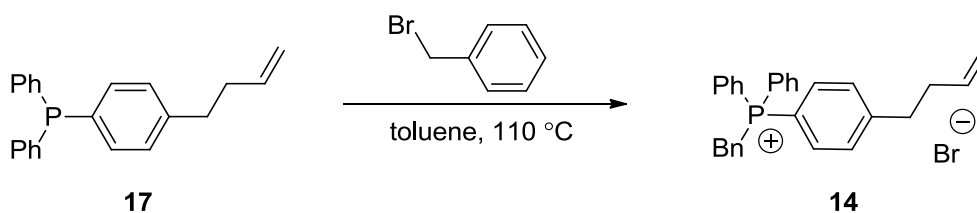
997, 912, 812, 742, 695  $\text{cm}^{-1}$ ;

$^1\text{H}$  NMR ( $\text{CDCl}_3$ , 500 MHz):  $\delta$  7.36 – 7.28 (m, 10H), 7.24 (t,  $J = 7.5$  Hz, 2H), 7.17 (d,  $J = 7.5$  Hz, 2H), 5.91 – 5.81 (m, 1H), 5.05 (d,  $J = 17.0$  Hz, 1H), 4.99 (d,  $J = 9.5$  Hz, 1H), 2.72 (t,  $J = 8.0$  Hz, 2H); 2.41 – 2.34 (m, 2H).

$^{13}\text{C}$  NMR ( $\text{CDCl}_3$ , 125 MHz):  $\delta$  142.6, 137.8 (d,  $J = 1.9$  Hz); 137.5 (d,  $J = 11$  Hz), 134.0 (d,  $J = 9.8$  Hz), 133.8 (d,  $J = 19$  Hz), 133.6 (d,  $J = 19$  Hz), 128.6 (d,  $J = 7.4$  Hz), 128.5, 128.4 (d,  $J = 6.5$  Hz), 115.0, 35.2, 35.1;

HRMS (ESI)  $m/z$  calculated for  $\text{C}_{22}\text{H}_{21}\text{P}^+$  ( $[\text{M}+\text{H}]^+$ ) 317.1459, found 317.1461.

benzyl(4-(but-3-en-1-yl)phenyl)diphenylphosphonium bromide, **14**



A Schlenk flask was charged with phosphine **17** (0.36 g, 1.2 mmol), benzyl bromide (0.15 mL, 1.3 mmol, 1.1 equiv.) and toluene (5.0 mL). The solution was stirred at 110 °C overnight to produce a white precipitate. The product **14** was isolated in 92% yield (0.51 g) by filtration and washed with pentane.

$^1\text{H}$  NMR ( $\text{DMSO-}d_6$ , 500 MHz):  $\delta$  7.08 (t,  $J = 7.5$  Hz, 2H), 6.95 – 6.88 (m, 4H), 6.86 – 6.72 (m, 8H), 6.47 (t,  $J = 7.0$  Hz, 1H), 6.40 (t,  $J = 8.0$  Hz, 2H), 6.14 (d,  $J = 7.0$  Hz, 2H), 5.07 – 4.96 (m, 1H), 4.31 (d,  $J = 15.5$  Hz, 2H), 4.23 (d,  $J = 17.0$  Hz, 1H), 4.18 (d,  $J = 10.5$  Hz, 1H), 2.01 (t,  $J = 7.5$  Hz, 2H), 1.57 (m, 2H);

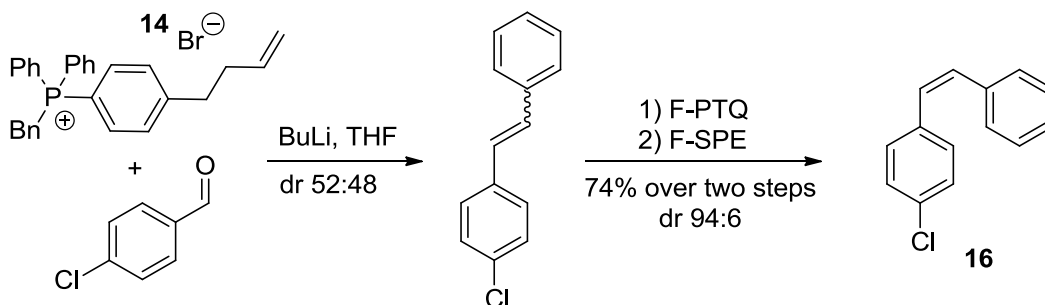
$^{13}\text{C}$  NMR ( $\text{DMSO-}d_6$ , 125 MHz):  $\delta$  149.5 (d,  $J = 3.3$  Hz), 137.4 (d,  $J = 6.5$  Hz); 135.0 (d,  $J = 3.3$  Hz), 134.0 (d,  $J = 9.3$  Hz), 133.9 (d,  $J = 9.8$  Hz), 130.5 (d,  $J = 80$  Hz), 130.0, 130.0, 128.5 (d,  $J = 56$  Hz), 128.0 (d,  $J = 8.4$  Hz), 118.4, 117.7, 115.6, 115.0, 114.3, 34.1 (d,  $J = 21$  Hz), 28.2 (d,  $J =$



47 Hz);

HRMS (ESI)  $m/z$  calculated for  $C_{29}H_{28}P^+$  ( $[M - Br]$ ) 407.1929, found 407.1909.

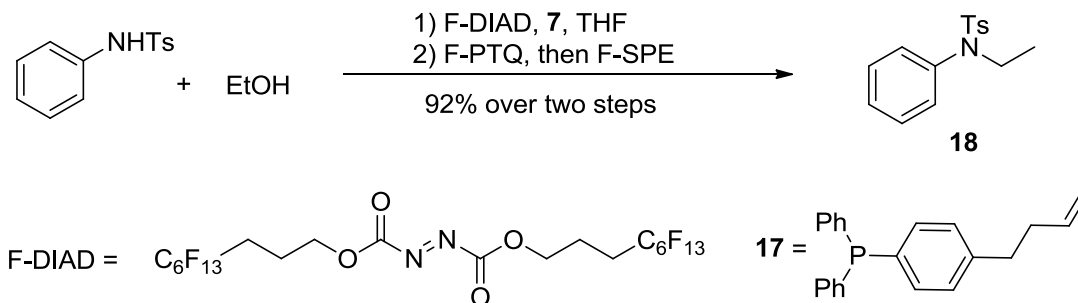
### Procedure for Wittig reaction:



To a suspension of phosphonium bromide **14** (0.12 g, 0.25 mmol) and anhydrous THF (4.0 mL) was added *n*-BuLi (0.10 mL, 0.25 mmol, 2.5 M) dropwise at 0 °C. The reaction mixture was stirred at 0 °C for 1 h. A solution of 4-chlorobenzaldehyde (34 mg, 0.24 mmol, 0.95 equiv.) and anhydrous THF (1.0 mL) was added dropwise over 0.25 h at 0 °C. The reaction mixture was then allowed to reach room temperature followed by stirring for 1 h (100% conversion according to TLC). The reaction mixture was concentrated *in vacuo* and then redissolved in MeCN/MeOH (3.5 mL, 4:3). To this solution was added  $CF_3(CF_2)_7I$  (88  $\mu$ L, 0.33 mmol, 1.3 equiv.) and  $Ru(bpy)_3Cl_2$  (2.2 mg, 2.5  $\mu$ mol, 1.0 mol%) followed by sparging with argon for 0.25 h. Sodium ascorbate (17 mg, 88  $\mu$ mol, 0.35 equiv.) was added and the reaction mixture was degassed by sparging for another 2 to 3 min. The reaction mixture was irradiated with visible light (blue LEDs) for 3 h whereupon another portion of sodium ascorbate (17 mg, 88  $\mu$ mol, 0.35 equiv.) was added. The reaction mixture was stirred for 15 h under visible light irradiation and was then concentrated *in vacuo* onto celite. The celite was loaded onto a cotton plugged glass pipette and washed with hexanes/EtOAc (8:2). The filtrate was concentrated *in vacuo*. F-SPE (2 g cartridge) was performed using MeCN/H<sub>2</sub>O (7:3) as the fluorophobic eluent. The product fraction was treated with brine (5 mL) and EtOAc (10 mL). The organic phase was dried over  $Na_2SO_4$  and

concentrated *in vacuo* to generate **16** as a white solid (38 mg) in 74% yield (Z/E ratio 1:0.13).<sup>77</sup>

**Procedure for Mitsunobu reaction:**



To a stirred solution of *N*-Ts-aniline (0.25 g, 1.0 mmol), EtOH (90  $\mu$ L, 1.5 mmol), and **17** (0.48 g, 1.5 mmol) in anhydrous THF (2.0 mL) was added F-DIAD<sup>78</sup> (1.3 g, 1.5 mmol) dropwise at 0  $^{\circ}$ C, and the resulting solution was stirred at RT overnight and checked by TLC to confirm full conversion. To the mixture, EtOAc (3 mL) was added and the mixture was washed with 1 M HCl (2 mL) and brine (2 mL). After the organic layer was dried over MgSO<sub>4</sub> and solvents were evaporated, the crude was redissolved in MeCN/MeOH (21 mL, 4:3). To this solution was added CF<sub>3</sub>(CF<sub>2</sub>)<sub>7</sub>I (0.53 mL, 1.1 g, 2.0 mmol, 1.3 equiv.) and Ru(bpy)<sub>3</sub>Cl<sub>2</sub> (1.1 mg, 1.5 mmol, 0.10 mol%) followed by sparging with argon for 0.25 h. Sodium ascorbate (0.11 mg, 0.53 mmol, 0.35 equiv.) was added and the reaction mixture was degassed by sparging for another 2 to 3 min. The reaction mixture was irradiated with visible light (blue LEDs) for 2.5 h and was then concentrated *in vacuo*. F-SPE (2 g cartridge) was performed using MeCN/H<sub>2</sub>O (7:3) as the fluorophobic eluent. The product fraction was treated with brine (5 mL) and EtOAc (10 mL). The organic phase was dried over Na<sub>2</sub>SO<sub>4</sub> and concentrated *in vacuo* to afford **18** (0.253 g, 92%) *R<sub>f</sub>* (EtOAc/hexane 1:19): 0.08;

IR (neat): 3064, 2977, 2935, 2874, 1596, 1493, 1452, 1345, 1305, 1234, 1169, 1150, 1088, 1065,

<sup>77</sup> Spectroscopic data matches with previously reported literature values: *J. Am. Chem. Soc.* **2003**, *125*, 6034.

<sup>78</sup> F-DIAD is available from Fluorous Technologies Inc. ([www.fluorous.com](http://www.fluorous.com))

1026, 955, 899, 815, 767, 712, 697, 653  $\text{cm}^{-1}$ ;

$^1\text{H}$  NMR ( $\text{CDCl}_3$ , 500 MHz):  $\delta$  7.46 (d,  $J = 8.0$  Hz, 2H), 7.31 – 7.25 (m, 2H), 7.21 (d,  $J = 8.0$  Hz, 2H), 7.04 – 7.00 (m, 2H), 3.57 (q,  $J = 7.0$  Hz, 2H), 2.39 (s, 3H), 1.04 (t,  $J = 7.0$  Hz, 3H);

$^{13}\text{C}$  NMR ( $\text{CDCl}_3$ , 125 MHz):  $\delta$  143.1, 138.6, 135.1, 129.1, 128.7, 128.6, 127.6, 127.4, 45.2, 21.1, 13.8;

HRMS (ESI)  $m/z$  calculated for  $\text{C}_{15}\text{H}_{17}\text{NO}_2\text{S}^+$  ( $[\text{M}+\text{H}]^+$ ) 276.1058, found 276.1056.

## Chapter 4. Photochemical Strategy for Lignin Degradation at Room Temperature

\*Portions of this chapter have been published in Nguyen, J. D.; Matsuura, B. S.; Stephenson, C. R. *J. Am. Chem. Soc.* **2014**, *136*, 1218.

### Introduction

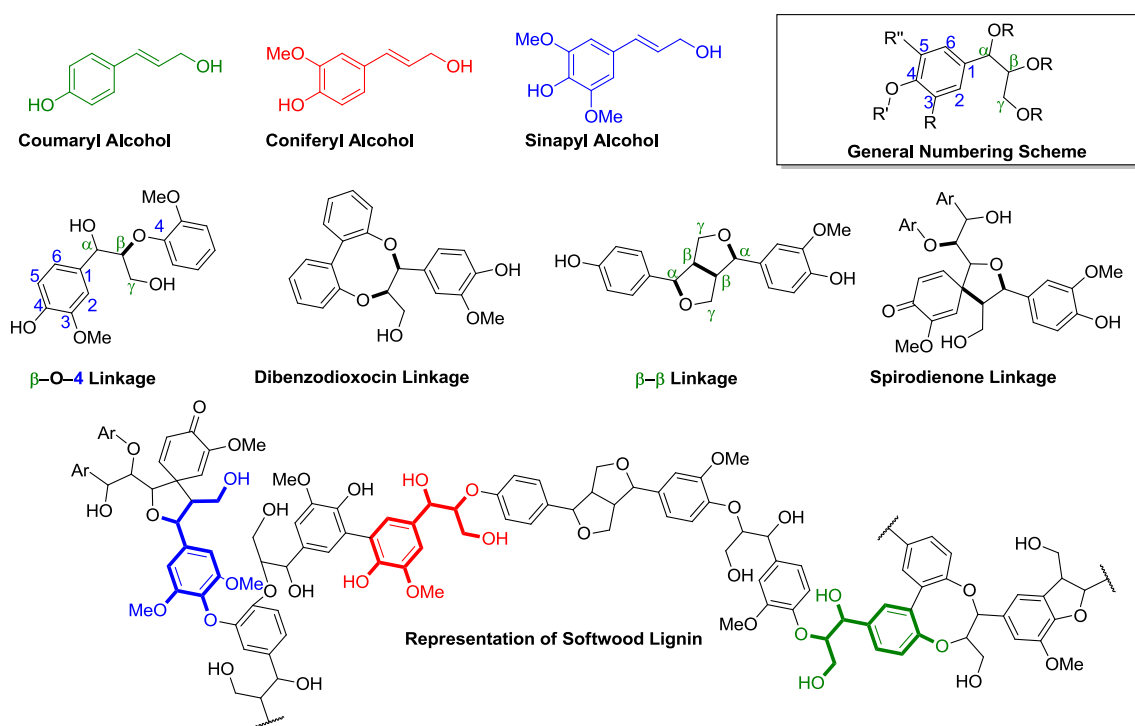
Lignin is the second most abundant biopolymer in the world, comprising 20-30% of available biomass. The amount of total biomass that is currently produced is sufficient to replace petroleum as a carbon feedstock for fine chemicals.<sup>159</sup> However, the lack of enabling technologies has hampered this potential application for biomass; consequently, it remains a largely unexploited resource. Due to its high chemical stability and irregular structure, the majority of lignin is unused as a chemical commodity. Instead, it is employed commercially for its bulk properties, as insulation or as a dispersant in the dye industry, where macroscopic form is more important than chemical properties. The high aromatic content of lignin makes it a potentially attractive feedstock for commodity chemicals such as benzene, toluene, and xylene, complimenting the chemicals derived from cellulose. However, the standard pretreatment and processing technologies render lignin untenable for further refinement. Furthermore, known lignin processing technologies are very energy intensive and typically require temperatures of >100°C and high pressures. On top of this, the yield of commodity chemicals from lignin biomass is very low. For example, the oxidative degradation of lignin is highly inefficient, producing between 7-10% yield of vanillin from Kraft lignin.<sup>160</sup> Moreover, much of the available lignin is not suitable for catalysis due to the high sulfur content that is introduced in the

pretreatment stage. Most of lignin is therefore converted through high temperature pyrolysis to generate syngas, a mixture of CO and H<sub>2</sub> using extremely high temperatures (400-1000 °C). The resultant char is highly stable at 750 °C, and is considered a very poor feedstock for the formation of polyaromatic hydrocarbons.<sup>161</sup> Unlike cellulose, fermentation on a large scale is still not an option, as only certain types of fungi can degrade lignocellulose, rendering this strategy, although attractive, immature from a development standpoint. In fact, there have been significant advances in the “molecular domestication” of feedstock plants that express lower amounts of lignin, an effort that reflects the processing difficulty lignin recalcitrance poses.<sup>162</sup>

Undoubtedly, petroleum is a critically important commodity for the maintenance of modern society as both a fuel source and as the primary chemical feedstock for pharmaceuticals and materials. Due to economic, political and supply pressures, the price of crude petroleum exhibits a high degree of price volatility that consequently affects the economy on a large scale.<sup>163</sup> As a consequence, there is an ongoing intense effort towards developing energy sources from wind, solar, nuclear power and biomass to meet electrical energy needs. Despite these significant strides in those areas, replacement technology for energy needs cannot replace the demand for transportation fuel and fine chemicals. It is with this in mind that biomass processing has materialized as a promising solution. Presently, the technology to replace petroleum for transportation purposes is unfeasible because the current annual production of biomass is still one tenth current agricultural yields.<sup>164</sup> Realistic estimates put United States biomass production at around 250 million tons a year, enough to completely replace petroleum as the carbon feedstock for fine chemicals.<sup>165</sup> The Department of Energy recently released a study on the feasibility of increasing this feedstock to 1-1.3 billion tons by 2050, without detrimentally

affecting the food supply and other essential agricultural commodities.<sup>166</sup> These goals were deemed feasible, relying on realistic projections of increases in crop yields and modest reallocation of land use.

Around 10% of refined petroleum is eventually processed into the petrochemicals that make up pure solvents and simple chemical building blocks, representing a significant fraction of petroleum consumed. Indeed, efforts towards utilizing biomass as chemical feedstock are currently under intense investigation. Research is primarily focused on using cellulose as the



**Figure 4.1** Representation of lignin biopolymer and common linkages.

main carbon source, because it comprises over 70% of overall biomass produced.<sup>167</sup> Cellulose is converted into commodity chemicals that represent the olefin/alkane fraction of petroleum distillate. Aside from cellulose, there is a very significant fraction of biomass that is very difficult to process and is unused. Lignocellulose is a biopolymeric matrix that contains a high amount of crosslinked hemicellulose and lignin. Lignin monomers can be classified into three

types of monomers derived from coumaryl alcohol, coniferyl alcohol, and sinapyl alcohol. These monomers, called monolignols, polymerize in a variety of configurations. The most common motif is the  $\beta$ -O-4 linkage, comprising 70-80% of all the linkages found in lignocelluloses.<sup>168</sup> Other crosslinking motifs are found as well, occurring in varying degrees

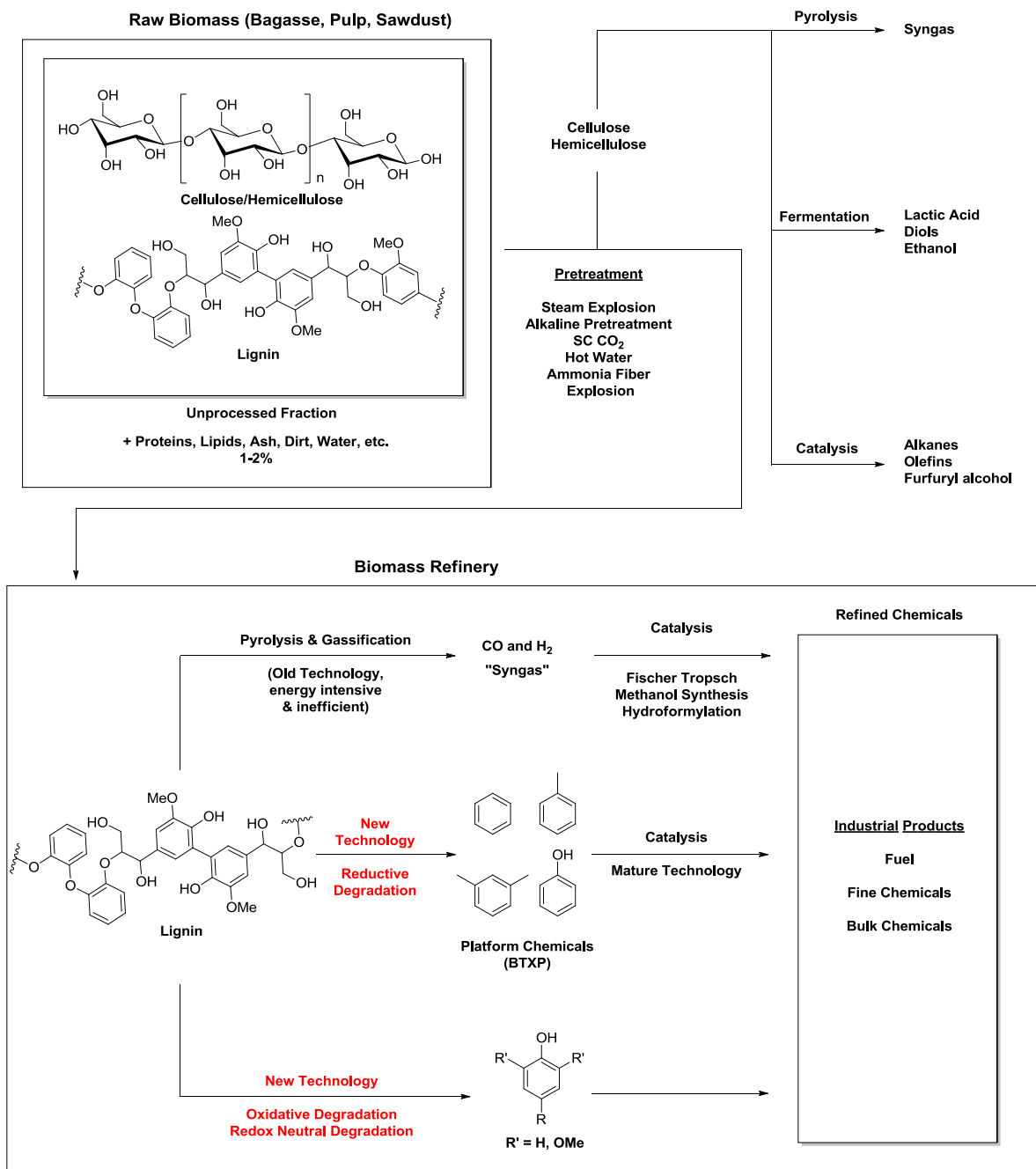


Figure 4.2 Summary of biorefinery.

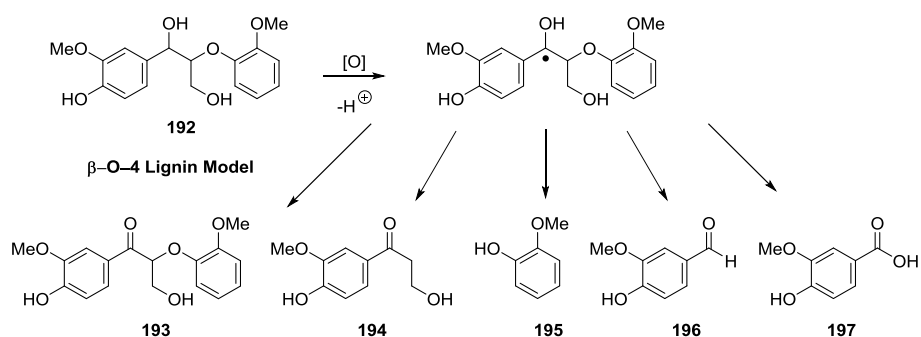
depending on the species of plant and part of the plant from which the raw material was harvested (Figure 4.1).<sup>168</sup> These linkages allow for a high degree of branching, resulting in a crosslinked aromatic polymer that is water resistant, structurally rigid, and resistant to oxidation. Due to these recalcitrant properties, lignin is largely used in applications such as fuel, as pulp for newspaper and composite boards where the bulk properties are more important than its chemical properties. With a lack of enabling technologies, pyrolysis of pretreated lignin yields syngas in about 15-20% yield plus an intractable char that is rich in polyaromatic hydrocarbons (Figure 4.2). With a suitable processing technique, lignin degradation could yield high value aromatics.

There are four major lignin processing techniques that are currently in use. These include the Kraft process (sulfide pulping), organosolv (pulping via extraction with organic solvent), sulfite process (solubilization of lignin via sulfonation of the aromatic rings), as well as mechanical pulping.<sup>168</sup> The harsh conditions necessary to break lignin down to more manageable sizes, often renders it untenable to further chemical refinement. The Kraft process, for example, requires the use of strong bases and sulfur to cleave the various bonds found in lignin. Both the sulfite and the Kraft process produce lignin that is high in sulfur content, which is notorious for deactivating transition metal catalysts (catalyst poisoning).<sup>169</sup> Consequently, technologies for lignin degradation are underdeveloped and present an opportunity for innovation.

In nature, the fungal enzyme lignin peroxidase degrades lignin through the generation of hydroxy radicals. This process is relatively slow, taking many months to fully degrade higher molecular weight lignin. Initial synthetic efforts to perform this chemistry have largely concentrated on the study of the mechanism of oxidative cleavage by metal based oxidants such as Co(II)/Mn(II)<sup>170a,b</sup> and CAN<sup>170d</sup> as well as enzymatic peroxidases such as horse radish



peroxidase,<sup>170a,d</sup> laccase,<sup>170e</sup> and lignin peroxidase.<sup>170b,d</sup> These studies clearly demonstrate the importance radicals play in the degradation of lignin and also showcase the difficult challenges

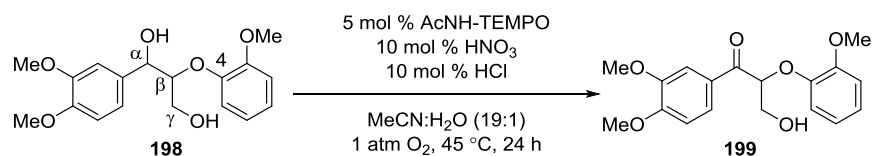


**Figure 4.3** Products formed from oxidative degradation of  $\beta$ -O-4 lignin model systems.

associated with oxidative lignin degradation. Substrate **192** (see Figure 4.3), a  $\beta$ -O-4 motif that comprises up to 70% of the linkages found in lignocellulose is the model system which has been utilized in the majority of preliminary studies to date.<sup>168</sup> These groundbreaking strategies produce a wide array of products, often requiring a stoichiometric amount of metal oxidant, or have high reaction temperatures. Although oxidative degradation tends to completely consume **192**, practical application of this strategy has been hampered by poor mass recovery or production of an intractable mixture of oxidation products. The oxidation of lignin model systems often generates compound **193** as a byproduct. A report by the Stahl identified the remarkable chemoselectivity of oxoammonium salts for the oxidation of the benzylic alcohol of lignin  $\beta$ -O-4 model systems and on lignin itself (Figure 4.4).<sup>171</sup> This compound represents a dead-end reaction pathway as it is highly resistant to further oxidative degradation to more useful basic building blocks. It is important to note that many current oxidative, reductive and redox neutral degradation techniques do not have the capacity to process this structural motif that is undoubtedly found in pretreated lignin.

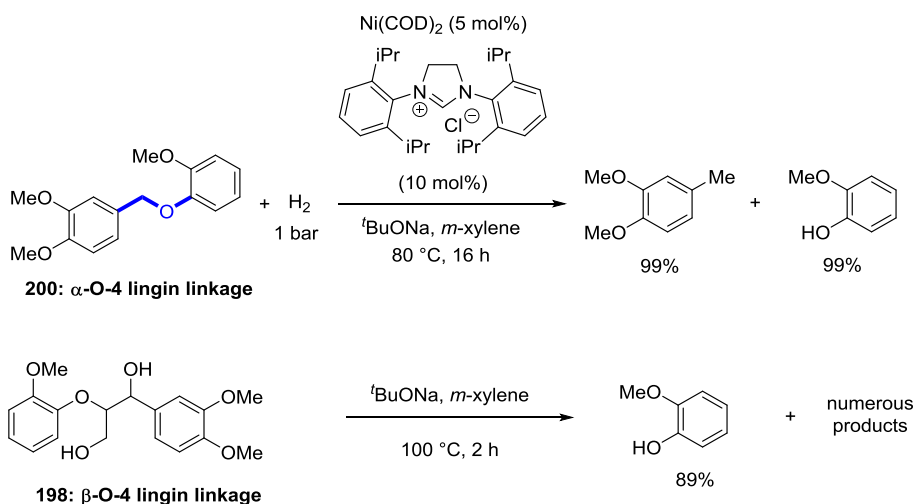
Catalytic hydrogenation of lignin has been known since the 1930s,<sup>172</sup> and has experienced significant advancements.<sup>173</sup> Typical hydrogenolysis of lignin is conducted under

harsh conditions, often at high temperatures, high pressures, and long reaction times. These reactions tend to produce a range of reduction products and exhibit low control over the product



**Figure 4.4** Stahl's chemoselective oxidation of  $\beta$ -O-4 lignin model systems.

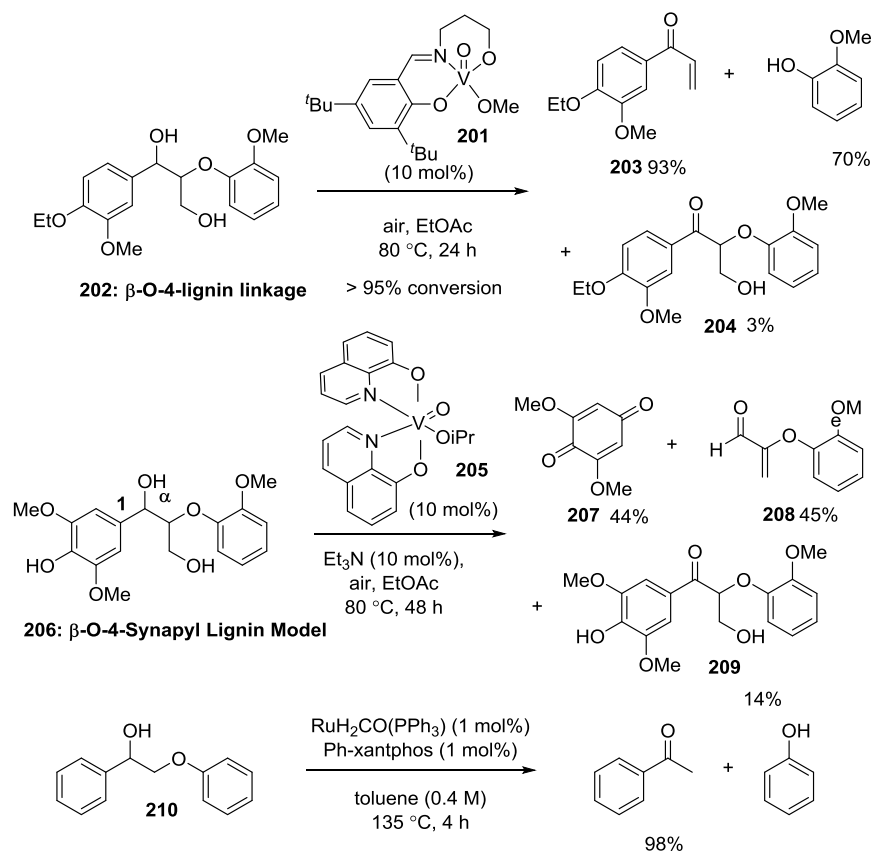
distribution.<sup>173</sup> In a recent report in *Science*, Hartwig and coworkers reported the use of a Ni-NHC system to reduce aryl ether bonds (Figure 4.5).<sup>174</sup> However, when the lignin model system **198** was subjected to their reaction conditions in the absence of the Ni-NHC system, guaiacol was isolated in high yield, presumably via a simple elimination reaction, along with an intractable mixture. This result indicates that there are significant side reactions on lignin model systems, and presumably on lignin itself, with the use of a strong base at high temperatures. On the basis of these important observations, my colleagues and I expect that it will be necessary to avoid strong base and elevated temperatures for efficient lignin degradation.



**Figure 4.5** Hartwig's reductive cleavage of  $\beta$ -O-4 lignin model systems.

A redox neutral degradation of lignin models was recently reported by the Toste lab,<sup>175</sup> utilizing a homogenous vanadium catalyst **201**, producing novel acrolein derivative **203**. This

catalyst suppresses the direct benzylic oxidation of **202** typical of other vanadium catalysts in this class (Figure 4.6).<sup>176</sup> Further exploration of this strategy by the Silks group revealed how subtle ligand effects and judicious substrate choice can generate an array of unique products<sup>177</sup>. Complex **205**, upon oxidation of substrate **206**, exhibited a unique “ $\alpha$ -1” C-C bond cleavage resulting in the formation of quinone **207** and acrolein derivative **208**. Another strategy, developed by the Bergman/Ellman groups, relied on a ruthenium based redox neutral transfer hydrogenation mediated cleavage of a simplified  $\beta$ -O-4 model system (**210**). This system was highly efficient, nearly quantitative yield on all substrates, and short reaction times (<1.5 h) and 100% atom economy. This method was even robust enough to completely depolymerize a 7,000 MW polymeric lignin analogue in quantitative yield.



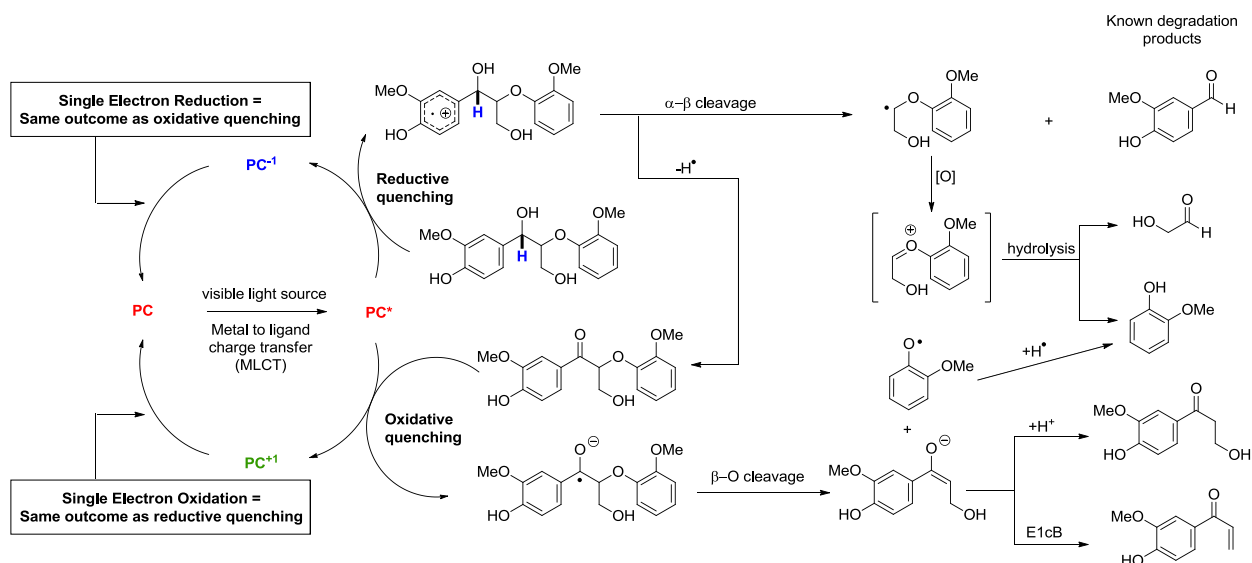
**Figure 4.6** Redox-neutral degradation of  $\beta$ -O-4 lignin model systems.

These methods represent the highly diverse and creative strategies that are possible with modern organic reactions, each having their associated advantages and disadvantages. The major disadvantage common to these protocols is the harsh reaction conditions. The detailed mechanistic studies performed by Silks *et. al.* demonstrates the degree of chemoselectivity the catalysts like **201** and **205** can impart<sup>177</sup>, however, the nature of the substrate can drastically influence the reaction. For example, when catalyst **201** is used to degrade model system **206**, 40% of the benzylic oxidation product, **209**, is formed. The ethylation of the hydroxy group on the  $\beta$ -O-4 model system appears to attenuate the benzylic oxidation since the degradation of model system **202** with vanadium catalyst **201** produces the benzylic oxidation product **204** in only 3% yield instead of 40% that is produced when reacted with **206**.<sup>177</sup> Finally, current catalysts do not appear to tolerate alkyl substitution on the secondary benzylic alcohol ( $\alpha$ -O-4 linkage).

I envisioned that photocatalytic methods could be used to mildly degrade lignin model systems and tuning the reaction conditions to chemoselectively generate an array of products depending on the chosen conditions. I anticipate the highly robust nature of these complexes to be compatible with a wide pH range, have high stability in aqueous, aerobic conditions, and unaffected by the presence of sulfides, sulfites and sulfones.

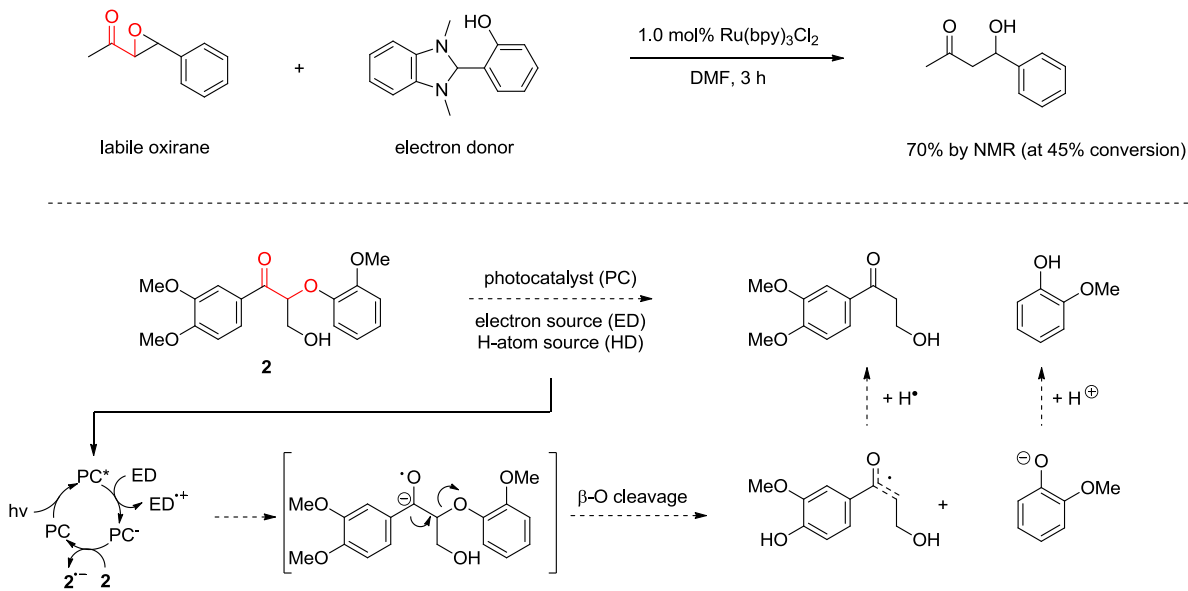
## Strategy

My intention was to utilize the oxidative quenching and reductive quenching to explore the degradation studies of lignin model systems and lignin. In particular, I focused on the cleavage of  $C_{\beta}$ -OAr bonds and  $C_{\alpha}$ - $C_{\beta}$  bonds of  $\beta$ -O-4 linkages not only because these are novel transformations for visible light photoredox catalysis, but also because they represent the most important bond cleavages for lignin degradation due to the high prevalence of  $\beta$ -O-4 linkages. As



**Figure 4.7** Strategic photoredox approach to degradation of lignin model systems.

shown in Figure 4.7, the excited state of a photocatalyst ( $PC^*$ ) as well as the oxidized form of the catalyst ( $PC^{+1}$ ) can act as an oxidant to perform a single electron oxidation. Oxidation of lignin and lignin model systems is known to occur readily with various mild and strong oxidants due to the fact that lignin is composed of many electron rich aromatic rings.<sup>178</sup> These single electron oxidations will generate radical cations that are capable of undergoing fragmentation via  $\alpha$ - $\beta$



**Figure 4.8** Hasegawa's reductive opening of epoxides (top). Reductive cleavage of  $C_{\alpha}$ -O bond (bottom).

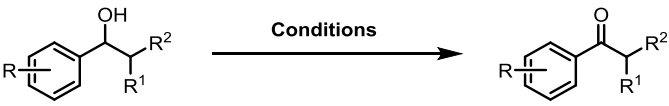
cleavage or benzylic oxidation. The benzylic ketone can react further and undergo fragmentation because the reduced form of the catalyst ( $PC^{-1}$ ) and the excited state of a photocatalyst can act as single electron reductants to generate radical anion and undergo  $\beta$ -O fragmentation. Ideally, the judicious choice of photocatalyst, additives, solvent, and temperature will impart a high level of control to efficiently generate a predictable supply of chemical feedstock.

Although there have been no reports on the use of photoredox catalysis for the depolymerization of lignin, literature precedent suggests that this approach is feasible. In particular, Hasegawa has shown that  $Ru(bpy)_3Cl_2$  can be used to reductively cleave the  $C_{\alpha}$ -O bond of an oxirane in the presence of an  $\alpha$ -carbonyl moiety (Figure 4.8, top).<sup>179</sup> Based upon this precedent, I hypothesized that lignin model systems that have been oxidized at the benzylic position, to generate  $\alpha$ -aryl ether ketones, will undergo  $C_{\alpha}$ -O bond cleavage with the use of an appropriate photocatalyst and reductive quencher.

### **Chemoselective Benzylic Oxidation**

Although many types of C–O bonds are found in the lignin biopolymer, the most common type is the  $\beta$ -O–4 linkage (see Figure 4.1), comprising over 70% of all linkages found in lignocelluloses. DFT calculations have indicated that the C–O bond of the  $\beta$ -O–4 linkage is significantly weakened upon the oxidation of the  $\alpha$ - or  $\gamma$ -carbon by ca. 14 kcal/mol.<sup>180</sup> Based upon these calculations, I postulated that it would be possible to chemoselectively cleave the C–O bond of the  $\beta$ -O–4 linkage after selective oxidation (benzylic or primary) utilizing a single electron transfer event to allow access to complementary fragmentation partners.

Therefore, Bryan Matsuura and I began by exploring the development of a chemoselective benzylic oxidation. The utilization of ammonium persulfate, titanium dioxide, or the photocatalyst  $[Ir(ppy)_2(dtbbpy)]PF_6$  to oxidize simple benzylic alcohols such as 1-

		
Entry	Reaction Conditions	Yield
1	1-phenylethyl alcohol (1 equiv), ammonium persulfate (1.5 equiv), visible light, H <sub>2</sub> O, 24 h	15%
2	1-phenylethyl alcohol (1 equiv), ammonium persulfate (3.0 equiv), visible light, H <sub>2</sub> O, 24 h	40%
3	1-phenylethyl alcohol (1 equiv.), TiO <sub>2</sub> (anatase), visible light, air balloon, MeCN, 48 h	22%
4	1-phenylethyl alcohol (1 equiv.), TiO <sub>2</sub> (anatase), visible light, air balloon, SiO <sub>2</sub> , MeCN, 48 h	30%
5	1-phenylethyl alcohol (1 equiv.), TiO <sub>2</sub> (anatase), visible light, continuous airflow, SiO <sub>2</sub> , MeCN, 48 h	45%
6	1-(4-methylphenoxy)ethanol (1 equiv), 5.0 mol% methyl viologen dichloride, [Ir(ppy) <sub>2</sub> (dtbbpy)]PF <sub>6</sub> , visible light, MeCN, 12 h	80%
7	211 (1 equiv), 5.0 mol% methyl viologen dichloride, visible light, [Ir(ppy) <sub>2</sub> (dtbbpy)]PF <sub>6</sub> , MeCN, 12 h	Decomp.

<sup>a</sup>Yields of products determined by <sup>1</sup>H NMR

**Table 4.1** Investigation of Visible Light-Mediated Oxidation of Benzylic Alcohols.

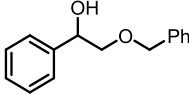
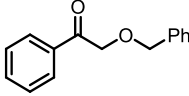
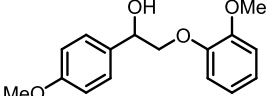
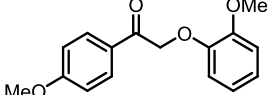
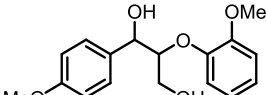
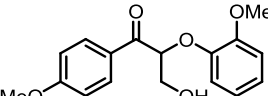
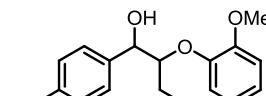
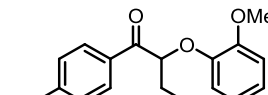
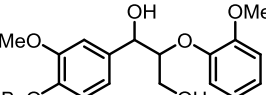
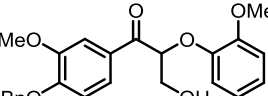
phenylethyl alcohol and 1-(4-methylphenoxy)ethanol gave yields ranging from 15% to 80%, but

the application of these conditions to the lignin model system substrate **214** (*vide infra*) provided mainly decomposition.

During the investigation of viable oxidation conditions,<sup>189</sup> the Stahl group reported an elegant catalytic aerobic benzylic alcohol oxidation of lignin model systems utilizing 4-AcNH-TEMPO (5 mol%), HNO<sub>3</sub> (10 mol%), and HCl (10 mol%).<sup>171</sup> This set of conditions can be applied to produce ketones such as **217–222**, which can subsequently be used as substrates for reductive C<sub>α</sub>-O bond cleavage reaction. Unfortunately, Bryan and I have not yet been able to successfully implement Stahl's oxidation conditions in concert with the photocatalytic reductive fragmentation (*vide infra*), precluding a one-pot procedure. It is possible that the presence of 4-AcNH-TEMPO may be interfering with the catalytic turnover of the photocatalyst. Consequently, I turned to [4-AcNH-TEMPO]BF<sub>4</sub> due to three main reasons. First, [4-AcNH-TEMPO]BF<sub>4</sub> has been shown to selectively oxidize benzylic alcohols at room temperature. Second, the hydroxylamine byproduct can be removed from the reaction mixture by adsorption onto silica. Third, the spent oxidant can be recycled using hydrogen peroxide and fluoroboric acid. As predicted, substrates **211–216** were efficiently oxidized to benzylic ketones with [4-AcNH-TEMPO]BF<sub>4</sub> and simple filtration provided the products in high purity.<sup>181</sup>

Entry	Substrate <sup>a</sup>	Time (h)	Product <sup>b,c</sup>	Yield
1	 <b>211</b>	1.5	 <b>217</b>	95%



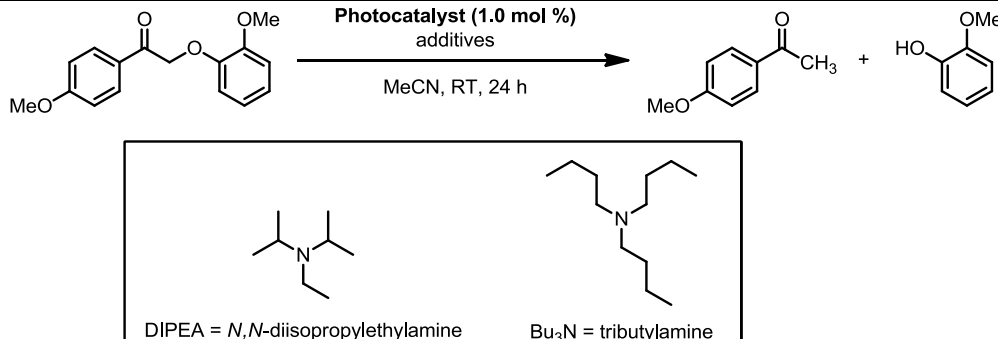
2	 <b>212</b>	<b>20</b>	 <b>218</b>	<b>95%</b>
3	 <b>213</b>	<b>15</b>	 <b>219</b>	<b>97%</b>
4	 <b>214</b>	<b>18</b>	 <b>220</b>	<b>98%</b>
5	 <b>215</b>	<b>15</b>	 <b>221</b>	<b>94%</b>
6	 <b>216</b>	<b>24</b>	 <b>222</b>	<b>94%</b>
<p><sup>a</sup>Unless otherwise noted, reactions were conducted on a 1.0 mmol scale. <sup>b</sup>Yields of products isolated by column chromatography. <sup>c</sup>Isolated yields based on an average of two runs.</p>				

**Table 4.2** Selective benzylic oxidation with [4-AcNH-TEMPO]BF<sub>4</sub>.

### Photoredox-Mediated Reductive Cleavage of C<sub>α</sub>-O Bonds

The cleavage of C–O bonds utilizing visible light-active photocatalysts have been reported by Hasegawa,<sup>182</sup> Ollivier,<sup>183</sup> and the Stephenson group.<sup>57</sup> In particular, Hasegawa and Ollivier studied the reductive cleavage of strained C–O bonds of ketoepoxides with the photocatalyst Ru(bpy)<sub>3</sub>Cl<sub>2</sub> to generate β-hydroxy ketones. However, a generalized visible light-mediated reductive cleavage of C<sub>α</sub>–O bonds (C<sub>β</sub> in lignin is the equivalent to C<sub>α</sub> for a carbonyl) has not yet been reported. I identified this opportunity to develop such a method in the context of a long term goal toward a mild and chemoselective lignin degradation.

I began my investigation by exploring C $\alpha$ -O bond cleavage of ketones and aldehydes. Based on previous successes with cleaving C-X bonds,<sup>30,58</sup> I hypothesized that photoredox catalysis<sup>107,108</sup> could be applied toward the C $\alpha$ -O bond cleavage of lignin model substrate **219**. Evaluation of a series of common photoredox catalysts including Ru(bpy)<sub>3</sub>Cl<sub>2</sub>,<sup>184</sup> *fac*-Ir(ppy)<sub>3</sub>,<sup>185</sup> [Ir(ppy)<sub>2</sub>(dtbbpy)]PF<sub>6</sub>, [Ir{dF(CF<sub>3</sub>)ppy}<sub>2</sub>(dtbbpy)]PF<sub>6</sub>,<sup>186</sup> Cu(dap)<sub>2</sub>Cl,<sup>187</sup> and eosin Y<sup>188</sup> revealed that *fac*-Ir(ppy)<sub>3</sub> and [Ir(ppy)<sub>2</sub>(dtbbpy)]PF<sub>6</sub> could effectively promote the C $\alpha$ -O bond cleavage of **219** to give 4'-methoxyacetophenone and guaiacol in high conversions.<sup>189</sup> Upon discovering that [Ir(ppy)<sub>2</sub>(dtbbpy)]PF<sub>6</sub> could be employed without degassing, I was able to develop optimized reaction conditions capable of fully fragmenting **219** in 12 h to generate 4'-methoxyacetophenone and guaiacol in 88% and 89% yield, respectively (Table 4.3).



DIPEA = *N,N*-diisopropylethylamine      Bu<sub>3</sub>N = tributylamine

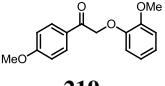
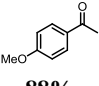
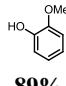
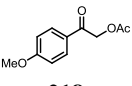
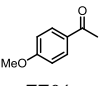
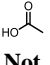
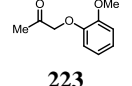
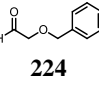
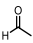
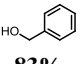
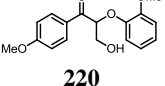
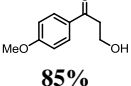
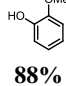
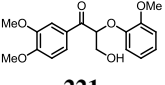
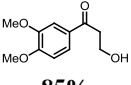
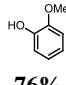
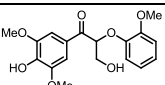
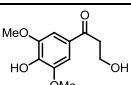
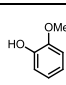
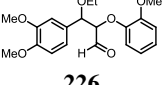
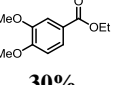
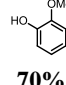
Entry	Conditions <sup>a</sup>	Conversion <sup>b</sup>
1	<i>fac</i> -Ir(ppy) <sub>3</sub> , Bu <sub>3</sub> N (5 equiv), HCO <sub>2</sub> H (5 equiv) visible light, degassed	100
2	<i>fac</i> -Ir(ppy) <sub>3</sub> , DIPEA (5 equiv), HCO <sub>2</sub> H (5 equiv) visible light, degassed	100
3	<i>fac</i> -Ir(ppy) <sub>3</sub> , DIPEA (3 equiv), HCO <sub>2</sub> H (3 equiv) visible light, degassed	100
4	<i>fac</i> -Ir(ppy) <sub>3</sub> , DIPEA (3 equiv), HCO <sub>2</sub> H (3 equiv) visible light, not degassed	0
5	Ru(bpy) <sub>3</sub> Cl <sub>2</sub> , DIPEA (3 equiv), HCO <sub>2</sub> H (3 equiv) visible light, not degassed	17
6	[Ir{dF(CF <sub>3</sub> )ppy} <sub>2</sub> (dtbbpy)]PF <sub>6</sub> , DIPEA (3 equiv), HCO <sub>2</sub> H (3 equiv) visible light, not degassed	37
7	Cu(dap) <sub>2</sub> Cl, DIPEA (3 equiv), HCO <sub>2</sub> H (3 equiv) visible light, not degassed	0
8	eosin Y, DIPEA (3 equiv), HCO <sub>2</sub> H (3 equiv)	10

	visible light, not degassed	
9	[Ir(ppy) <sub>2</sub> (dtbbpy)]PF <sub>6</sub> , DIPEA (3 equiv), HCO <sub>2</sub> H (3 equiv) visible light, not degassed	100
10	[Ir(ppy) <sub>2</sub> (dtbbpy)]PF <sub>6</sub> , DIPEA (3 equiv) visible light, not degassed	80
11	[Ir(ppy) <sub>2</sub> (dtbbpy)]PF <sub>6</sub> , HCO <sub>2</sub> H (3 equiv) visible light, not degassed	0
12	No photocatalyst, DIPEA (3 equiv), HCO <sub>2</sub> H (3 equiv) visible light, not degassed	0
13	[Ir(ppy) <sub>2</sub> (dtbbpy)]PF <sub>6</sub> , DIPEA (3 equiv), HCO <sub>2</sub> H (3 equiv) no light, not degassed	0
14	[Ir(ppy) <sub>2</sub> (dtbbpy)]PF <sub>6</sub> visible light, not degassed	0
<sup>a</sup> Unless otherwise noted, reactions were conducted on a 0.1 mmol scale. <sup>b</sup> Conversion based upon <sup>1</sup> H NMR with 1,3-dimethoxybenzene as an internal standard.		

**Table 4.3** Optimization of Reductive C<sub>α</sub>-O Bond Cleavage & Control Reactions.

Bryan and I next examined the C<sub>α</sub>-O bond cleavage in more detail by varying the ether substituents. A substrate bearing an α-acetoxy group instead of guaiacol reached full conversion in significantly less time, indicating that the reaction rate is strongly influenced by the pK<sub>a</sub> of the leaving group. The reaction is also influenced by the reactivity of the carbonyl portion of the molecule, as illustrated by the absence of fragmentation products upon substitution of the phenyl ketone with a methyl ketone (**223**), presumably due to the larger reduction potential of methyl ketones in comparison to phenyl ketones.<sup>190</sup> On the contrary, commercially available 2-(benzyloxy)acetaldehyde (**224**), underwent efficient fragmentation, cleaving the much stronger C-O bond, to give benzyl alcohol in high yield. Substrates **220**, **221**, **225**, and **226** were selected to test the generality of the catalytic C-O bond cleavage reaction on relevant lignin model systems. Specifically, substrates **220**, **221**, and **225** represent products of a benzylic oxidation on each of the different phenylpropanol monomers, whereas substrate **226** represents a lignin model system of coniferyl alcohol that has been oxidized at the primary alcohol (see Figure 4.1). As expected, lignin model systems **220**, **221**, **225**, and **226** all underwent efficient fragmentation. However, although the fragmentation of substrate **226** gave good yields of guaiacol, the

complementary aldehyde fragment could not be isolated (Table 4.4, entry 8), possibility due to polymerization of the expected cinnamaldehyde product. Instead, Bryan was able to isolate ethyl 3,4-dimethoxybenzoate in 30% isolated yield, which represents a unique oxidative cleavage of the  $\alpha$ - $\beta$  linkage.<sup>189</sup>

$\text{X}-\text{C}(=\text{O})-\text{CH}(\text{R}^1)-\text{OR}^2 \xrightarrow[\text{visible light, MeCN, RT}]{[\text{Ir}(\text{ppy})_2(\text{dtbbpy})]\text{PF}_6 (1.0 \text{ mol } \%), \text{DIPEA} (3 \text{ equiv}), \text{HCO}_2\text{H} (3 \text{ equiv})} \text{X}-\text{C}(=\text{O})-\text{R}^1 + \text{R}^2\text{OH}$				
entry	substrate	time (h)	product 1 <sup>a,b</sup>	product 2 <sup>a,b</sup>
1	 <b>219</b>	<b>12</b>	 <b>88%</b>	 <b>89%</b>
2	 <b>218</b>	<b>4</b>	 <b>77%</b>	 <b>Not isolated</b>
3	 <b>223</b>	<b>24</b>	<b>No reaction</b>	
4	 <b>224</b>	<b>12</b>	 <b>Not isolated</b>	 <b>83%</b>
5	 <b>220</b>	<b>15</b>	 <b>85%</b>	 <b>88%</b>
6	 <b>221</b>	<b>18</b>	 <b>85%</b>	 <b>76%</b>
7	 <b>225</b>	<b>48</b>	 <b>90%</b>	 <b>95%</b>
8	 <b>226</b>	<b>24</b>	 <b>30%</b>	 <b>70%</b>

<sup>a</sup>Yields of products isolated by column chromatography. <sup>b</sup>Isolated yields based on an average of two runs.

**Table 4.4** Substrate Scope of Visible Light-Mediated C $\alpha$ -O Bond Cleavage.

Overall, the mild reaction conditions allow for the atom-economical reductive fragmentation of the lignin model systems to generate guaiacol and  $\beta$ -hydroxy phenyl ketones. No evidence of undesired oxidation or further fragmentation of the guaiacol was observed, and

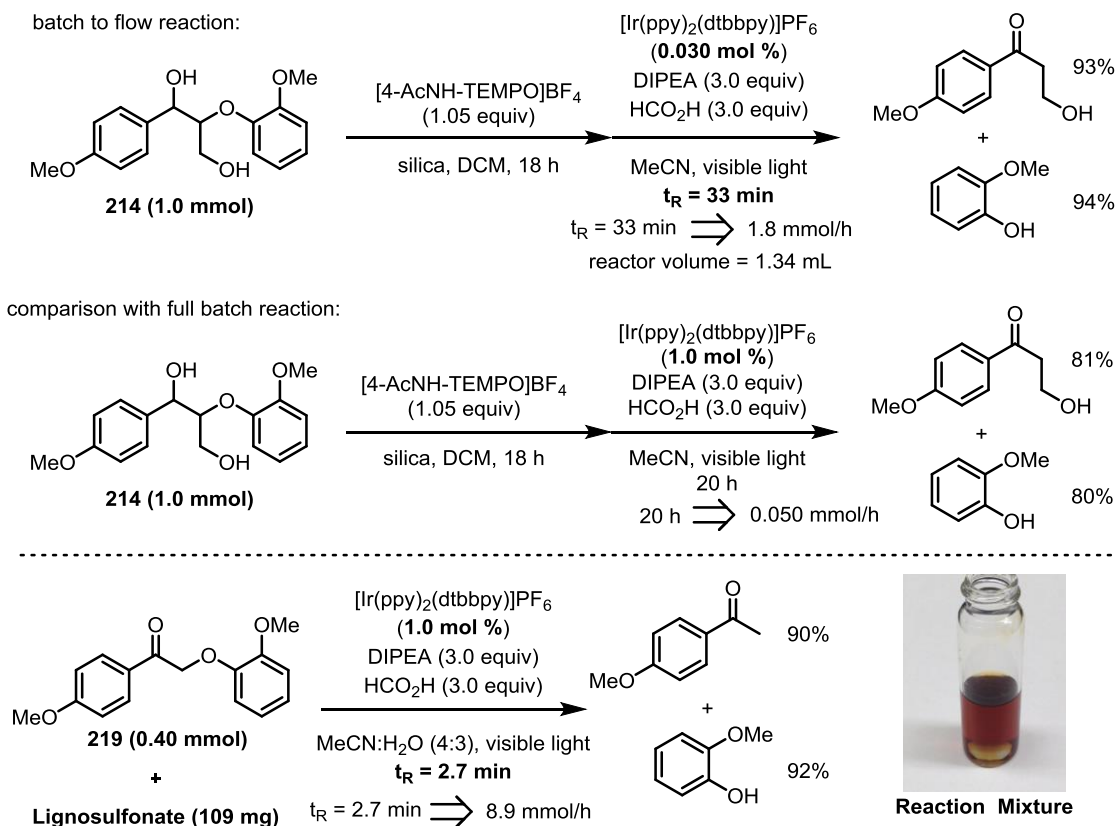
the  $\beta$ -hydroxy phenyl ketones did not undergo retro-aldol or elimination reactions. The ability to generate these fragmentation products under mild conditions and in high yields highlights the potential ability of this method to assist in the production of commodity compounds. In addition, the successful fragmentation of substrate **226** highlights the versatility of this lignin degradation strategy because primary alcohols typically survive lignin pulping methods, whereas benzylic alcohols are known to undergo substitution to form benzylic thiols (kraft), benzylic sulfones (sulfite), and benzylic ethers (organosolv). Furthermore, the  $\beta$ -hydroxy phenyl ketone fragments produced from substrates **220**, **221**, and **225** have not been generated by any other lignin degradation method in high yields, particularly **225**, which is a difficult substrate due to the free phenol.

### **Two-Step Protocol for Lignin Degradation**

By combining the chemoselective benzylic oxidation utilizing [4-AcNH-TEMPO]BF<sub>4</sub> and the visible light-mediated C <sub>$\alpha$</sub> -O bond cleavage, I successfully developed a lignin degradation method that can be performed at ambient temperature. Substrates **213–215** were cleanly oxidized to benzylic ketones by mixing a slight excess of [4-AcNH-TEMPO]BF<sub>4</sub> and silica. Upon completion of the oxidation the mixture was filtered and dichloromethane was removed in vacuo. Next, DIPEA, formic acid, [Ir(ppy)<sub>2</sub>(dtbbpy)]PF<sub>6</sub>, and MeCN were added and the reaction mixture was irradiated with blue LEDs to produce the fragmentation products in high yields. This system is particularly amenable to a batch-to-flow<sup>65,191</sup> reaction set-up in which the oxidation is performed in batch and the reductive cleavage is performed in flow. Utilizing an easily assembled flow reactor,<sup>189</sup> the rate of substrate consumption for **214** could be increased to 1.8 mmol/hour in flow from 0.050 mmol/hour in batch even when the catalyst loading is reduced from 1.0 mol% to 0.030 mol%. The ability to perform the reductive C <sub>$\alpha$</sub> -O bond cleavage reaction at lower catalyst loading is not exclusive to flow reactions, as is demonstrated by the gram-scale

batch fragmentation of substrate **214** with only 0.030 mol% catalyst loading. Surprisingly, in both of these cases the use of 0.030 mol% catalyst loading gave slightly improved yields for both fragmentation products as compared to 1.0 mol% (Figure 4.9, top).

At the onset, I was aware of the potential difficulty of irradiating darkly colored solutions of lignin. Therefore, I performed the photocatalytic reduction of **219** (0.4 mmol) in the presence of an equivalent weight of lignosulfonate. The dark brown color of the resulting solution prevented efficient irradiation of the reaction medium in batch, which resulted in no conversion after 48 hours. However, when the same reaction was carried out in flow, I observed full consumption of **219**, providing a high yield of both guaiacol and 4-methoxyacetophenone, despite reduced light transmittance (Figure 4.9, bottom). This clearly demonstrates the ability of

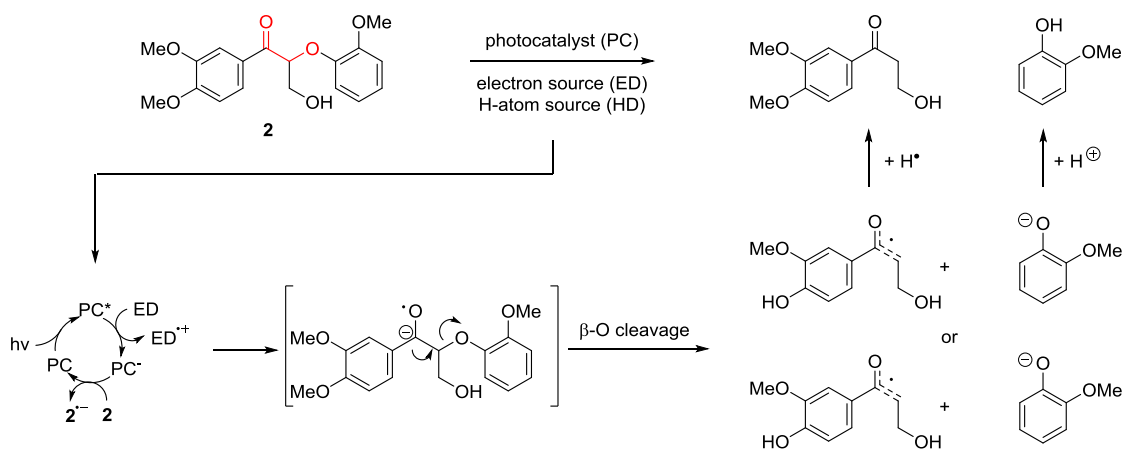


**Figure 4.9** Utilizing Continuous Flow and Lower Catalyst Loading.

the reductive cleavage reaction to operate in the presence of sulfonate groups, solvent quantities of water, and dark color impurities found in liginosulfonate.

### Mechanism and Mechanistic Studies

The proposed mechanism of the reductive C<sub>α</sub>-O bond cleavage is based on the well-established reductive quenching cycle of [Ir(ppy)<sub>2</sub>(dtbbpy)]PF<sub>6</sub> and is analogous to the reductive dehalogenation mechanism previously studied by my former colleague, Joseph Tucker. Visible light absorption by the photocatalyst initiates a metal-to-ligand charge transfer to generate the excited state [Ir]<sup>3+</sup>\*. This excited state accepts an electron from the amine or amine-formate complex to generate [Ir]<sup>2+</sup>, a strong reductant (-1.51 V vs SCE). The [Ir]<sup>2+</sup> complex performs a single electron transfer to the benzylic ketone or aliphatic aldehyde to generate a radical anion, which undergoes a fragmentation to generate an alkoxy anion and the corresponding C<sub>α</sub>-radical. Protonation of the alkoxy anion and H-atom abstraction by C<sub>α</sub>-radical produces the fragmentation products.



**Figure 4.10** Proposed mechanism of C-O bond cleavage.

### Conclusions

In conclusion, my colleagues and I have described a potential mild and efficient two-stage lignin degradation strategy that proceeds through a selective [4-AcNH-TEMPO]BF<sub>4</sub>-

mediated oxidation and a photoredox catalyzed reductive C–O bond cleavage. The separation of the oxidation and reduction steps, as well as the mild nature of the reaction conditions, allows for greater control of bond construction and cleavage to ultimately maintain the integrity of the fragmentation products. This proof-of-principle approach addresses many of the challenges in the chemoselective degradation of lignin which include functional group tolerance and mild reaction conditions, however aspects of scalability, stoichiometric waste, and cost remain to be addressed. Further development of a photocatalytic depolymerization that obviates the need for superstoichiometric additives are currently ongoing.

## **Experimental**

### **General Procedure A: Benzylic Oxidation with [4-AcNH-TEMPO]BF<sub>4</sub>.**

A 5 dram vial with a magnetic stir bar was charged with the corresponding benzylic alcohol (1.00 mmol, 1.00 equiv), dichloromethane (10.0 mL), silica gel (100 wt. % of benzylic alcohol), and [4-AcNH-TEMPO]BF<sub>4</sub> (1.05 mmol, 1.05 equiv). The vial was capped and the heterogenous mixture was stirred at room temperature until it was complete (as judged by TLC analysis). The reaction mixture was vacuum filtered through a pad of silica on a glass-fritted funnel (pore size C) and an additional 30 mL of dichloromethane (10 mL portions) was used to rinse the product from the silica. The filtrate was concentrated in vacuo and the crude residue can be used directly in General Procedure B or purified by chromatography on silica gel to afford the desired product.

### **General Procedure B: Reductive C–O Bond Cleavage.**

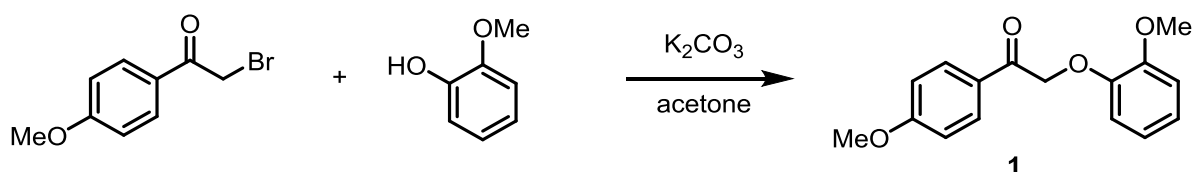
A 5 dram vial with a magnetic stir bar was charged with the corresponding benzylic ketone (1.00 mmol, 1.00 equiv), MeCN (5.0 mL), *N,N*-diisopropylamine (3.0 mmol, 3.0 equiv), formic acid (3.0 mmol, 3.0 equiv) and [Ir(ppy)<sub>2</sub>(dtbbpy)]PF<sub>6</sub> (0.010 mmol, 0.010 equiv). The vial was capped and the reaction mixture was stirred at room temperature until it was complete (as judged



by TLC analysis). The solvent was removed from the crude mixture *in vacuo* and was dissolved in EtOAc. The contents were poured into a separatory funnel containing 25 mL of EtOAc and 25 mL of deionized water. The layers were separated and the aqueous layer was extracted with EtOAc (2 × 25 mL). The combined organic layers were washed with brine, dried (Na<sub>2</sub>SO<sub>4</sub>), and concentrated in vacuo. The residue was purified by chromatography on silica gel to afford the desired products.

### **General Procedure C: Two-Step Degradation Protocol.**

A 5 dram vial with a magnetic stir bar was charged with the corresponding benzylic alcohol (1.00 mmol, 1.00 equiv), dichloromethane (10.0 mL), silica gel (100 wt. % of benzylic alcohol), and [4-AcNH-TEMPO]BF<sub>4</sub> (1.05 mmol, 1.05 equiv). The vial was capped and the heterogenous mixture was stirred at room temperature until it was complete (as judged by TLC analysis). The reaction mixture was vacuum filtered through a pad of silica on a glass-fritted funnel (pore size C) and an additional 30 mL of dichloromethane (10 mL portions) was used to rinse the product from the silica. The filtrate was concentrated in vacuo and the crude residue was combined with MeCN (5.0 mL), *N,N*-diisopropylamine (3.0 mmol, 3.0 equiv), formic acid (3.0 mmol, 3.0 equiv) and [Ir(ppy)<sub>2</sub>(dtbbpy)]PF<sub>6</sub> (0.010 mmol, 0.010 equiv) in a 5 dram vial. The vial was capped and the reaction mixture was stirred at room temperature until it was complete (as judged by TLC analysis). The solvent was removed from the crude mixture in vacuo and was dissolved in EtOAc. The contents were poured into a separatory funnel containing 25 mL of EtOAc and 25 mL of deionized water. The layers were separated and the aqueous layer was extracted with EtOAc (2 × 25 mL). The combined organic layers were washed with brine, dried (Na<sub>2</sub>SO<sub>4</sub>), and concentrated in vacuo. The residue was purified by chromatography on silica gel to afford the desired products.



**2-(2-methoxyphenoxy)-1-(4-methoxyphenyl)ethanone (1)**: Substrate **1** was prepared according to a literature procedure.<sup>79</sup> A round bottom flask equipped with a reflux condenser was charged with 2-bromo-1-(4-methoxyphenyl)ethanone (13.7 g, 60 mmol), potassium carbonate (12.3 g, 89 mmol), guaiacol (8.2 mL, 74 mmol), and acetone (250 mL). The resulting suspension was stirred and heated to reflux for 3 h, after which it was filtered through celite and concentrated in vacuo. The resulting solid purified by chromatography on  $SiO_2$  (70:30, hexanes/EtOAc) afforded **1** (13.9 g, 51 mmol, 86%) as a colorless solid.

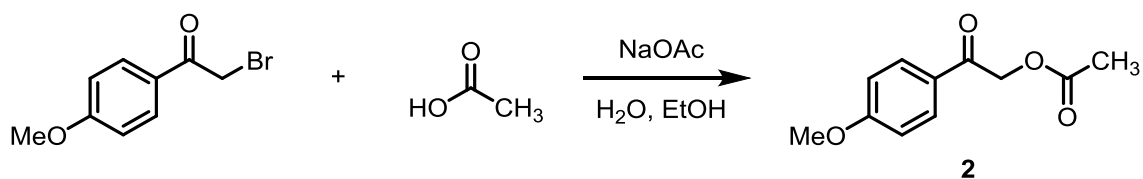
$R_f$ (EtOAc/hexane 1:3): 0.20;

IR (neat): 2936, 2837, 1689, 1597, 1501, 1212, 1168, 1127, 1023, 832, 739  $cm^{-1}$ ;

$^1H$  NMR ( $CDCl_3$ , 400 MHz):  $\delta$  8.03 (d,  $J = 8.4$  Hz, 2H), 7.00–6.90 (m, 2H), 6.97 (d,  $J = 8.4$  Hz, 2H), 6.88–6.84 (m, 2H), 5.29 (s, 2H), 3.89 (s, 6H);

$^{13}C$  NMR ( $CDCl_3$ , 175 MHz):  $\delta$  193.1, 163.9, 149.7, 147.6, 130.5, 127.7, 122.3, 120.8, 114.7, 113.9, 112.2, 72.0, 55.9, 55.5;

HRMS (ESI)  $m/z$  calculated for  $C_{16}H_{16}O_4^+$  ( $[M+H]^+$ ) 273.1121, found 273.1110.

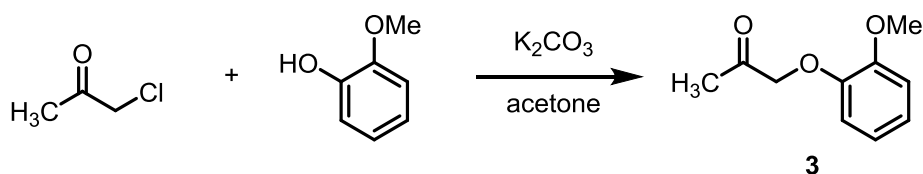


<sup>79</sup> *J. Am. Chem. Soc.* **2010**, *132*, 12554.

**2-(4-methoxyphenyl)-2-oxoethyl acetate (2):** Substrate **2** was prepared according to literature procedure.<sup>80</sup> A suspension of 2-bromo-1-(4-methoxyphenyl)ethanone (4.8 g, 21 mmol) in 22 mL of ethanol was prepared round-bottomed flask, and a solution of sodium acetate trihydrate (3.2 g, 24 mmol) in 11 mL of water and 1.1 mL of acetic acid was added. The mixture was heated at reflux for 2.5 h, then cooled to room temperature, and refrigerated overnight. In some cases, a solid separated that was collected by filtration and was found to be pure acetate. In other cases, most of the ethanol was removed under reduced pressure, and the resulting oily mixture was distributed between 30 mL EtOAc and 20 mL of a semisaturated, ice-cold NaHCO<sub>3</sub> solution. The organic extracts were washed in sequence with 10 mL of semisaturated brine, dried with sodium sulfate, and evaporated in vacuo. Purified by chromatography on SiO<sub>2</sub> (70:30, hexanes/EtOAc) afforded **2** (4.0 g, 19 mmol, 90%) as a colorless solid. Spectral data are consistent with those reported in the literature.<sup>81</sup>

$R_f$ (EtOAc/hexanes 1:3): 0.20;

<sup>1</sup>H NMR (CDCl<sub>3</sub>, 400 MHz):  $\delta$  7.78 (d,  $J$  = 7.4 Hz, 2H), 6.83 (d,  $J$  = 7.3 Hz, 2H), 5.19 (s, 2H), 3.74 (s, 3H), 2.11 (s, 3H).



**1-(2-methoxyphenoxy)propan-2-one (3):** Substrate **3** was prepared according to a literature procedure.<sup>82</sup> A mixture of guaiacol (0.62 g, 5.0 mmol), chloroacetone (0.69 g, 7.5 mmol) and K<sub>2</sub>CO<sub>3</sub> (1.0 g, 7.5 mmol) in acetone (10 mL) was stirred at 60 °C for 3 hours. Then, K<sub>2</sub>CO<sub>3</sub> was

<sup>80</sup> *J. Med. Chem.* **2007**, *50*, 21.

<sup>81</sup> *Chin. J. Chem.* **2010**, *28*, 294.

<sup>82</sup> *Eur. J. Org. Chem.* **2012**, *2012*, 1499.

filtered and the solvent removed under reduced pressure and purification by chromatography on SiO<sub>2</sub> (75:25, hexanes/EtOAc) afforded **3** (0.74 g, 4.1 mmol, 82%) as a clear and colorless oil.

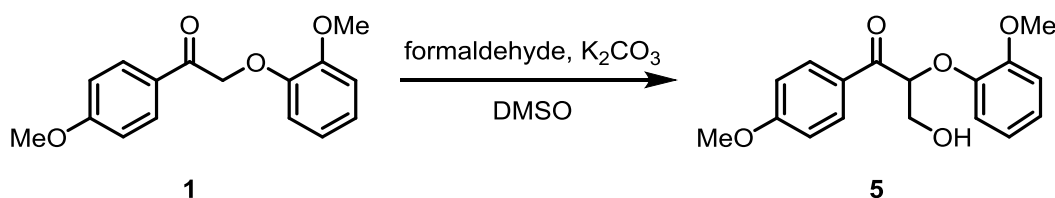
*R<sub>f</sub>*(EtOAc/hexanes 1:3): 0.25;

IR (neat): 2918, 2837, 1717, 1592, 1501, 1250, 1125, 1024, 965, 740 cm<sup>-1</sup>;

<sup>1</sup>H NMR (CDCl<sub>3</sub>, 400 MHz): δ 7.00 (dt, *J* = 8.2, 1.4 Hz, 1H), 6.94 (dd, *J* = 8.2, 1.8 Hz, 1H), 6.89 (dt, *J* = 8.0, 1.8 Hz, 1H), 6.79 (dd, *J* = 8.0, 1.4 Hz, 1H), 4.60 (s, 2H), 3.90 (s, 3H), 2.30 (s, 3H);

<sup>13</sup>C NMR (CDCl<sub>3</sub>, 175 MHz): δ 205.9, 149.4, 147.1, 122.3, 120.6, 114.1, 112.0, 74.1, 55.6, 26.2;

HRMS (ESI) *m/z* calculated for C<sub>10</sub>H<sub>12</sub>O<sub>3</sub><sup>+</sup> ([M+H]<sup>+</sup>) 181.0859, found 181.0855.



**3-hydroxy-2-(2-methoxyphenoxy)-1-(4-methoxyphenyl)propan-1-one (5)**: Substrate **5** was prepared according to a literature procedure.<sup>83</sup> A solution of **1** (1.5 g, 5.5 mmol) in DMSO (30 mL) containing K<sub>2</sub>CO<sub>3</sub> (1.5 g, 11 mmol) was stirred for 30 min at room temperature before adding formaldehyde (37 %) (0.82 mL, 11 mmol). The resulting solution was stirred for 3 h and 2 N NaOH (15 mL) was added and stirred for 1 h. After addition of 1 N HCl, the solution was extracted with ethyl acetate. The extracts were dried, concentrated in vacuo, and purification by chromatography on SiO<sub>2</sub> (50:50, hexanes/EtOAc) afforded **5** (0.83 g, 2.8 mmol, 50%) as a colorless solid.

*R<sub>f</sub>*(EtOAc/hexanes 3:2): 0.31;

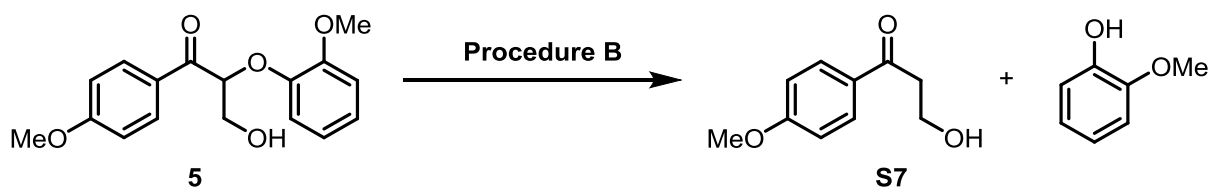
IR (neat): 3474, 2942, 2840, 1684, 1599, 1504, 1254, 1173, 1128, 1026, 974, 840, 742 cm<sup>-1</sup>;

<sup>83</sup> *J. Org. Chem.* **2010**, *75*, 6549.

$^1\text{H}$  NMR ( $\text{CDCl}_3$ , 400 MHz):  $\delta$  8.06 (d,  $J = 8.6$  Hz, 2H), 7.02 (t,  $J = 7.6$  Hz, 1H), 6.98–6.89 (m, 4H), 6.83 (t,  $J = 7.2$  Hz, 1H), 5.40–5.35 (m, 1H), 4.07 (t,  $J = 5.1$  Hz, 2H), 3.89 (s, 3H), 3.87 (s, 3H), 3.00 (t,  $J = 5.6$  Hz, 1H);

$^{13}\text{C}$  NMR ( $\text{CDCl}_3$ , 175 MHz):  $\delta$  195.0, 164.0, 150.5, 146.9, 131.3, 127.9, 123.6, 121.1, 118.6, 114.0, 112.3, 84.7, 63.6, 55.8, 55.5;

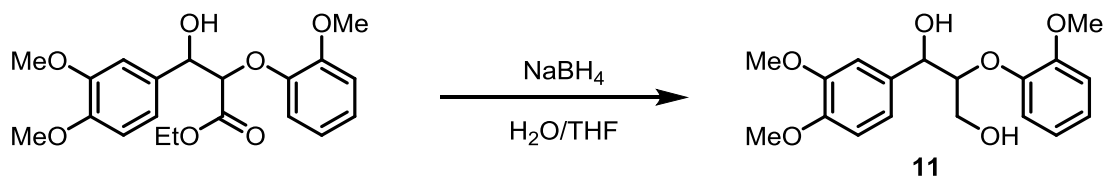
HRMS (ESI)  $m/z$  calculated for  $\text{C}_{17}\text{H}_{18}\text{O}_5^+$  ( $[\text{M}+\text{H}]^+$ ) 303.1227, found 303.1225.



**3-hydroxy-1-(4-methoxyphenyl)propan-1-one** (table 1, entry 5, product 1): According to General Procedure B, **5** (0.30 g, 1.0 mmol), DIPEA (0.52 mL, 0.39 g, 3.0 mmol), formic acid (0.11 mL, 0.14 g, 3.0 mmol) and  $[\text{Ir}(\text{ppy})_2(\text{dtbbpy})]\text{PF}_6$  (9.2 mg, 10  $\mu\text{mol}$ ) in MeCN (5.0 mL) afforded **S7** (0.15 g, 0.85 mmol, 85%) and guaiacol (0.11 g, 0.88 mmol, 88%) after purification by chromatography on  $\text{SiO}_2$  (50:50, hexanes/EtOAc). Spectral data are consistent with those reported in the literature.<sup>84</sup>

$R_f$  (EtOAc/hexanes 3:2): 0.28;

$^1\text{H}$  NMR ( $\text{CDCl}_3$ , 400 MHz):  $\delta$  7.93 (d,  $J = 9.0$  Hz, 2H), 6.93 (d,  $J = 9.0$  Hz, 2H), 4.00 (t,  $J = 5.5$  Hz, 2H), 3.89 (s, 3H), 3.16 (t,  $J = 5.5$  Hz, 2H), 2.74 (br s, 1H).

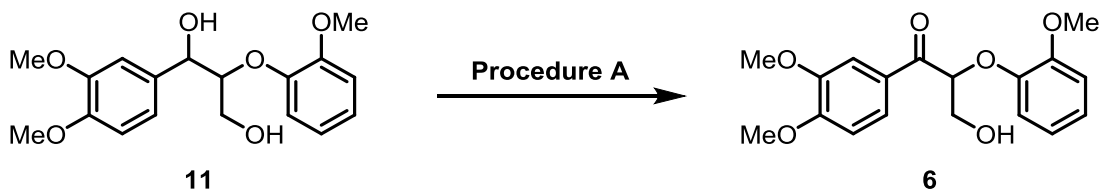


<sup>84</sup> *Tetrahedron* **2010**, *66*, 3995.

**1-(3,4-dimethoxyphenyl)-2-(2-methoxyphenoxy)propane-1,3-diol (11):** The synthesis of **11** was adapted from the literature procedure.<sup>85</sup> To a solution of  $\beta$ -hydroxyester<sup>85</sup> (3.4 g, 9.0 mmol) in THF/H<sub>2</sub>O (5 mL, 3:1 ratio) was added sodium borohydride (1.7 g, 45 mmol) in portions. The reaction was allowed to stir at room temperature overnight. The reaction was diluted with ethyl acetate and washed with water and brine, then dried over sodium sulfate. The organic layer was then concentrated and purified by chromatography on SiO<sub>2</sub> (60:40, hexanes/EtOAc) afforded **11** (2.7 g, 89%) as a 2.5:1 mixture of diastereomers. Spectral data are consistent with those reported in the literature.<sup>86</sup>

*R<sub>f</sub>* (hexanes/DCM/acetone/MeOH 6:2:1.5:0.5): 0.40;

<sup>1</sup>H NMR (CDCl<sub>3</sub>, 500 MHz):  $\delta$  7.14 (dd, *J* = 7.9, 1.5 Hz, 1H, minor diastereomer), 7.11-7.05 (m, 1H, major diastereomer, 1H minor diastereomer, overlap), 7.01-6.89 (m, 5H, major diastereomer, 2H, minor diastereomer, overlap), 6.87-6.83 (m, 1H, major diastereomer, 1H, minor diastereomer, overlap), 4.99 (d, *J* = 4.7 Hz, 1H, minor diastereomer), 4.98 (t, *J* = 4.7 Hz, 1H, major diastereomer), 4.16 (ddd, *J* = 6.0, 4.7, 3.4 Hz, 1H, major diastereomer), 4.04 (m, 1H, minor diastereomer), 3.95-3.89 (m, 1H, major diastereomer), 3.92 (s, 3H, minor diastereomer), 3.88 (s, 3H, major diastereomer, 3H, minor diastereomer), 3.88 (s, 3H, major diastereomer, 3H minor diastereomer), 3.69 (m, 1H, minor diastereomer) 3.66 (m, 1H, major diastereomer), 3.63 (m, 1H minor diastereomer), 3.48 (dd, *J* = 12.5, 3.9 Hz, 1H, minor diastereomer).



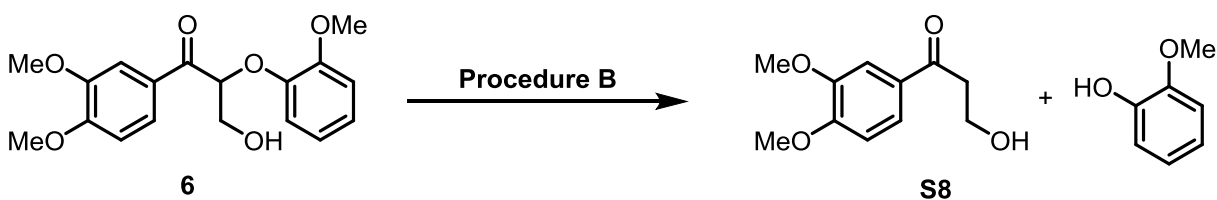
<sup>85</sup> *Angew. Chem. Int. Ed.* **2012**, *51*, 3410.

<sup>86</sup> *Chem. Eur. J.* **2011**, *17*, 13877.

**1-(3,4-dimethoxyphenyl)-3-hydroxy-2-(2-methoxyphenoxy)propan-1-one (6):** According to General Procedure A, **11** (334 mg, 1.0 mmol), [4-AcNH-TEMPO]BF<sub>4</sub> (315 mg, 1.1 mmol), and silica (334 mg) in DCM (10 mL) afforded **6** (314 mg, 94%) after purification by chromatography on SiO<sub>2</sub> (60:40,hexanes/EtOAc). Spectral data are consistent with those reported in the literature.<sup>87</sup>

*R<sub>f</sub>* (hexanes/DCM/acetone/MeOH 6:2:1.5:0.5): 0.36;

<sup>1</sup>H NMR (CDCl<sub>3</sub>, 500 MHz): δ 7.76 (dd, *J* = 8.6, 2.2 Hz, 1H), 7.62 (d, *J* = 2.0 Hz, 1H), 7.00 (td, *J* = 7.7, 7.7, 1.2 Hz, 1H), 6.91 (ddd, *J* = 8.3, 8.3, 1.5 Hz, 1H), 6.89 (d, *J* = 8.31 Hz, 1H), 6.83 (td, *J* = 7.26, 7.26 Hz, 1H), 5.40 (t, *J* = 5.4, 5.4 Hz, 1H), 4.07, (d, *J* = 5.4 Hz, 2H), 3.95 (s, 3H), 3.92 (s, 3H), 3.86 (s, 3H), 3.06 (br s, 1H).



**1-(3,4-dimethoxyphenyl)-3-hydroxypropan-1-one (table 1, entry 6, product 1):** According to General Procedure B, **6** (0.38 g, 1.14 mmol), DIPEA (0.60 mL, 0.44 g, 3.4 mmol), formic acid (0.13 mL, 0.16 g, 3.4 mmol) and [Ir(ppy)<sub>2</sub>(dtbbpy)]PF<sub>6</sub> (10 mg, 11.0 μmol) in MeCN (10.0 mL) afforded **S8** (141 mg, 85%) and guaiacol (239 mg, 76%) after purification by chromatography on SiO<sub>2</sub> (70:20:5:5 hexanes/DCM/MeOH/acetone).

### 5.2 mmol Scale One-Pot Reductive Fragmentation of **11** to **S8**

According to General Procedure C, **11** (1.75 g, 5.22 mmol) in DCM (50.0 mL), silica gel (1.75 g, 100 wt. %), and [4-AcNH-TEMPO]BF<sub>4</sub> (1.65 g, 5.5 mmol). The vial was capped and the heterogenous mixture was stirred at room temperature until it was complete (as judged by TLC

<sup>87</sup> *J. Am. Chem. Soc.* **2013**, *135*, 6415.

analysis). The reaction mixture was vacuum filtered through a pad of silica on a glass-fritted funnel (pore size C) and an additional 90 mL of DCM (30 mL portions) was used to rinse **6** from the silica. The organic layer was concentrated and then the crude was reacted with DIPEA (2.75 mL, 2.0 g, 16 mmol), formic acid (0.60 mL, 0.73 g, 16 mmol) and [Ir(ppy)<sub>2</sub>(dtbbpy)]PF<sub>6</sub> (2 mg, 2.0 μmol) in MeCN (50 mL) afforded **S8** (1.05 g, 95%) and guaiacol (0.65 g, 99%) after purification by chromatography on SiO<sub>2</sub> (70:20:5:5 hexanes/DCM/MeOH/acetone).

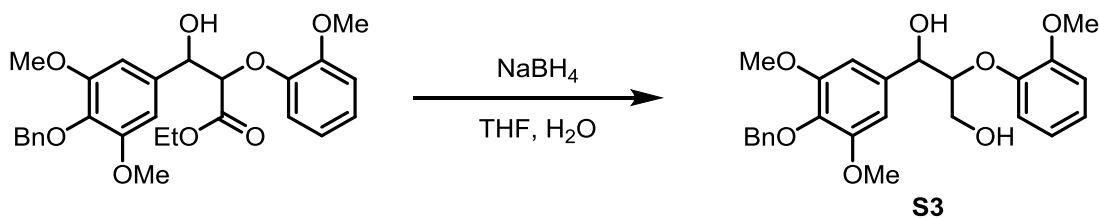
*R<sub>f</sub>* (hexanes/DCM/MeOH/acetone 7:2:0.5:0.5): 0.21;

IR (neat): 3437, 2938, 1667, 1586, 1514, 1464, 1418, 1347, 1264, 1201, 1150, 1021, 888, 808, 766 cm<sup>-1</sup>;

<sup>1</sup>H NMR (CDCl<sub>3</sub>, 700 MHz): δ 7.59 (d, *J* = 8.3 Hz, 1H), 7.52 (s, 1H), 6.89 (d, *J* = 8.3 Hz, 1H), 4.02 (m, 2H), 3.95 (s, 3H), 3.93 (s, 3H), 3.19 (t, *J* = 5.3 Hz, 2H);

<sup>13</sup>C NMR (CDCl<sub>3</sub>, 175 MHz): δ 231.5, 129.9, 123.0, 110.0, 109.9, 58.3, 56.1, 56.0, 39.8;

HRMS (ESI) *m/z* calculated for C<sub>11</sub>H<sub>15</sub>O<sub>4</sub><sup>+</sup> ([M+H]<sup>+</sup>) 211.0965, found 211.0960.



**1-(4-(benzyloxy)-3,5-dimethoxyphenyl)-2-(2-methoxyphenoxy)propane-1,3-diol (S3):**

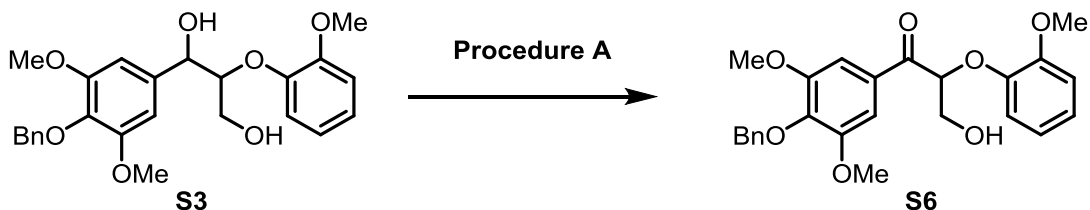
Substrate **S3** was synthesized according the literature procedure.<sup>85</sup> To a solution of β-hydroxyester<sup>85</sup> (5.0 g, 9.5 mmol) in THF/H<sub>2</sub>O (5 mL, 3:1 ratio) was added sodium borohydride (1.8 g, 47 mmol) in portions. The reaction was allowed to stir at room temperature overnight. The reaction was diluted with ethyl acetate and washed with water and brine, then dried over sodium sulfate. The organic layer was then concentrated and purified by chromatography on



SiO<sub>2</sub> (60:40, hexanes/EtOAc) afforded **S3** (3.8 g, 91%, 2.5:1 diastereomeric ratio). Spectral data are consistent with those reported in the literature.<sup>85</sup>

*R<sub>f</sub>* (hexanes:EtOAc 7:1): 0.10;

<sup>1</sup>H NMR (CDCl<sub>3</sub>, 500 MHz): δ 7.47 (d, *J* = 6.8 Hz, 2H, minor diastereomer), 7.47 (d, *J* = 6.8 Hz, 2H, major diastereomer), 7.33 (m, 2H, minor diastereomer), 7.33 (m, 2H, major diastereomer) 7.29 (d, *J* = 6.8 Hz, 1H, minor diastereomer), 7.29 (d, *J* = 6.8 Hz, 1H, major diastereomer), 7.10 (m, 1H, minor diastereomer), 6.95 (m, 3H), 6.67 (s, 0.82H, minor diastereomer), 6.60 (s, 2H, major diastereomer), 4.99 (m, 2H, major diastereomer), 4.97 (d, *J* = 4.4 Hz, 1.3H, minor diastereomer), 4.16 (m, 1H, major diastereomer), 4.02 (m, 0.6H, minor diastereomer), 3.92 (s, 1.4H, minor diastereomer), 3.90 (s, 3H, major diastereomer), 3.82 (s, 1.83H, minor diastereomer), 3.81 (s, 6H, major diastereomer), 3.66 (m, 1H, major diastereomer), 3.51 (m, 0.5H, minor diastereomer).



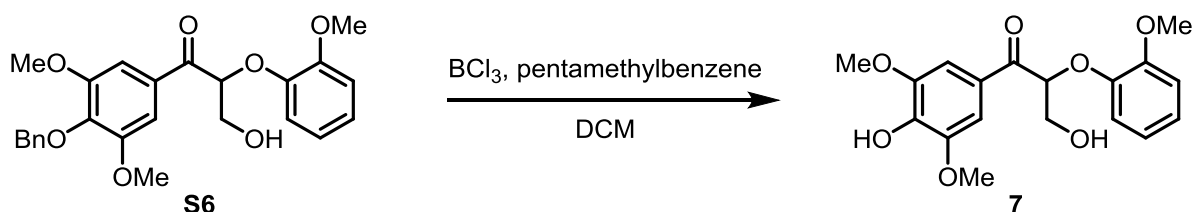
### 1-(4-(benzyloxy)-3,5-dimethoxyphenyl)-3-hydroxy-2-(2-methoxyphenoxy)propan-1-one

**(S6):** According to General Procedure A, **S3** (1.0 g, 2.3 mmol), [4-AcNH-TEMPO]BF<sub>4</sub> (0.72 g, 2.4 mmol), and silica (1.0 g) in DCM (20 mL) afforded **S6** (0.94 g, 94%) after purification by chromatography on SiO<sub>2</sub> (60:40, hexanes/EtOAc). Spectral data are consistent with those reported in the literature.<sup>88</sup>

*R<sub>f</sub>* (hexanes/EtOAc 4:1): 0.15;

<sup>88</sup> *J. Photochem. Photobiol. A* 2003, 156, 253.

$^1\text{H}$  NMR ( $\text{CDCl}_3$ , 500 MHz):  $\delta$  7.46-7.43 (m, 2H), 7.34-7.31 (m, 2H), 7.32 (s, 2H), 7.02 (ddd,  $J = 7.8, 7.8, 1.6$  Hz, 1H), 6.92 (ddd,  $J = 8, 1.5, 1.5$  Hz, 2H), 6.85 (ddd,  $J = 7.7, 7.7, 1.5$  Hz, 1H), 5.35 (d,  $J = 5.1, 5.1$  Hz, 1H), 5.10 (s, 2H), 4.09-4.07 (m, 2H), 3.82 (s, 6H), 2.93 (dd,  $J = 6.0, 6.0$  Hz, 1H).

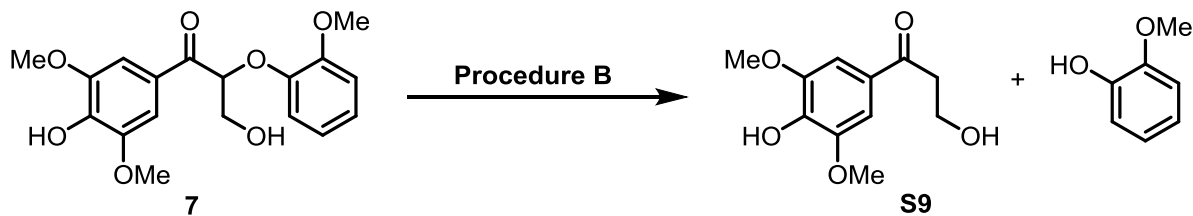


**3-hydroxy-1-(4-hydroxy-3,5-dimethoxyphenyl)-2-(2-methoxyphenoxy)propan-1-one (7):** A solution of **S6** (150 mg, 0.23 mmol) and pentamethylbenzene (101 mg, 0.69 mmol) in dichloromethane was cooled to  $-78^\circ\text{C}$  in a dry ice/acetone bath. To this,  $\text{BCl}_3$  (450  $\mu\text{L}$ , 1M solution in DCM, 0.45 mmol) was added dropwise.<sup>89</sup> This was allowed to stir at  $-78^\circ\text{C}$  for 30 minutes upon which the reaction was quenched with MeOH. This organic layer was immediately loaded onto celite and purified by chromatography on  $\text{SiO}_2$  (50:50, hexanes/EtOAc) to afford **7** (75 mg, 95%) as a colorless solid. Spectral data are consistent with those reported in the literature.<sup>85</sup>

$R_f$ (hexanes/EtOAc, 8:2): 0.06;

$^1\text{H}$  NMR ( $\text{CDCl}_3$ , 500 MHz):  $\delta$  7.41 (s, 2H), 7.01 (ddd,  $J = 8.1, 7.3, 1.5$  Hz, 1H), 6.91 (ddd,  $J = 9.5, 8.5, 1.7$  Hz, 2H), 6.83 (ddd,  $J = 7.6, 7.6, 1.5$  Hz, 1H), 6.01 (br s, 1H), 5.34 (dd,  $J = 6.5, 4.3$  Hz, 1H), 4.09 (d,  $J = 5.4$  Hz, 1H), 4.08 (d,  $J = 3.2$  Hz, 1H), 3.91 (s, 6H), 3.86 (s, 3H).

<sup>89</sup> *Synlett* **2008**, 13, 1977.

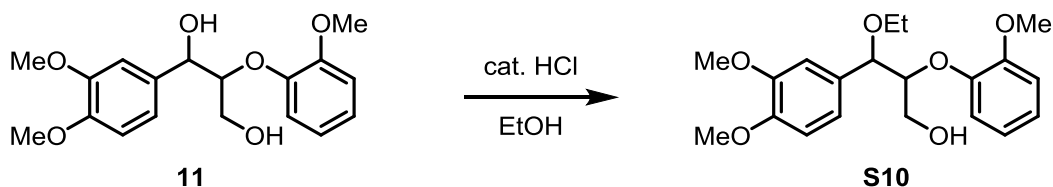


**3-hydroxy-1-(4-hydroxy-3,5-dimethoxyphenyl)propan-1-one (table 1, entry 7, product 1):**

According to General Procedure B, **7**<sup>90</sup> (71 mg, 0.19 mmol), DIPEA (0.13 mL, 96 mg, 0.75 mmol), formic acid (28  $\mu$ L, 34 mg, 0.75 mmol) and [Ir(ppy)<sub>2</sub>(dtbbpy)]PF<sub>6</sub> (1.7 mg, 2.0  $\mu$ mol) in MeCN (0.5 mL) afforded **S9** (41 mg, 90%) and guaiacol (22 mg, 95%) after purification by chromatography on SiO<sub>2</sub> (70:10:10:10, hexanes/DCM/MeOH/acetone). Spectral data are consistent with those reported in the literature.<sup>90</sup>

*R<sub>f</sub>* (hexanes/DCM/acetone/MeOH 7:1:1:1) 0.05;

<sup>1</sup>H NMR (CDCl<sub>3</sub>, 700 MHz):  $\delta$  7.26 (s, 2H), 5.99 (br s, 1H), 4.03 (q, *J* = 8.4 Hz, 2H), 3.96 (s, 3H), 3.20 (t, *J* = 5.3 Hz, 2H), 2.67 (t, *J* = 6.3 Hz, 1H).



**3-(3,4-dimethoxyphenyl)-3-ethoxy-2-(2-methoxyphenoxy)propan-1-ol (S10):** Compound **S10**

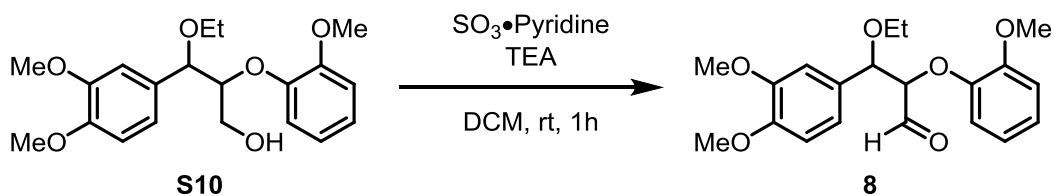
was made according to literature precedent.<sup>91</sup> 1 drop of conc. HCl was added a solution of **11** (0.75 g, 2.2 mmol) in ethanol (6 mL) and heated to 60°C for 3 hours. The reaction was concentrated and purified by chromatography over SiO<sub>2</sub> (75:25, hexanes/EtOAc) to afford **S10** (0.68 g, 84% 1:4:1 mixture of diastereomers) as a clear and colorless oil. Spectral data are consistent with those reported in the literature.<sup>91</sup>

<sup>90</sup> *J. Chem. Soc. Pak.* **2009**, *31*, 126.

<sup>91</sup> *Holzforchung* **1991**, *45*, 37.

$R_f$  (hexanes/EtOAc 3:1): 0.26;

$^1\text{H NMR}$  ( $\text{CDCl}_3$ , 500 MHz):  $\delta$  7.29 (dd,  $J = 7.8, 1.5$  Hz, 1H, minor diastereomer), 7.02 (m, 1H, minor diastereomer), 6.97-6.89 (m, 3H, major diastereomer, 4H, minor diastereomer), 6.86-6.82 (m, 2H, major diastereomer, 1H, minor diastereomer), 6.75 (ddd,  $J = 7.7, 7.7, 1.7$  Hz, 1H, major diastereomer), 6.50 (dd,  $J = 7.8, 1.5$  Hz, 1H, major diastereomer), 4.53 (d,  $J = 7.3$  Hz, 1H, major diastereomer), 4.50 (d,  $J = 7.3$  Hz, 1H, minor diastereomer), 4.18 (ddd,  $J = 7.0, 7.0, 3.7$  Hz, 1H, minor diastereomer), 4.08 (m, 1H, major diastereomer), 3.93 (br. s., 1H, major diastereomer), 3.89 (s, 3H, minor diastereomer), 3.88 (s, 3H, minor diastereomer), 3.88 (s, 3H, major diastereomer), 3.87 (s, 3H, minor diastereomer), 3.86 (s, 3H, major diastereomer), 3.82 (s, 3H, major diastereomer), 3.52-3.38 (m, 2H, major diastereomer, 2H, minor diastereomer), 3.39 (br. s., 1H, major diastereomer), 3.23 (br. s., 1H, major diastereomer, 1H, minor diastereomer), 1.21 (t,  $J = 7, 7$  Hz, 3H major diastereomer), 1.19 (t,  $J = 7, 7$  Hz, 3H, minor diastereomer).



**3-(3,4-dimethoxyphenyl)-3-ethoxy-2-(2-methoxyphenoxy)propanal (8)**: To a solution of **S10** (108 mg, 0.30 mmol) in a 1:1 mixture of  $\text{DCM}/\text{DMSO}$  (2 mL), was added  $\text{SO}_3 \cdot \text{Pyridine}$  (190 mg, 1.2 mmol) and triethylamine (0.17 mL, 1.2 mmol). This reaction was allowed to stir at room temperature for 3 hours upon which it was diluted with ethyl acetate and washed with five portions of water and one portion of brine. The organic layer was dried over sodium sulfate and concentrated to afford **8** as a yellow oil (97 mg as a 1.5:1 mixture of diastereomers). This was found to be unstable to chromatography and was used directly in the next step.

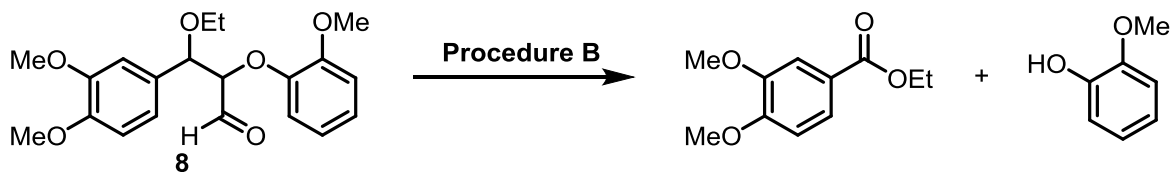
$R_f$  (hexanes/EtOAc 1:3): 0.25;

IR (neat): 3452, 2972, 2933, 1734, 1594, 1502, 1456, 1258, 1118, 1113, 1027, 750  $\text{cm}^{-1}$ ;

$^1\text{H}$  NMR ( $\text{CDCl}_3$ , 500 MHz):  $\delta$  9.88 (d,  $J = 2.0$  Hz, 1H, minor diastereomer), 9.76 (d,  $J = 2.9$ , 1H, major diastereomer), 7.12 (d,  $J = 2.0$  Hz, 1H, minor diastereomer), 7.00 (d,  $J = 2.0$ , 1H, major diastereomer), 6.97-6.91 (m, 2H, major diastereomer, 2H, minor diastereomer), 6.84 (dd,  $J = 8.3, 1.5$  Hz, 2H, major diastereomer), 6.82 (dd,  $J = 8.3, 1.5$  Hz, 2H, minor diastereomer), 6.75–6.79 (m, 1H, major diastereomer), 6.72–6.68 (m, 1H, major diastereomer, 1H minor diastereomer), 6.53 (dd,  $J = 8.3, 1.5$ , 1H, minor diastereomer), 4.77 (d,  $J = 3.4$  Hz, 1H, minor diastereomer), 4.71 (d,  $J = 5.9$  Hz, 1H, major diastereomer), 4.44 (dd,  $J = 5.9, 2.4$  Hz, 1H, major diastereomer), 4.23 (dd,  $J = 3.2, 2.2$  Hz, 1H, minor diastereomer), 3.90 (s, 3H, minor diastereomer), 3.87 (s, 6H, major diastereomer), 3.87 (3H, minor diastereomer), 3.75 (s, 3H, major diastereomer), 3.74 (s, 3, minor diastereomer), 3.51-3.36 (m, 2H, major diastereomer, 2H, minor diastereomer), 1.19 (t,  $J = 7.1$  Hz, 3H, minor diastereomer), 1.18 (t,  $J = 7.1$  Hz, 3H, major diastereomer);

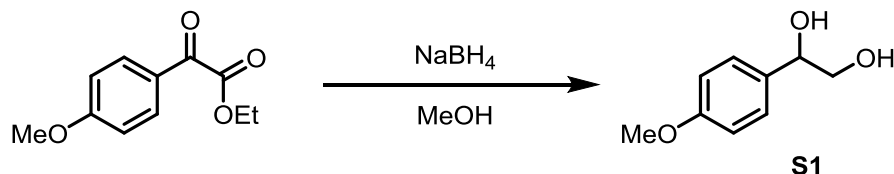
$^{13}\text{C}$  NMR ( $\text{CDCl}_3$ , 125 MHz):  $\delta$  203.0, 200.4, 150.3, 149.0, 147.4, 130.2, 130.0, 123.6, 123.5, 120.9, 120.9, 120.2, 119.8, 118.8, 118.7, 112.4, 112.2, 110.7, 110.7, 110.6, 88.4, 87.0, 82.1, 81.0, 65.2, 64.7, 55.9, 55.9, 55.9, 55.9, 55.6, 55.4, 15.1, 15.0;

HRMS (ESI)  $m/z$  calculated for  $\text{C}_{20}\text{H}_{24}\text{O}_6\text{Na}^+$  ( $[\text{M}+\text{Na}]^+$ ) 383.1471, found 383.1461.



**Fragmentation of Compound 9 (Table 1, Entry 9):** According to General Procedure B crude aldehyde **9** (117 mg, 0.33 mmol), DIPEA (0.17 mL, 126 mg, 0.97 mmol), formic acid (0.04 mL, 45 mg, 0.97 mmol) and  $[\text{Ir}(\text{ppy})_2(\text{dtbbpy})]\text{PF}_6$  (3.0 mg, 3.3  $\mu\text{mol}$ ) in MeCN (0.5 mL) afforded

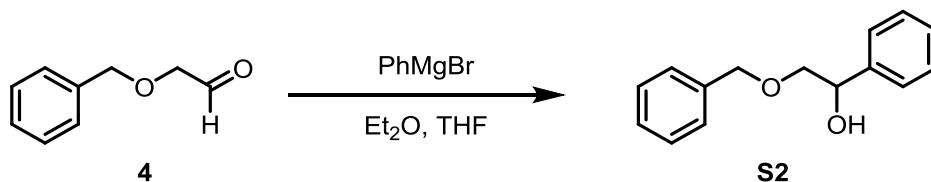
ethyl 3,4-dimethoxybenzoate<sup>92</sup> (21 mg, 30%) and guaiacol (28 mg, 70%) after purification by chromatography on SiO<sub>2</sub> (70:20:5:5, hexanes/DCM/MeOH/acetone). Spectral data are consistent with those reported in the literature.



**1-(4-methoxyphenyl)ethane-1,2-diol (S1):** Substrate **S1** was prepared according to a literature procedure.<sup>84</sup> In a flask, the  $\alpha$ -ketoester (1.0 mmol) was dissolved in methanol (5 mL). Then NaBH<sub>4</sub> (3.0 equiv) was added portion wise. The reaction mixture was stirred at room temperature until the reaction was completed based on TLC monitoring. Upon completion of the reaction, the mixture was acidified using 5.0 M HCl until pH 6. The solvent was then evaporated using rotary evaporator. The residue was dissolved in brine solution and the crude material was extracted using EtOAc. The organic layer was dried using anhydrous Na<sub>2</sub>SO<sub>4</sub>, filtered, and the solvent was evaporated. Purification by chromatography on SiO<sub>2</sub> (25:75, hexanes/EtOAc) afforded **S1** (0.17 g, 1.0 mmol, 100%). Spectral data are consistent with those reported in the literature.<sup>93</sup>

$R_f$  (EtOAc/hexanes 3:2): 0.18;

<sup>1</sup>H NMR (CDCl<sub>3</sub>, 400 MHz):  $\delta$  7.30 (d,  $J$  = 8.4 Hz, 2H), 6.90 (d,  $J$  = 8.8 Hz, 2H), 4.83–4.74 (m, 1H), 3.81 (s, 3H), 3.76–3.63 (m, 2H), 2.51 (br s, 1H), 2.12 (br s, 1H).



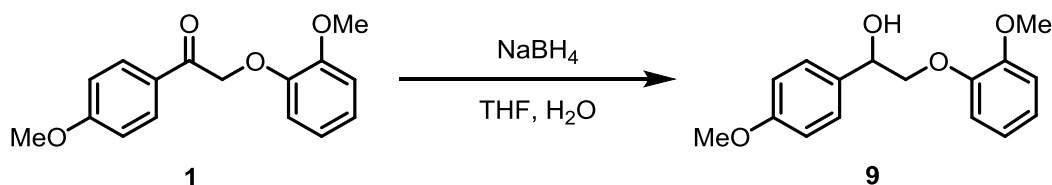
<sup>92</sup> *Org. Biomol. Chem.* **2012**, *10*, 506.

<sup>93</sup> *J. Am. Chem. Soc.* **2010**, *132*, 14409.

**2-(benzyloxy)-1-phenylethanol (S2):** Substrate **S2** was prepared according to a literature procedure.<sup>94</sup> To a solution of 2-(benzyloxy)acetaldehyde (**4**) (20 mmol) in THF (40 mL) was added PhMgBr 3.0 M in Et<sub>2</sub>O (22 mmol, 1.1 eq.) at 0 °C. After the mixture was stirred for 10 min at 0 °C, the mixture was warmed up to room temperature and was stirred for another 2 hours. The mixture was carefully quenched with saturated aq. NH<sub>4</sub>Cl at 0 °C, and the organic layer was separated and aqueous layer was extracted with Et<sub>2</sub>O twice. The combined organic layer was washed with brine and dried over anhydrous Na<sub>2</sub>SO<sub>4</sub>. The solvent was removed under reduced pressure and the residue was purified by chromatography on SiO<sub>2</sub> (90:10, hexanes/EtOAc) to afford **S2** (3.9 g, 17 mmol, 85%) as a clear and colorless oil. Spectral data are consistent with those reported in the literature.<sup>94</sup>

$R_f$ (EtOAc/hexanes 1:3): 0.48;

<sup>1</sup>H NMR (CDCl<sub>3</sub>, 400 MHz):  $\delta$  7.40–7.29 (m, 10H), 4.98 (dd,  $J = 9.0, 3.3$  Hz, 1H), 4.63 (d,  $J = 12.0$  Hz, 1H), 4.59 (d,  $J = 12.0$  Hz, 1H), 3.67 (dd,  $J = 9.6, 3.3$  Hz, 1H), 3.54 (dd,  $J = 9.6, 9.0$  Hz, 1H), 2.87 (br s, 1H).



**2-(2-methoxyphenoxy)-1-(4-methoxyphenyl)ethanol (9):** Substrate **9** was prepared according to a literature procedure.<sup>79</sup> A round bottom flask was charged with **1** (1.7 g, 6.2 mmol), THF (28 mL), and water (7 mL). Sodium borohydride (0.47 g, 12.4 mmol) was added portion-wise to maintain a gentle evolution of gas over 5 minutes, after which the reaction mixture was stirred for 3 h at room temperature. The reaction was quenched with saturated aqueous NH<sub>4</sub>Cl (50 mL)

<sup>94</sup> *J. Am. Chem. Soc.* **2012**, *134*, 10329.

and then the reaction mixture was diluted with water (50 mL). The aqueous portion was extracted with Et<sub>2</sub>O (3 x 50 mL). The combined organic extracts were washed twice with brine, dried over MgSO<sub>4</sub>, filtered, and concentrated in vacuo. Purification by chromatography on SiO<sub>2</sub> (75:25, hexanes/EtOAc) afforded **9** (1.4 g, 5.0 mmol, 80%) as a clear and colorless oil.

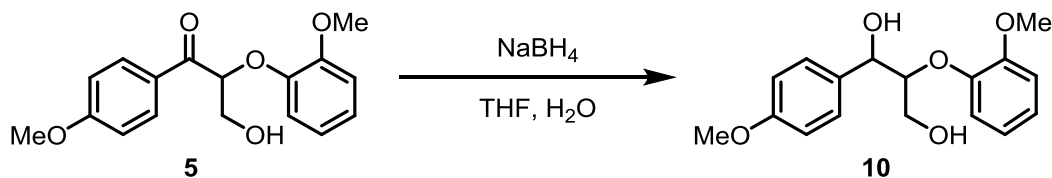
*R<sub>f</sub>*(EtOAc/hexanes 1:1): 0.43;

IR (neat): 3454, 2933, 2836, 1612, 1593, 1505, 1455, 1250, 1177, 1124, 1027, 832, 745 cm<sup>-1</sup>;

<sup>1</sup>H NMR (CDCl<sub>3</sub>, 400 MHz): δ 7.37 (d, *J* = 9.0 Hz, 2H) 7.03–6.88 (m, 6H), 5.06 (d, *J* = 9.0 Hz, 1H), 4.16 (dd, *J* = 10, 2.8 Hz, 1H), 4.01–3.93 (m, 1H), 3.90 (s, 3H), 3.82 (s, 3H), 3.38 (br s, 1H);

<sup>13</sup>C NMR (CDCl<sub>3</sub>, 175 MHz): δ 159.3, 150.0, 148.0, 131.7, 127.5, 122.4, 121.0, 115.8, 113.8, 111.9, 76.1, 71.9, 55.8, 55.2;

HRMS (ESI) *m/z* calculated for C<sub>16</sub>H<sub>18</sub>O<sub>4</sub><sup>+</sup> ([M+H]<sup>+</sup>) 292.1543, found 292.1537.



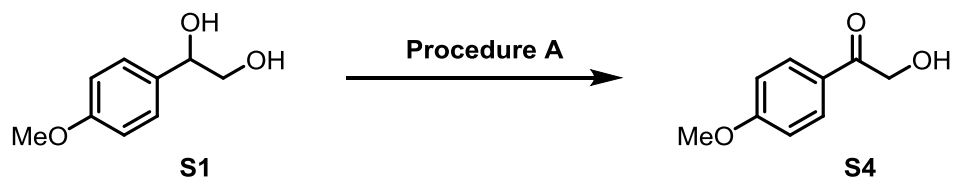
**2-(2-methoxyphenoxy)-1-(4-methoxyphenyl)propane-1,3-diol (10)**: Substrate **10** was prepared according to a literature procedure.<sup>87</sup> Substrate **5** (1.1 g, 3.5 mmol) was dissolved in the mixture of THF:H<sub>2</sub>O (5:1) (25 mL), and sodium borohydride (0.26 g, 7.0 mmol) was added portion-wise to maintain a gentle evolution of gas. Then, the mixture was stirred for 6 h at room temperature. The reaction mixture was quenched with saturated aqueous NH<sub>4</sub>Cl (50 mL) and diluted with 30 mL water. The aqueous portion was extracted with ethyl acetate (3 × 30 mL). The organic portions were combined, dried over MgSO<sub>4</sub>, filtered and concentrated in vacuo. Purification by chromatography on SiO<sub>2</sub> (40:60, hexanes/EtOAc) afforded **10** as a mixture of diastereomers



(0.75: 1) and a thick colorless oil (0.80 g, 2.6 mmol, 75%). Spectral data are consistent with those reported in the literature.<sup>86</sup>

$R_f$ (EtOAc/hexanes 3:2): 0.31;

$^1\text{H}$  NMR ( $\text{CDCl}_3$ , 400 MHz):  $\delta$  7.38 (d,  $J = 7.8$  Hz, 2H, major diastereomer), 7.32 (d,  $J = 7.4$  Hz, 2H, minor diastereomer), 7.14 (d,  $J = 7.6$  Hz, 1H, major diastereomer), 7.11–7.04 (m, 1H, both diastereomers), 7.01–6.87 (m, 4H, major diastereomer, 5H, minor diastereomer), 5.04–4.98 (m, 1H, both diastereomers), 4.20–4.14 (m, 1H, minor diastereomer), 4.07–4.01 (m, 1H, major diastereomer), 3.96–3.87 (m, 1H, minor diastereomer), 3.93 (s, 3H, major diastereomer), 3.90 (s, 3H, minor diastereomer), 3.82 (s, 3H, both diastereomers), 3.70–3.59 (m, 2H, major diastereomer, 1H, minor diastereomer), 3.51–3.39 (m, 1H, both diastereomers), 2.78–2.67 (m, 1H, both diastereomers).

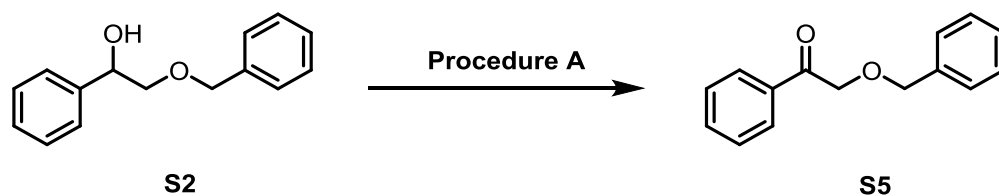


**2-hydroxy-1-(4-methoxyphenyl)ethanone (S4):** According to General Procedure A, S1 (0.17 g, 1.0 mmol), [4-AcNH-TEMPO]BF<sub>4</sub> (0.32 g, 1.05 mmol), and silica (0.17 g) in DCM (10 mL) afforded S4 (0.16 g, 95%) after purification by chromatography on SiO<sub>2</sub> (60:40, hexanes/EtOAc) as a colorless solid. Spectral data are consistent with those reported in the literature.<sup>95</sup>

$R_f$ (EtOAc/hexanes 1:3): 0.13;

$^1\text{H}$  NMR ( $\text{CDCl}_3$ , 400 MHz):  $\delta$  7.92 (d,  $J = 8.4$  Hz, 2H), 6.98 (d,  $J = 8.4$  Hz, 2H), 4.83 (s, 2H), 3.90 (s, 3H), 3.57 (br s, 1H).

<sup>95</sup> *J. Organomet. Chem.* **2009**, 694, 3452.

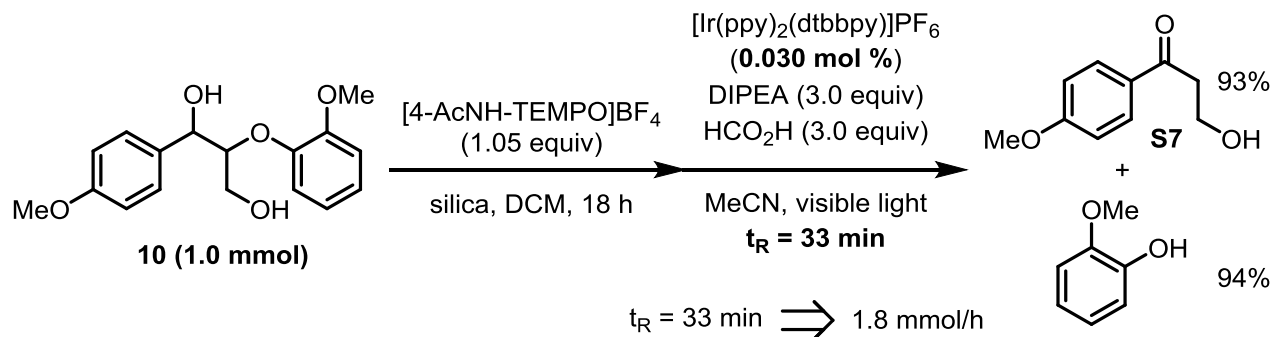


**2-(benzyloxy)-1-phenylethanone (S5):** According to General Procedure A, **S2** (0.23 g, 1.0 mmol), [4-AcNH-TEMPO]BF<sub>4</sub> (0.32 g, 1.05 mmol), and silica (0.23 g) in DCM (10 mL) afforded **S5** (0.21 g, 95%) after purification by chromatography on SiO<sub>2</sub> (75:25, hexanes/EtOAc) as a colorless solid. Spectral data are consistent with those reported in the literature.<sup>96</sup>

*R<sub>f</sub>*(EtOAc/hexanes 3:2): 0.77;

<sup>1</sup>H NMR (CDCl<sub>3</sub>, 400 MHz): δ 7.93 (d, *J* = 7.6 Hz, 2H), 7.59 (t, *J* = 7.6 Hz, 1H), 7.47 (t, *J* = 8.0 Hz, 2H), 7.43–7.27 (m, 5H), 4.77 (s, 2H), 4.71 (s, 2H).

#### Batch to Flow Reaction:

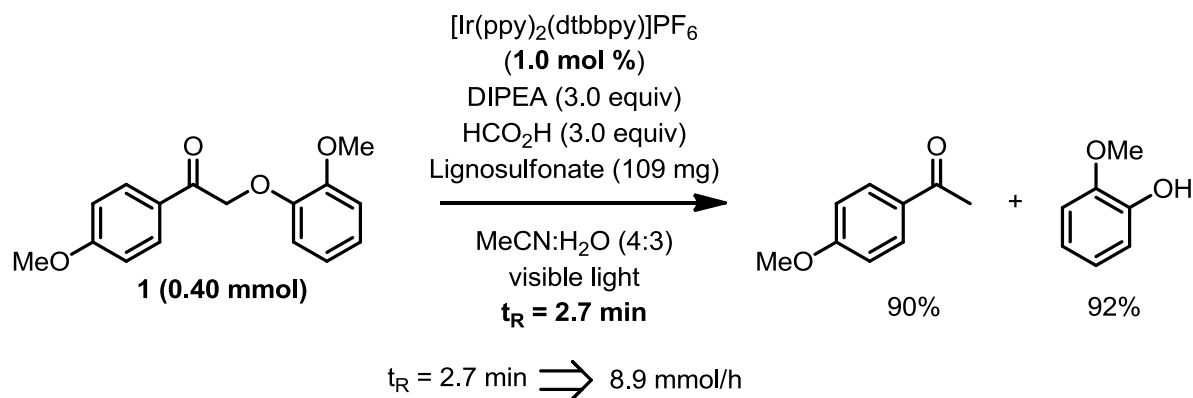


According to General Procedure A, **10** (0.30 g, 1.0 mmol), [4-AcNH-TEMPO]BF<sub>4</sub> (0.32 g, 1.05 mmol), and silica (0.30 g) in DCM (10 mL) afforded **5**, which was then mixed with DIPEA (0.52 mL, 0.39 g, 3.0 mmol), formic acid (0.11 mL, 0.14 g, 3.0 mmol) and [Ir(ppy)<sub>2</sub>(dtbbpy)]PF<sub>6</sub> (0.27 mg, 0.30 μmol) in MeCN (5.0 mL) and submitted to the photoreactor at a flow rate of 0.41

<sup>96</sup> *J. Org. Chem.* **2011**, *76*, 3576.

$\mu\text{L}/\text{min}$  ( $t_{\text{R}} = 33 \text{ min}$ ) to afford **S7** (0.17 g, 0.93 mmol, 93%) and guaiacol (0.12 g, 0.94 mmol, 94%) after purification by chromatography on  $\text{SiO}_2$ .

### Reductive C–O Bond Cleavage of Substrate **1** in the Presence of Lignosulfonates:



Lignosulfonic acid sodium salt (lignosulfonate) is dissolved by a mixture of MeCN (4.0 mL) and H<sub>2</sub>O (3.0 mL) in a 5 dram vial. The following components are then added: Substrate **1** (0.11 g, 0.40 mmol), DIPEA (0.21 mL, 0.16 g, 1.2 mmol), formic acid (44  $\mu\text{L}$ , 56 mg, 1.2 mmol) and  $[\text{Ir}(\text{ppy})_2(\text{dtbbpy})]\text{PF}_6$  (3.7 mg, 4.0  $\mu\text{mol}$ ). The reaction mixture is then submitted to the photoreactor at a flow rate of 0.50 mL/min ( $t_{\text{R}} = 2.7 \text{ min}$ ) to afford 4'-methoxyacetophenone (54 mg, 0.36 mmol, 90%) and guaiacol (47 mg, 0.37 mmol, 92%) after purification by chromatography on  $\text{SiO}_2$ .

Below is a photo of the reaction mixture.



## Chapter 5: Conclusion and Future Prospects

The advancement of visible light-mediated photoredox catalysis over the past six years has been showcased via a myriad of synthetic methods as well as applications to total syntheses. The diversity of these synthetic methods relies upon the ability of photoredox catalysts such as  $[\text{Ru}(\text{bpy})_3]\text{Cl}_2$ ,  $[\text{Ir}(\text{ppy})_2(\text{dtbbpy})]\text{PF}_6$ ,  $[\text{Ir}\{\text{dF}(\text{CF}_3)\text{ppy}\}_2(\text{dtbbpy})]\text{PF}_6$ , and *fac*- $\text{Ir}(\text{ppy})_3$  to undergo several productive quenching pathways from the excited state (*i.e.* reductive quenching, oxidative quenching, and energy transfer). This versatility has allowed for the development of a series of methods such as reductive radical dehalogenation,  $\alpha$ -amino functionalization, olefin/alkyne difunctionalization, and cycloaddition reactions. In addition, these photocatalysts possess a series of advantages uncommon to most organometallic complexes as well as reagents commonly associated with radical chemistry including stability in the presence of moisture and air, reactivity at room temperature, and accessibility via commercial vendors or simple synthetic routes.

Several general conclusions can be reached based upon my work and others concerning visible light-mediated photoredox catalysis: 1) The reaction conditions are typically mild; 2) Reactions that are not oxygen-dependent can be performed without degassing, but degassing typically provides lower reaction times and higher isolated yields; 3) Photocatalysts have been shown to work cooperatively with organocatalysts and organometallic complexes; 4) Redox potentials, excited state lifetimes, and maximum absorbance wavelengths are properties that have shown to correlate well with reactivity.

Undoubtedly, the discovery and development of new methods utilizing visible light-mediated photoredox catalysis will continue to grow in the next decade, particularly due to the ability of photocatalysts to be merged with other types of catalysis. However, an in-depth study of how factors such as light intensity, solvent choice, Lewis acid or Brønsted acid additives, etc... affect the reaction outcome and/or reaction kinetics has not been performed. These studies will be necessary to understand how to better improve existing methods and develop new methods. More importantly, these studies may provide answers to many of the existing anomalous results that have been observed by practitioners in the field of photoredox catalysis. One example of an observation that could possibly be explained with more rigorous mechanistic studies involves the specific role of water and lithium bromide or lithium tetrafluoroborate in the ATRA reaction. Another observation pertains to the unexpected partial hydrodehalogenation of unactivated alkyl and aryl bromides utilizing catalysts that possess reduction potentials more than 1.0 V less than the reduction potential of the substrate.

Last, but not least, the development of new photoredox catalysts specifically designed for organic transformations performed in solution is an underdeveloped area of study. Preliminary results in the Stephenson group indicate that particular reactions are prone to a high level of catalyst deactivation via radical functionalization and ligand dissociation. The design of catalysts that could inhibit these side reactions would generate a new class of robust photoredox catalysts that would surely improve many existing methods.

## BIBLIOGRAPHY

- 
- <sup>1</sup> Juris, A.; Balzani, V.; Barigelletti, F.; Campagna, S.; Belser, P.; Von Zelewsky, V. *Coord. Chem. Rev.* **1988**, *84*, 85.
- <sup>2</sup> Slinker, J. D.; Gorodetsky, A. A.; Lowry, M. S.; Wang, J.; Parker, S.; Rohl, R.; Bernhard, S.; Malliaras, G. G. *J. Am. Chem. Soc.* **2004**, *126*, 2763.
- <sup>3</sup> Lowry, M. S.; Goldsmith, J. I.; Slinker, J. D.; Rohl, R.; Pascal, R. A., Jr.; Malliaras, G. G.; Bernhard, S. *Chem. Mater.* **2005**, *17*, 5712.
- <sup>4</sup> Dedeian, K.; Djurovich, P. I.; Garces, F. O.; Carlson, G.; Watts, R. J. *Inorg. Chem.* **1991**, *30*, 1685.
- <sup>5</sup> Prier, C. K.; Rankic, D. A.; MacMillan, D. W. C. *Chem. Rev.* **2013**, *113*, 5322.
- <sup>6</sup> Burstall, F. H. *J. Chem. Soc. (Resumed)*. **1936**, 173.
- <sup>7</sup> Juris, A.; Balzani, V.; Belser, P.; von Zelewsky, A. *Helv. Chim. Acta* **1981**, *64*, 2175.
- <sup>8</sup> (a) Kalyanasundaram, K. *Coord. Chem. Rev.* **1982**, *46*, 159; (b) Kalyanasundaram, K.; Grätzel, M. *Coord. Chem. Rev.* **1998**, *177*, 347; (c) Balzani, V.; Bergamini, G.; Campagna, S.; Puntoriero, F. In *Photochemistry and Photophysics of Coordination Compounds I*; Balzani, V., Campagna, S., Eds.; Springer Berlin Heidelberg: **2007**; Vol. 280, p 1-36; (d) Campagna, S.; Puntoriero, F.; Nastasi, F.; Bergamini, G.; Balzani, V. *Photochemistry and Photophysics of Coordination Compounds I*; Balzani, V., Campagna, S., Eds.; Springer Berlin Heidelberg: **2007**, 280, 117-214; (e) Flamigni, L.; Barbieri, A.; Sabatini, C.; Ventura, B.; Barigelletti, F. In

---

*Photochemistry and Photophysics of Coordination Compounds II*; Balzani, V., Campagna, S., Eds.; Springer Berlin Heidelberg: **2007**; Vol. 281, p 143-203.

<sup>9</sup> Meyer, T. J. *Acc. Chem. Res.* **1989**, *22*, 163; (b) Bard, A. J.; Fox, M. A. *Acc. Chem. Res.* **1995**, *28*, 141.

<sup>10</sup> O'Regan, B.; Gratzel, M. *Nature*. **1991**, *353*, 737.

<sup>11</sup> Gray, H. B.; Maverick, A. W. *Science*. **1981**, *214*, 1201.

<sup>12</sup> For Ru(bpy)<sub>3</sub>Cl<sub>2</sub>,  $\tau_0$  ranges between 575 - 1000 ns in various organic and aqueous solvents, see: Ding, Z.; Wellington, R. G.; Brevet, P. F.; Girault, H. H. *J. Phys. Chem.* **1996**, *100*, 10658.

<sup>13</sup> Demas, J. N.; Taylor, D. G. *Inorg. Chem.* **1979**, *18*, 3177.

<sup>14</sup> For selected examples of energy transfer from photoredox catalyst excited states, see: (a) Wrighton, M.; Markham, J. *J. Phys. Chem.* **1973**, *77*, 3042. (b) Demas, J. N.; Harris, E. W.; McBride, R. P. *J. Am. Chem. Soc.* **1977**, *99*, 3547.

<sup>15</sup> Tucker, J. W.; Stephenson, C. R. J. *J. Org. Chem.* **2012**, *77*, 1617.

<sup>16</sup> Flynn, C. M. Jr.; Demas, J. N. *J. Am. Chem. Soc.* **1974**, *96*, 1959.

<sup>17</sup> King, K. A., Spellane, P. J., Watts, R. J. *J. Am. Chem. Soc.* **1985**, *107*, 1431.

<sup>18</sup> Balzani, V.; Bolletta, F.; Gandolfi, M. T.; Maestri, M. *Top. Curr. Chem.* **1978**, *75*, 1.

<sup>19</sup> (a) Shih, H. W., Vander Wal, M. N., Grange, R. L., MacMillan, D. W. C. *J. Am. Chem. Soc.* **2010**, *132*, 13600. (b) McNally, A., Prier, C. K., MacMillan D. W. C. *Science* **2011**, *334*, 1114. (c) Ju, X.; Liang, Y.; Jia, P.; Li, W.; Yu, W. *Org. Biomol. Chem.* **2012**, *10*, 498. (d) Nguyen, J. D.; D'Amato, E. M.; Narayanam, J. M. R.; Stephenson, C. R. J. *Nature Chem.* **2012**, *4*, 854. (e) Yasu, Y.; Koike T.; Akita, M. *Angew. Chem., Int. Ed.* **2012**, *51*, 9567. (f) Nguyen, J. D.; Reiss, B.; Dai, C., Stephenson, C R. J. *Chem. Commun.* **2013**, *49*, 4352.

- 
- <sup>20</sup> Cano-Yelo, H.; Deronzier, A. *J. Chem. Soc., Perkin Trans. 2* **1984**, 1093-1098; (b) Cano-Yelo, H.; Deronzier, A. *Tetrahedron Lett.* **1984**, 25, 5517.
- <sup>21</sup> Okada, K.; Okamoto, K.; Morita, N.; Okubo, K.; Oda, M. *J. Am. Chem. Soc.* **1991**, 113, 9401.
- <sup>22</sup> Van Bergen, T. J.; Hedstrand, D. M.; Kruizinga, W. H.; Kellogg, R. M. *J. Org. Chem.* **1979**, 44, 4953.
- <sup>23</sup> Fukuzumi, S.; Mochizuki, S.; Tanaka, T. *J. Phy. Chem.* **1990**, 94, 722.
- <sup>24</sup> Nicewicz, D. A.; MacMillan, D. W. C. *Science* **2008**, 322, 77.
- <sup>25</sup> Ischay, M. A.; Anzovino, M. E.; Du, J.; Yoon, T. P. *J. Am. Chem. Soc.* **2008**, 130, 12886.
- <sup>26</sup> (a) Xi, Y. M.; Yi, H.; Lei, A. W. *Org. Biomol. Chem.* **2013**, 11, 2387; (b) Prier, C. K.; Rankic, D. A.; MacMillan, D. W. *Chem. Rev.* **2013**, 113, 5322; (c) Narayanam, J. M.; Stephenson, C. R. *Chem. Soc. Rev.* **2011**, 40, 102; (d) Teplý, F. *Collect. Czech. Chem. Commun.* **2011**, 76, 859.
- <sup>27</sup> (a) Yoon, T. P.; Ischay, M. A.; Du, J. *Nat Chem* **2010**, 2, 527; (b) Zeitler, K. *Angew. Chem., Int. Ed* **2009**, 48, 9785.
- <sup>28</sup> Hironaka, K.; Fukuzumi, S.; Tanaka, T. *J. Chem. Soc., Perkin Trans. 2* **1984**, 1705.
- <sup>29</sup> Kern, J.-M.; Sauvage, J.-P. *J. Chem. Soc., Chem. Commun.* **1987**, 546.
- <sup>30</sup> Narayanam, J. M. R.; Tucker, J. W.; Stephenson, C. R. J. *J. Am. Chem. Soc.* **2009**, 131, 8756.
- <sup>31</sup> Tucker, J. W.; Narayanam, J. M. R.; Krabbe, S. W.; Stephenson, C. R. J. *Org. Lett.* **2009**, 12, 368.
- <sup>32</sup> Snider, B. B. *Chem. Rev.* **1996**, 96, 339.
- <sup>33</sup> (a) Magolan, J.; Kerr, M. A. *Org. Lett.* **2006**, 8, 4561; (b) Magolan, J.; Carson, C. A.; Kerr, M. A. *Org. Lett.* **2008**, 10, 1437.
- <sup>34</sup> Tucker, J. W.; Nguyen, J. D.; Narayanam, J. M. R.; Krabbe, S. W.; Stephenson, C. R. J. *Chem. Commun.* **2010**, 46, 4985.



- 
- <sup>35</sup> Furst, L.; Matsuura, B. S.; Narayanam, J. M. R.; Tucker, J. W.; Stephenson, C. R. J. *Org. Lett.* **2010**, *12*, 3104.
- <sup>36</sup> Condie, A. G.; González-Gómez, J. C.; Stephenson, C. R. J. *J. Am. Chem. Soc.* **2010**, *132*, 1464.
- <sup>37</sup> Li, Z.; Li, C.-J. *J. Am. Chem. Soc.* **2005**, *127*, 3672.
- <sup>38</sup> (a) Freeman, D. B.; Furst, L.; Condie, A. G.; Stephenson, C. R. J. *Org. Lett.* **2011**, *14*, 94; (b) Bergonzini, G.; Schindler, C.; Wallentin, C.-J.; Jacobsen, E. N.; Stephenson, C. *Chem. Sci.* **2013**, *5*.
- <sup>39</sup> Hu, J.; Wang, J.; Nguyen, T. H.; Zheng, N. *Beilstein J. Org. Chem.* **2013**, *9*, 1977.
- <sup>40</sup> Ruiz Espelt, L.; Wiensch, E. M.; Yoon, T. P. *J. Org. Chem.* **2013**, *78*, 4107.
- <sup>41</sup> Yoon, T. P. *ACS Catal* **2013**, *3*, 895.
- <sup>42</sup> Lin, S.; Ischay, M. A.; Fry, C. G.; Yoon, T. P. *J. Am. Chem. Soc.* **2011**, *133*, 19350.
- <sup>43</sup> Crutchley, R. J.; Lever, A. B. P. *J. Am. Chem. Soc.* **1980**, *102*, 7128; (b) Haga, M.; Dodsworth, E. S.; Eryavec, G.; Seymour, P.; Lever, A. B. P. *Inorg. Chem.* **1985**, *24*, 1901.
- <sup>44</sup> Maity, S.; Zhu, M.; Shinabery, R. S.; Zheng, N. *Angew. Chem., Int. Ed.* **2012**, *51*, 222.
- <sup>45</sup> Furst, L.; Narayanam, J. M. R.; Stephenson, C. R. J. *Angew. Chem., Int. Ed.* **2011**, *50*, 9655.
- <sup>46</sup> Schnermann, M. J.; Overman, L. E. *Angew. Chem., Int. Ed.* **2012**, *51*, 9576.
- <sup>47</sup> Andrews, R. S.; Becker, J. J.; Gagné, M. R. *Angew. Chem., Int. Ed.* **2010**, *49*, 7274.
- <sup>48</sup> Lackner, G. L.; Quasdorf, K. W.; Overman, L. E. *J. Am. Chem. Soc.* **2013**, *135*, 15342.
- <sup>49</sup> Nguyen, J. D.; Tucker, J. W.; Konieczynska, M. D.; Stephenson, C. R. *J. Am. Chem. Soc.* **2011**, *133*, 4160.
- <sup>50</sup> Wallentin, C.-J.; Nguyen, J. D.; Finkbeiner, P.; Stephenson, C. R. J. *J. Am. Chem. Soc.* **2012**, *134*, 8875.

- 
- <sup>51</sup> Yasu, Y.; Koike, T.; Akita, M. *Angew. Chem., Int. Ed.* **2012**, *51*, 9567.
- <sup>52</sup> Calculated from the reported value in Ref 51 (−0.75 V vs. Cp<sub>2</sub>Fe in MeCN).
- <sup>53</sup> Nagib, D. A.; MacMillan, D. W. C. *Nature* **2011**, *480*, 224.
- <sup>54</sup> Skarda, V.; Cook, M. J.; Lewis, A. P.; McAuliffe, G. S. G.; Thomson, A. J.; Robbins, D. J. J. *Chem. Soc., Perkin Trans. 2.* **1984**, 1309.
- <sup>55</sup> Tamayo, A. B.; Alleyne, B. D.; Djurovich, P. I.; Lamansky, S.; Tsyba, I.; Ho, N. N.; Bau, R.; Thompson, M. E. *J. Am. Chem. Soc.* **2003**, *125*, 7377.
- <sup>56</sup> Excited state potentials were calculated from the reported ground state values.
- <sup>57</sup> Tucker, J. W.; Narayanam, J. M.; Shah, P. S.; Stephenson, C. R. *Chem. Commun.* **2011**, *47*, 5040.
- <sup>58</sup> Nguyen, J. D.; D'Amato, E. M.; Narayanam, J. M. R.; Stephenson, C. R. J. *Nature Chem.* **2012**, *4*, 854.
- <sup>59</sup> (a) Kim, H.; Lee, C. *Angew. Chem., Int. Ed.* **2012**, *51*, 12303; (b) Garnier, J.; Kennedy, A. R.; Berlouis, L. E. A.; Turner, A. T.; Murphy, J. A. *Beilstein J. Org. Chem.* **2010**, *6*, 73.
- <sup>60</sup> Tucker, J. W.; Zhang, Y.; Jamison, T. F.; Stephenson, C. R. J. *Angew. Chem., Int. Ed.* **2012**, *51*, 4144.
- <sup>61</sup> Bou-Hamdan, F. R.; Seeberger, P. H. *Chem. Sci.* **2012**, *3*, 1612.
- <sup>62</sup> Andrews, R. S.; Becker, J. J.; Gagné, M. R. *Angew. Chem., Int. Ed.* **2012**, *51*, 4140.
- <sup>63</sup> Knowles, J. P.; Elliott, L. D.; Booker-Milburn, K. I. *Beilstein J. Org. Chem.* **2012**, *8*, 2025.
- <sup>64</sup> Dai, C.; Narayanam, J. M. R.; Stephenson, C. R. J. *Nat Chem.* **2011**, *3*, 140.
- <sup>65</sup> Nguyen, J. D.; Reiss, B.; Dai, C.; Stephenson, C. R. J. *Chem. Commun.* **2013**, *49*, 4352.
- <sup>66</sup> Garegg, P. J.; Samuelsson, B. *J. Chem. Soc., Chem. Commun.* **1979**, 978.
- <sup>67</sup> Fors, B. P.; Hawker, C. J. *Angew. Chem., Int. Ed.* **2012**, *51*, 8850.

- 
- <sup>68</sup> Leibfarth, F. A.; Mattson, K. M.; Fors, B. P.; Collins, H. A.; Hawker, C. J. *Angew. Chem., Int. Ed.* **2013**, *52*, 199.
- <sup>69</sup> Balzani, V. *Electron Transfer in Chemistry*; Wiley-VCH: Weinheim, 2001; Vol. 1.
- <sup>70</sup> (a) Marsden, S. P.; Depew, K. M.; Danishefsky, S. J. *J. Am. Chem. Soc.* **1994**, *116*, 11143; (b) J. Kim, J. A. Ashenhust and M. Movassaghi, *Science* **2009**, *324*, 238.
- <sup>71</sup> For selected reviews on cascade reactions mediated by free radicals, see: (a) Albert, M.; Fensterbank, L.; Lacôte, E.; Malacria, M. *Top. Curr. Chem.* **2006**, *264*, 1 (b) McCarroll, A. J.; Walton, J. C. *Angew Chem. Int. Ed.* **2001**, *40*, 2224.
- <sup>72</sup> Curran, D. P.; Rakiewicz, D. M. *J. Am. Chem. Soc.* **1985**, *107*, 1448.
- <sup>73</sup> For examples of the hazards and reactivity of other radical initiation systems, see: (a) Molander, G. A. *Org. React.* **1994**, *46*, 211; (b) Khattab, M. A.; Elgamal, M. A.; El-Batouti, M. *Fire Mater.* **1996**, *20*, 253; (c) O'Mahony, G. *Synlett*, **2004**, 572.
- <sup>74</sup> Alonso, F., Beletskaya, I. P.; Yus, M. *Chem. Rev.* **2002**, *102*, 4009.
- <sup>75</sup> Bailey, W. F.; Patricia, J. J. *J. Organomet. Chem.* **1988**, *352*, 1.
- <sup>76</sup> Knochel, P., Dohle, W., Gommermann, N., Kneisel, F. F., Kopp, F., Korn, T., Sapountzis, I.; Ahn Vu, V. *Angew. Chem., Int. Ed.* **2003**, *42*, 4302.
- <sup>77</sup> Yoon, N. M. *Pure Appl. Chem.* **1996**, *68*, 843.
- <sup>78</sup> Chen, J.; Zhang, Y.; Yang, L.; Zhang, X.; Liu, J.; Li, L.; Zhang, H. *Tetrahedron* **2007**, *63*, 4266.
- <sup>79</sup> Curran, D. P.; Rakiewicz, D. M. *J. Am. Chem. Soc.* **1985**, *107*, 1448.
- <sup>80</sup> Depew, K. M.; Marsden, S. P.; Zatorska, D.; Zatorski, A.; Bornmann, W. G.; Danishefsky, S. *J. Am. Chem. Soc.* **1999**, *121*, 11953.
- <sup>81</sup> Kim, J.; Ashenhust, J. A.; Movassaghi, M. *Science* **2009**, *324*, 238.

- 
- <sup>82</sup> Neumann, W. P. *Synthesis* **1987**, 665.
- <sup>83</sup> Sanchez, J. & Myers, T. N. *Kirk-Othmer Encyclopedia of Chemical Technology* 4th edn, 431-460 (John Wiley & Sons, 2000).
- <sup>84</sup> Krief, A.; Laval, A. *Chem. Rev.* **1999**, 99, 745.
- <sup>85</sup> Miura, K.; Ichinose, Y.; Nozaki, K.; Fugami, K.; Oshima, K.; Utimoto, K. *Bull. Chem. Soc. Jpn.* **1989**, 62, 143.
- <sup>86</sup> Medeiros, M. R.; Schacherer, L. N.; Spiegel, D. A.; Wood, J. L. *Org. Lett.* **2007**, 9, 4427.
- <sup>87</sup> Murphy, J. A.; Khan, T. A.; Zhou, S. Z.; Thomson, D. W.; Mahesh, M. *Angew. Chem., Int. Ed.* **2005**, 44, 1356.
- <sup>88</sup> Cahard, E.; Schoenebeck, F.; Garnier, J.; Cutulic, S. P. Y.; Zhou, S.; Murphy, J. A. *Angew. Chem., Int. Ed.* **2012**, 51, 3673.
- <sup>89</sup> Weiss, M. E.; Kreis, L. M.; Lauber, A.; Carreira, E. M. *Angew. Chem., Int. Ed.* **2011**, 50, 11125.
- <sup>90</sup> Ueng, S. H.; Fensterbank, L.; Lacôte, E.; Malacria, M.; Curran, D. P. *Org. Biomol. Chem.* **2011**, 9, 3415.
- <sup>91</sup> Spiegel, D. A.; Wiberg, K. B.; Schacherer, L. N.; Medeiros, M. R.; Wood, J. L. *J. Am. Chem. Soc.* **2005**, 127, 12513.
- <sup>92</sup> Gansäuer, A.; Behlendorf, M.; Cangönül, A.; Kube, C.; Cuerva, J. M.; Friedrich, J.; van Gastel, M. *Angew. Chem., Int. Ed.* **2012**, 51, 3266.
- <sup>93</sup> Neumann, M.; Földner, S.; Burkhard, K.; Zeitler, K. *Angew. Chem., Int. Ed.* **2011**, 50, 951.
- <sup>94</sup> Nagib, D. A.; Scott, M. E.; MacMillan, D. W. C. *J. Am. Chem. Soc.* **2009**, 131, 10875.
- <sup>95</sup> Tucker, J. W.; Stephenson, C. R. J. *Org. Lett.* **2011**, 13, 5468.

- 
- <sup>96</sup> Hill, H. A. O.; Pratt, J. M.; O'Riordan, M. P.; Williams, F. R.; Williams, R. J. P. *J. Chem. Soc. A* **1971**, 1859.
- <sup>97</sup> Rondinini, S.; Romana, P.; Paolo, M.; Guido, S. *Electrochimica Acta*. **2001**, *46*, 3245.
- <sup>98</sup> Fry, A. J.; Krieger, R. L. *J. Org. Chem.* **1976**, *41*, 54.
- <sup>99</sup> Pause, L.; Robert, M.; Savéant, J. *J. Am. Chem. Soc.* **1999**, *121*, 7158.
- <sup>100</sup> McNally, A.; Prier, C. K.; MacMillan D. W. C. *Science* **2011**, *334*, 1114.
- <sup>101</sup> (a) Larock, R. C. *Comprehensive Organic Transformations*, 2nd ed.; Wiley-VCH: New York, 1999; pp 49; (b) Veith, G. E.; Beckmann, E.; Burke, B. J.; Boyer, A.; Maslen, S. L.; Ley, S. V. *Angew. Chem. Int. Ed.* **2007**, *46*, 7629; (c) Palacios, D. S.; Anderson, T. M.; Burke, M. D. *J. Am. Chem. Soc.* **2007**, *129*, 13804.
- <sup>102</sup> *Handbook of Chemistry and Physics*, 81st Edition CRC Press.
- <sup>103</sup> (a) Barton, D. H. R.; McCombie, S.W. *J. Chem. Soc. Perkin Trans.1* **1975**, 1574; (b) Crich, D.; Quintero, L. *Chem. Rev.* **1989**, *89*, 1413; (c) Clive, D. L. J.; Wang, J. *J. Org. Chem.* **2002**, *67*, 1192.
- <sup>104</sup> (a) Saito, I.; Ikehira, H.; Kasatani, R.; Watanabe, M.; Matsuura, T. *J. Am. Chem. Soc.* **1986**, *108*, 3115; (b) Lam, K.; Markó, I. E. *Org. Lett.*, **2008**, *10*, 2919; (c) Lam, K.; Markó, I. E. *Chem. Commun.* **2009**, 95; (d) Lam, K.; Markó, I. E. *Org. Lett.* **2011**, *13*, 406.
- <sup>105</sup> (a) Zhang, L.; Koreeda, M. *J. Am. Chem. Soc.* **2004**, *126*, 13190; (b) Jordan, P. A.; Miller, S. *J. Angew. Chem. Int. Ed.* **2012**, *51*, 2907.
- <sup>106</sup> For examples of molecular editing of complex molecules, see: (a) Szpilman, A. M.; Carreira, E. M. *Angew. Chem. Int. Ed.* **2010**, *49*, 9592; (b) Palacios, D. S.; Dailey, I.; Siebert, D. M.; Wilcock, B. C.; Burke, M. D. *Proc. Natl. Acad. Sci. USA* **2011**, *108*, 6733.

---

<sup>107</sup> For recent examples of the applications of photoredox catalysis, see: (a) Nicewicz, D.; MacMillan, D. W. C. *Science* **2008**, *322*, 77; (b) Ischay, M. A.; Anzovino, M. E.; Du, J.; Yoon, T. P. *J. Am. Chem. Soc.* **2008**, *130*, 12886; (c) Andrews, R. S.; Becker, J. J.; Gagne, M. R. *Angew. Chem., Int. Ed.* **2010**, *49*, 7274; (d) Kalyani, D.; McMurtrey, K. B.; Neufeldt, S. R.; Sanford, M. S. *J. Am. Chem. Soc.* **2011**, *133*, 18566; (e) Hari, D. P.; König, B. *Org. Lett.* **2011**, *13*, 3852; (f) Nagib, D. A.; MacMillan, D. W. C. *Nature* **2011**, *480*, 224; (g) Ye, Y.; Sanford, M. S. *J. Am. Chem. Soc.* **2012**, *134*, 9034; (h) DiRocco, D. A.; Rovis, T. *J. Am. Chem. Soc.* **2012**, *134*, 8094-8097; (i) Wallentin, C. J.; Nguyen, J. D.; Finkbeiner, P.; Stephenson, C. R. J. *J. Am. Chem. Soc.* **2012**, *134*, 8875; (j) Fors, B. P.; Hawker, C. J. *Angew. Chem. Int. Ed.* **2012**, *51*, 8850; (k) Hari, D. P.; Schroll, P.; König, B. *J. Am. Chem. Soc.* **2012**, *134*, 2958; (l) Lu, Z.; Yoon, T. P. *Angew. Chem. Int. Ed.* **2012**, *51*, 10329; (m) Kohls, P.; Jadhav, D.; Pandey, G.; Reiser, O. *Org. Lett.* **2012**, *14*, 672; (n) Tarantino, K. T.; Liu, P.; Knowles, R. R. *J. Am. Chem. Soc.* **2013**, *135*, 10022; (o) Perkowski, A. J.; Nicewicz, D. A. *J. Am. Chem. Soc.* **2013**, *135*, 10334; (p) Guillaume, R.; McCallum, T.; Morin, M.; Gagosz, F.; Barriault, L. *Angew. Chem. Int. Ed.* **2013**, *52*, 13342; (q) Bergonzini, G.; Schindler, C. S.; Wallentin, C.-J.; Jacobsen, E. N.; Stephenson, C. R. J. *Chem. Sci.* **2014**, *5*, 112.

<sup>108</sup> For recent review of photoredox catalysis in synthetic applications, see: (a) Zietler, K. *Angew. Chem., Int. Ed.* **2009**, *48*, 9785; (b) Yoon, T. P.; Ischay, M. A.; Du, J. *Nature Chem.* **2010**, *2*, 527; (c) Narayanam, J. M. R.; Stephenson, C. R. J. *Chem. Soc. Rev.* **2011**, *40*, 102; (d) Teplý, F. *Collect. Czech. Chem. Commun.* **2011**, *76*, 859; (e) Tucker, J. W.; Stephenson, C. R. J. *J. Org. Chem.* **2012**, *77*, 1617; (f) Xuan, J.; Xiao, W.-J. *Angew. Chem. Int. Ed.* **2012**, *51*, 6828.

<sup>109</sup> Garegg, P. J.; Samuelsson, B. J. *J. Chem. Soc., Chem. Commun.* **1979**, 978.

- 
- <sup>110</sup> For examples, see: (a) Garegg, R. Johansson, P. J.; Ortega, C.; Samuelsson, B. J. *J. Chem. Soc. Perkin Trans. I* **1982**, 681; (b) Starr, J. T.; Koch, G.; Carreira, E. M. *J. Am. Chem. Soc.*, **2000**, *12*, 8793; (c) Fernandez, J. M. G.; Gabelle, A.; Defaye, J. *Carbohydr. Res.* **1994**, *265*, 249.
- <sup>111</sup> (a) Bou-Hamdan, F. R.; Seeberger, P. H. *Chem. Sci.* **2012**, *3*, 1612; (b) Andrews, R. S.; Becker, J. J.; Gagné, M. R. *Angew. Chem. Int. Ed.* **2012**, *51*, 4140; (c) Tucker, J. W.; Zhang, Y.; Jamison, T. F.; Stephenson, C. R. J. *Angew. Chem. Int. Ed.* **2012**, *51*, 4144; (d) Neumann, M.; Zeitler, K. *Org. Lett.* **2012**, *14*, 2658.
- <sup>112</sup> Kim, H.; Lee, C. *Angew. Chem. Int. Ed.* **2012**, *51*, 12303.
- <sup>113</sup> Barriault, L.; Revol, G.; McCallum, T.; Morin, M.; Gagozs *Angew Chem, Int. Ed.* **2013**, *52*, 13342.
- <sup>114</sup> Jiang, H.; Bak, J. R.; Lopez-Delgado, F. J.; Joergensen, K. A. *Green Chem.* **2013**, *15*, 3355.
- <sup>115</sup> Baugley, P. A.; Walton, J. C. *Angew. Chem., Int. Ed.* **1998**, *37*, 3072.
- <sup>116</sup> Trost, B. M. *Science* **1991**, *254*, 1471.
- <sup>117</sup> Muñoz-Molina, J. M.; Belderrain, T. M.; Pérez, P. J. *Eur. J. Inorg. Chem.* **2011**, *21*, 3155.
- <sup>118</sup>(a) Kharasch, M. S.; Skell, P. S.; Fischer, P. *J. Am. Chem. Soc.* **1948**, *70*, 1055; (b) Kharasch, M. S.; Jensen, E. V.; Urry, W. H. *Science* **1945**, *102*, 128.
- <sup>119</sup> (a) Curran, D. P.; Bosch, E.; Kaplan, J.; Newcomb, M. *J. Org. Chem.* **1989**, *54*, 1826; (b) Curran, D. P.; Chang, C.-T. *J. Org. Chem.* **1989**, *54*, 3140; (c) Curran, D. P.; Chen, M.-H.; Spletterz, E.; Seong, C. M.; Chang, C.-T. *J. Am. Chem. Soc.* **1989**, *111*, 8872; (d) Curran, D. P.; Seong, C. M. *J. Am. Chem. Soc.* **1990**, *112*, 9401; (e) Curran, D. P.; Tamine, J. *J. Org. Chem.* **1991**, *56*, 2746; (f) Curran, D. P.; Kim, D. *Tetrahedron* **1991**, *47*, 6171. (g) Curran, D. P.; Kim, D.; Ziegler, C. *Tetrahedron* **1991**, *47*, 6189.

- 
- <sup>120</sup> (a) Yorimitsu, H.; Nakamura, T.; Shinokubo, H.; Oshima, K. *J. Org. Chem.* **1998**, *63*, 8604; (b) Yorimitsu, H.; Nakamura, T.; Shinokubo, H.; Oshima, K.; Omoto, K.; Fujimoto, H. *J. Am. Chem. Soc.* **2000**, *122*, 11041; (c) Yorimitsu, H.; Shinokubo, H.; Matsubara, S.; Oshima, K.; Omoto, K.; Fujimoto, H. *J. Org. Chem.* **2001**, *66*, 7776.
- <sup>121</sup> Cao, L.; Li, C. *Tetrahedron Lett.* **2008**, *49*, 7380.
- <sup>122</sup> Gilbert, B. C.; Kalz, W.; Lindsay, C. I.; McGrail, P. T.; Parsons, A. F.; Whittaker, D. T. E. *J. Chem. Soc., Perkin Trans. I* **2000**, 1187.
- <sup>123</sup> (a) Yang, Z.-Y.; Burton, D. J. *J. Org. Chem.* **1991**, *56*, 5125; (b) Metzger, J. O.; Mahler, R. *Angew. Chem., Int. Ed.* **1995**, *34*, 902.
- <sup>124</sup> Forti, L.; Ghelfi, F.; Libertini, E.; Pagnoni, U. M.; Soragni, E. *Tetrahedron* **1991**, *53*, 17761.
- <sup>125</sup> Quebatte, L.; Scopelliti, R.; Severin, K. *Angew. Chem., Int. Ed.* **2004**, *43*, 1520.
- <sup>126</sup> Lübbers, T.; Schäfer, H. J. *Synlett* **1991**, 861.
- <sup>127</sup> For examples of oxidative quenching in visible light photoredox catalysis, see: (a) Cano-Yelo, H.; Deronzier, A. *J. Chem. Soc., Faraday Trans. I* **1984**, *80*, 3011; (b) Cano-Yelo, H.; Deronzier, A. *Tetrahedron Lett.* **1984**, *25*, 5517; (c) Zeh, J. M.; Liou, S. L.; Kumar, A. S.; Hsia, M. S. *Angew. Chem., Int. Ed.* **2003**, *42*, 577.
- <sup>128</sup> LiBr is required only for the reactions of  $\alpha$ -bromo esters and presumably serves to assist in activating the bromo ester towards reduction.
- <sup>129</sup> Curran has previously reported that iodomalونات only add efficiently to terminal and 1,1-disubstituted olefins.
- <sup>130</sup> Kirk, K. *J. Fluorine Chem.* **1999**, *100*, 127.
- <sup>131</sup> Jeschke, P. *ChemBioChem* **2004**, *5*, 570.
- <sup>132</sup> Extrand C. W. *J. Fluorine Chem.* **2003**, *122*, 121.



- 
- <sup>133</sup> For examples of the preparation of vinyl trifluoromethane using (a) Cross coupling, see: Xiao, J.; Weisblum, B.; Wipf, P. *J. Am. Chem. Soc.* **2005**, *127*, 5742. (b) Cross metathesis, see: Imhof, S.; Randl, S.; Blechert, S. *Chem. Commun.* **2001**, 1692. (c) Elimination, see: Bazhin, D. N.; Gorbunova, T. I.; Zapevalov, A. Y.; Salouti, V. I. *J. Fluorine Chem.* **2009**, *130*, 438.
- <sup>134</sup> For synthetic uses of 1,1-cyclopropane diesters, see: (a) Pohlhaus, P. D.; Johnson, J. S. *J. Org. Chem.* **2005**, *70*, 1057. (b) Perreault, C.; Goudreau S. R.; Zimmer L. E.; Charette, A. B. *Org. Lett.* **2008**, *10*, 689. (c) Lebold, T. P.; Kerr, M. A. *Pure Appl. Chem.* **2010**, *82*, 1797.
- <sup>135</sup> Ru(bpy)<sub>3</sub>Cl<sub>2</sub> is synthesized in one step from RuCl<sub>3</sub> (5.0 g for \$157.00 from Sigma Aldrich), whereas [Ir{dF(CF<sub>3</sub>)ppy}<sub>2</sub>(dtbbpy)]PF<sub>6</sub> is synthesized in three steps from IrCl<sub>3</sub> (5.0 g for \$396.50 from Sigma Aldrich).
- <sup>136</sup> Mitani, M; Kiriyaama, T; Kuratate, T. *J. Org. Chem.* **1994**, *59*, 1279.
- <sup>137</sup> Dunbar, R. C.; Hays, J. D.; Honovich, J. P.; Lev, N. B. *J. Am. Chem. Soc.* **1980**, *102*, 3951.
- <sup>138</sup> For a recent difluoromethylation protocol initiated by (Zn(SO<sub>2</sub>CF<sub>2</sub>H)<sub>2</sub>, DFMS, see: Fujiwara, Y; Dixon, J. A.; Rodriguez, R. A.; Baxter, R. D.; Dixon, D. D.; Collins, M. R.; Blackmond, D. G.; Baran P. S. *J. Am. Chem. Soc.* **2011**, *134*, 1494.
- <sup>139</sup> Horvath, I. T.; Rabai, J. *Science* **1994**, *266*, 72.
- <sup>140</sup> Gladysz, J. A.; Curran, D. P.; Horvath, I. T. *Handbook of Fluorous Chemistry*; WILEY-VCH Verlag GmbH & Co. KGaA: Weinheim, 2004.
- <sup>141</sup> Curran, D. P. *Synlett* **2001**, 1488.
- <sup>142</sup> Curran, D. P. *Angew. Chem., Int. Ed.* **1998**, *37*, 1175.
- <sup>143</sup> Curran, D. P.; Luo, Z. Y. *J. Am. Chem. Soc.* **1999**, *121*, 9069.
- <sup>144</sup> (a) Filler, R.; Kobayashi, Y.; *Biomedical Aspects of Fluorine Chemistry*; Kodansha Ltd.: Tokyo, 1982. (b) Resnati, G. *Tetrahedron* **1993**, *49*, 9385; (c) Kirsh, P. *Modern Fluoroorganic*

---

*Chemistry: Synthesis, Reactivity, Applications*; John Wiley & Sons: New York, 2004; (d)

Uneyama, K. *Organofluorine Chemistry*, Blackwell Publishing Ltd, 2006.

<sup>145</sup> Hope, E. G.; Kemmitt, R. D. W.; Paige, D. R.; Stuart, A. M.; Wood, D. R. W. *Polyhedron* **1999**, *18*, 2913.

<sup>146</sup> (a) Kainz, S.; Koch, D.; Baumann, W.; Leitner, W. *Angew. Chem., Int. Ed.* **1997**, *36*, 1628; (b) Xiao, J. L.; Chen, W. P.; Xu, L. J.; Hu, Y. L.; Osuna, A. M. B. *Tetrahedron*, **2002**, *58*, 3889; (c) Sanford, M. S.; Loy, R. N. *Org. Lett.* **2011**, *13*, 2548.

<sup>147</sup> (a) Haszeldine, R. N. *J. Chem. Soc.* **1953**, 3565; (b) Hauptchein, M.; Braid, M.; Lawler, F. E. *J. Am. Chem. Soc.* **1957**, *79*, 2549; (c) Lu, X.; Ma, S.; Zhu, J. *Tetrahedron Lett.*, **1988**, *29*, 5129; (d) Cirkva, V.; Ameduri, B.; Boutevin, B.; Kvicala, J.; Paleta, O. *J. Fluorine Chem.* **1995**, *74*, 97; (e) Ryu, I.; Kerimerman, S.; Niguma, T.; Minakata, S.; Komatsu, M.; Luo, Z.; Curran, D. P. *Tetrahedron Lett.* **2001**, *42*, 947; (f) Iizuka, M.; Yoshida, M. *J. Fluorine Chem.* **2009**, *130*, 926.

<sup>148</sup> Koshechko, V. G.; Kiprianova, L. A. *Theor. Exp. Chem.* **1999**, *35*, 18.

<sup>149</sup> Flamigni, L.; Barbieri, A.; Sabatini, C.; Ventura, B.; Barigelletti, F. *Top. Curr. Chem.* **2007**, *281*, 143.

<sup>150</sup> Kalyanasundaram, K. *Coord. Chem. Rev.* **1982**, *46*, 159.

<sup>151</sup> Dolbier, W. R. *Chem. Rev.* **1996**, *96*, 1557.

<sup>152</sup> (a) Guo, X. C.; Chen, Q. Y. *J. Fluorine Chem.* **1999**, *93*, 81; (b) Yoshida, M.; Ohkoshi, M.; Aoki, N.; Ohnuma, Y.; Iyoda, M. *Tetrahedron Lett.* **1999**, *40*, 5731; (c) Barata-Vallejo, S.; Postigo, A. *J. Org. Chem.* **2010**, *75*, 6141.

<sup>153</sup> One gram of Ru(bpy)<sub>3</sub>Cl<sub>2</sub> is capable of converting 14 mol (1.4 kg of 5-hexen-1-ol) of substrate based on the results from preparative reactions.

- 
- <sup>154</sup> (a) Curran, D. P.; Hadida, S.; Studer, A.; He, M.; Kim, S. Y.; Luo, Z.; Larhed, M.; Hallberg, M.; Linclau, B. "Fluorous Synthesis: A User's Guide", In *Combinatorial Chemistry: A Practical Approach*; Fenniri, H. Ed.; Oxford Univ Press: Oxford, 2000; Vol. 2; pp 327-352; (b) Curran, D. P. "Fluorous Techniques for the Synthesis of Organic Molecules: A Unified Strategy for Reaction and Separation", in *Stimulating Concepts in Chemistry*, Wiley-VCH: Weinheim, 2000, 25-37; (c) Luo, Z.; Zhang, Q.; Oderaotshi, Y.; Curran, D. P. *Science* **2001**, *291*, 1766.
- <sup>155</sup> Dandapani, S.; Newsome, J. J.; Curran, D. P. *Tetrahedron Lett.* **2004**, *45*, 6653.
- <sup>156</sup> (a) Zhang, Q. S.; Luo, Z. Y.; Curran, D. P. *J. Org. Chem.* **2000**, *65*, 8866; b) Dandapani, S.; Curran, D. P. *Tetrahedron* **2002**, *58*, 3855.
- <sup>157</sup> Wrighton, M.; Markam, J. *J. Phys. Chem.* **1973**, *77*, 3042.
- <sup>158</sup> Wayner, D. D. M.; Houmam, A. *Acta Chem. Scand.* **1998**, *52*, 377.
- <sup>159</sup> Vennestrøm, P. N. R.; Osmundsen, C. M.; Christensen, C. H.; Taarning, E. *Angew. Chem. Int. Ed.* **2011**, *50*, 10502.
- <sup>160</sup> Fargues, C.; Mathias, Á.; Rodrigues, A. *Ind. Eng. Chem. Res.* **1996**, *35*, 28.
- <sup>161</sup> Sharma, R. K.; Wooten, J. B.; Baliga, V. L.; Lin, X.; Chan, W. G.; Hajaligol, M. R. *Fuel*, **2004**, *83*, 1469.
- <sup>162</sup> For a recent advance in tall grass engineering see (a) Fu, C.; Mielenz, J. R.; Xiao, X.; Ge, Y.; Hamilton, C. Y. *et al. Proc. Natl. Acad. Sci.* **2011**, *108*, 3803. For recent advances in modified commodity wood plants see: (b) Hisano, H.; Nandakumar, R.; Wang, Z.-Y. *In Vitro Cell. Dev. Biol.—Plant* **2009**, *45*, 306 (c) Pilate, G.; Guiney, E.; Holt, K.; Petit-Conil, M.; Lapierre, C. *et al. Nature Biotechnol.* **2002**, *20*, 607 (d) Williams, C. G. *Nature Biotechnol.* **2005**, *23*, 530.
- <sup>163</sup> Guo, H.; Kliesen, K. L. *Federal Reserve Bank of St. Louis Review*, **2005**, *87*, 669.
- <sup>164</sup> Henry, R. J. *Plant Biotechnol. J.* **2010**, *8*, 1467.

- 
- <sup>165</sup> (a) Perlack, R. D.; Wright, L. L.; Turhollow, A. F.; Graham, R. L.; Stokes, B. J.; Erbach, D. *C. Biomass as Feedstock for a Bioenergy and Bioproducts Industry: The Technical Feasibility of a Billion-Ton Annual Supply*; U.S. Department of Energy. DOE/GO-102005-2135 (2005). (b) This figure takes into account of these high C/O content of biofuels.
- <sup>166</sup> R.D. Perlack and B.J. Stokes (Leads), *U.S. Department of Energy. 2011. U.S. Billion-Ton Update: Biomass Supply for a Bioenergy and Bioproducts Industry*. Oak Ridge National Laboratory, Oak Ridge, TN. ORNL/TM-2011/224 (2011).
- <sup>167</sup> *Alternative, Renewable, and Novel Feedstocks for Producing Chemicals*; U.S. Department of Energy. Oak Ridge National Laboratory, Oak Ridge, T.N. (2006).
- <sup>168</sup> Zakzeski, J.; Bruijninx, P. C. A.; Jongerius, A. L.; Weckhuysen, B. M. *Chem. Rev.* **2010**, *110*, 3552.
- <sup>169</sup> Deem, A. G.; Kaveckis, J. E. *Ind. Eng. Chem.* **1941**, *33*, 1373.
- <sup>170</sup> (a) DiCosimo, R.; Szabo, H.-C. *J. Org. Chem.* **1988**, *53*, 1673 (b) Baciocchi, E.; Fabbri, C.; Lanzalunga, O. *J. Org. Chem.* **2003**, *68*, 9061 (c) Kawai, S.; Kobayashi, Y.; Nakagawa, M.; Ohashi, H. *J. Wood Sci.* **2006**, *52*, 363 (d) Crestini, C.; Caponi, M. C.; Argyropoulos, D. S.; Saladino, R. *Bioorg. Med. Chem.* **2006**, *14*, 5292 (e) Bohlin, C.; Persson, P.; Gorton, L.; Lundquist, K.; Jeonsson, L. *J. Mol. Catal. B* **2005**, *35*, 100.
- <sup>171</sup> Rahimi, A.; Azarpira, A.; Kim, H.; Ralph, J.; Stahl, S. S. *J. Am. Chem. Soc.* **2013**, *135*, 6415.
- <sup>172</sup> Harris, E. E.; D'Ianni, J.; Adkins, H. *J. Am. Chem. Soc.* **1938**, *60*, 1467.
- <sup>173</sup> (a) Barta, K.; Matson, T. D.; Fettig, M. L.; Scott, S. L.; Iretskii, A. V.; Ford, P. C. *Green Chem.* **2010**, *12*, 1640; (b) Matson, T. D.; Barta, K.; Iretskii, A. V.; Ford, P. C. *J. Am. Chem. Soc.* **2011**, *133*, 14090; (c) Parsell, T. H.; Owen, B. C.; Klein, I.; Jarrell, T. M.; Marcum, C. L.;

---

Hauptert, L. J.; Amundson, L. M.; Kenttämä, H. I.; Ribeiro, F.; Miller, J. T.; Abu-Omar, M. M. *Chem. Sci.* **2013**, *4*, 806.

<sup>174</sup> (a) Sergeev, A. G.; Hartwig, J. F. *Science*, **2011**, *332*, 439. For recent report detailing the reductive degradation of lignin models utilizing heterogenous catalysis, see: (b) Parsell, T. H.; Owen, B. C.; Klein, I.; Jarrell, T. M.; Marcum, C. L.; Hauptert, L. J.; Amundson, L. M.; Kenttämä, H. I.; Ribeiro, F.; Miller, J. T.; Abu-Omar, M. M. *Chem. Sci.* **2013**, *4*, 806.

<sup>175</sup> Son, S.; Toste, F. D. *Angew. Chem. Int. Ed.* **2010**, *49*, 1.

<sup>176</sup> For general reactivity see: (a) Jiang, N.; Ragauskas, A. J. *J. Org. Chem.* **2007**, *72*, 7030. (b) Pawar, V. D.; Bettigeri, S.; Weng, S.-S.; Chen, C.-T. *J. Am. Chem. Soc.* **2006**, *128*, 6308 (c) Radosevich, A. T.; Musich, C.; Toste, F. D. *J. Am. Chem. Soc.* **2005**, *127*, 1090 (d) Maeda, Y.; Kakiuchi, N.; Matsumura, S.; Nishimura, T.; Kawamura, T.; Uemura, S. *J. Org. Chem.*, **2002**, *67*, 6718 (e) Hanson, S. K.; Baker, R. T.; Gordon, J. C.; Scott, B. L.; Sutton, A. D.; Thorn, D. L. *J. Am. Chem. Soc.* **2009**, *131*, 428. (f) Hanson, S. K.; Baker, R. T.; Gordon, J. C.; Scott, B. L.; Silks, L. A.; Thorn, D. L. *J. Am. Chem. Soc.* **2010**, *132*, 17804. Studies using these catalysts on lignin models: (g) Hanson, S. K.; Baker, R. T.; Gordon, J. C.; Scott, B. L.; Thorn, D. L. *Inorg. Chem.* **2010**, *49*, 5611 (h) Sedai, B.; Díaz-Urrutia, C.; Baker, R. T.; Wu, R.; Silks, L. A.; Hanson, S. K. *ACS Catal.* **2011**, *1*, 794.

<sup>177</sup> Hanson, S. K.; Wu, R.; Silks, L. A. *Angew. Chem. Int. Ed.* **2012**, *51*, 3410.

<sup>178</sup> DiCosimo, R.; Szabo, H.-C. *J. Org. Chem.* **1988**, *53*, 1673

<sup>179</sup> Hasegawa, E.; Takizawa, S.; Seida, T.; Yamaguchi, A.; Yamaguchi, N.; Chiba, N.; Takahashi, T.; Ikeda, H.; Akiyama, K. *Tetrahedron* **2006**, *62*, 6581.

<sup>180</sup> Kim, S.; Chmely, S. C.; Nimlos, M. R.; Bomble, Y. J.; Foust, T. D.; Paton, R. S.; Beckham, G. *T. J. Phys. Chem. Lett.* **2011**, *2*, 2846.

---

<sup>181</sup> See Table 4.2.

<sup>182</sup> Hasegawa, E.; Takizawa, S.; Seida, T.; Yamaguchi, A.; Yamaguchi, N.; Chiba, N.; Takahashi, T.; Ikeda, H.; Akiyama, K. *Tetrahedron* **2006**, *62*, 6581.

<sup>183</sup> Larraufie, M.-L.; Pellet, R.; Fensterbank, L.; Goddard, J.-P.; Lacôte, E.; Malacria, M.; Ollivier, C. *Angew. Chem., Int. Ed.* **2011**, *50*, 4463.

<sup>184</sup> Juris, A.; Balzani, V.; Barigelletti, F.; Campagna, S.; Belser, P.; Von Zelewsky, V. *Coord. Chem. Rev.* **1988**, *84*, 85.

<sup>185</sup> Dedeian, K.; Djurovich, P. I.; Garces, F. O.; Carlson, G.; Watts, R. J. *Inorg. Chem.* **1991**, *30*, 1685.

<sup>186</sup> Lowry, M. S.; Goldsmith, J. I.; Slinker, J. D.; Rohl, R.; Pascal, R. A., Jr.; Malliaras, G. G.; Bernhard, S. *Chem. Mater.* **2005**, *17*, 5712.

<sup>187</sup> Kern, J.-M.; Sauvage, J.-P. *J. Chem. Soc. Chem. Commun.* **1987**, 546.

<sup>188</sup> Sivaraja, M.; Goodin, D. B.; Smith, M.; Hoffman, B. M. *Science* **1989**, *245*, 738.

<sup>189</sup> See Table 4.3.

<sup>190</sup> Montalti, M.; Credi, A.; Prodi, L.; Gandolfi, M. T. Ionization Energies, Electron Affinities, and Reduction Potentials. In *Handbook of Photochemistry*, 3rd ed.; CRC Press; Boca Raton, FL, 2006; pp 495-527.

<sup>191</sup> For recent examples of visible light photoredox catalysis in flow, see: (a) Bou-Hamdanab, F. R.; Seeberger, P. H. *Chem. Sci.* **2012**, *3*, 1612; (b) Andrews, R. S.; Becker, J. J.; Gagné, M. R. *Angew. Chem. Int. Ed.* **2012**, *51*, 4140; (c) Tucker, J. W.; Zhang, Y.; Jamison, T. F.; Stephenson, C. R. J. *Angew. Chem. Int. Ed.* **2012**, *51*, 4144; (d) Neumann, M.; Zeitler, K. *Org. Lett.* **2012**, *14*, 2658. For a recent review on flow photochemistry, see: Knowles, J. P.; Elliott, L. D.; Booker-Milburn, K. I. *Beilstein J. Org. Chem.* **2012**, *8*, 2025.